



University  
of Glasgow

Holmes, Ashleigh (2012) *Characterising virulence factors from pathogenic bacteria using fluorescent reporters*. PhD thesis.

<http://theses.gla.ac.uk/3317/>

Copyright and moral rights for this thesis are retained by the author

A copy can be downloaded for personal non-commercial research or study, without prior permission or charge

This thesis cannot be reproduced or quoted extensively from without first obtaining permission in writing from the Author

The content must not be changed in any way or sold commercially in any format or medium without the formal permission of the Author

When referring to this work, full bibliographic details including the author, title, awarding institution and date of the thesis must be given



University of Glasgow | Institute of Infection,  
Immunity & Inflammation

# Characterising virulence factors from pathogenic bacteria using fluorescent reporters

A thesis submitted to the University of Glasgow for the degree of  
Doctor of Philosophy

By

Ashleigh Holmes M.Sci

Submitted September 2011

College of Medical, Veterinary and Life Sciences  
Glasgow Biomedical Research Centre  
Glasgow University  
120 University Place  
Glasgow G12 8TA

## **Acknowledgements**

First and foremost, I would like to thank Prof. Tim Mitchell and Dr. Andrew Roe for the opportunity to work with them and for their support, enthusiasm and wisdom, which has been invaluable. Thanks to both past and present members of the Mitchell and Roe labs, there are just too many to name individually, for making the past four years enjoyable.

Many thanks to my family for their continued support and belief in my abilities, it has been a great help. Last but not least, thanks to Raymond for his support during the good times and the bad, helping me achieve all that I can.

## **Author's declaration**

This thesis is the original work of the author unless otherwise stated.

Ashleigh Holmes

September 2011

## Abstract

Protein translocation systems are invaluable to pathogenic bacteria, facilitating the display of virulence factors on their surface or their release into the extracellular environment. Some protein export systems are ubiquitous and essential to cell survival whereas others are horizontally acquired on prophages or pathogenicity islands (PAI), in many cases providing the bacterium with pathogenic advantages. For the majority of the known protein export systems, their structure, function and secreted substrates have been characterised, yet some proteins have been identified that are secreted via unknown mechanisms.

Enterohaemorrhagic *Escherichia coli* (EHEC) O157:H7 is an important cause of human foodborne disease worldwide. The pathogenicity of this bacterium is mainly attributed to the secretion of toxins and the presence of a Type III Secretion System (T3SS). The T3SS can translocate bacterial proteins, known as effectors, into the host cell which mediate an effect culminating in the formation of a characteristic attaching and effacing (A/E) lesion. This system is encoded on a horizontally acquired PAI termed the locus of enterocyte effacement (LEE). The LEE not only encodes the T3SS apparatus but also several effectors secreted by the system and transcription factors which regulate its expression. However, it was recently found that T3SS not only secretes LEE encoded effectors but can also secrete proteins encoded on other prophages present in the EHEC genome. Characterisation of these non-LEE encoded effectors is ongoing and this study investigates the expression, regulation and function of non-LEE encoded effector H1 (NleH1) and H2 (NleH2). Non-LEE encoded effector H1 (NleH1) and H2 (NleH2) are secreted by the T3SS but are encoded on different prophages. This study demonstrates that expression of NleH1 and NleH2 is induced in the same conditions which stimulate the expression of the LEE but expression is diminished upon initial host cell contact *in vitro*. Transcription of *nleH1* and *nleH2* is dependent upon factors specific to *E. coli* O157:H7 and these factors are regulated by LEE encoded regulators Ler and GrlA, as they have a positive effect on *nleH* transcription. NleH1 and H2 are predicted serine/threonine protein kinases and are able to autophosphorylate. Yeast two hybrid screening and 2D differential gel electrophoresis did not elucidate a eukaryotic protein binding partner of NleH1 or NleH2 and they do not

have a significant effect upon NF- $\kappa$ B activation. Determining the expression, regulation and function of non-LEE encoded effectors contributes towards further understanding of how this pathogen causes disease.

*Streptococcus pneumoniae*, also known as the pneumococcus, is another globally important human pathogen. It is a very diverse pathogen, with over 90 capsular serotypes and is naturally competent for DNA uptake. Pneumococcal pathogenesis is facilitated by the production of a pore-forming toxin, pneumolysin. Pneumolysin's activities in pneumococcal pathogenesis extend beyond its cytolytic function as it can also activate the complement pathway and modulate the host cytoskeleton. Pneumolysin is a member of a conserved family of toxins known as the cholesterol dependent cytolysins but differs due to the lack of a secretion signal peptide within its sequence. This indicates that it is not secreted from the bacterium however it has been reported that some strains can release pneumolysin in a cell lysis-independent manner. Additional to this, pneumolysin can also localise to the cell wall, and this localisation is not strain dependent. This study characterised codon-optimised N-terminally labelled pneumolysin constructs were characterised and used to assess the localisation of pneumolysin. In addition, the importance of autolysin and genes which are co-transcribed with Ply upon the localisation/secretion of pneumolysin was investigated by construction of a pneumococcal strain carrying an autolysin-pneumolysin fusion which naturally occurs in equine strains. These genes were not required for the translocation of pneumolysin or its association with the cell wall. Growth of this strain, and its isogenic parent, *in vitro* at a low density and low temperature resulted in the pneumolysin being detected in the broth culture. This indicates that pneumolysin can be released from the cell wall and that this action is not dependent upon the genes which were deleted in the mutant. The distribution of pneumolysin on the pneumococcal surface was assessed with immunofluorescence, and Lumio<sup>TM</sup> substrate fluorescence, microscopy and found to have a general distribution. As a contribution to future pneumococcal research, codon-optimised fluorescent protein reagents were developed and can be used as reporters for gene expression and protein localisation.

## Table of Contents

Acknowledgements.....	2
Abstract.....	4
Table of Contents .....	6
List of Tables.....	9
List of Figures.....	10
Abbreviations .....	12
1 Introduction.....	15
1.1 Secretion systems in bacteria.....	15
1.1.1 Overview.....	15
1.1.2 Translocation across the cytoplasmic membrane.....	16
1.1.3 Translocation of proteins across the outer membrane.....	22
1.2 Enterohaemorrhagic <i>E. coli</i> (EHEC).....	25
1.2.1 Locus of Enterocyte Effacement (LEE) .....	27
1.2.2 Regulation of the LEE.....	34
1.2.3 Non-LEE encoded effector proteins.....	40
1.3 <i>Streptococcus pneumoniae</i> .....	50
1.3.1 Pneumococcal virulence factors.....	51
1.3.2 Pneumolysin .....	55
1.4 Aims of the project.....	63
2 Materials and Methods.....	64
2.1 Bacterial strains, growth conditions & storage .....	64
2.2 Preparation of genomic DNA.....	66
2.2.1 <i>E. coli</i> .....	66
2.2.2 <i>S. pneumoniae</i> .....	66
2.3 Molecular cloning.....	67
2.3.1 Plasmid DNA preparation .....	67
2.3.2 PCR amplification.....	67
2.3.3 Restriction enzyme digestion .....	68
2.3.4 Ligation reaction.....	68
2.4 Transformation of <i>E. coli</i> .....	69
2.5 Construction & analysis of NleH translational fusions.....	70
2.5.1 GFP/RFP fusions .....	70
2.5.2 ILOV fusions .....	71
2.5.3 Analysis of bacterial fluorescence .....	71
2.6 Quantitative PCR (Q-PCR) .....	74
2.7 Construction of NleH knockouts.....	75
2.7.1 Rationale of Lambda Red-mediated recombination.....	75
2.7.2 Rationale of allelic exchange .....	76
2.7.3 Creation of DNA products for knockouts .....	78
2.8 Transfection of HEK293T cells .....	81
2.9 2-D Fluorescence Difference Gel Electrophoresis (2-D DIGE) .....	82
2.10 Yeast-two hybrid analysis.....	84
2.11 <i>S. pneumoniae</i> codon-optimised constructs .....	86
2.11.1 Fluorescent proteins and pneumolysin.....	86
2.11.2 Transcriptional reporter construct .....	87
2.12 Transformation of <i>S. pneumoniae</i> .....	89
2.13 Characterisation of codon-optimised proteins.....	89
2.13.1 Preparation of samples.....	89
2.13.2 SDS-PAGE and western blotting .....	89
2.13.3 Haemolytic assay.....	90

2.13.4	Analysis of <i>S. pneumoniae</i> fluorescence .....	91
2.14	Fluorescence microscopy of pneumococci .....	92
2.14.1	Immunofluorescence.....	92
2.14.2	Lumio™ fluorescence.....	92
2.15	Construction of LytA-Ply fusion in TIGR4NO1 .....	93
2.16	Characterisation of TIGR4NO1ΔLytA-Ply::Chl .....	94
2.16.1	Confirmation of successful mutation.....	94
2.17	Fractionation of <i>S. pneumoniae</i> .....	94
2.17.1	Cell wall digestion buffer .....	95
3	Expression and regulation of Non-LEE encoded effectors (Nle) H1 and H2..	96
3.1	Summary .....	96
3.2	Expression of NleH in different media types .....	96
3.2.1	Expression of GFP translational fusions .....	97
3.3	Expression of NleH in defined regulatory deletions .....	101
3.3.1	Expression in stationary phase regulator knockouts.....	101
3.3.2	Expression in LEE regulator knockouts .....	102
3.3.3	Expression in nleH knockouts .....	108
3.4	Expression of NleH upon host cell contact.....	112
3.5	Discussion.....	114
4	Function of Non-LEE encoded effector H (NleH) .....	119
4.1	Summary .....	119
4.2	Bioinformatics.....	119
4.3	Investigating the effects of NleH on NF-κB signalling.....	122
4.4	Elucidating the host protein targets of NleH .....	125
4.4.1	2D Differential Gel Electrophoresis .....	125
4.4.2	Yeast-two hybrid screen.....	127
4.5	Translocation reporter iLOV .....	129
4.6	Discussion.....	133
5	Enhancing the fluorescent toolbox of <i>Streptococcus pneumoniae</i> .....	137
5.1	Summary .....	137
5.2	Codon-optimised fluorescent proteins .....	140
5.3	Characterisation of <i>S. pneumoniae</i> codon-optimised GFP, YFP and RFP	142
5.3.1	Expression of fluorescence during growth .....	142
5.3.2	Fluorescence microscopy.....	144
5.3.3	Detection of Lumio™ and FLAG tags.....	147
5.4	Application of fluorescent proteins for the pneumococcus .....	149
5.4.1	Transcriptional reporter .....	149
5.5	Discussion.....	153
6	Localisation of pneumolysin (Ply) within the pneumococcus.....	156
6.1	Summary .....	156
6.2	Ply constructs and expression analysis .....	156
6.2.1	Western blotting and Lumio™ analysis .....	157
6.2.2	Analysis of haemolytic activity .....	160
6.2.3	Binding of RFP-Ply to erythrocytes.....	161
6.3	Construction of isogenic mutant TIGR4ΔLytA-Ply::Chl .....	162
6.3.1	Rationale for construction of LytA-Ply fusion in TIGR4 .....	162
6.3.2	Confirmation of successful lytA-ply deletion in TIGR4.....	166
6.4	Pneumococcal localisation of Ply. ....	172
6.4.1	Fractionation analysis.....	172
6.4.2	Fluorescence microscopy analysis.....	177
6.5	Virulence analysis of TIGR4ΔLytA-Ply::Chl.....	185
6.6	Discussion.....	186

7 Final Discussion.....	193
Publications .....	198
List of References .....	200
Appendix.....	241

## List of Tables

Table 1-1 Effector proteins encoded on the LEE PAI .....	32
Table 1-2 Characterised non-LEE encoded T3S effectors (O Island designation is according to the systematic nomenclature design in (Perna <i>et al.</i> , 2001)).....	41
Table 1-3 Characterised pneumococcal virulence factors.....	52
Table 2-1 Strains used in study .....	65
Table 2-2 Typical PCR reaction and cycle conditions .....	67
Table 2-3 Primers used for NleH-FP translational fusions .....	71
Table 2-4 Primers used for making NleH-iLOV translational fusions.....	71
Table 2-5 Q-PCR primers .....	74
Table 2-6 Primers for NleH knockouts .....	79
Table 2-7 Plasmids used for NF- $\kappa$ B assay in HEK293T cells.....	81
Table 2-8 Primers used to create Y2H entry clones .....	85
Table 2-9 Pneumolysin and fluorescent protein constructs .....	86
Table 2-10 Primers used for transcriptional reporter constructs.....	88
Table 2-11 Primers for LytA-Ply fusion .....	93
Table 4-1 Properties of GFP and iLOV.....	129
Table 5-1 Details of codon-optimised fluorescent protein constructs.....	141
Table 6-1 Ply vectors .....	157
Table 6-2 Haemolytic activity of whole cell lysates from D39 $\Delta$ PlySTOP episomally complemented with Ply .....	161

## List of Figures

Figure 1-1 Outer layer arrangement of bacteria .....	16
Figure 1-2 Schematic representation of protein secretion via the Sec system...	18
Figure 1-3 Schematic diagram of Gram-negative bacteria secretion systems ....	23
Figure 1-4 Genetic arrangement of EHEC LEE .....	28
Figure 1-5 Model of Type III Secretion Apparatus.....	30
Figure 1-6 Schematic diagram of LEE regulation in EHEC O157:H7 .....	36
Figure 1-7 T3 effector modulation of the canonical NF- $\kappa$ B activation pathway	46
Figure 1-8 Structure of a typical cholesterol dependent cytolysin (CDC) .....	55
Figure 1-9 Two models of pore formation by CDCs; adapted from (Gilbert, 2002) .....	56
Figure 2-1 Representation of the promoters and coding sequence cloned upstream of GFP .....	70
Figure 2-2 Allelic exchange gene replacement and deletion. ....	77
Figure 2-3 In-Fusion cloning of multiple fragments into a single vector .....	79
Figure 2-4 The yeast-two hybrid system .....	84
Figure 2-5 Promoterless YFP construct pAHS12 .....	88
Figure 2-6 Putative promoter sequences of NanA cloned upstream of YFP.....	88
Figure 3-1: Sequence alignment of the 5' UTR of <i>E. coli</i> O157:H7 NleH1 and NleH2 .....	98
Figure 3-2 Expression of NleH-GFP constructs in <i>E. coli</i> O157:H7 grown in minimal media.....	100
Figure 3-3 Expression of NleH-GFP and Tir-GFP in <i>E. coli</i> K-12, $\Delta$ rpoS and $\Delta$ qseC mutants .....	102
Figure 3-4 Expression of NleH-GFP and Tir-GFP in <i>E. coli</i> O157:H7 defined LEE regulator mutants .....	104
Figure 3-5 Quantitative PCR of NleH transcripts in LEE regulator knockouts....	105
Figure 3-6 Fluorescence microscopy of NleH-GFP .....	108
Figure 3-7 PCR to confirm replacement or deletion of NleH1 in EHEC strain TUV93-0 .....	109
Figure 3-8 PCR to confirm NleH1 and NleH2 replacement or deletion in EHEC strain 85-170 .....	110
Figure 3-9 NleH-GFP expression in NleH knockouts .....	111
Figure 3-10 Expression of NleH-GFP upon <i>E. coli</i> O157:H7 ZAP193 contact with EBL cells .....	113
Figure 4-1 Amino acid sequence alignment of NleH1, NleH2 and OspG .....	120
Figure 4-2 NF- $\kappa$ B activation in the presence of NleH variants .....	124
Figure 4-3 Typhoon scans of NleH1 WT and K159A .....	126
Figure 4-4 Example view of DeCyder analysis software.....	127
Figure 4-5 Yeast-two hybrid screen with vectors described by (Stellberger <i>et al.</i> , 2010) .....	128
Figure 4-6 Fluorescence microscopy of NleH-iLOV upon contact with EBL cells .....	131
Figure 4-7 Three dimensional viewing of bacteria adhering to EBL cells. ....	132
Figure 5-1 Nucleotide sequence added upstream of the ATG start codon in designed constructs from DNA2.0. ....	141
Figure 5-2 Expression of fluorescent proteins during growth in <i>S. pneumoniae</i> D39 .....	143
Figure 5-3 Fluorescence microscopy of D39 pAHS4/5/8 .....	145
Figure 5-4 Immunofluorescence microscopy with fluorescent pneumococci ....	146
Figure 5-5 Z-stack (thickness) of D39 pAHS5 labelled with Cy5 .....	147

Figure 5-6 In-Gel Lumio™ Tag Detection.....	148
Figure 5-7 Western detection of FLAG-Fluorescent protein - monoclonal $\alpha$ -FLAG antibodies .....	148
Figure 5-8 Putative promoter sequences of NanA .....	150
Figure 5-9 Expression of NanA promoter reporter fusions in <i>S. pneumoniae</i> strain R6 .....	152
Figure 6-1 Western blot analysis of pneumococcal lysates - polyclonal antibody .....	158
Figure 6-2 Western blot analysis of pneumococcal lysates - monoclonal antibody .....	159
Figure 6-3 Lumio™ tag detection of Ply complements in D39 $\Delta$ PlySTOP .....	160
Figure 6-4 Erythrocytes treated with PBS and D39 $\Delta$ PlySTOP pAHS6 lysate .....	162
Figure 6-5 Genes surrounding Ply in TIGR4 .....	163
Figure 6-6 Artemis Comparison Tool (ACT) of TIGR4 at position SP_1923 (Ply) and A45 .....	165
Figure 6-7 Introducing the LytA-Ply genetic fusion from A45 into TIGR4 genome. ....	167
Figure 6-8 Confirmation of successful deletion by PCR.....	168
Figure 6-9 Sequence alignment of TIGR4 Ply and LytA against A45 sequence, including the inserted Cat cassette.....	169
Figure 6-10 Analysis of pneumococcal chain length .....	170
Figure 6-11 Haemolytic assay of TIGR4 $\Delta$ LytA-Ply, isogenic parent and episomal complement whole cell lysates.....	171
Figure 6-12 Western blot of TIGR4 $\Delta$ LytA-Ply - polyclonal $\alpha$ -Ply antibody.....	172
Figure 6-13 Fractionation of TIGR4, TIGR4 $\Delta$ LytA-Ply (T $\Delta$ LP) and T $\Delta$ LP with pAHS3. ....	174
Figure 6-14 Gram staining of pneumococci after cell wall digestion treatment .....	175
Figure 6-15 Fractionation with alternative cell wall digestion buffer.....	176
Figure 6-16 Immunofluorescence microscopy of D39 $\Delta$ PlySTOP/pAHS3 and TIGR4 $\Delta$ LytA-Ply/pAHS3. ....	179
Figure 6-17 Lumio™ labeling of D39 $\Delta$ PlySTOP expressing tagged-Ply.....	183
Figure 6-18 3D analysis of D39 $\Delta$ PlySTOP/pAHS6 with Lumio™ substrate .....	183
Figure 6-19 Fluorescence microscopy of pneumococci incubated with Lumio™ reagent.....	184
Figure 6-20 3D analysis of TIGR4 $\Delta$ LytA-Ply/pAHS3 with Lumio™ substrate.....	185

## Abbreviations

°C	Degrees Celsius
α-	Anti
β-	Beta
Δ	Deletion
μl	micro litre
μm	micrometer
μM	micro molar
Ab	Antibody
ABC	ATP-binding cassette
Amp	Ampicillin
APS	Ammonium persulphate
BAB	Blood Agar Base
BBB	Blood Brain Barrier
BHI	Brain Heart Infusion
BLAST	Basic Local Alignment Search Tool
bp	Base pair
BSA	Bovine Serum Albumin
Cbp	Choline Binding Protein
CDC	Cholesterol-dependent Cytolysin
cDNA	Complementary DNA
CDS	Coding sequence
Ces	Chaperone of Escherichia coli secretion
CFU	Colony Forming Unit
Chl	Chloramphenicol
Cif	Cycle inhibiting factor
CPS	Capsule Polysaccharide
CR	Citrobacter rodentium
CSP	Competence Stimulating Peptide
CU	Chaperone/Usher
D39	<i>S. pneumoniae</i> serotype 2 strain D39 (NCTC number: 7466)
dH <sub>2</sub> O	Distilled water
DMEM	Dulbelcco's Modified Eagle Medium
DNA	Deoxyribonucleic acid
dNTP	deoxyribonucleotide triphosphate
DTT	Dithiothreitol
EBL	Embryonic bovine lung
ECL	Enhanced chemi-luminescence
EHEC	Enterohaemorrhagic Escherichia coli
EPEC	Enteropathogenic Escherichia coli
Ery	Erythromycin
Esc	Escherichia secretion
Esp	Escherichia secreted protein
FAS	Fluorescent-actin staining
FCS	Foetal Calf Serum
FITC	Fluorescein isothiocyanate
g	Gram
gDNA	Genomic DNA
Gent	Gentamycin
GFP	Green fluorescent protein
GrlA/R	Global regulator of LEE-activator/repressor

H <sub>2</sub> O <sub>2</sub>	Hydrogen peroxide
HEK	Human Embryonic Kidney
Hfq	Host factor required for phage QB RNA replication
His-Tag	Histidine Affinity tag
HlyA	Alpha-hemolysin
H-NS	Histone-like nucleoid-structuring protein
HPA	Health Protection Agency, Colindale, London
hr	Hour
HRP	Horseradish peroxidase
HU	Haemolytic Units
HUS	Haemolytic uraemic syndrome
Hyl	Hyaluronidase
IAA	Isoamyl alcohol
IL	Interleukin
ILY	Intermedilysin
IM	Inner membrane
IPD	Invasive pneumococcal disease
IPTG	Isopropyl- $\beta$ -D-Thiogalactopyranoside
IRTKS	Insulin receptor tyrosine kinase substrate
Kan	Kanamycin
Kb	Kilobase
kDa	Kilodalton
L	Litre
LB	Luria Broth
LEE	Locus of enterocyte effacement
Ler	LEE-encoded regulator
LPS	Lipopolysaccharide
LytA	Autolysin A
M	Molar
mAb	Monoclonal Antibody
Map	Mitochondria associated protein
MEM	Minimum Essential Medium
mg	Milligram(s)
min	Minute(s)
ml	Millilitre
mM	Millimolar
Mpc	Multiple point controller
mRNA	Messenger Ribonucleic acid
MW	Molecular weight
Nck	Non-catalytic region of tyrosine kinase adaptor
NF- $\kappa$ B	Nuclear Factor kappa B
Nle	Non-LEE-Encoded
nm	Nanometre
nM	Nanomole
N-WASP	Neuronal Wiskott-Aldrich Syndrome protein
OD <sub>600nm</sub>	Optical Density measured at 600 nm
OM	Outer membrane
Omp	Outer membrane protein
ORF	Open reading frame
Osp	Outer Shigella protein
PAI	Pathogenicity island
PBS	Phosphate Buffered Saline
PCR	Polymerase Chain Reaction

PdT	Ply carrying triple mutations: D385N, C428G, W433F
Per	Plasmid-encoded regulator
PFO	Perfringolysin O
Pht	Pneumococcal histidine triad protein
Ply	Pneumolysin
PMF	Proton motive force
PpmA	Proteinase maturation protein A
PppA	Pneumococcal protective protein A
PS	Polysaccharide
Psa	Pneumococcal surface adhesion protein
Psp	Pneumococcal surface protein
Q-PCR	Quantitative PCR
QS	Quorum sensing
RBC	Red blood cell
RFP	Red fluorescent protein
RFU	Relative fluorescence units
RNA	Ribonucleic acid
rpm	Revolutions per minute
rRNA	Ribosomal ribonucleic acid
RT	Room Temperature (~20°C)
SDM	Site-directed mutagenesis
SDS-PAGE	Sodium Dodecyl Sulphate-Polyacrylamide Gel Electrophoresis
Sec	General secretory pathway
sec	Second(s)
Sep	Secretion of Escherichia coli proteins
SLO	Streptolysin O
Stx	Shiga toxin
T1/2/3/4/5/6SS	Type 1/2/3/4/5/6 secretion system
Tat	Twin-arginine translocation
TccP	Tir-cytoskeleton coupling protein
TE	TRIS-EDTA
TIGR	The Institute for Genomic Research
TIGR4	Serotype 4 S. pneumoniae sequenced by TIGR
Tir	Translocated intimin receptor
TLR	Toll-like Receptor
TNF	Tumour Necrosis Factor
TRITC	Rhodamine
U	Units
UK	United Kingdom
USA	United states of America
UTR	Untranslated region
V	Volts
v/v	Volume/volume
VT	Verocytotoxin
VTEC	Verocytotoxin producing E.coli
WHO	World Health Organisation
WT	Wild type
xg	centrifugal force
X-GAL	5-Bromo-4-chloro-3-indolyl β-D-galactopyranoside
YFP	Yellow fluorescent protein
ZmpB	Zinc metalloprotease B

# 1 Introduction

## 1.1 Secretion systems in bacteria

### 1.1.1 Overview

Bacterial pathogenicity depends greatly on the ability to secrete virulence factors which are displayed on the bacterial cell surface, secreted into the extracellular milieu or even translocated directly into the host cell (Finlay & Falkow, 1997; Lee & Schneewind, 2001). Gram-positive and Gram-negative bacteria have cell envelopes across which to secrete proteins; one with a thin layer of peptidoglycan and an outer cell membrane (Gram-negative) or one with a thick layer of peptidoglycan (Gram-positive) surrounding the plasma membrane, Figure 1-1.

Peptidoglycan consists of glycan chains with repeating sugar molecules, N-acetylglucosamine and N-acetylmuramic acid connected by  $\beta$ -1,4 linkages. The glycan chains are linked together by oligopeptides, the amino acids used and the number of cross-links can differ between bacterial species (Madigan *et al.*, 2003). Teichoic and lipoteichoic acids (LTA) contribute to the negative charge of the Gram positive cell wall, and can attract cations such as magnesium and calcium providing cell rigidity. Lipopolysaccharide (LPS) contributes to the negative charge and structure of Gram negative cell walls and is comprised of Lipid A, core polysaccharide and O-specific polysaccharide (also known as O-antigen). The O-antigen of LPS can differ between bacteria which can allow classification of bacteria of the same species by serotype, for example *Escherichia coli* O157, *E. coli* O22 and *E. coli* O104. As peptidoglycan, LTA and LPS have repetitive structures the host innate immune system has evolved receptors that recognise these structures, also known as pathogen-associated molecular patterns (PAMPs) as non-self (Akira *et al.*, 2001).

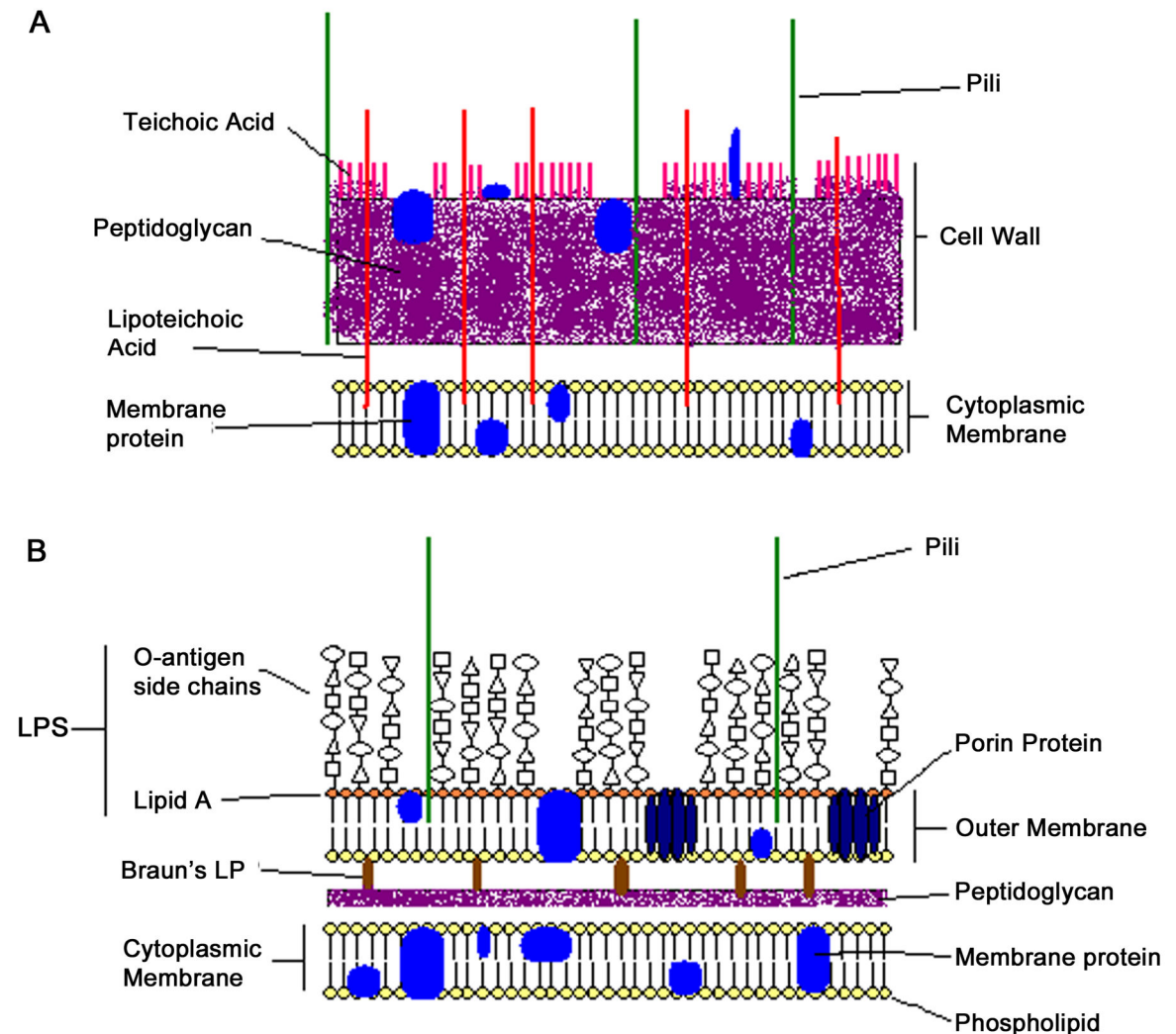


**Figure 1-1 Outer layer arrangement of bacteria**

**A.** Gram positive bacteria are characterised by the presence of a thick layer of peptidoglycan (purple). The peptidoglycan provides an anchor for pili (green), wall-associated proteins (blue) and (lipo)teichoic acids (pink), together constitute the cell wall.

**B.** Gram negative bacteria are characterised by the additional membrane layer which surrounds the thin peptidoglycan layer. This outer membrane differs to the cytoplasmic membrane due to the incorporation of lipopolysaccharide (LPS). The outer membrane is tethered to the peptidoglycan layer by Braun's lipoprotein (LP; brown), and incorporates outer membrane associated proteins, porin proteins and pili. The space between the inner and outer membranes is called the periplasm. Figure is based on (Madigan *et al.*, 2003)

### 1.1.2 Translocation across the cytoplasmic membrane

Protein translocation across the cytoplasmic membrane can follow one of 6 different pathways; the general secretory (Sec) system, twin-arginine translocation (TAT) system, Flagellar Export Apparatus (FEA), Fimbrilin-Protein Exporter (FPE), the holins, and the ESX-1/Type VII secretion system (Nguyen *et al.*, 2000; Desvaux & Hebraud, 2006; Saier, 2006; Abdallah *et al.*, 2007). With reference to translocation across the cytoplasmic membrane, only the Sec and TAT system will be described further.

### 1.1.2.1 The general secretary (Sec) system

The Sec System is well conserved, and essential, among both prokaryotes and eukaryotes. In eukaryotes, a Sec system analogue is necessary for translocation of proteins across the endoplasmic reticulum. In prokaryotes, the Sec system is utilized for protein transport across the cytoplasmic membrane. The structure and mechanism of this secretion system has largely been studied in Gram-negative bacterium *Escherichia coli* (Economou, 2002), and Gram-positive bacterium *Bacillus subtilis* (van Wely *et al.*, 2001). The Sec system consists of three integral membrane proteins, SecY, SecE and SecG, which form the translocon pore, a cytoplasmic ATPase SecA and accessory membrane proteins SecD, SecF and YajC, Figure 1-2. It has been proposed that SecA recruits and assembles four SecYEG complexes to form the translocase (Manting *et al.*, 2000). However, the oligomeric state of functioning SecYEG translocase still appears to be inconclusive as recent reports have shown that active translocation occurs with SecYEG dimers (Gold *et al.*, 2010; Deville *et al.*, 2011) and that preprotein secretion can occur via a single SecYEG complex (Kedrov *et al.*, 2011). The SecYEG translocase is closely associated with accessory membrane proteins SecDF/YajC and YidC. YidC is responsible for membrane protein insertion into the cytoplasmic membrane (Scotti *et al.*, 2000). SecDF is proposed to facilitate protein translocation by SecYEG (Matsuyama *et al.*, 1993). SecA is a homodimeric ATP-binding protein, which is involved in providing the system with energy, and acts as a receptor for precursor proteins (Driessen *et al.*, 1998; Economou, 1998). It exists in a compact, ADP-bound state and an extended, ATP-bound state (den Blaauwen & Driessen, 1996). When associated with SecYEG, it is activated for precursor stimulated cycles of ATP binding and hydrolysis (Lill *et al.*, 1990), which results in cycles of SecA membrane insertion and precursor translocation. The proton motive force also assists this cyclic reaction by ensuring unidirectional translocation and providing a source of ATP (Driessen, 1992; Nishiyama *et al.*, 1999).

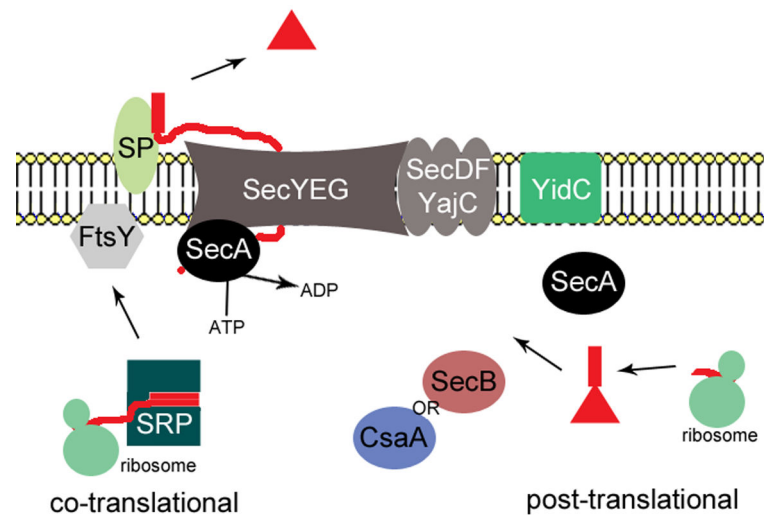


**Figure 1-2 Schematic representation of protein secretion via the Sec system**  
 Secretion can occur via one of two pathways: co-translational or post-translational for reasons explained in the text. In the co-translational pathway, the secretion signal peptide is recognised by the signal recognition particle (SRP). The SRP/ribosome complex interacts with FtsY to bring the polypeptide to be secreted in close proximity with SecA. In the post-translational pathway, the protein is synthesised and the signal peptide recognised by SecA or SecB/CsaA chaperones, which maintain the protein in a secretion-permissible conformation. SecB/CsaA chaperones interact with SecA to 'deliver' the protein for secretion through SecYEG. Signal peptidase (SP) cleaves the signal peptide from the polypeptide and the protein is secreted.

Proteins that are to be translocated by the Sec system are synthesised as precursor with an N-terminal signal peptide, which is recognised by the translocase. The signal peptide has a tripartite structure: a positively charged N-domain (normally due to presence of lysine and/or arginine residues), a hydrophobic H-domain and a C-domain which specifies the cleavage site for signal peptidase (Tjalsma *et al.*, 2000). Signal peptidase is present on the outer surface of the plasma membrane and is responsible, as its name suggests, for the cleavage of the signal peptide from the precursor protein to give rise to a mature protein. Prior to translocation, the precursor protein associates with a cytosolic chaperone protein (also known as targeting factors) either co-translationally or post-translationally, which maintains the precursor in a translocation-competent state by preventing their folding and aggregation (Tjalsma *et al.*, 2000; Tjalsma *et al.*, 2004). The signal-recognition particle (SRP) is a complex consisting of Ffh (fifty-four homologue) protein, so-called as it is a GTPase which is homologous to the 54-kDa subunit of the eukaryotic SRP, and RNA (Keenan *et al.*, 2001). The SRP complex binds to the signal peptide of emerging polypeptide chains from the ribosome, and is targeted to the

membrane via FtsY protein, a SRP receptor protein. In *E. coli*, the post-translational targeting of preproteins to the Sec translocon is mediated by SecB. SecB binds to the precursor protein with low affinity, but to the C-terminus of SecA with high affinity (Knoblauch *et al.*, 1999). Therefore, it is considered that SecB acts as a general chaperone to the Sec translocase, by enabling the interaction of precursor proteins with SecA if they present the appropriate signal peptide. A SecB homologue has not been found in *B. subtilis*, however a possible analogue is CsaA. CsaA is a suppressor of the *E. coli* SecA (temperature sensitive) mutant, and was subsequently shown to have shared properties with SecB, such as an affinity for precursor proteins and SecA (Muller *et al.*, 1992; Muller *et al.*, 2000). However, it does not bind SecA at the same conserved domain as SecB. The pathway by which a precursor protein follows to be chaperoned to SecA, i.e. via SRP or SecB/CsaA, depends on the hydrophobicity of the signal peptide as more hydrophobic proteins follow the SRP pathway. This may provide reason as to why *B. subtilis* does not have a SecB chaperone, as *B. subtilis* proteins tend to have more hydrophobic signal peptides (Tjalsma *et al.*, 2000) and are therefore targeted to the translocase via SRP. Also, the hydrophobicity of a protein is greatly enhanced by the presence of transmembrane domains, which are present in cytoplasmic (or inner) membrane proteins. However, proteins to be inserted into the outer membrane of gram negative organisms, e.g. porins, have a  $\beta$ -barrel conformation and thus a lower hydrophobicity, so these proteins are chaperoned by SecB.

The distribution of the Sec translocon has been investigated in *E. coli*, *B. subtilis* and streptococcal species. The SecA in *Streptococcus pyogenes* localises to a focal point in the cell surface, at the position of the old pole, which has been termed the ExPortal (Rosch & Caparon, 2004; Rosch & Caparon, 2005). The ExPortal has also been characterised in *S. mutans* using immunogold electron microscopy (Hu *et al.*, 2008) and also in *Enterococcus faecalis* (Kline *et al.*, 2009). When the ExPortal was first characterised it was hypothesised that this could be a central paradigm for the localisation of the Sec system in all Gram-positive bacteria, however studies in *Bacillus subtilis* demonstrated that the Sec system was distributed in a helical array along the longitudinal axis of the cell (Campo *et al.*, 2004). In *E. coli*, conflicting reports have been made on the distribution of the Sec translocon; that it is uniformly distributed around the

cytoplasmic membrane (Brandon *et al.*, 2003) or in a helical array like that for *B. subtilis* (Shiomi *et al.*, 2006). It is proposed that the Sec translocons cluster in areas where cell wall synthesis occurs, as the cell wall is more permeable allowing the proteins to travel to the surface or extracellular environment (Campo *et al.*, 2004; Rosch & Caparon, 2004). It is also hypothesised that the presence of the Sec systems in clusters facilitates the interactions of secreted polypeptides with chaperones or other accessory factors for processing or efficient folding (Campo *et al.*, 2004; Rosch & Caparon, 2005).

### 1.1.2.2 Accessory Sec system

Additional *secA* homologs have been identified in a number of Gram positive and Mycobacterial species (Rigel & Braunstein, 2008). The second SecA shares less homology with the SecA of the general secretory pathway, and is therefore termed SecA2. Staphylococci and Streptococci species have an accessory *secY2* which is part of an operon with *secA2* and additional genes involved in the synthesis, glycolysis and transport of an adhesin. The genetic arrangement of the accessory Sec system locus is conserved but the locus is not present in all strains, which indicate that these loci have been horizontally acquired (Rigel & Braunstein, 2008). SecA2/Y2 systems in these species are responsible for the translocation of glycosylated serine-rich proteins (Bensing & Sullam, 2002; Obert *et al.*, 2006). In *S. pneumoniae* SecA2/Y2 translocates pneumococcal serine-rich repeat protein (PsrP), which is an adhesin that contributes to pneumococcal colonisation and pathogenesis (Hava & Camilli, 2002; Obert *et al.*, 2006; Rose *et al.*, 2008; Shivshankar *et al.*, 2009; Sanchez *et al.*, 2010). Proteins which are translocated by the SecA2/SecY2 system have an N-terminal signal sequence with the traditional tripartite structure described for the Sec system. However, glycine residues within the hydrophobic region have been shown to be necessary for translocation via SecA2/SecY2 and also interfere with translocation via the Sec system (Bensing *et al.*, 2007). A 20 amino acid motif present after the signal peptidase cleavage site has been shown to be essential for translocation via the SecA2/SecY2 system and termed the accessory Sec transport (AST) domain (Bensing & Sullam, 2010). Characterisation of the translocation mechanism of this accessory secretion system and how its substrates are recognised is ongoing (Bensing & Sullam, 2010).

### 1.1.2.3 The Twin-Arginine Translocation (TAT) pathway

The Tat system is so called due to the signal sequences of proteins translocated by this system contain two arginines (R-R) (Sargent *et al.*, 1998). The interesting aspect of the Tat system is its ability to secrete fully folded proteins and even multimeric enzyme complexes. TatA monomers assemble to form a transmembrane channel, which is able to change diameter, presumably through the addition or loss of TatA monomers, enabling the passage of folded proteins of differing molecular weights and sizes (Gohlke *et al.*, 2005). The TatBC complex recognizes and binds a pre-protein containing a twin-arginine motif in its signal sequence before associating with the TatA oligomer in a proton-motive force dependent manner. The secretory machinery is fully assembled to translocate the protein across the membrane via the channel formed by TatA monomers. Once the protein has been translocated, the system returns to a resting state with the TatA complex dissociating from the TatBC complex (Palmer *et al.*, 2005).

The Tat system has been shown to be important for virulence, for example an *E. coli* O157:H7 strain with the Tat operon deleted significantly reduced its virulence *in vitro* (Pradel *et al.*, 2003). It was determined that the lack of a Tat system affected the secretion of Shiga-like toxin 1 (Stx1) and affected motility by abolishing the synthesis/stability of flagellin H7, both of which are important virulence factors of *E. coli* O157 (Pradel *et al.*, 2003).

### 1.1.2.4 Non-classical secretion

Proteomic analyses of the secretome or surface subproteomes of bacterial species have identified cytoplasmic proteins in the extracellular fractions, without obvious evidence of cell lysis. Often, these cytoplasmic proteins have demonstrated an alternative function extracellularly compared to their function within the cell. Such proteins with multiple unrelated functions are described as 'moonlighting' proteins (Jeffery, 1999). Across a number of Gram-positive bacteria, including *Listeria*, *Streptococcus*, *Staphylococcus* and *Bacillus* species, the cytoplasmic protein enolase is displayed on the bacterial cell surface, and when extracellular, binds plasmin(ogen) (Pancholi & Fischetti, 1998; Bergmann *et al.*, 2001; Bergmann *et al.*, 2003; Carneiro *et al.*, 2004; Ge *et al.*, 2004;

Schaumburg *et al.*, 2004; Tjalsma *et al.*, 2004; Agarwal *et al.*, 2008; Esgleas *et al.*, 2008). Recently, a study investigating non-classical secretion in *B. subtilis* found that secretion of predicted cytoplasmic proteins, including enolase, occurred during early stationary phase of growth (Yang *et al.*, 2011). Secretion of enolase was demonstrated to occur in an autolysin-negative strain and in the absence of cell lysis, indicated by viable count, secretion without active protein synthesis and lack of SecA protein in the extracellular milieu. However, enolase secretion was abolished by the mutation of an  $\alpha$ -helical membrane-embedding domain present in its protein structure (Yang *et al.*, 2011). This provides evidence that protein structure contributes to non-classical secretion in *Bacillus*. However, secretion of proteins via this non-classical pathway is controversial as the mechanism of translocation and whether it is an active form of secretion remains to be elucidated.

### **1.1.3 Translocation of proteins across the outer membrane**

In Gram-negative bacteria, specialized secretion systems have evolved in order to translocate proteins across the largely impenetrable outer membrane. These secretion systems have been categorized in a number system (I-VI) and some pathways are dependent on the ubiquitous pathways present in the cytoplasmic membrane and others are not, Figure 1-3.

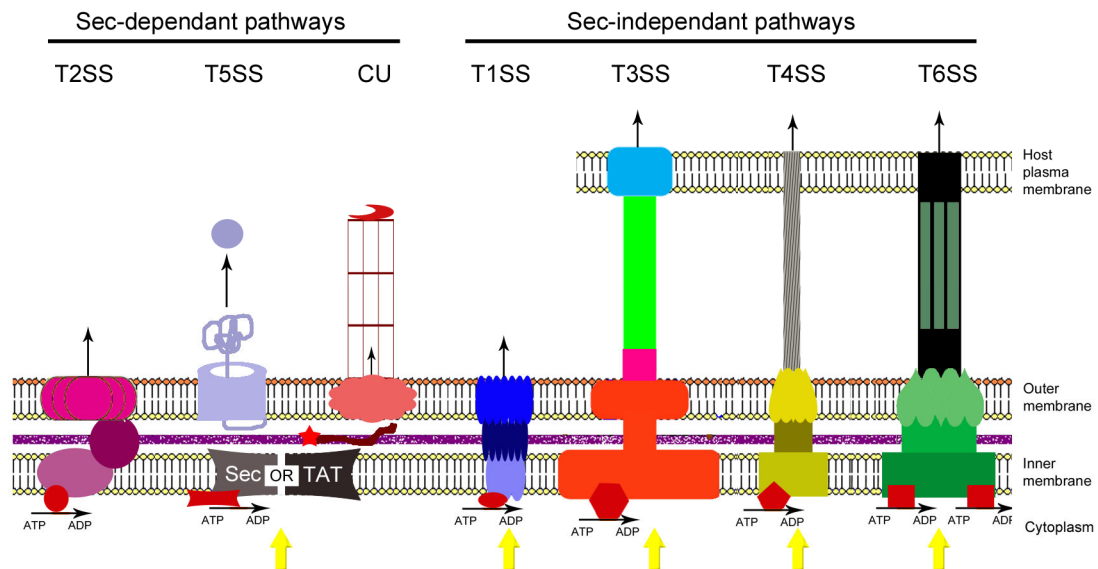


**Figure 1-3 Schematic diagram of Gram-negative bacteria secretion systems**  
 Simple representation of secretion systems, which is not to any scale and complexes consist of multiple proteins. ATPase, is represented by dark red symbol, which provides energy for protein secretion by ATP hydrolysis. The red star represents a chaperone, complexed with an 'unfolded' protein, as part of the chaperone usher (CU) pathway. Protein secretion via type 2, type 5 and CU pathways is a two-step process, where the protein is translocated into the periplasm via the general secretory (Sec) or Twin-Arginine Translocation pathway before translocation across the outer membrane. Protein secretion via type 1, type 3, type 4 or type 6 occurs across both membranes in one step and is therefore described as Sec-independent.

The Type I secretion system (T1SS) is described as a Sec-independent system, as proteins, up to 800kDa in size (Holland *et al.*, 2005), are secreted across both the cytoplasmic and outer membrane. The prototypical example of this system consists of an ABC transporter (HylB), membrane fusion protein (HylD) and outer membrane protein (TolC) which together translocate alpha-haemolysin (HylA) from *E.coli* (Hartlein *et al.*, 1983; Lee & Schneewind, 2001). Type II secretion (T2S) is a two step process where the protein is first translocated across the cytoplasmic membrane via the Sec or Tat system (Coulthurst & Palmer, 2008; Ferrandez & Condemine, 2008) then across the outer membrane via a secretin (Nunn, 1999). The Type III Secretion System (T3SS) is Sec-independent, like Type I, and is dedicated to the translocation of proteins directly into host cells. The genes encoding the apparatus required for Type III secretion are usually encoded on horizontally acquired islands, which are regions on genomes/plasmid of pathogenic strains; they are absent in closely related non-pathogenic strains. T3SS have been identified in a broad range of Gram negative bacterial species including *Yersinia*, *Salmonella*, *Shigella*, *Escherichia coli*, *Pseudomonas*, and *Erwinia* (Galan & Collmer, 1999). This system is described further in Section 1.2.1.1. The Type IV secretion system (T4SS) is related to the conjugative pilus

system in bacteria and can translocate proteins, protein-DNA complexes or DNA across both membranes in a one step process (Cascales & Christie, 2003). However, the pertussis toxin from *Bordetella pertussis* is translocated via a Sec-dependent Type IV secretion pathway into the extracellular environment (Rambow-Larsen & Weiss, 2004). The Type V secretion system (T5SS) includes the autotransporter (AT) and two-partner (TpsA and TpsB) proteins, which are first translocated into the periplasm via the Sec system, AT or TpsA are processed by signal peptidase into an active proenzyme, the C-terminal end of the AT protein or TpsB inserts into the outer membrane in a  $\beta$ -barrel conformation assisted by the BAM complex (Knowles *et al.*, 2009), providing a pore for the N-terminal end of the AT protein or TpsA respectively, to translocate to the surface (Henderson *et al.*, 2004). The Type VI secretion system (T6SS) is analogous to T4SS and has only recently been described. It is characterised by its requirement for a ring-forming AAA<sup>+</sup> ATPase (ClpV) to provide energy to the system (Mougous *et al.*, 2006; Bingle *et al.*, 2008; Filloux *et al.*, 2008).

## 1.2 Enterohaemorrhagic *E. coli* (EHEC)

Enterohaemorrhagic *E. coli* (EHEC) are Gram negative facultative anaerobic bacteria which are important causative agents of severe foodborne disease worldwide (Kaper *et al.*, 2004). EHEC was first identified in 1982 as a cause of bloody diarrhoea and HUS. EHEC causes sporadic but deadly outbreaks of haemorrhagic colitis (bloody diarrhoea), which can lead to the serious complication of haemolytic uremic syndrome, in developed countries such as Scotland, USA and Japan. The incidence of EHEC infections is greater in young children and the elderly. There are many serotypes of EHEC, such as O111, O26, O104, but the World Health Organisation considers EHEC serotype O157 as the most important serotype with regards to public health.

EHEC can colonize ruminants, such as sheep and cattle, asymptotically (Borczyk *et al.*, 1987; Orskov *et al.*, 1987; Chapman *et al.*, 1996). The persistence and tropism of EHEC O157 colonisation in cattle was assessed by experimental challenge of cattle, which determined that EHEC O157:H7 is found in high numbers in bovine faeces and displays a tropism for the mucosa of the terminal rectum of cattle (Naylor *et al.*, 2003). It was also found that the faeces from cattle with EHEC O157:H7 colonised terminal rectum displayed a high EHEC O157:H7 distribution on the outer surface of the faeces, whereas other colonising species of *E. coli* were distributed throughout (Naylor *et al.*, 2003). Further studies assessing the colonisation of cattle after slaughter confirmed EHEC O157:H7 tropism for this site of the intestinal tract and indicated that colonisation of this site facilitates bacterial shedding in the faeces (Low *et al.*, 2005). EHEC O157:H7 infections in humans typically arise from the consumption of faecal contaminated meat, vegetable or other animal by-products, such as milk. EHEC O157:H7 infections can also occur via the faecal-oral route which commonly occurs with children visiting petting zoos/farms, for example the outbreak in 2009 at Godstone Farm, Surrey resulted in 93 EHEC infections, of which 17 resulted in HUS (<http://www.griffininvestigation.org.uk/>).

EHEC O157 is considered to have evolved from an enteropathogenic *E. coli* (EPEC) O55 strain, through the acquisition of bacteriophages encoding Shiga toxins (Reid *et al.*, 2000). Shiga toxins (Stx-1 and Stx-2) are AB<sub>5</sub> toxins which have been shown to play an important role in EHEC pathogenesis, as these toxins are cytotoxic and can inhibit host cell protein synthesis (Endo *et al.*, 1988). Using purified toxin, it was shown that the toxin induces fluid accumulation and loss of adsorptive villus epithelial cells in rabbits *in vivo* (Keenan *et al.*, 1986). Stx is also known as verotoxin (VT) due to the cytotoxicity observed when incubated with Vero cells (Scotland *et al.*, 1985). The production of Stx has been linked to the pathology associated with haemolytic colitis and HUS (Karmali *et al.*, 1983). This is supported by a recent *E. coli* outbreak in Germany, with over 3,000 infections reported of which 25% resulted in HUS, caused by an *E. coli* O104:H4 strain acquiring the *stx* gene, as well as antibiotic resistance genes and alternative fimbrial adhesins (Rohde *et al.*, 2011). Therefore, EHEC is a subset of verotoxin/shiga-toxin producing *E. coli* (VTEC/STEC).

EHEC are members of the 'attaching and effacing' (A/E) family of bacterial pathogens, with enteropathogenic *E. coli* (EPEC) and *Citrobacter rodentium*, so named due to the lesion formed during the bacterium's colonization of the intestinal mucosa (Moon *et al.*, 1983). The histopathology is characterised by the loss of microvilli (effacement), cytoskeletal rearrangements resulting in the formation of a 'pedestal' structure and intimate bacterial attachment (10-12 nm gap) to the gut enterocyte (Polotsky *et al.*, 1977; Rothbaum *et al.*, 1982; Moon *et al.*, 1983; Knutton *et al.*, 1987). This lesion is caused by the effector proteins which are delivered into the host by way of a T3SS, hijacking the host cell cytoskeleton enabling an intimate attachment between the bacterium and the host cell to be formed. This T3SS is encoded by a pathogenicity island named the locus of enterocyte effacement (LEE) (McDaniel *et al.*, 1995).

### **1.2.1 Locus of Enterocyte Effacement (LEE)**

The LEE PAI is about 35kB (Perna *et al.*, 2001) and consists of at least 41 open reading frames (ORFs) arranged in five operons, Figure 1-4. LEE1, 2, and 3 contain 22 ORFs and primarily encode the constituents of the type III secretion apparatus, the *esc* (*E. coli* secretion) and *sep* (secretion of *E. coli*) proteins. LEE4 encodes the proteins which form the conduit between the bacterium and the host cells, namely the EscF needle complex protein and the translocator proteins EspA, B, and D. LEE5 contains the translocated intimin receptor (Tir), its chaperone CstT and the adhesin intimin. The LEE also carries its own transcriptional regulators, Ler (LEE encoded regulator) and GrlRA (global regulator of LEE repressor and activator).

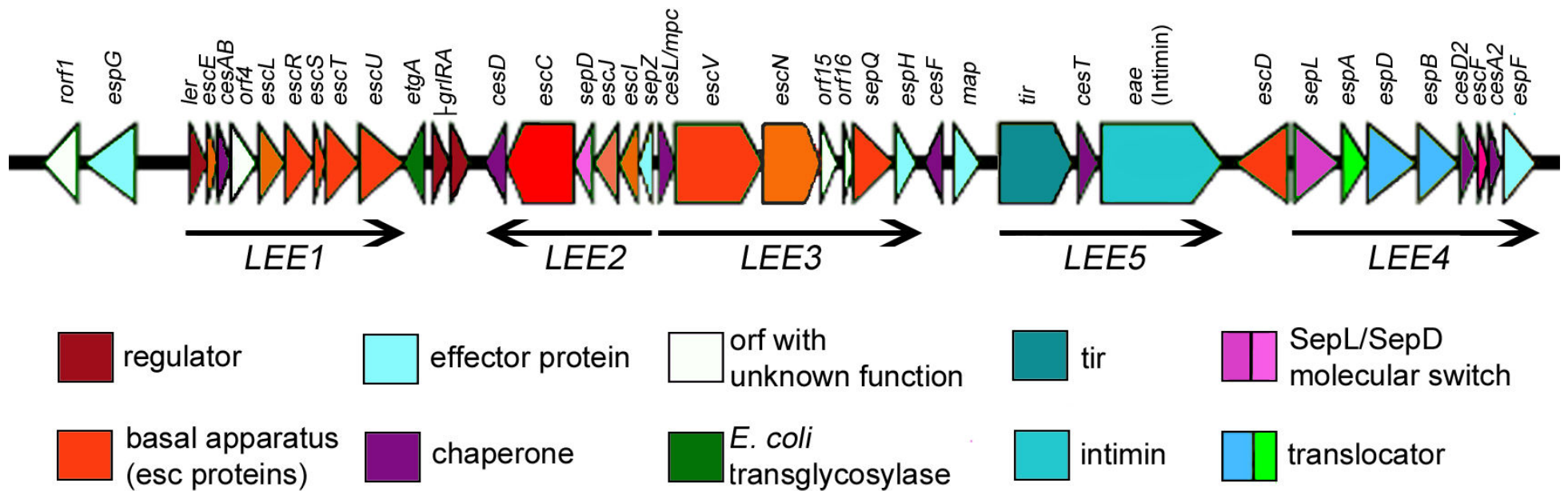
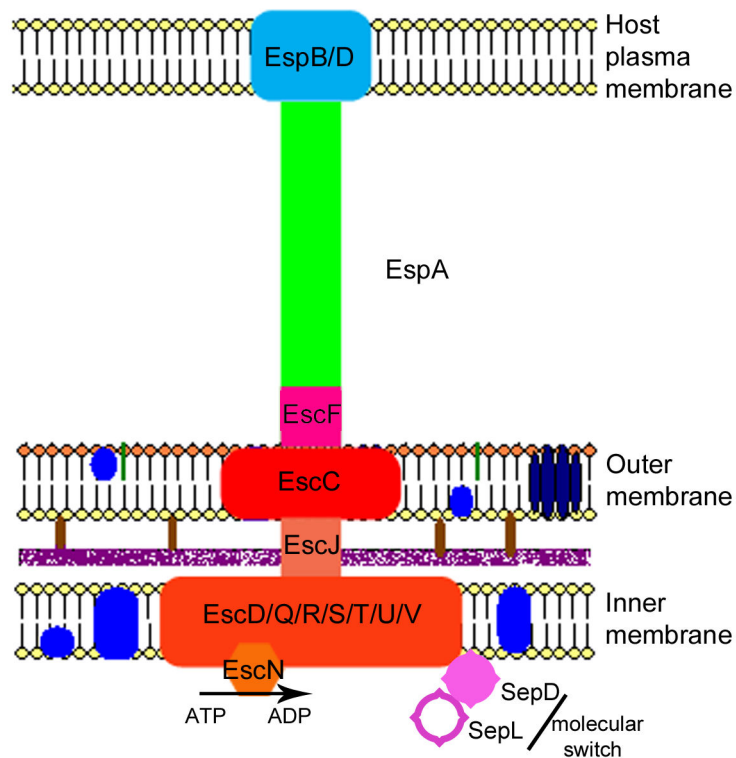


Figure 1-4 Genetic arrangement of EHEC LEE

The image was adapted from coliBASE (<http://www.xbase.ac.uk/genome/escherichia-coli-o157h7-edl933>). Additional annotations from (Garmendia *et al.*, 2005; Pallen *et al.*, 2005; Tsai *et al.*, 2006; Su *et al.*, 2008; Younis *et al.*, 2010; Yu *et al.*, 2010; Biemans-Oldehinkel *et al.*, 2011; Garcia-Gomez *et al.*, 2011).

### 1.2.1.1 T3SS apparatus

The T3SS is constructed from many different proteins, many of which are conserved across bacterial species, and some components also share protein homology with flagellar proteins. The Type III secretion apparatus has been shown to have a common evolutionary origin with the export apparatus for the flagellum (Cornelis, 2006). This is because they both consist of an ATP-dependent basal apparatus spanning the cytoplasmic membrane and a hollow needle-like complex spanning the periplasm and outer membrane. This structure allows the translocation of the proteins which form the filament structure that spans outwith the bacterium and mediates attachment with the host cell. T3SS translocates pore-forming toxins, via this filamentous structure (translocon), that perturb the host membrane for the translocation of T3 effector proteins. The components that make the basal apparatus are secreted by the Sec system. EscV forms the major component of the inner membrane part of the complex, and the protein is conserved in all T3SS. EscJ spans the periplasm, shares sequence similarity with the flagellar protein FliF and is required for the secretion of the distal components of the complex (Crepin *et al.*, 2005). EscC forms the main complex in the outer membrane of the bacterium, and the monomers are secreted via both the Sec and basal apparatus (Gauthier *et al.*, 2003). EscN is the ATPase which provides the system with energy for the secretion of translocators and effectors. EscN can also interact with effector proteins complexed with their chaperone, facilitating translocation (Gauthier & Finlay, 2003).



**Figure 1-5 Model of Type III Secretion Apparatus**

Representation of EHEC T3SS based upon (Pallen *et al.*, 2005; Tree *et al.*, 2009). EscC/D/J/Q-V proteins which make the basal apparatus which spans the bacterial membranes, EscF is the needle complex, EscN provides the energy for secretion/translocation, SepD and SepL form the gate and mediate the switch from secretion of translocon proteins (EspA/D/B), which form the filament extension to mediate attachment and pore formation in the host membrane developing a conduit between the two cell types, to effector protein translocation.

The T3SS apparatus in EPEC and EHEC differs from the *Yersinia* and *Salmonella* T3SS in that it has a filamentous extension from the needle EscF structure to ‘reach’ the host cell (Wilson *et al.*, 2001). This translocon filament is composed of EspA (Ebel *et al.*, 1998; Knutton *et al.*, 1998), with EspB and EspD forming the pore, of 3-5nm diameter, in the host cell membrane (Ide *et al.*, 2001). EspA has functional homology to flagellin, and it has been shown that the EspA filament extends in a similar mechanism to that of the flagella (Delahay *et al.*, 2005). Polymerisation of EspA is dependent on the presence of EspD that is proposed to act as the translocon cap (Kresse *et al.*, 1999; Daniell *et al.*, 2001). Once EspA-mediated cell contact is made, EspD oligomerises in the host cell membrane, and pores are formed in association with EspB. Translocation of effector proteins can then proceed.

### 1.2.1.2 Effector proteins of the LEE

The effectors encoded by the LEE PAI include Tir, Map, EspB, EspF, EspG, EspH, SepZ (EspZ), which have all been characterised over the years, some better than others, and are summarised in Table 1-1. Tir (translocated intimin receptor) mediates intimate attachment of the bacterium to the host cell, by translocating into the host cell, presenting itself on the host cell membrane to bind to the bacterial adhesin intimin (Kenny *et al.*, 1997; DeVinney *et al.*, 1999). Tir is therefore essential for the formation of the A/E lesion, as it also facilitates recruitment of N-WASP, resulting in the polymerisation of actin through Arp2/3 (Goosney *et al.*, 2001). The dynamics of actin polymerisation differs between EPEC and EHEC as it was observed that Tir<sub>EHEC</sub> did not complement a Tir deficient strain of EPEC (Kenny, 1999; Kenny, 2001). The recruitment of N-WASP differs between EPEC and EHEC, as EPEC Tir is tyrosine phosphorylated before recruiting N-WASP via host protein Nck, but EHEC Tir does not require Nck for actin polymerisation (DeVinney *et al.*, 2001; Gruenheid *et al.*, 2001; Kenny, 2001; Campellone *et al.*, 2002). It was hypothesised that for actin polymerisation, EHEC must also translocate an adaptor protein with Tir, and systematic deletion of O-Islands in *E. coli* O157:H7 EDL933 confirmed that this product was on prophage element CP-933U, homologous to EspF and called EspF<sub>U</sub> (Campellone *et al.*, 2004). Functional analysis of this effector *in vitro* by two independent groups demonstrated that it interacts with Tir and binds N-WASP acting as a functional homolog of Nck and was also named TccP (Tir cytoskeleton coupling protein) (Campellone *et al.*, 2004; Garmendia *et al.*, 2004). Recently, the interaction of Tir with EspF<sub>U</sub>/TccP has been shown to be mediated *in vitro* by a host insulin receptor tyrosine kinase substrate p53 (IRKSp53) (Vingadassalom *et al.*, 2009; Weiss *et al.*, 2009). However, actin polymerisation can occur in a mechanism independent of TccP *in vivo* as demonstrated using a bovine ligated ileal loop model of infection (Vlisidou *et al.*, 2006a). This study also shows that pedestal formation is not necessary for *E. coli* O157:H7 persistence in bovine and ovine models of infection. The polymerisation of actin at the base of bacterial attachment was exploited by (Knutton *et al.*, 1989) to develop a new method of lesion detection, other than through electron microscopy (EM), called Fluorescent actin staining (known as the 'FAS test'), whereby fluorescein-isothiocyanate (FITC) or rhodamine (TRITC) labelled phalloidin, a phallotoxin

that can specifically bind polymerised actin, labels this area underneath the attached bacteria. This technique has since been widely applied to test EHEC mutants to determine which genes affect intimate bacterial attachment and A/E lesion formation.

**Table 1-1 Effector proteins encoded on the LEE PAI**

Effector	Location	Role in pathogenesis
Tir (translocated intimin receptor)	LEE5	<p>Inserts into the host cell membrane and mediates intimate attachment with intimin (Kenny <i>et al.</i>, 1997; DeVinney <i>et al.</i>, 1999).</p> <p>Recruits N-WASP and Arp2/3 causing cytoskeletal rearrangement resulting in pedestal formation (Goosney <i>et al.</i>, 2001).</p> <p>Represses filopodia formation (Kenny <i>et al.</i>, 2002)</p> <p>Controls epithelium damage caused by EspG-mediated calpain activation (Dean <i>et al.</i>, 2010a)</p>
Map (mitochondrion associated protein)	LEE	<p>Localises to the mitochondria in the host cell (Kenny &amp; Jepson, 2000).</p> <p>Mediates filopodia formation at site of infection by activating Cdc42 GTPase (Kenny <i>et al.</i>, 2002)</p> <p>Disrupts host tight junctions and intestinal barrier, dependent upon the presence of intimin (Dean &amp; Kenny, 2004)</p> <p>Binds Na<sup>+</sup>/H<sup>+</sup> exchanger regulatory factor 2 (NHERF2) (Martinez <i>et al.</i>, 2010)</p>
EspB	LEE4	<p>Expression in host cells <i>in vitro</i> redistributes actin filaments resulting in a reduction of actin stress fibres observed (Taylor <i>et al.</i>, 1999)</p> <p>Directly interacts with <math>\alpha</math>-catenin, contributing to A/E lesion formation (Kodama <i>et al.</i>, 2002)</p> <p>Increases <math>\alpha</math>-catenin affinity for binding actin filaments to form bundles and inhibit Arp2/3 mediated actin polymerisation <i>in vitro</i> (Hamaguchi <i>et al.</i>, 2008)</p>
EspF	LEE4	<p>Is associated with reduction in transepithelial resistance and redistribution of tight junction proteins disrupting host intestinal barrier (McNamara <i>et al.</i>, 2001; Elliott <i>et al.</i>, 2002; Dean &amp; Kenny, 2004; Viswanathan <i>et al.</i>, 2004; Dean <i>et al.</i>, 2006; Guttman <i>et al.</i>, 2006; Peralta-Ramirez <i>et al.</i>, 2008)</p>

EspF (continued)		<p>Localises to the mitochondrion (Marches <i>et al.</i>, 2006)</p> <p>Inhibits phagocytosis of EPEC (Quitard <i>et al.</i>, 2006) and EHEC (Marches <i>et al.</i>, 2008)</p> <p>Modulates the host cytoskeleton (Marches <i>et al.</i>, 2006; Alto <i>et al.</i>, 2007; Peralta-Ramirez <i>et al.</i>, 2008)</p> <p>Targets the nucleolus once the mitochondrial membrane potential is reduced, redistributing nucleolin into the cytoplasm (Dean <i>et al.</i>, 2010b).</p> <p>Reviewed in (Holmes <i>et al.</i>, 2010)</p>
EspG/EspG2	LEE	<p>Mutant in <i>C. rodentium</i> displays reduced colonisation and unable to cause colonic hyperplasia (Hardwidge <i>et al.</i>, 2005)</p> <p>Binds to tubulin destabilising the microtubule networks, triggering the activation of GEF-H1 and induces the formation of actin stress fibres (Matsuzawa <i>et al.</i>, 2004; Hardwidge <i>et al.</i>, 2005; Matsuzawa <i>et al.</i>, 2005; Shaw <i>et al.</i>, 2005; Tomson <i>et al.</i>, 2005)</p> <p>Activates host cysteine protease calpain resulting in the destruction of the epithelium <i>in vitro</i> (Dean <i>et al.</i>, 2010a)</p>
EspH	LEE3	<p>Represses filopodia formation and promotes pedestal formation in a mechanism independent from Tir (Tu <i>et al.</i>, 2003)</p> <p>Mutant is attenuated in rabbit model of infection and reduced colonisation of GI tract (Ritchie &amp; Waldor, 2005)</p> <p>Binds Rho guanine exchange factors (RhoGEF) preventing Rho activation and disrupting the actin cytoskeleton. Also plays a role in inhibiting phagocytosis of EPEC <i>in vitro</i> (Dong <i>et al.</i>, 2010).</p>
SepZ (EspZ)	LEE2	<p>Binds CD98 counteracting cytopathic effect and facilitates host cell survival (Shames <i>et al.</i>, 2010)</p>

In summary, the effectors encoded on the LEE (Table 1-1) are required for bacterial intimate attachment, the formation of the A/E lesion and disrupting the intestinal barrier by modulating the host cytoskeleton and inhibits phagocytosis. The effectors can work in concert to mediate the multiple effects they exert upon the host cell.

### **1.2.2 Regulation of the LEE**

Horizontally acquired genetic elements require appropriate regulation of expression which can be managed by both endogenous and exogenous elements. LEE expression is extremely complex, influenced by a number of environmental signals and regulated by an interplay of LEE-encoded, global and other horizontally-acquired regulators.

The LEE encodes 3 regulatory elements; LEE-encoded regulator (Ler), Global Regulator of the LEE Activator (GlrA) and Glr repressor (GlrR). Ler is the first open reading frame of LEE1 (*orf1*) and belongs to the H-NS family of nucleoid-associated proteins which positively regulates transcription of both LEE and non-LEE genes (Elliott *et al.*, 2000; Haack *et al.*, 2003; Roe *et al.*, 2007). Ler activates gene transcription by counteracting the effects of global regulator H-NS (Bustamante *et al.*, 2001) which silences transcription of genes by binding to curved AT-rich regions (Dorman & Deighan, 2003). H-NS has been shown to repress the LEE, with LEE1 repression being dependent upon temperature in EPEC (Umanski *et al.*, 2002). In EHEC, H-NS represses *ler* and *LEE4* transcription (Beltrametti *et al.*, 1999; Laaberki *et al.*, 2006). Osmolarity can reduce the repression of gene transcription by H-NS owing to the change in DNA topology in these conditions (Dorman & Deighan, 2003), and it has been shown that the LEE PAI in EHEC is upregulated in conditions with high osmolarity (Sperandio *et al.*, 1999). GlrA and GlrR are encoded between LEE1 and LEE2, and were identified through analysis of a systematic deletion of each gene in the LEE of *C. rodentium* (Deng *et al.*, 2004). The genes are co-transcribed and their expression is dependent upon Ler (Deng *et al.*, 2004; Laaberki *et al.*, 2006). Expression of GlrA in turn positively regulates expression of Ler through

interacting with the LEE1 promoter (Laaberki *et al.*, 2006; Huang & Syu, 2008) forming a positive feedback loop (Barba *et al.*, 2005). GrlR binds GrlA (Barba *et al.*, 2005; Jobichen *et al.*, 2007; Huang & Syu, 2008) and this interaction is proposed to act as a check-point to downregulate the feedback loop. GrlA can also co-ordinate enterohaemolysin expression with the LEE (Saitoh *et al.*, 2008) and negatively regulates expression of the flagella (Iyoda *et al.*, 2006), ultimately facilitating intimate attachment of the bacterium to the host cells. This is controlled through the degradation of GrlR by ClpX protease (Iyoda & Watanabe, 2005), releasing GrlA and thereby reducing transcription of flagella genes, as overexpression of the flagella has been shown to have an overall negative effect on attachment (Iyoda *et al.*, 2006), and increasing transcription of the LEE. Hfq is a RNA chaperone which post-transcriptionally regulates Ler expression during stationary phase of growth, and GrlRA expression during the exponential phase (Hansen & Kaper, 2009; Shakhnovich *et al.*, 2009).

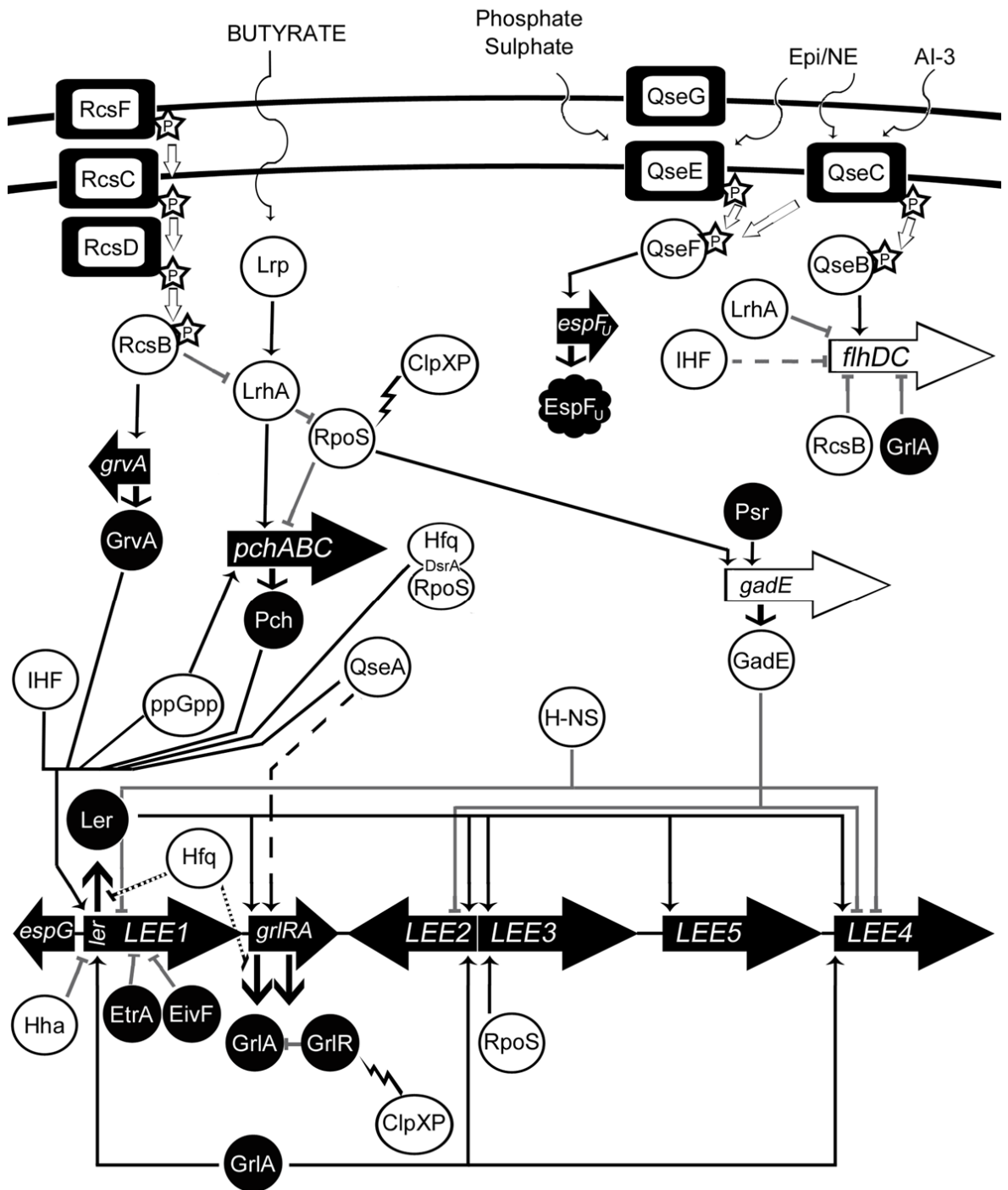


**Figure 1-6 Schematic diagram of LEE regulation in EHEC O157:H7**

The figure is adapted from (Mellies *et al.*, 2007). Thin black arrows represent positive regulatory signals, grey blunt arrows represent negative regulatory signals. Solid black arrows represent expression of protein from gene. Dashed arrows indicate an indirect effect on regulation of gene expression. Dotted line represents an effect on mRNA stability, seen with Hfq. Jagged line represents protein degradation by ClpXP protease. Star-P represents phosphorylation, and white arrows represent phosphate transfer. Horizontally acquired elements have a black background and elements endogenous to *E. coli* have a white background. See text for detailed explanation.

Quorum sensing regulates the LEE in EHEC through responding to environmental signals such as temperature, osmolarity and pH through signalling molecules (Sperandio *et al.*, 1999). These signalling molecules are hormone-like molecules

called autoinducers. AI-2 was the first quorum sensing molecule identified in *E. coli* due to its homology to lux genes in *Vibrio fischeri*, and *luxS* gene is required for its production in *E. coli*. Another autoinducer, AI-3, is part of an interkingdom communication system which enables cross-talk with epinephrine (Epi) and norepinephrine (NE) from mammals with bacteria. This cross-talk has been shown to be mediated through a histidine kinase QseC, which autophosphorylates upon sensing these hormone signals (Clarke *et al.*, 2006) and transfers this phosphate to its response regulator QseB. The transcription factor activated in this cascade is QseA which has been shown to directly interact with the distal promoter of *ler* (Sharp & Sperandio, 2007; Kendall *et al.*, 2010), thereby directly activating its expression, and through the action of Ler, indirectly activating expression of the LEE PAI (Sperandio *et al.*, 2002a). QseA can also activate *grlRA* transcription in a Ler-independent manner (Russell *et al.*, 2007). QseBC has also been shown to positively regulate motility through transcriptional regulation of the flagella regulator genes *flhDC* (Sperandio *et al.*, 2002b; Clarke & Sperandio, 2005b). An additional quorum sensing two-component system QseEF was identified in a microarray study comparing differential gene expression in EHEC and an isogenic *luxS* mutant (Sperandio *et al.*, 2001) and characterised (Reading *et al.*, 2007). This two-component system responds to phosphate, sulphate and Epi/NE, and is transcribed in an operon with an outer membrane protein QseG (Reading *et al.*, 2009). QseEF does not regulate LEE expression, like that of QseBC, but regulates the transcription of T3SS effector *espFu/TccP* (Reading *et al.*, 2007). The transcription of *espFu* is dependent upon the presence of QseF, but not QseE as QseF can be activated by other sensor kinases, such as QseC (Reading *et al.*, 2007). As mentioned previously, *EspFu/TccP* is required by EHEC Tir to form A/E lesions, therefore QseEF can regulate the expression of this effector in co-ordination with the LEE, and it has been demonstrated that Tir cannot be translocated without the presence of QseG *in vitro* (Reading *et al.*, 2009).

Other global regulators which regulate the LEE include stringent response signalling molecule ppGpp (Nakanishi *et al.*, 2006), stress sigma factor *rpoS* (Sperandio *et al.*, 1999; Iyoda & Watanabe, 2005; Laaberki *et al.*, 2006), RNA chaperone Hfq (Hansen & Kaper, 2009; Shakhnovich *et al.*, 2009), integrated host factor (IHF) (Friedberg *et al.*, 1999), and Hha (Sharma & Zuerner, 2004).

The stringent response molecule ppGpp accumulates in nutrient-starved cells, which mediates transcription of genes by binding RNA-polymerase in coordination with DksA, and together positively regulate the transcription of *ler* and *pch* (Nakanishi *et al.*, 2006). RpoS sigma factor, which is involved in gene regulation during stationary phase (Lange & Hengge-Aronis, 1991), directly activates LEE3 transcription (Sperandio *et al.*, 1999) and differentially controls *ler* transcription (Laaberki *et al.*, 2006; Dong & Schellhorn, 2009). Hfq is an RNA chaperone which in concert with small non-coding RNA (sRNA) binds mRNA, controlling translation and mRNA stability. Hfq has been shown to negatively regulate *ler* transcription and translation (Shakhnovich *et al.*, 2009) and *grlRA* mRNA stability during the exponential phase of growth, indirectly controlling LEE expression (Hansen & Kaper, 2009). Hfq is a global regulator, as it is involved in regulating the translation of RpoS and H-NS with sRNA DsrA. This regulation of RpoS translation by DsrA has been shown to promote the transcription of *ler* (Laaberki *et al.*, 2006), and *dsrA* transcription is positively regulated by QseA (Kendall *et al.*, 2010). IHF directly activates *ler* transcription demonstrated by gel motility shift assays and Dnasel footprinting (Friedberg *et al.*, 1999). IHF has also been shown to negatively regulate transcription of the flagella regulator genes *flhDC* indirectly via an un-identified EHEC specific factor (Yona-Nadler *et al.*, 2003). Hha was identified by transposon mutant screening of an EHEC O157:H7 strain expressing *esp::lacZ*, and purified Hha protein was shown to directly bind and negatively regulate *ler* transcription (Sharma & Zuerner, 2004).

Horizontally acquired elements which regulate the LEE include PerC (plasmid encoded regulator) in EPEC or PerC-like homologues (Pch) in EHEC, of which there are seven PchA-E, PchX and PchY. PchABC have been shown to globally positively effect transcription of LEE, via *ler*, and non-LEE encoded genes (Iyoda & Watanabe, 2004; Porter *et al.*, 2005; Abe *et al.*, 2008). Transcription of *pch* is negatively regulated by RpoS (Iyoda & Watanabe, 2005). GrvA (global regulator for virulence A) is an EHEC specific regulator of LEE1, and therefore *ler* (Tobe *et al.*, 2005). Pch and GrvA are transcriptionally regulated by the same His-Arp phosphorelay system RcsDCB, negatively and positively respectively (Tobe *et al.*, 2005). The authors propose that the RcsDCB system positively regulates the transcription of *grvA* directly. The negative regulation of *pch* by RcsB has been proposed to be an indirect effect as it was growth medium dependent,

indicating RcsB represses *pch* expression by the repression of another gene (Tobe *et al.*, 2005). The probable candidate for RcsB-dependent *pch* repression is LrhA (LysR-homologue A), which is a direct positive regulator of *pchABC* transcription in EHEC (Honda *et al.*, 2009) and RcsB represses *lrhA* transcription in *E. coli* K-12 (Peterson *et al.*, 2006). It has recently been demonstrated through microarray analysis of differential gene expression in EHEC and isogenic single mutants in  $\Delta qseE/F/G$ , that the QseEF two component system represses *rscB* transcription (Reading *et al.*, 2010), thereby contributing to the co-ordination of LEE expression with the effectors it secretes, such as EspF<sub>U</sub>/TccP. Expression of *pch* is also positively affected by butyrate concentrations in the extracellular media, which is sensed by Lrp (leucine-responsive regulatory protein) (Nakanishi *et al.*, 2009). The influence of Lrp on *pch* is also indirect, as chromatin-immunoprecipitation and sequence analysis did not reveal direct Lrp binding. The effect of Lrp on *pch* transcription is possibly mediated via Lrp positive regulation of *lrhA* transcription, which has been shown in *E. coli* K-12 (Cho *et al.*, 2008). LrhA is also involved in the negative regulation of the flagellar genes in K-12 strains (Lehnen *et al.*, 2002) and in O157 strains, independent from grlA (Honda *et al.*, 2009) and RcsB also negatively regulates flagellar gene expression directly in K-12 (Francez-Charlot *et al.*, 2003).

Other EHEC specific regulators of the LEE are the regulators *etrA* and *eivF* which are encoded alongside a second, non-functional, T3SS (ETT2). These regulators negatively regulate the LEE, demonstrated through microarray analysis of  $\Delta etrA$  and  $\Delta eivF$  compared to wildtype and reduced protein secretion when introduced episomally in a high secretor EHEC strain (Zhang *et al.*, 2004). Prophage-encoded secretion regulator (Psr) genes were identified through a systematic analysis of the level of T3S dependent secreted proteins from TUV93-0 O-Island mutants, and found to indirectly repress LEE expression (Tree *et al.*, 2011). This study demonstrates that PsrA positively regulates the GAD acid stress response by inducing transcription of *gadE*, particularly after adhering to host cells. GadE is a member of the LuxR regulator family which represses the LEE by interacting with the promoter regions of LEE1 and LEE2/3 (Tatsuno *et al.*, 2003; Tree *et al.*, 2011). GadE is also positively regulated by RpoS (Dong & Schellhorn, 2009) and negatively regulated by *pch* (Abe *et al.*, 2008).

Overall, regulation of LEE expression is complex, as expression is controlled by LEE-encoded regulators (Ler and GrlRA), global endogenous regulators (H-NS and IHF), and other horizontally acquired regulators (Pch). The regulation of LEE has integrated into the complex endogenous regulatory network including quorum-sensing (QseABCDEFG), phosphorelay systems (RcsBCD) and metabolite activated factors (Lrp). This demonstrates the strict control of LEE expression so that it is only expressed at the optimum moment cued by environmental signals such as bicarbonate ions (Abe *et al.*, 2002), when flagellar expression is repressed, and in co-ordination with the effectors that is translocated by the T3SS.

### **1.2.3 Non-LEE encoded effector proteins**

#### **1.2.3.1 Overview**

It was soon discovered that the T3SS apparatus not only translocated proteins encoded within the LEE but also others encoded elsewhere in the genome. As described previously, EspF<sub>U</sub>/TccP is encoded on CP-933U, and is required for Tir dependent actin polymerisation and pedestal formation by acting as an Nck mimic (Campellone *et al.*, 2004; Garmendia *et al.*, 2004). Cycle inhibiting factor (Cif) was identified through a transposon mutant of EPEC strain E22 screen for the inhibition of the cytopathic effect, identified by focal adhesion plaques, in FAS-test positive cells (Marches *et al.*, 2003). EspI/NleA was identified from two independent approaches; signature-tagged mutagenesis of *C. rodentium* (Mundy *et al.*, 2004) and proteomic analysis of culture supernatants from EHEC and a T3SS deficient mutant (Gruenheid *et al.*, 2004).

Studies in *C. rodentium*, an A/E bacterial pathogen of mice, thus routinely used as small animal *in vivo* model of A/E infections, shown that SepL and SepD acts as a switch controlling the secretion of translocators (EspA, B, D) and effectors (e.g. Map, EspH) (Deng *et al.*, 2004). When tested in EHEC and EPEC, SepL and SepD deletion mutants were shown to hypersecrete effector proteins, but cease to secrete translocators (Deng *et al.*, 2005). Studies of these ‘hypersecretor’ mutants lead to the discovery of additional proteins, or putative effectors, translocated through the T3SS apparatus which were not encoded on the LEE.

These 7 proteins were named Non-LEE encoded effectors (Nle): NleA, NleB, NleC, NleD, NleE, NleF, and NleG. This led to the speculation that ‘the repertoire of *E. coli* effector genes might be much larger than (currently) recognised’ and this hypothesis was tested using a systematic bioinformatics and proteomics approach (Tobe *et al.*, 2006), identifying a total of 39 putative effectors, classed into 20 families. Since the publication of this study, research into determining the function of these non-LEE encoded effector, and how they contribute to EHEC, and EPEC, pathogenicity has increased and ongoing. The function(s), and/or contribution to pathogenesis, of non-LEE encoded effectors are summarised in Table 1-2. It can be seen that many of these non-LEE encoded effectors contribute towards colonisation *in vivo* but only EspF<sub>U</sub>/TccP is required for the formation of A/E lesions *in vitro*.

**Table 1-2 Characterised non-LEE encoded T3S effectors (O Island designation is according to the systematic nomenclature design in (Perna *et al.*, 2001)**

Effector	Location	Function(s)
TccP/EspF <sub>U</sub>	OI-79	Interacts with Tir via IRKSp53 and binds N-WASP for actin polymerisation via Arp2/3 for pedestal formation (Campellone <i>et al.</i> , 2004; Garmendia <i>et al.</i> , 2004; Vingadassalom <i>et al.</i> , 2009; Weiss <i>et al.</i> , 2009).
Cif (cycle inhibiting factor)	OI-71	A cyclomodulin which inhibits mitosis, recruits focal adhesion plaques and induces stress fibres (Marches <i>et al.</i> , 2003; Charpentier & Oswald, 2004; Nougayrede <i>et al.</i> , 2005; Taieb <i>et al.</i> , 2006)  Inhibits cell cycle transition by blocking the proteosomal degradation of cyclin-dependent kinase inhibitors (Samba-Louaka <i>et al.</i> , 2008) by binding NEDD8 blocking E3 ubiquitin ligase function (Cui <i>et al.</i> , 2010; Jubelin <i>et al.</i> , 2010; Morikawa <i>et al.</i> , 2010). Induces apoptosis (Samba-Louaka <i>et al.</i> , 2009)
NleA (EspI)	OI-71	Required for full virulence in <i>C. rodentium</i> mouse infection and EHEC gnotobiotic pig model of infection (Gruenheid <i>et al.</i> , 2004; Mundy <i>et al.</i> , 2004).  Localises to the Golgi apparatus (Gruenheid <i>et al.</i> , 2004; Creuzburg <i>et al.</i> , 2005).  Interferes with protein trafficking and secretion in mammalian cells through binding with Sec24, part of the COPII complex (Kim <i>et al.</i> , 2007).

		<p>Has a PDZ binding domain which is necessary for binding to Sec24 and NHERF (Lee <i>et al.</i>, 2008; Martinez <i>et al.</i>, 2010).</p> <p>Involved in disrupting intestinal tight junctions in concert with EspF and Map (Thanabalasuriar <i>et al.</i>, 2010).</p>
EspJ	OI-79	<p><i>E. coli</i> O157:H7Δ<i>espJ</i> persists longer than wild-type in animal models of infection (Dahan <i>et al.</i>, 2005).</p> <p>Inhibits opsono-phagocytosis (Marches <i>et al.</i>, 2008).</p> <p>Localises to the mitochondrion (Kurushima <i>et al.</i>, 2010).</p>
EspK	OI-50	<p>Localises to host cytosol. EspK deficient EHEC is less persistent than WT in colonising calves, but no effect seen in mouse model with <i>C. rodentium</i> (Vlisidou <i>et al.</i>, 2006b)</p>
EspM (M1 and M2)	OI-71 (1) OI-108 (2)	<p>Modulates actin dynamics through RhoA activation forming stress fibres and regulates actin pedestal formation (Arbeloa <i>et al.</i>, 2008; Arbeloa <i>et al.</i>, 2010; Simovitch <i>et al.</i>, 2010)</p>
EspV	(Pseudogene present in Sp4 in EHEC Sakai strain).	<p>EPEC homolog identified in 10% EHEC strains by PCR. Locations in EHEC are not characterised. When ectopically expressed in mammalian and yeast cells it induces morphological changes (Arbeloa <i>et al.</i>, 2011)</p>
NleB	OI-122	<p>Essential for <i>C. rodentium</i> colonisation and development of colonic hyperplasia (Kelly <i>et al.</i>, 2006)</p> <p>Inhibits IL-1<math>\beta</math> stimulated NF-<math>\kappa</math>B activation (Nadler <i>et al.</i>, 2010; Newton <i>et al.</i>, 2010)</p>
NleC	OI-36	<p>Does not contribute to <i>E. coli</i> O157:H7 virulence or colonisation in animal models (Marches <i>et al.</i>, 2005).</p> <p>Is a zinc metalloprotease which cleaves p65 (Yen <i>et al.</i>, 2010; Baruch <i>et al.</i>, 2011; Muhlen <i>et al.</i>, 2011; Pearson <i>et al.</i>, 2011) and p300 (Shames <i>et al.</i>, 2011), thereby inhibiting transcription of NF-<math>\kappa</math>B dependent genes, modulating the host immune response.</p> <p>Inhibits p38 MAPK activation (Sham <i>et al.</i>, 2011)</p>

		Mutant in <i>C. rodentium</i> leads to greater pathology <i>in vivo</i> and greater chemokine induction in cecal loop model of infection (Sham <i>et al.</i> , 2011)
NleD	OI-36	Does not contribute to <i>E. coli</i> O157:H7 virulence or colonisation in animal models (Marches <i>et al.</i> , 2005)  Is a zinc metalloprotease which cleaves the JNK serine/threonine protein kinase, modulating the host immune response (Baruch <i>et al.</i> , 2011)
NleE	OI-122	Mutant in <i>C. rodentium</i> is attenuated in mouse model of infection and colonisation (Wickham <i>et al.</i> , 2007)  Modulates NF- $\kappa$ B activation by inhibiting phosphorylation of IKK by an unknown mechanism (Nadler <i>et al.</i> , 2010; Newton <i>et al.</i> , 2010)  Inhibits IL-1 $\beta$ stimulation of NF- $\kappa$ B activation in dendritic cells (Vossenkamper <i>et al.</i> , 2010)
NleF	OI-71	Localises to cytosol of host cell and plays a role in colonisation (Echtenkamp <i>et al.</i> , 2008). No host protein interactions have been characterised.
NleG	OI-71, OI-57, CP-933R, OI-108	E3 ubiquitin ligase activity (alleles G2-3, G5-1, G6-2 and G9') (Wu <i>et al.</i> , 2010)
NleH (H1 and H2)	OI-36 (1), OI-71 (2)	Section 1.2.3.2
NleI	OI-57 OI-71 CP-933R OI-58	EPEC NleI localises to host cytosol and membranes and translocation is dependent upon CstT (Li <i>et al.</i> , 2006). Only 1 allele in EPEC; four in EHEC and CR. No host protein interactions have been characterised.
NleL (EspX7)	OI-50	E3 ubiquitin ligase activity which specifically regulates pedestal formation (Piscatelli <i>et al.</i> , 2011); not present in EPEC.

### 1.2.3.2 Non-LEE encoded effector H

NleH1 and NleH2 were identified in the aforementioned bioinformatic and proteomic screen as putative T3SS effector proteins and BLAST analysis revealed that they are homologs of a characterised *Shigella flexneri* T3S effector (Tobe *et al.*, 2006). With this preliminary data, NleH became an interesting candidate for further research into its role in A/E pathogenesis.

*Citrobacter rodentium* was found to contain only one NleH gene, which shares the same gene organization as to that of NleH1 in EHEC and EPEC but a higher predicted protein identity with NleH2 (Garcia-Angulo *et al.*, 2008). The same study of *C. rodentium* NleH (CRNleH) show that secretion and translocation into an intestinal cell line *in vitro* required a functional T3SS, and that it is post-transcriptionally regulated in coordination with the LEE.

NleH may be required during the early stages of infection, as a CRNleH knockout has a reduced ability to colonise the mouse (Garcia-Angulo *et al.*, 2008) and is outcompeted by wild-type *C. rodentium* in a mixed infection (Hemrajani *et al.*, 2008). Similar results were found with an EHEC O157 $\Delta$ nleH1nleH2 double mutant in the bovine and ovine models of infection, where the mutant was shed in greater numbers than, or outcompeted by, the wild-type strain in the respective models (Hemrajani *et al.*, 2008).

NleH share protein homology with OspG, an effector protein of *Shigella flexneri*. Using a yeast two hybrid screen, OspG was found to interact with E2 ubiquitin-conjugating enzymes, thereby inhibiting NF- $\kappa$ B activation and interfering with the host innate immune response (Kim *et al.*, 2005). The effects of NleH on NF- $\kappa$ B activation with regards to A/E infections have been investigated, and its effects appear to depend on the A/E pathogen studied. CRNleH has been shown to activate NF- $\kappa$ B *in vivo* (Hemrajani *et al.*, 2008); EHEC NleH1 represses, and NleH2 activates, NF- $\kappa$ B dependent promoters *in vitro* (Gao *et al.*, 2009). Conflicting reports arise for EPEC NleH, where it does not affect NF- $\kappa$ B signalling (Ruchaud-Sparagano *et al.*, 2007) or both alleles attenuate its activation *in vitro* (Royan *et al.*, 2010). Through three independent co-immunoprecipitation assays, NleH has been shown to interact with ribosomal protein subunit-3 (RPS3) (Gao *et al.*, 2009) modulating the activation of NF- $\kappa$ B; Bax inhibitor-1 (BI-1) (Hemrajani *et al.*, 2010) interfering with host cell apoptosis pathways; and NHERF2 (NleH1 only) (Martinez *et al.*, 2010). NleH appears to be a multifunctional effector protein, which is not an uncommon trait for these proteins; as described previously, EspF is able to elicit various responses in the host, reviewed in (Holmes *et al.*, 2010).

### **1.2.3.3 Modulation of NF- $\kappa$ B activation by bacterial T3S effector proteins**

NF- $\kappa$ B is a transcription factor which can be made up of a homodimer or heterodimer of Rel proteins; p65 (RelA), RelB, c-Rel, p50 and p52. Under resting conditions, free NF- $\kappa$ B is sequestered by I $\kappa$ B (inhibitors of NF- $\kappa$ B), which under stimulating conditions is phosphorylated by IKK and subsequently ubiquitinated for degradation by the proteasome, thereby releasing NF- $\kappa$ B enabling it to travel from the cytoplasm into the nucleus (Winston *et al.*, 1999). When in the nucleus, it can bind to its promoters, known as  $\kappa$ B sites, and activate transcription of many genes involved in cellular processes, including the immune response. The canonical NF- $\kappa$ B pathway is stimulated by a number of receptors such as TNF receptor, IL-1 receptor, TLR and T-cell receptor but all cascades converge at IKK-mediated phosphorylation of I $\kappa$ B (Chen & Greene, 2004; Hayden & Ghosh, 2004). Bacterial T3S effector proteins have evolved many different strategies to alter the transcription of NF- $\kappa$ B dependent genes, modulating the hosts' responses to bacterial infection.

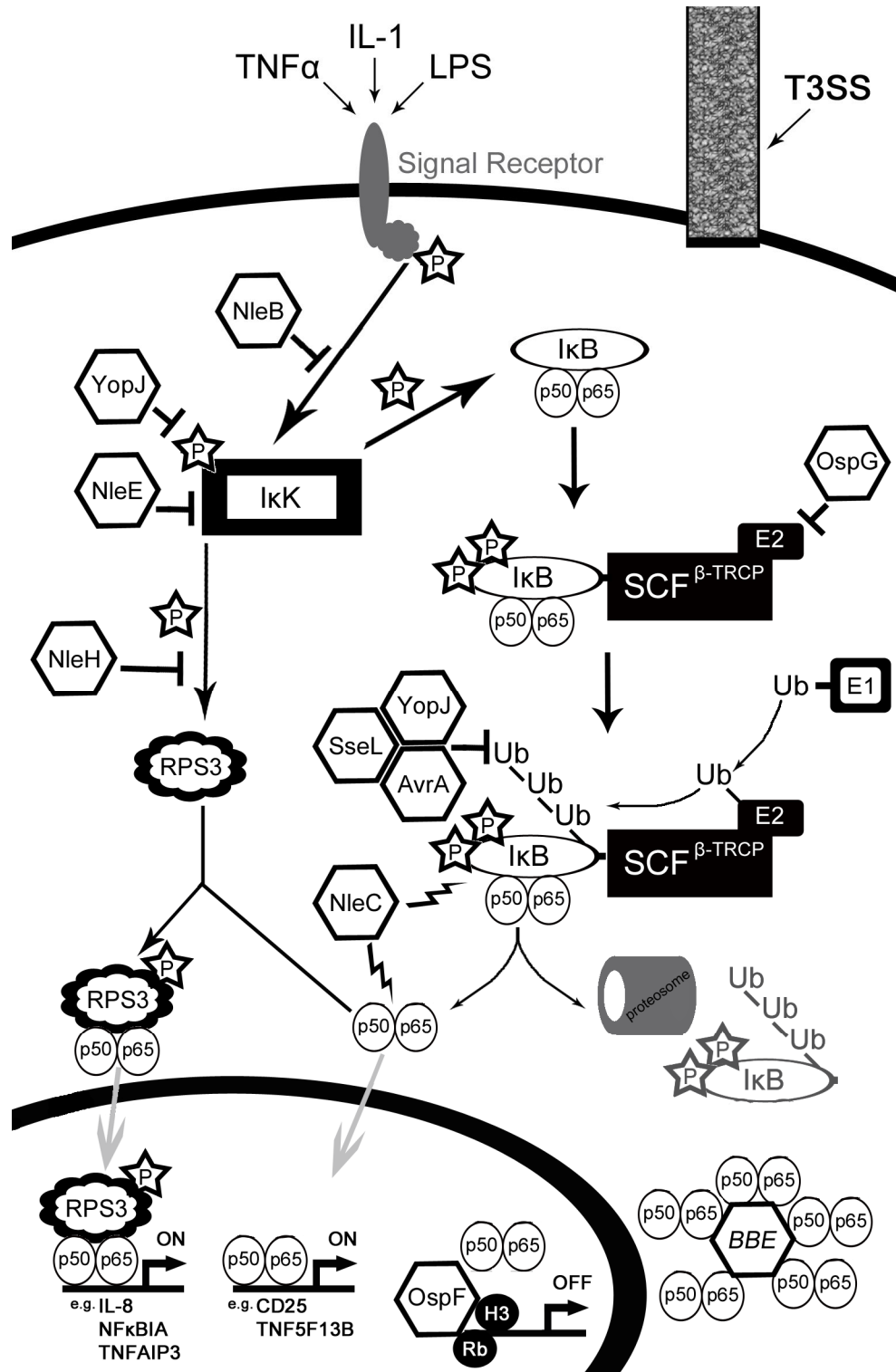


**Figure 1-7 T3 effector modulation of the canonical NF-κB activation pathway**  
Hexagons represent T3S effector proteins; note *B. bronchiseptica* T3 effector (BBE) has not been identified or characterised fully. Blunt arrows indicate inhibition of the pathway, details of which are in the text. Jagged arrows indicates degradation.

NleC is a metalloprotease which cleaves p65 demonstrated by *in vitro* infections of HeLa cells with various EPEC strains and analysing cell lysates for p65 degradation by western blotting (Yen *et al.*, 2010; Baruch *et al.*, 2011; Pearson

*et al.*, 2011) and by an *in vitro* digestion assay with recombinant NleC, which is dependent upon a functional protease domain HExxH (Yen *et al.*, 2010; Baruch *et al.*, 2011). Additional work from Prof Brendan Kenny's group demonstrate using transfection assays that NleC can also degrade p50 and I $\kappa$ B in a proteasome-independent manner (Muhlen *et al.*, 2011). Host acetyltransferase p300 was identified as a substrate of NleC by stable isotope labelling of amino acids in cell culture (SILAC) (Shames *et al.*, 2011). This interaction was confirmed by co-immunoprecipitation, and *in vitro* protease assay confirmed NleC mediated degradation of p300. p300 is necessary for the expression of IL-8 and p65 is acetylated by p300 (Shames *et al.*, 2011).

NleE inhibits phosphorylation of IKK $\beta$  and its activity is enhanced by NleB (Nadler *et al.*, 2010). *In vitro* assay tested IKK $\beta$  and I $\kappa$ B phosphorylation by extracting proteins from cells infected with EPEC strains, WT,  $\Delta$ *nleE*, and  $\Delta$ *escV* then adding TNF $\alpha$ /IL-1 $\beta$  to stimulate phosphorylation. Western blotting analysis showed that TNF $\alpha$  and IL-1 $\beta$  stimulated phosphorylation of IKK $\beta$  in uninfected cells and cells infected with EPEC $\Delta$ *escV* and  $\Delta$ *nleE* but not EPEC WT. Complementing the  $\Delta$ *nleE* mutant with a plasmid expressing NleE only partially restored the inhibition of IKK $\beta$  phosphorylation. NleB is proposed to enhance the activity of NleE as an *nleBE* double mutant inhibited I $\kappa$ B degradation greater than the *nleE* single mutant. NleE inhibition of IL-1 $\beta$  stimulated NF- $\kappa$ B activation has also been demonstrated by EPEC infection of dendritic cells (Vossenkamper *et al.*, 2010). The inhibition of I $\kappa$ B degradation and nuclear translocation of p65 by NleE and NleB was supported by work from Prof Elizabeth Hartland's group (Newton *et al.*, 2010). The authors demonstrate through a transfection assay that NleB inhibits TNF $\alpha$  stimulated NF- $\kappa$ B activation to similar levels as NleE, but does not have an effect on the IL-1 $\beta$  stimulated pathway. Therefore, the authors propose that NleB acts upstream of NleE in the NF- $\kappa$ B activation pathway. NleH EHEC inhibits IKK $\beta$  mediated phosphorylation of RPS3, inhibiting its translocation from the cytoplasm into the nucleus, inhibiting transcription of RPS3-dependent NF- $\kappa$ B genes (Gao *et al.*, 2009; Wan *et al.*, 2011).

Using yeast-two hybrid analysis OspG was shown to interact with ubiquitinated E2 enzymes, and this interaction was confirmed by co-IP and *in vitro* binding assays (Kim *et al.*, 2005). This results in OspG inhibiting proteosomal degradation of phosphorylated I $\kappa$ B and subsequently inhibits NF- $\kappa$ B activation,

which is dependent upon the inherent kinase activity of OspG (Kim *et al.*, 2005). OspF from *Shigella* affects NF- $\kappa$ B recruitment at subset of genes through dephosphorylation of MAP kinase preventing subsequent phosphorylation of Histone 3 thereby modulating chromatin structure (Arbibe *et al.*, 2007). OspF interacts with retinoblastoma protein (Rb), which recruits other factors which post-translationally modify histones, thereby controlling chromatin remodelling and gene transcription, specifically repressing IL-8 secretion (Zurawski *et al.*, 2009).

YopJ from *Yersinia* has deubiquitinase activity (Orth, 2002; Zhou *et al.*, 2005) and removes ubiquitin from I $\kappa$ B (Zhou *et al.*, 2005). YopJ can also act as an acetyltransferase, acetylating functional residues in the activation loop of kinases (Collier-Hyams *et al.*, 2002; Mittal *et al.*, 2006; Mukherjee *et al.*, 2006). The acetylation of serine or threonine residues in these loops blocks subsequent phosphorylation and IKK $\beta$  undergoes acetylation by YopJ (Mittal *et al.*, 2006; Mukherjee *et al.*, 2006). The acetylation activity of YopJ has recently been shown to be activated by binding a eukaryotic host factor, inositol hexakisphosphate (IP<sub>6</sub>) (Mittal *et al.*, 2010).

AvrA from *Salmonella* is a member of YopJ/Avr family of deubiquitinases (Orth, 2002). Transfection of HEK293T cells with an NF- $\kappa$ B reporter and plasmids expressing AvrA, MEKK1, IKK $\beta$  and p65 shows that AvrA inhibits NF- $\kappa$ B activation downstream of IKK $\beta$  without affecting phosphorylation of I $\kappa$ B (Collier-Hyams *et al.*, 2002). Recombinant AvrA can deubiquitinate I $\kappa$ B *in vitro*, thereby preventing its degradation by the proteasome and subsequently inhibiting NF- $\kappa$ B activation (Ye *et al.*, 2007). SseL (*Salmonella* secreted factor L) is encoded on SPI-2 and can also deubiquitinate I $\kappa$ B *in vitro* and *in vivo* (Le Negrate *et al.*, 2008).

*Bordetella bronchiseptica* infection of rat lung epithelium cell line results in NF- $\kappa$ B aggregation in the cytoplasm, suppressing its activation and this was dependent upon the T3SS (Yuk *et al.*, 2000). Reduced transcription of antimicrobial peptide genes from *B. bronchiseptica* infected bovine tracheal epithelial cells is also dependent upon the presence of the T3SS (Legarda *et al.*, 2005). The authors also report that they did not observe any differences in I $\kappa$ B

phosphorylation or ubiquitination levels, therefore this mechanism of NF- $\kappa$ B modulation differs from YopJ, AvrA and SseL (Legarda *et al.*, 2005).

### 1.3 *Streptococcus pneumoniae*

*Streptococcus pneumoniae* (the pneumococcus) is a Gram positive facultative anaerobic bacterium and an important human pathogen worldwide. Pneumococci are a common cause of invasive diseases (septicaemia and meningitis) and respiratory-tract infections, such as otitis media, sinusitis, and community-acquired pneumonia. Diseases are caused particularly in young children, the elderly and immuno-compromised persons (Bogaert *et al.*, 2004). In 2008, just over 5,500 cases of invasive pneumococcal disease (IPD) were reported in the UK, contributing to a total of approximately 15,000 IPD cases reported across Europe (Annual epidemiological report on communicable diseases in Europe 2010 <http://ecdc.europa.eu>). *S. pneumoniae* infections can result in an estimated 40,000 hospitalisations, 40,000 GP consultations and 63,000 cases of otitis media annually in England and Wales ([http://www.hpa.org.uk/web/HPAweb&HPAwebStandard/HPAweb\\_C/1203008864027](http://www.hpa.org.uk/web/HPAweb&HPAwebStandard/HPAweb_C/1203008864027)). Pneumococci are classed by the immunochemistry of the polysaccharide present in the capsule that surrounds them, using the Quellung reaction. The Quellung reaction is evident under a microscope where incubation of positive reactive antibodies against a capsular serotype results in the bacterium 'swelling'. Currently, there are 93 different serotypes of the pneumococcus identified (Henrichsen, 1995; Park *et al.*, 2007; Jin *et al.*, 2009; Calix & Nahm, 2010), which include cross-reactive subtypes, such as the serotype 6 group (A, B, C and D).

Although *S. pneumoniae* is a serious human pathogen, it is part of the normal flora of the upper respiratory tract (URT), i.e. the nasopharynx, of healthy individuals. Colonisation of the nasopharynx is pivotal to pneumococcal spread and disease but can be limited to asymptomatic carriage (Bogaert *et al.*, 2004). Risk factors for *S. pneumoniae* nasopharyngeal colonisation include antibiotic use, asthma, smoking, ethnicity and over-crowding (Hoge *et al.*, 1994; Greenberg *et al.*, 2006; Roche *et al.*, 2007; Cardozo *et al.*, 2008). Bacterial colonisation of nasopharynx is complex as pneumococci have to compete for the same niche as *Haemophilus influenzae*, *Neisseria meningitidis*, *Staphylococcus aureus* and other Streptococcal species (Bogaert *et al.*, 2004). Therefore colonisation of the nasopharynx is a dynamic process due to the continuous

turnover of colonising species and serotypes present. Nasopharyngeal colonisation is likely to happen to every individual at some stage of life (Bogaert *et al.*, 2004).

The ability of the pneumococcus to colonise the URT, and to cause disease, largely depends on the virulence factors the bacterium produces. For example, neuraminidase, an enzyme which decreases the viscosity of the mucus layer protecting the epithelium and thereby exposes host-cell receptors, e.g. N-acetyl-glycosamine. NanA gene expression is upregulated in pneumococci in the nasopharynx, but not in lungs or blood (LeMessurier *et al.*, 2006), indicating a role in pneumococcal colonisation. Exposing the host cell receptors enables interaction with other pneumococcal surface-associated proteins, e.g. pneumococcal surface protein A (PspA). Expression of NanA also facilitates pneumococcal growth in the presence of other colonising species, such as *N. meningitidis*, as NanA removes the sialic acid that these species use to decorate their cell walls to evade the innate immune response (Shakhnovich *et al.*, 2002). The pneumococcus produces hydrogen peroxide (H<sub>2</sub>O<sub>2</sub>) during growth which can inhibit the growth of, and kill, other nasopharyngeal colonising species (Pericone *et al.*, 2000). The pneumococcus expresses a pore-forming toxin, pneumolysin (Ply), which can allow peptidoglycan from another bacterial species, such as *H. influenzae*, to translocate into the host cell (Ratner *et al.*, 2007), inducing an immune response against the other bacteria. These actions provide the pneumococcus with a competitive advantage over other colonising species to eliminate them and colonise the common niche.

### **1.3.1 Pneumococcal virulence factors**

The pneumococcus produces a number of virulence factors which contribute to the bacterium's ability to colonise and cause disease and/or pathology. Well characterised factors include the polysaccharide capsule and the toxin pneumolysin (Ply). Additional putative virulence factors have been identified through signature-tagged mutagenesis (Polissi *et al.*, 1998; Lau *et al.*, 2001; Hava & Camilli, 2002), lambda-phage libraries (Beghetto *et al.*, 2006) and full genome sequencing (Tettelin *et al.*, 2001; Hiller *et al.*, 2007). A large number

of these putative factors remain uncharacterised, yet studies are regularly being published demonstrating ongoing research in this area (Frolet *et al.*, 2010), and Table 1-3 outlines the virulence factors important in pneumococcal colonisation and/or pathogenesis. It should be noted that not all of the virulence factors are conserved amongst different strains of pneumococci, with some displaying variance (PspA, PspC, ZmpB and IgA protease) or have been horizontally acquired (pilus pathogenicity islands and PsrP) or not present (Pht proteins) (Donati *et al.*, 2010).

Proteins can be linked to the cell surface of the pneumococcus by way of one of three processes; via a sortase recognizing an LPXTG-motif for covalent linkage to the peptidoglycan present in the cell wall, via non-covalent linkage to phosphorylcholine in the cell wall teichoic and lipoteichoic acids (choline-binding proteins) or via signal peptidase II-mediated covalent integration into the plasma membrane (lipoproteins). The importance of protein display on the cell surface is evident in *S. pneumoniae* where the sortase A gene has been deleted, resulting in attenuation of pneumococcal colonisation and pathogenesis *in vivo* (Chen *et al.*, 2005; Paterson & Mitchell, 2006). Before these proteins can be expressed on the cell wall surface, or secreted into the extracellular milieu, they must be exported across the cytoplasmic membrane, by way of the Sec system. The Sec system was shown to be significantly ( $P=0.004$ ) up-regulated by 2.2-fold when in contact with an epithelial cell line by microarray analysis (Orihuela *et al.*, 2004b).

**Table 1-3 Characterised pneumococcal virulence factors**

<b>Virulence Factor</b>	<b>Role in colonisation/pathogenesis</b>	<b>Pneumococcal Location</b>
Capsule	Protects the bacterium from opsonisation and phagocytosis  Provides protection from complement  Hides pneumococcal antigens from the innate immune system (Abeyta <i>et al.</i> , 2003)	Covers the entire surface area above the cell wall
Autolysin A (LytA)	Degrades pneumococcal peptidoglycan cell wall, leading to cell lysis (Howard & Gooder, 1974)	Cell wall; choline binding

LytA (continued)	<p>Has a role in murine models of pneumonia and bacteraemia (Berry <i>et al.</i>, 1989a; Berry <i>et al.</i>, 1992; Berry &amp; Paton, 2000)</p> <p>Contributes to pneumococcal replication in the lung (Orihuela <i>et al.</i>, 2004a)</p> <p>Has a role in the rat model of pneumococcal meningitis (Hirst <i>et al.</i>, 2008)</p> <p>Related enzymes LytB and LytC contribute to colonisation (Gosink <i>et al.</i>, 2000)</p>	
Pneumococcal surface protein A (PspA)	<p>Contributes to pneumococcal virulence (Berry &amp; Paton, 2000)</p> <p>Inhibits alternative pathway of complement (Yuste <i>et al.</i>, 2005)</p> <p>Required for pneumococcal colonisation, pneumonia and bacteraemia (Ogunniyi <i>et al.</i>, 2007b)</p>	Cell wall; choline binding
Pneumococcal surface protein C [PspC; aka choline binding protein A (CbpA) or SpsA]	<p>Contributes to pneumococcal colonisation (Rosenow <i>et al.</i>, 1997; Ogunniyi <i>et al.</i>, 2007b)</p> <p>Binds factor H (Dave <i>et al.</i>, 2001) facilitating pneumococcal invasion of tissues <i>in vivo</i> (Quin <i>et al.</i>, 2007b)</p> <p>Mutants show reduced virulence in pneumonia and bacteraemia (Iannelli <i>et al.</i>, 2004; Kerr <i>et al.</i>, 2006)</p>	Cell wall; choline binding
IgA1 protease	<p>Degrades host IgA thereby evading the immune response (Poulsen <i>et al.</i>, 1996; Wani <i>et al.</i>, 1996)</p> <p>Processed IgA by protease may promote pneumococcal adherence to host cells (Weiser <i>et al.</i>, 2003)</p>	Cell wall; LPXTG anchored
Pili	<p>Adheres to respiratory and epithelial cells and the extracellular matrix (ECM) (Barocchi <i>et al.</i>, 2006; LeMieux <i>et al.</i>, 2006; Nelson <i>et al.</i>, 2007; Hilleringmann <i>et al.</i>, 2008; Izore <i>et al.</i>, 2010)</p> <p>Second pilus type has been identified and shown to be involved in host cell adhesion (Bagnoli <i>et al.</i>, 2008)</p>	Cell wall; LPXTG anchored

Pneumococcal serine rich protein (PsrP)	<p>Promotes pneumococcal persistence in the lung and antibodies against this antigen protects against challenge (Rose <i>et al.</i>, 2008)</p> <p>Bacterial adhesin which interacts with Keratin-10 on lung epithelial cells (Shivshankar <i>et al.</i>, 2009)</p>	Cell wall; LPXTG anchored
Zinc metalloprotease (Zmp)	Induces inflammation in the lower respiratory tract by stimulating TNF- $\alpha$ production (Blue <i>et al.</i> , 2003)	Cell wall; LPXTG anchored
Hyaluronidase (Hyl)	<p>Degrades hyaluronic acid present in the host connective tissues and associated ECM, possibly promoting pneumococcal dissemination (Paton <i>et al.</i>, 1993)</p> <p>Contributes to pneumococcal meningitis (Kostyukova <i>et al.</i>, 1995)</p>	Cell wall; LPXTG anchored Also secreted
Neuraminidase A (NanA)	<p>Cleaves sialic acid from mucin, glycoprotein and gangliosides (Scanlon <i>et al.</i>, 1989), possibly to reveal host receptors for pneumococcal adherence</p> <p>Removes sialic acid from the cell walls of competitor colonising species (Shakhnovich <i>et al.</i>, 2002)</p> <p>Role in pneumococcal colonisation and infection of the respiratory tract, and bacteraemia (Manco <i>et al.</i>, 2006)</p>	Cell wall; LPXTG anchored Also secreted
Pneumococcal Histidine Triad (Pht) proteins	Reduce complement binding to pneumococci by recruitment of human factor H (Ogunniyi <i>et al.</i> , 2009)	Lipoprotein, surface exposed
Pneumococcal surface antigen A (PsaA)	<p>Essential for pneumococcal colonisation, bacteraemia and pneumonia (Berry &amp; Paton, 1996; Johnson <i>et al.</i>, 2002)</p> <p>Substrate (Manganese) binding lipoprotein of <i>psa</i> ABC transporter (Dintilhac <i>et al.</i>, 1997)</p>	Lipoprotein, surface exposed
Protease maturation protein (PpmA)	Contributes to pneumococcal virulence (Overweg <i>et al.</i> , 2000) and colonisation (Cron <i>et al.</i> , 2009)	Lipoprotein, surface exposed
PavA	Binds fibronectin and is essential for pneumococcal virulence (Holmes <i>et al.</i> , 2001)	Surface exposed

Pneumolysin (Ply)	<p>Cytolytic toxin which binds to cholesterol-containing membranes, such as respiratory epithelium (Feldman <i>et al.</i>, 1990)</p> <p>Required for exponential pneumococcal growth in the blood to cause acute sepsis (Benton <i>et al.</i>, 1995)</p> <p>Mutant is unable to cause pneumococcal meningitis (Hirst <i>et al.</i>, 2008)</p>	Cytoplasm; Cell wall
-------------------	---	----------------------

### 1.3.2 Pneumolysin

Pneumolysin (Ply) is a member of a family of toxins called cholesterol dependent cytolysins (CDCs), which are present in over 20 species of Gram positive bacteria including *Clostridia* and *Bacillus*. CDCs are pore-forming toxins which bind to cholesterol containing membranes (Johnson *et al.*, 1980). The CDCs are highly conserved and play important roles in the pathogenesis of the organisms that produce them.

The molecular structure of two cytolysins has been resolved, perfringolysin (PFO) from *Clostridium perfringens* and intermedilysin (Ily) from *Streptococcus intermedius* (Polekhina *et al.*, 2004). Many of the structure and function studies of Ply are based on the structure model of PFO, Figure 1-8. CDCs consist of four domains, labelled 1-4, each playing a role in the function of the molecule.

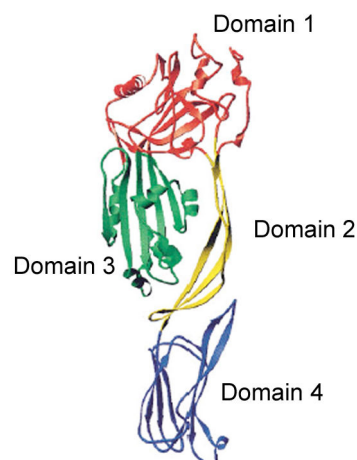


**Figure 1-8 Structure of a typical cholesterol dependent cytolysin (CDC)**  
 CDC comprises of four domains in its tertiary structure, figure adapted from (Rossjohn *et al.*, 1997) co-ordinates available at Protein Data Bank ref 1M3I (<http://www.pdb.org/pdb/explore/explore.do?structureId=1M3I>).

Domain 4 has been shown to be the domain responsible for cholesterol binding, due to the presence of a conserved 11 amino acid (ECTGLAWEWWR) region within the domain (Jacobs *et al.*, 1999). The exception to the family of CDCs is intermedilysin as it has specific toxicity to human cells (Nagamune *et al.*, 1996) due to its requirement for a receptor, CD59, to bind to host membranes (Giddings *et al.*, 2004; Soltani *et al.*, 2007). Domain 4 can bind to the membrane prior to oligomerisation (Nakamura *et al.*, 1995) and recombinant domain 4 protein competes for binding with full-length toxin (Baba *et al.*, 2001). There are two proposed models for pore formation, whereby the individual monomers insert into the membrane then oligomerise to form pores or they bind first to the membrane, oligomerise to form a pre-pore, then insert into the phospholipid bilayer.

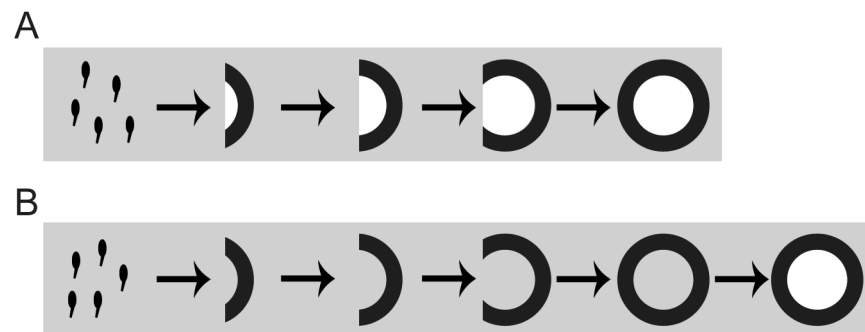


**Figure 1-9 Two models of pore formation by CDCs; adapted from (Gilbert, 2002)**  
**A Model of toxin insertion followed by oligomerisation leading to gradual pore formation (Palmer *et al.*, 1998)** **B Model of toxin monomer binding, oligomerisation to form a prepore followed by membrane insertion to create the pore (Shepard *et al.*, 2000)**

The insertion followed by oligomerisation model was first proposed through studies with streptolysin O, where electron-microscopy of treated red blood cells shown arc-like structures on the membrane surface alongside complete pores (Palmer *et al.*, 1998). The formation of these arc structures was investigated further using SLO mutants that inhibit oligomerisation and it was found the membrane was permeable to small molecules in the absence of complete pores (Palmer *et al.*, 1998). The pre-pore theory was proposed by Tweten and coworkers through their studies with perfringolysin (Shepard *et al.*, 2000). They have shown that toxin insertion is coupled with oligomerisation therefore a prepore is formed (Hotze *et al.*, 2001), and pore formation is controlled by monomer-monomer interactions (Hotze *et al.*, 2002). Studies with Ply show that the monomers can oligomerise in high concentrations without the need for

cholesterol or membranes (Gilbert *et al.*, 1998). Ply pore formation fits with the pre-pore theory as the oligomeric structure first assembles on the membrane prior to membrane insertion, shown through cryo-EM (Gilbert *et al.*, 1999; Tilley *et al.*, 2005). By rigid-body fitting the structure of PFO onto a cryo-EM map of Ply pores, the conformational changes from pre-pore to pore were determined (Tilley *et al.*, 2005). Domain 3 is responsible for oligomerisation once the prepore assembles, Domain 2 folds in half, dissociating away from Domain 3. Domain 3 can then undergo further conformational change to insert 2 amphipathic  $\beta$ -sheets into the membrane (Tilley *et al.*, 2005). A tryptophan in Domain 4 (W433) has been shown to be essential for lysis as it penetrates the upper leaflet of the phospholipid bilayer after Domain 3 has undergone its conformational change (Mitchell *et al.*, 1992; Hill *et al.*, 1994).

The Ply gene was first sequenced in 1987 from a serotype 2 strain of pneumococcus, D39, and termed allele 1 (Walker *et al.*, 1987). Due to its ability to form pores on cholesterol containing membranes, Ply is toxic to most eukaryotic cell types, including epithelial and endothelial cells present in the respiratory tract and brain (Rubins *et al.*, 1992; Rubins *et al.*, 1993; Zysk *et al.*, 2001). The pore forming activity can also induce apoptosis of neutrophils (Zysk *et al.*, 2000), brain cells (Braun *et al.*, 2002; Braun *et al.*, 2007), macrophages (Srivastava *et al.*, 2005; Garcia-Suarez Mdel *et al.*, 2007), cochlear cells (Beurg *et al.*, 2005) and dendritic cells (Littmann *et al.*, 2009). Ply can also inhibit the ciliary beat of respiratory epithelium and this inhibition was relieved by addition of cholesterol or anti-Ply antibodies (Steinfort *et al.*, 1989; Feldman *et al.*, 1990). Ply was originally thought to be produced in a lytic form in all disease causing strains, until the identification of reduced haemolytic versions in serotype 7F and 8 strains (Lock *et al.*, 1996) and non-lytic form in serotype 1, ST306 (Kirkham *et al.*, 2006) which is a prevalent cause of invasive pneumococcal disease in Scotland. This ST306 Ply was able to bind the membrane but cannot form pores, only arc structures could be seen with transmission EM, and analysis of the sequence identified 6 amino acid mutations (Tyr150His, Thr172Iso, Lys224Arg, Ala265Ser,  $\Delta$ Val270, and  $\Delta$ Lys271) compared to allele 1 (Kirkham *et al.*, 2006). The mutation of tyrosine to histidine at position 150 had not been previously described with the other 5 mutations found in the previous study (Lock *et al.*, 1996). Therefore the abrogation of

haemolytic activity seen in ST306 Ply allele was attributed to the combinational effect of T172I and Y150H mutations (Kirkham *et al.*, 2006). It was demonstrated before identification of this Ply allele that the function of Ply extends beyond that of cell lysis; it can interact with the classical complement pathway (Paton *et al.*, 1984).

Ply is able to interact with C1q both directly due to its homology to C-reactive protein (CRP) and indirectly through interaction with the Fc region of IgG (Mitchell *et al.*, 1991). This activation of complement inhibits C3 deposition on *S. pneumoniae* thereby reducing opsonophagocytosis and, using Ply deficient strains, it is specifically dependent upon Ply *in vitro* (Yuste *et al.*, 2005) and *in vivo* (Quin *et al.*, 2007a). Ply can also induce cytokine production which has been shown to be both pore-formation dependent and independent (Baba *et al.*, 2002). The relationship between cytolytic activity and complement activation has been shown to act independently of one another during experimental infection models (Benton *et al.*, 1997a).

### **1.3.2.1 Role of Ply in pneumococcal colonisation**

The role of Ply in colonisation is not well defined due to conflicting reports. Studies comparing a Ply deficient strain with its isogenic parent indicate that Ply contributes to pneumococcal adherence to respiratory epithelium *in vitro* however, in the murine model of colonisation the mutant is present in comparable or greater numbers than wild-type (Rayner *et al.*, 1995; Rubins *et al.*, 1998). The role of Ply in colonisation is considered minor in comparison to other virulence factors, such as PspC and PspA (Ogunniyi *et al.*, 2007a; Ogunniyi *et al.*, 2007b). The effects of Ply on the host innate immune response can contribute to both pneumococcal persistence and bacterial clearance, thus implying that a fine balance must be mediated. The evidence that supports this is that Ply can induce the apoptosis of many inflammatory cell types such as macrophages, neutrophils and monocytes. Ply induces nitric oxide production in macrophages, leading to macrophage apoptosis (Braun *et al.*, 1999; Marriott *et al.*, 2004). However, Ply can also induce inflammatory response thereby increasing pneumococcal clearance (van Rossum *et al.*, 2005). Host-mediated

apoptosis of alveolar macrophages promotes bacterial clearance in a murine model of resolving pneumococcal lung infection (Dockrell *et al.*, 2003). Pneumococcal clearance by the host has been shown to be dependent upon the direct interaction of Ply with Toll-like Receptor (TLR) 4, as TLR4 deficient mice are more susceptible to colonisation by Ply producing pneumococci (Malley *et al.*, 2003). The interaction of Ply with TLR4 also induces host-mediated macrophage apoptosis in the upper respiratory tract, promoting pneumococcal clearance in a murine model (Srivastava *et al.*, 2005). The role of Ply in pneumococcal persistence in the nasopharynx is seen in the colonisation model described by Richards and authors, where a Ply deficient mutant is cleared within 7-14 days but its serotype 2 isogenic parent can still be detected 28 days post-infection (Richards *et al.*, 2010).

### **1.3.2.2 Role of Ply in pneumococcal disease**

The contribution of Ply to pneumococcal pathogenesis has been tested in many animal models of infection, including bacteraemia, pneumonia, meningitis and otitis media. In the murine model of pneumonia, Ply deficient mutants are attenuated compared to their isogenic parent strains (Berry *et al.*, 1989b; Berry & Paton, 2000; Ogunniyi *et al.*, 2007a; Ogunniyi *et al.*, 2007b). Production of Ply enables the pneumococci to replicate in the alveoli and penetrate the interstitium of the lung (Rubins *et al.*, 1995). The lytic and complement activating functions of Ply play two distinct roles in the progression of pneumonia (Rubins *et al.*, 1996). The cytolytic function contributes towards neutrophil recruitment and the complement activating function accumulates T cells (Jounblat *et al.*, 2003). Sublytic concentrations of Ply are present *in vivo* and contributes towards pathology in the lung by inducing apoptosis of host cells and localised inflammation (Garcia-Suarez Mdel *et al.*, 2007). The role and importance of Ply in pneumococcal pneumonia is further supported by the observations where immunisation of mice with Ply protein or  $\alpha$ -Ply antibodies offers protection from subsequent pneumococcal infection (Musher *et al.*, 2001; Briles *et al.*, 2003; Garcia-Suarez Mdel *et al.*, 2004).

Bacteraemia commonly arises from the progression of pneumococcal infection in the lungs to the blood and Ply production has been shown to be an important influence in this transition (Rubins *et al.*, 1995; Jounblat *et al.*, 2003). Ply production is advantageous for exponential pneumococcal replication in the blood, and growth of a type 2 strain with its Ply mutant shows that the production of Ply from the parent can contribute to the growth of the mutant in the blood *in vivo* (Benton *et al.*, 1995). Further studies demonstrated that the contribution of Ply to pneumococcal replication in the blood can depend upon the genetic background of the mouse used in the model of infection (Benton *et al.*, 1997a). The same study also showed that the complement activating and cytolytic properties of Ply do not contribute individual roles to virulence in the blood (Benton *et al.*, 1997a). This may be due to the route of challenge as Jounblat and authors report that these two functions can influence the progression of bacteraemia when mice were challenged via an intranasal route of infection (Jounblat *et al.*, 2003). Pneumococci expressing Ply with its complement activating activity inactivated were detected in the blood 6 hours after infection, pneumococci expressing wild-type toxin were detected after 12 hours and pneumococci expressing Ply with its cytolytic activity inactivated were not detected until 24 hour post-infection (Jounblat *et al.*, 2003). In a rat model of infection, Ply contributes to survival in the blood by inhibiting clearance and reducing the opsonising activity of serum (Alcantara *et al.*, 1999; Alcantara *et al.*, 2001).

Ply has been reported to be an important contributing factor to the progression of pneumococcal meningitis (Kostyukova *et al.*, 1995). Ply can destroy brain ependymal cells and reduce ciliary beat, shown by using an *ex vivo* model and comparing recombinantly expressed Ply with a cytolytic inactivated mutant (Mohammed *et al.*, 1999) and D39 pneumococci with its Ply deficient mutant PLN-A (Hirst *et al.*, 2000). The production of hydrogen peroxide by pneumococci works in concert with Ply to induce pathology and apoptosis of brain cells (Hirst *et al.*, 2000; Braun *et al.*, 2002; Braun *et al.*, 2007). Ply causes damage to cerebral endothelial cells in an *in vitro* blood brain barrier (BBB) model, and the authors postulate that this Ply-mediated damage may enable pneumococci to traverse the BBB to cause meningitis (Zysk *et al.*, 2001). This is supported by results from animal models of meningitis where pneumococci were injected

directly into the brain. Murine models of meningitis infection demonstrate that pneumococcal strains deficient in Ply, but not neuraminidases or hyaluronidase, are attenuated compared to the parent type 2 strain (Wellmer *et al.*, 2002). This importance of Ply in the pathogenesis of meningitis is supported by additional corroborating reports using rabbit (Braun *et al.*, 2002) and rat (Hirst *et al.*, 2008) models of pneumococcal meningitis. Sub-lytic concentrations of Ply have important implications in the pathology associated with pneumococcal meningitis. Ply can activate Rho and Rac GTPases resulting in the formation of actin stress fibres, filopodia and lamellipodia (Iliev *et al.*, 2007). The authors show that this activation occurs prior to macropore formation, and postulate membrane depolarisation induced by toxin binding, results in lamellipodia formation (Iliev *et al.*, 2007). Ply can also induce microtubule stabilisation and bundling in an *in vivo* rabbit model of pneumococcal meningitis and *in vitro* with neuronal and non-neuronal cell lines (Iliev *et al.*, 2009). The authors demonstrated that this action depended upon cholesterol binding but not macropore forming abilities of the toxin by using sub-lytic concentrations, 0.1 µg/ml, which are found in pneumococcal meningitis patients (Iliev *et al.*, 2009). Further studies showed that the pore-forming ability of Ply does play a role in affecting the host cytoskeleton *in vitro* by comparing wild-type toxin to two pore-forming mutants (W433F and ΔA146R147), which can still bind to cholesterol (Förtsch *et al.*, 2011).

### **1.3.2.3 Ply release and localisation**

Ply exerts its function outwith the pneumococcal cell, however Ply differs from the other CDCs in that it does not possess a consensus N-terminal secretion signal (Walker *et al.*, 1987). This correlated with earlier reports that Ply was retained in the pneumococcal cytoplasm (Johnson, 1977) and resulted in the observation that Ply was not detected until the onset of cell lysis mediated by autolysin A (LytA) in stationary phase cultures *in vitro*.

Autolysin (LytA) is a choline-binding protein with N-acetylmuramyl-L-alanine amidase activity. This enzyme degrades the peptidoglycan of the bacterial cell wall (Howard & Gooder, 1974). The enzyme naturally degrades the cell wall during cell growth, for cell wall turn-over and cell-cell separation (Jedrzejewski, 2001). This action releases cell wall components into the external milieu which

can trigger an immune response. When a cell enters stationary phase of growth, or is exposed to antibiotics and/or detergents, it can lead to complete cell lysis, and cell death, by autolysin.

LytA mutants have reduced virulence in murine models of pneumonia and bacteraemia, and rabbit model of meningitis, compared to isogenic parent strains of pneumococci (Berry *et al.*, 1989a; Berry *et al.*, 1992; Canvin *et al.*, 1995; Orihuela *et al.*, 2004a; Hirst *et al.*, 2008). Pre-immunisation of mice with autolysin antigen protects mice from subsequent pneumococcal challenge, to a level comparable with Ply, but no additive effect is seen when both antigens were administered (Lock *et al.*, 1992). This indicates that the main role of LytA in pneumococcal virulence is to induce cell lysis for the release of Ply, and other immunogenic factors, into the external milieu. The contribution of Ply to the virulence of pneumococci with different capsular types was investigated, and this study discovered that *in vitro* haemolytic titres of Ply are first detected intracellularly at late exponential phase in the majority of strains. An extracellular pool of Ply could be detected before stationary phase in a select number of strains, including serotype 3 strain WU2 (Benton *et al.*, 1997b). The release of Ply in this strain was investigated further and, using defined mutants of LytA and *in vitro* growth in the presence of choline, it was shown that this release was autolysin-independent (Balachandran *et al.*, 2001). The authors hypothesise that Ply is not secreted *in vitro* by other strains of *S. pneumoniae*, such as D39, due to the lack of an unknown stimulus in the growth conditions tested. This report of autolysin-independent transport of Ply by the pneumococcus was further supported by results from Andrew Camilli's group. The authors report that Ply can localise to the pneumococcal cell wall and that this phenomenon was not dependent upon capsular serotype or LytA (Price & Camilli, 2009). The results from these three studies suggest that Ply can transverse the cytoplasmic membrane in all pneumococcal strains, by an as yet uncharacterised mechanism, but secretion of Ply from the cell wall may only occur in certain strains or in certain conditions. These reports raise the questions: how is Ply secreted?; how it is sequestered to and released from the cell wall?; what controls Ply secretion, i.e. are there particular genes involved?; and what implications does Ply secretion have upon pneumococcal colonisation and pathogenesis?.

## 1.4 Aims of the project

The aims of this project were to assess the regulation, expression and function of two non-LEE encoded Type III secretion system effectors of *E. coli* O157:H7, NleH1 and NleH2. Fluorescent proteins are commonly used as reporters of gene expression and protein localisation, and were employed in the characterisation of NleH. Conversely, fluorescent proteins have not been utilised extensively in pneumococcal research. To address this, fluorescent proteins with the codon usage optimised for expression in *S. pneumoniae* were developed as reagents for future research. These reagents were characterised in the pneumococcus, using parallel techniques from NleH experiments, and used to assess the localisation of pneumolysin. Determining the localisation and distribution of Ply on the pneumococcal cell can offer further insight into how this toxin contributes to pneumococcal pathogenesis.

## 2 Materials and Methods

### 2.1 Bacterial strains, growth conditions & storage

Strains used in this study are listed in Table 1. *E. coli* were grown from a single colony in Luria-Bertani (LB) broth, M9 minimal media (M9), Minimal Essential Media with HEPES modification (MEM; Sigma M7278), or Dulbecco's Minimal Essential Media (DMEM; Sigma D5671). Glucose was added to MEM to give a final concentration of 0.2%. Antibiotics were included where necessary at the following concentrations: 50 µg/ml kanamycin (Kan), 12.5 µg/ml chloramphenicol (Chl), 100 µg/ml ampicillin (Amp), 1 mg/ml erythromycin (Ery), 15 µg/ml gentamycin (Gent).

*S. pneumoniae* were initially grown on BAB (Blood Agar Base No.2; Oxoid, UK) supplemented with 5% horse blood (E&O Laboratories, Bonnybridge, UK). BHI (Blood-Heart Infusion broth; Oxoid, UK) was inoculated with a single colony and grown statically at 37°C until mid-log phase ( $OD_{600nm} = 0.6$ ) was reached. Strain purity and optochin sensitivity was tested by streaking onto BAB with an optochin disc (Mast, UK). Antibiotics were included where necessary at the following concentrations: 12.5 µg/ml Chl; 1 µg/ml Ery.

For frozen bacterial stocks, sterile glycerol was added to an overnight LB culture of *E. coli* or mid-log ( $OD_{600nm} = \sim 0.6$ ) BHI culture of *S. pneumoniae* to 15% (v/v) and stored at -80°C in 1ml aliquots.

**Table 2-1 Strains used in study**

Strain	Description
<b>E. coli</b>	
TUV 93-0	Shiga toxin negative ( <i>stx</i> <sup>-</sup> ) derivative (Campellone <i>et al.</i> , 2004) of EHEC O157:H7 strain EDL933 [sequenced strain (Perna <i>et al.</i> , 2001)]
ZAP193	EHEC O157:H7 strain NCTC 12900 <i>stx</i> <sup>-</sup>
ZAP193Δ <i>ler</i>	Clean deletion of <i>ler</i> gene. Received from Sean McAteer, ZAP Laboratories, University of Edinburgh.
ZAP193Δ <i>grlA</i> -Tn-Kan	Transposon insertion in <i>grlA</i> gene; received from Sean McAteer, ZAP Laboratories, University of Edinburgh.
BW25113	<i>E. coli</i> K-12 (Baba <i>et al.</i> , 2006); received from Dr Gail Ferguson.
BW25113 rpos:Kan	BW25113 Keio mutant of <i>rpoS</i> (Baba <i>et al.</i> , 2006). Received from Dr Gail Ferguson.
85-170	Spontaneous Stx <sub>1</sub> and Stx <sub>2</sub> EHEC O157:H7 strain (Tzipori <i>et al.</i> , 1987). Received from Prof Gad Frankel.
85-170 Δ <i>nlcH1nlcH2</i>	Received from Prof Gad Frankel. Mutants generated by one-step PCR λ-Red-mediated mutagenesis Kan <sup>R</sup> Amp <sup>R</sup>
85-170Δ <i>nlcH1</i>	Generated by allelic exchange with pKO3bH1 by AH
MC1000	<i>araD139 Δ(araABC-leu)7679 galU galK Δ(lac)X74 rpsL thi</i> (Casadaban & Cohen, 1980). Received from Dr Vanessa Sperandio.
VS184	MC1000Δ <i>qseC</i> (Sperandio <i>et al.</i> , 2002b). Received from Dr Vanessa Sperandio.
XL1-Blue	<i>recA1 endA1 gyrA96 thi-1 hsdR17 supE44 relA1 lac</i> [F' <i>proAB lacI<sup>q</sup>ΔM15 Tn10 (Tet<sup>r</sup>)</i> ] (www.stratagene.com)
<b>S. pneumoniae</b>	
D39	Avery's type 2 strain NCTC 7466 (Avery <i>et al.</i> , 1944) sequenced strain (Lanie <i>et al.</i> , 2007)
TIGR4NO1	Serotype 4 sequenced strain (Aaberge <i>et al.</i> , 1995; Tettelin <i>et al.</i> , 2001)
R6	Unencapsulated derivative of D39 (Hoskins <i>et al.</i> , 2001)
A45	Serotype 3 strain isolated from a horse (Whatmore <i>et al.</i> , 1999)
D39Δ <i>PlySTOP</i>	Created by Dr Calum Johnston, Janus mutagenesis of D39 to introduce early stop codon in <i>Ply</i> sequence.
FP28	D39Δ <i>pspC</i> , with <i>cat</i> cassette described in (Iannelli <i>et al.</i> , 2004)
TIGR4NO1Δ <i>LytA-Ply</i>	Generated by allelic exchange with pUCLytA27R:: <i>Chl</i> into TIGR4 by AH

## 2.2 Preparation of genomic DNA

### 2.2.1 *E. coli*

Cells were pelleted from 1ml overnight LB culture and genomic DNA (gDNA) was extracted using ChargeSwitch™ gDNA Mini Bacteria kit (Invitrogen; Scotland), as per manufacturer's protocol. DNA was resuspended in 200 µl molecular grade water (dH<sub>2</sub>O) (Sigma, UK) and stored at 4°C until required.

### 2.2.2 *S. pneumoniae*

Genomic DNA (gDNA) was extracted from *S. pneumoniae* cultures using a method previously described (Blue *et al.*, 2003), with modifications. Typically, strains were grown overnight in 20ml BHI at 37°C, and a BAB plate aseptically streaked to test for purity, and an optochin disc added to confirm identity. The culture was centrifuged in a 4K15 centrifuge (Sigma, UK) at 4,000xg for 15 minutes at 4°C, and the supernatant carefully removed. The pellet was resuspended in 1ml lysis buffer (10mM Tris, 100mM EDTA and 0.5% SDS) and subsequently incubated at 37°C for 1 hour. Proteinase K (Invitrogen, Scotland) was then added to a final concentration of 100 µg/ml and incubated at 50°C for 3 hours. Next, RNase (Invitrogen, Scotland) was added to the mixture to a final concentration of 20 µg/ml and incubated at 37°C for 30 minutes before adding an equal volume of phenol:chloroform:isoamyl alcohol (25:24:1) (Sigma, UK). The tubes were then inverted sharply several times to mix the samples, and centrifuged at 12,000xg for 3 min. The upper phase of the solution was then removed and placed into a fresh 1.5ml tube, before addition of 0.2 volumes of 10M ammonium acetate (Sigma-Aldrich, UK) and ~700 µl absolute ethanol (Fisher Scientific, UK, analytical reagent grade). The tubes were then gently inverted, and centrifuged at 12,000xg for 30 min in a benchtop centrifuge (Centrifuge 5417C, Eppendorf, UK) to pellet the DNA, before careful removal of the supernatant. The pellets were then air dried for 30 minutes to remove any remaining ethanol, before being resuspended in ~200 µl molecular grade dH<sub>2</sub>O (Sigma, UK). The samples were then stored at 4°C until required.

## 2.3 Molecular cloning

### 2.3.1 Plasmid DNA preparation

Plasmid DNA was prepared from 3ml overnight *E. coli* LB culture using Qiaprep Spin Miniprep Kit (QIAGEN) as per manufacturer's instructions, except DNA was eluted in molecular grade water (dH<sub>2</sub>O) for downstream applications.

### 2.3.2 PCR amplification

Polymerase chain reaction (PCR) was used for two purposes: to amplify DNA for molecular cloning or for bacterial colony screening. For molecular cloning and sequencing, a high fidelity DNA polymerase, Phusion DNA polymerase (Finnzymes/NEB, UK), was used. For bacterial colony screening, GoTaq DNA polymerase (Promega, UK) with Green buffer was used. Both DNA polymerases were used as outlined by the manufacturer guidelines; a typical reaction and cycle conditions are outlined in Table 2-2.

**Table 2-2 Typical PCR reaction and cycle conditions**

Colony PCR with GoTaq polymerase	PCR for cloning with Phusion polymerase
<u>Reaction Mix: 25 µl</u> 5 µl GoTaq Green Buffer (x5) 3 µl 2.5mM dNTPs (Invitrogen, UK) 0.2 µl Forward Primer (10 µM) 0.2 µl Reverse Primer (10 µM) 0.2 µl GoTaq polymerase (10 U/µl) 16.4 µl dH <sub>2</sub> O	<u>Reaction Mix: 50 µl</u> 10 µl Phusion Buffer (x5) 4 µl 2.5mM dNTPs (Invitrogen, UK) 2.5 µl Forward Primer (10 µM) 2.5 µl Reverse Primer (10 µM) 0.5 µl DNA template (gDNA/plasmid) 0.5 µl Phusion polymerase (10 U/µl) 30 µl dH <sub>2</sub> O
<u>Cycle conditions:</u> 1 x 95°C 5 minutes; 30 x 94°C 50 seconds, 50°C 50 seconds, 72°C 1 minute/kb product 1 x 72°C 5 minutes Hold at 4°C	<u>Cycle conditions:</u> 1 x 98°C 1 minute; 30 x 98°C 10 seconds, (lowest melting temp of primers + 3)°C 20 seconds, 72°C 20 seconds/kb product 1 x 72°C 5 minutes Hold at 4°C

PCR products were diluted 1:3 in DNA loading buffer before loading, or loaded directly if GoTaq Green buffer used, into a 0.8% agarose (Sigma, UK) gel with 0.05% SYBR safe DNA stain (Invitrogen, Scotland) alongside 1Kb+ DNA ladder

(Invitrogen). The gel was run at 100V for 20 minutes in TAE buffer and viewed under ultraviolet light in an UVIpro Gold Gel-doc system (UVItec, UK) to confirm successful PCR.

### **2.3.3 Restriction enzyme digestion**

Restriction enzymes were supplied by New England Biolabs (NEB, UK) or Promega. Typically 1 µg of plasmid DNA, or a 30 µl PCR product after being cleaned by Qiaquick PCR purification kit (QIAGEN, UK) and eluted in dH<sub>2</sub>O, was mixed with 1 µl chosen restriction enzyme, recommended buffers (1x) and bovine serum albumin (BSA; 1 mg/ml) in a total volume of 50 µl. After incubation at 37°C for 3 hours, the DNA of interest was either cleaned by QIAquick PCR purification kit (QIAGEN, UK) or extracted from an agarose gel slice using QIAquick Gel Extraction kit (QIAGEN, UK). Both kits were used as per manufacturer's instructions, with DNA eluted in dH<sub>2</sub>O.

### **2.3.4 Ligation reaction**

DNA is mixed in an insert:vector molecular ratio of 3:1 in a total of 8 µl, then 1 µl T4 DNA ligase buffer and 1 µl T4 DNA ligase (NEB, UK) is added. The reaction is incubated either at room temperature for 3 hours or 16°C overnight. 5 µl of this mixture is then used for transformation into XL1-Blue *E. coli*.

## 2.4 Transformation of *E. coli*

For molecular cloning, XL1-Blue chemically competent *E. coli* was used. Once a 100 µl frozen aliquot of competent bacteria was thawed on ice, DNA was added and incubated on ice for a further 20 minutes. The sample was heat-shocked at 42°C for 45 seconds followed immediately by incubation on ice for 2 minutes. 700 µl of LB broth was added to the heat-shocked sample and incubated at 37°C, with shaking at 180 rpm, for 60 minutes. 150 µl culture was plated onto LB plates with appropriate antibiotics added and incubated overnight.

*E. coli* O157:H7 strains were made electrocompetent by repeated suspension of cells in ice-cold 10% glycerol; ½ volumes, ¼ volumes and finally 1/250 volumes. Typically ~500ng DNA was mixed with 40 µl competent cells in an electroporation cuvette (Bio-Rad) and incubated for 10 minutes on ice prior to electroporation using a Bio-Rad GenePulser™. Immediately after electroporation, 700 µl LB was added and the cells incubated for 1 hour at 37°C, 180rpm. 150 µl culture was plated onto LB plates with appropriate antibiotics added and incubated overnight.

## 2.5 Construction & analysis of NleH translational fusions

### 2.5.1 GFP/RFP fusions

Promoter regions of NleH1 and NleH2, and an indicated number of amino acids of coding sequence, were PCR amplified from TUV-930 gDNA using primers described in Table 2-3, and cloned into pAJR70 (Roe *et al.*, 2003) for translational fusions to GFP. Figure 2-1 shows the areas of the genome amplified to make the constructs pAHE8 and pAHE18-22. The upstream primers had a BamHI restriction enzyme site, the downstream CDS primers a KpnI site, introduced into the sequence to allow sub-cloning into the reporter vectors by ligation. All constructs were confirmed with restriction digest analysis prior to sequencing at Dundee Sequencing Service (Dundee University, UK) using primers PrAJR70F and PrGFPR.

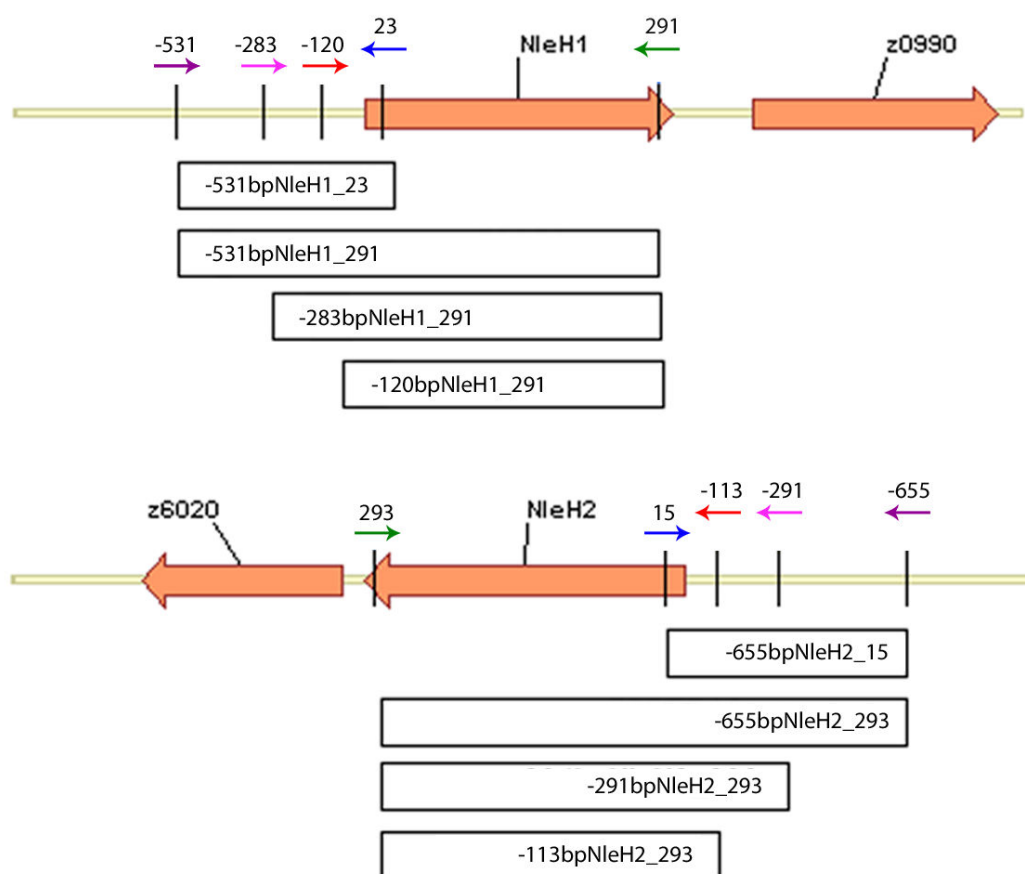


**Figure 2-1 Representation of the promoters and coding sequence cloned upstream of GFP**  
Arrangement of genes from Vector NTi software (Invitrogen), arrows indicate primers labelled with reference to their name, in Table 2-3, and boxes show primer pairs used for fragment.

**Table 2-3 Primers used for NleH-FP translational fusions**

Primer	Sequence (5' → 3')
	Introduced restriction enzyme recognition sites are in lower case.
NleH15bam	CGggatccATTGTACAGGTCCATTGC
NleH1pro23kpn	CGggatccAGGCGAAGTCAGGTTTCTGGT
NleH1ser291kpn	CGggatccACTAATAAGATCTTGCTTTCC
NleH1 5 120bp	CggatccGGAAGGATGAATTAGTTGCC
NleH1 5 283bp	CGggatccGCTGCAGATTTAGATATTGC
NleH25bam	CGggatccCGACATACTCATTAGCT
NleH2ser15kpn	CGggatccAGAATTCATGAACATCCCAA
NleH2leu293kpn	CGggatccAGCTTTCTCCGTGATAAGA
NleH2 5 113bp	CGggatccGAAGTAACCCGATAGCTTC
NleH2 5 291bp	CGggatccAGCAATGATTCGTGCCAC
PrAJR70F	AGCCCGAAGTGGCGAGCCCG
PrGFPR	CTCGGCGCGGGTCTTGTAGTTGCC

## 2.5.2 ILOV fusions

The coding sequences of NleH1 and NleH2 were PCR amplified from TUV93-0 gDNA using primers detailed in Table 2-4. The 5' primer includes an NdeI site at the ATG start codon of the ORF and the 3' primer includes a KpnI site before the natural stop codon of NleH. This PCR product was cloned into pJ284:iLOV to create a translational fusion to iLOV, which is under the control of an IPTG inducible (ptac) promoter.

**Table 2-4 Primers used for making NleH-iLOV translational fusions**

Primer	Sequence (5' → 3')
	INTRODUCED RESTRICTION ENZYME SITES ARE IN LOWER CASE
NleH1 LOV 5 NdeI	GGCcatatgGTATGTTATCGCCATATTC
NleH1 LOV 3 KpnI	CGCggtaccAATTTTACTTAATACCACAC
NleH2 LOV 5 NdeI	GTTGAAAcatatgTTATCGCCCTC
NleH2 LOV 3 KpnI	GGATAAAAggtaccTATCTTACTTAATAC
pJ284F	CGCTCAAGGCGCACTCCCG
eLOVR	CCGTCCCTGATCAGTCTCCGGG

## 2.5.3 Analysis of bacterial fluorescence

### 2.5.3.1 Population based assay

Constructs pAHE8 and 18-22 were assessed by growing ZAP193, and their mutants where indicated, transformants overnight in LB+Chl media then the

next morning diluted to a final OD<sub>600nm</sub> of 0.08 into 20ml DMEM+Chl or MEM+Chl in 100ml Erlenmeyer flasks. Flasks were incubated at 180rpm, 37°C. At hourly intervals, 1ml of culture was removed from the flask, an OD<sub>600nm</sub> measurement taken using spectrophotometer, and 200 µl aliquots were analysed in triplicate in a clear 96 flat-well microtitre plate (Costar, UK) using FLUOstar plate reader (BMG Labtech, UK). For any combination of strain and medium, cultures containing promoterless gfp (pAJR70) acted as a control for background fluorescence. Background fluorescence was plotted against OD<sub>600nm</sub> using Microsoft Excel software and a line of best fit obtained. Using this method, data were corrected for background fluorescence, and the corrected data was plotted using GraphPad Prism 5 (GraphPad Software, USA).

### 2.5.3.2 Single cell analysis

Expression of gfp in individual bacteria was analysed by fluorescence microscopy. Strains were grown in MEM and at OD<sub>600nm</sub> 0.8, a 100 µl aliquot was removed and diluted 1:1 in 4% paraformaldehyde (PFA; Sigma, UK). 20 µl was dried onto a microscope slide and EspA filaments stained as described previously (Roe *et al.*, 2003). Briefly, 20 µl of α-EspA antibody diluted to 1:100 in Phosphate Buffered Saline (PBS) + 0.1% BSA was incubated on each spot overnight at 4°C in a humidity chamber. The primary antibody was washed off with three 5 minute washes in PBS + 0.1% BSA; 20 µl α-rabbit AlexaFluor-555 conjugated secondary antibody (1:1000; Invitrogen, UK) was then incubated on each spot for 45 minutes at room temperature in the dark. After four 5 minute washes with PBS + 0.1% BSA, the spots were dried before a coverslip was mounted with fluorescence mounting media (Dako, USA).

The slides were examined on a Zeiss M1 Axioskopp microscope, using the appropriate filter sets and x100 objective, a Z-stack of 16 images was captured at a spacing of 0.15 µm using Volocity software (PerkinElmer, UK). These images were used to create a composite image that reduces the spatial effects of bacteria in different focal planes. The average gfp units per voxel (cubic pixel) was quantified, for at least 100 bacteria with a minimum volume of 4 µm<sup>3</sup>, using Volocity Quantification software. These values were exported and plotted in GraphPad Prism 5 (GraphPad Software, USA).

### 2.5.3.3 Upon contact with host cells

Embryonic bovine cells (German Collection of Microorganisms and Cell Cultures, no. ACC192) were prepared and cultured as described previously (Roe et al., 2004). Typically, cells were cultured in MEM (M2279; Sigma, UK) supplemented with 1mM L-Glutamine, 10% Foetal Calf Serum (FCS; Invitrogen), 100 U/ml penicillin and 100 µg/ml streptomycin. Cells were seeded at a density of  $1 \times 10^5$  into an 8-chamber microscope slide (Nunc/ThermoScientific, UK) and incubated at 37 °C, 5% CO<sub>2</sub> for at least 24 hours before bacterial co-culture.

ZAP193 transformed with the appropriate GFP reporter plasmids were cultured in MEM-HEPES to OD<sub>600nm</sub> = 0.8 at 37 °C, added to the multichamber slide at a multiplicity of infection (MOI) of 100:1, and centrifuged onto the EBL cells (1000xg) for 5 min, to begin the infection. Time points analysed were 0, 5, 30 and 180 min after infection. ZAP193 strain transformed with the appropriate iLOV reporter plasmids were cultured in MEM-HEPES + IPTG to OD<sub>600nm</sub> = 0.6 at 37 °C, before addition to the EBL cells. The cells were stained at intervals by removal of the culture and addition of CellMask™ Deep Red plasma membrane stain (5 µg/ml; Invitrogen), incubated for 5 minutes at 37 °C/5% CO<sub>2</sub>, washed in PBS three times, before addition of 4% PFA to fix the cells. After 20 minutes, the slide was washed with PBS two times and a coverslip applied with fluorescence mounting media (Dako, USA).

Images were acquired on a Zeiss M1 Axioskopp at x100 magnification; z-stacks are acquired using Volocity software (PerkinElmer, UK) with 0.15 µm spacing between images for 4 µm. Z-stack images were used to create a composite image where background and refractive light fluorescence is reduced. Volocity software allows 3D restoration and the ability to manipulate the composite image and view from different aspects.

## 2.6 Quantitative PCR (Q-PCR)

Triplicate ZAP193, ZAP193 $\Delta$ *grlA* and ZAP193 $\Delta$ *ler* were cultured in MEM-HEPES media to an OD<sub>600nm</sub> = 1.2. Bacterial pellets were suspended in RNAProtect Bacteria Reagent (QIAGEN, UK). Total RNA was extracted using RNeasy Mini kit (QIAGEN, UK) and cDNA synthesis was carried out using a QuantiTect™ Reverse Transcription kit (QIAGEN, UK). Duplicate Q-PCRs were carried out using a Quantifast™ SYBR® green PCR kit (QIAGEN, UK) and Stratagene MX3000 and primers listed in Table 2-5. All the experiments were performed according to manufacturer's instructions. The RNA extraction, cDNA synthesis and Q-PCR were carried out by Dr Dai Wang.

**Table 2-5 Q-PCR primers**

Primer	Sequence 5' → 3'
H1 RT F	CCGAGTGTGGACTATAACAGGTTG
H1 RT R	TCGTTGTCACCTCTTCATTGC
H2 RT F	GCCGAGGGTTAGCAACAATA
H2 RT R	ACGAACTTCGCTTGTACCT

## 2.7 Construction of NleH knockouts

There are two methods developed for gene deletions and gene replacements in pathogenic *E. coli*; Lambda Red-mediated recombination and allelic exchange with a suicide vector.

### 2.7.1 Rationale of Lambda Red-mediated recombination

This technique uses the Red recombinase enzyme from bacteriophage Lambda ( $\lambda$ ) to recombine linear fragments of DNA into the bacterial chromosome. This enzyme and Gam, an  $\alpha$ -RecBCD exonuclease, is provided to the *E. coli* strain to be mutated in a low copy temperature sensitive plasmid, named pKM201 (Murphy & Campellone, 2003). Homologous DNA sequence which flanks the gene of interest is added to a chosen antibiotic resistance cassette by PCR. Gene deletions can be made with only 50bp of homologous sequence in *E. coli* K-12 strains (Datsenko & Wanner, 2000), however due to the lower efficiency of recombination in *E. coli* O157:H7 strains, the homologous sequence flanking the Kan cassette was increased to 500bp.

Once the PCR product for recombination has been constructed, an *E. coli* O157:H7 strain which has previously been transformed with pKM201 is made electrocompetent as follows. 20ml of pre-warmed (30°C) LB+Amp is inoculated with four colonies of *E. coli* O157:H7 pKM201 and incubated at 30°C, 180rpm until  $OD_{600nm} = 0.4$ . Red recombinase and Gam endonuclease production is induced by addition of IPTG (1mM) for 75 minutes at 30°C. The cells are heat shocked for 15 minutes at 42°C before chilling on ice for 10 minutes. The culture is centrifuged at 4,000rpm for 10 minutes, 4°C. The cell pellet is resuspended in 2ml ice-cold 20% glycerol, and centrifuged again as before but only for 3 minutes. The cell pellet was resuspended in 1ml ice-cold 20% glycerol and transferred to a 1.5ml centrifuge tube. The mixture was centrifuged in at 8,000rpm for 1 minute, 4°C, and the pellet resuspended in 400  $\mu$ l ice-cold 20% glycerol. To an 80  $\mu$ l aliquot of competent cells, 50-1000 ng PCR product (in a maximum volume of 15  $\mu$ l) was added prior to transfer to a pre-chilled electroporation cuvette (Bio-Rad, UK). The sample was electroporated as described in Section 1.1.

### **2.7.2 Rationale of allelic exchange**

The technique uses Chl, Kan and levansucrase (SacB) as positive selection markers on a temperature sensitive plasmid (Emmerson *et al.*, 2006). The plasmid is first transformed into the strain of choice at 28°C (Figure 2-2, A). Positive colonies are then subjected to periods of high temperatures (42°C) and antibiotic selection (Chl), to promote a recombination event in the homologous sequence adjacent to the gene of interest (Figure 2-2, B), integrating the plasmid into the chromosome. The culture is then returned to low temperature (28°C) and antibiotic selection (Kan) and this selects bacteria where a second homologous recombination event has occurred, thereby excising the plasmid from the chromosome (Figure 2-2, C). After overnight culture in LB to promote plasmid loss, successful recombinants are selected for the Kan<sup>R</sup>Chl<sup>S</sup> phenotype, by replica plating on LB+Kan and LB+Chl plates (Figure 2-2, D). To inhibit selection of bacteria which have not resolved the plasmid, replica plating can also be carried out on 6% sucrose agar without sodium chloride. This media inhibits growth of strains which have retained the SacB cassette as levansucrase cleaves sucrose resulting in toxic levels of levans. The kanamycin cassette can be excised from the chromosome by transforming the plasmid pCP20 into successful recombinants; this temperature sensitive plasmid expresses FLP recombinase which catalyses the recombination between two neighbouring FRT sites, flanking the Kan gene, generating a clean deletion (Figure 2-2, E).

Although suicide-driven allelic exchange vectors provide a method of targeted gene manipulation, it should be noted that inadvertent secondary mutations in the neighbouring sequence to the gene manipulated has been previously reported.

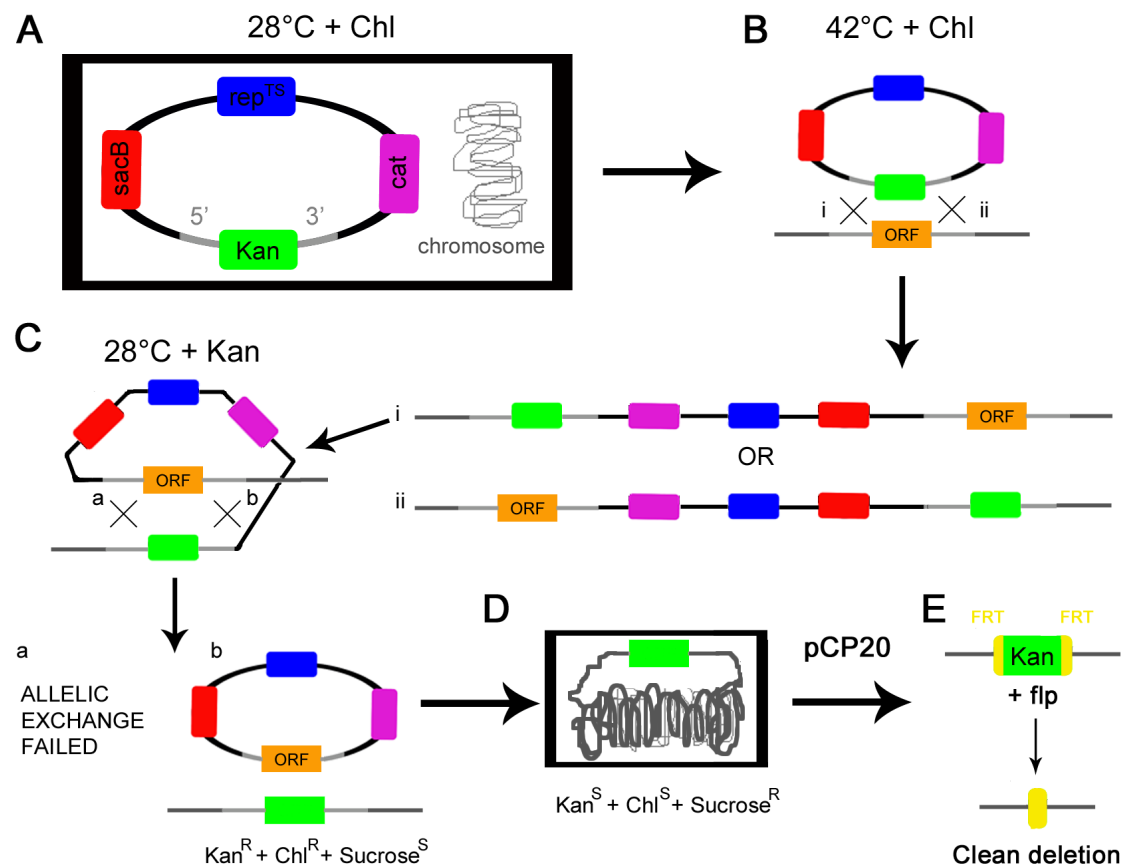


**Figure 2-2 Allelic exchange gene replacement and deletion.** The figure was adapted from (Emmerson *et al.*, 2006). **A.** The allelic exchange vector carries a temperature sensitive system of replication ( $rep^{TS}$ ), the chloramphenicol transferase ( $cat$ ) gene to confer chloramphenicol resistance, the levan sucrose ( $sacB$ ) gene which is toxic to *E. coli* in the presence of sucrose and a kanamycin ( $Kan$ ) gene to confer kanamycin resistance, flanked by the homologous upstream (5') and downstream (3') sequence to the chromosomal gene to be replaced (ORF). This plasmid is transformed into the strain and transformants selected on LB+Chl plates at 28°C. **B.** The transformant is then grown at 42°C in LB+Chl, which is not permissible for plasmid replication, and the plasmid integrates into the chromosome, generating two possible primary integrants (i and ii). **C.** Primary integrant i is grown at 28°C in LB+Kan, which allows the plasmid to replicate so a second recombination event (a or b) occurs, excising it from the chromosome. This can result in the original plasmid excising from the chromosome, leaving the ORF in the chromosome (a) or replacing the ORF with the Kan cassette (b). **D.** The recombinants are grown in LB to promote plasmid loss, then replica plated on LB+Kan and LB+Chl plates to select the colony with the correct recombinant phenotype Kan<sup>R</sup>Chl<sup>S</sup>. The addition of sucrose to media inhibits the growth of strains which retain the SacB cassette. **E.** Transformation of pCP20 into the recombinant can generate a clean deletion by excising the kanamycin cassette through recombination of the flanking FRT sites catalysed by FLP recombinase expressed by the plasmid.

## **2.7.3 Creation of DNA products for knockouts**

### **2.7.3.1 In-Fusion cloning**

This cloning method uses a Vaccinia virus DNA polymerase which has 3' → 5' exonuclease activity which exposes a 15bp fragment of single stranded DNA allowing it to anneal to complementary sequence (Hamilton *et al.*, 2007). Transformation of the construct into *E. coli* then repairs any gaps or nicks in the DNA sequence (Zhu *et al.*, 2007). This allows not just the cloning of one sequence into any vector of choice, but the possibility to clone multiple fragments into the same vector. First, the three PCR sequences are amplified, 5' NleH flank, Kan cassette and 3' NleH flank using primers listed in Table 2-6, with the homologous sequences introduced for complementary base-pairing when exposed by the In-Fusion enzyme. The vector of choice, in this case pUC18, linearised with EcoRI and HindIII, and all the fragments are mixed together with the In-Fusion reaction mix, Figure 2-3 A. This is then transformed into XL1-Blue competent *E. coli* as described in Section 1.1, and selection is through blue-white screening.

**Table 2-6 Primers for NleH knockouts**

Primer	Sequence
NleH1.3.R	CTCCTAGTCTGGAAGAGTTG
NleH1.5.F	GTACAGGTCCATTGCAGCAAC
NleH1.ext.F	CAACAGTACAGCTATAAATCG
NleH1.ext.R	CCACAGGGATATTCAACTGC
NleH1.nest.F	GGCTTAAAGCTTGTATTAATC
NleH1.nest.R	GCCAATCTTATCGAGTGCTG
NleH1.P1.5.R	GGAACTTCGAAGCAGCTCCAGCCTCATTTCAAC CTTCAAATAAACC
NleH1.P2.3.F	GGATATTCATATGGACCATGGCTAATTCCCAGT GTAGTGGATTTGTTGC
NleH2.3.R	CCATATAGCTCTGAAGAGTG
NleH2.5.F	GCGGAAACCGCTTTACCTTCTGCG
NleH2.ext.F	GCTGCACGGGTTGTTGTTAC
NleH2.ext.R	GTAAGTAAGATCTGGTACCC
NleH2.nest.F	CAGTGAGCGGTTTGTCCGGC
NleH2.nest.R	CTTTGCCTTGTCTACTTTCTC
NleH2.P1.5.R	GGAACTTCGAAGCAGCTCCAGCCTCATTTCAAC CTTCAAATAAACC
NleH2.P2.F3	GGATATTCATATGGACCATGGCTAATTCGTTAA GGGGGTTTTGATATG
P1 cassette 5	GTGTAGGCTGGAGCTGCTTC
P2 cassette 3	ATGGGAATTAGCCATGGTCC

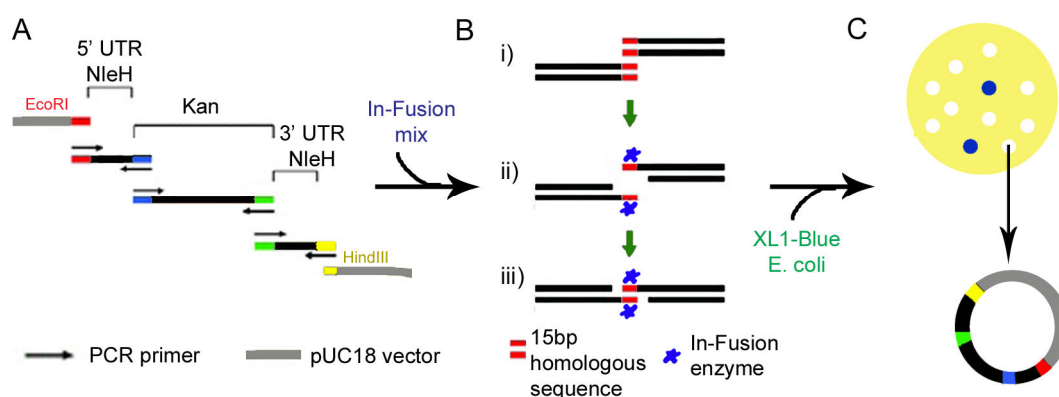


**Figure 2-3 In-Fusion cloning of multiple fragments into a single vector**

The method used to genetically fuse multiple DNA fragments together in a single reaction. First, the DNA fragments are amplified using primers that add 15bp of homologous sequence to the ends of each fragment (A). The PCR products and linearised pUC18 vector were mixed together with the In-Fusion mix, which contains In-Fusion enzyme. The In-Fusion enzyme binds to double stranded DNA ends (Bi) and with its 3'→5' exonuclease activity exposes single strand DNA (Bii) allowing it to pair with homologous sequence (Biii). Transformation of the mixture into *E. coli* results in antibiotic resistant clones (C), where blue colonies are pUC18 plasmid parent and white colonies contain the insert, interrupting the β-galactosidase gene. The figure was adapted from (Zhu *et al.*, 2007).

### 2.7.3.2 Splice overlap extension PCR

In-Fusion cloning was unsuccessful for NleH2 after three attempts, so the homologous sequence introduced into each PCR product was utilised for splice overlap extension, whereby during the PCR reaction, the single strands of DNA can complementary base-pair over the homologous region, allowing a PCR product to be amplified across using a forward primer that binds to one product and the reverse primer binds to the other. Constructing one PCR product from three individual PCR products in a single reaction was difficult therefore it was approached in a step-by-step process as follows. The 5' NleH flank, Kan cassette and 3' NleH flank were amplified and the PCR products cleaned of dNTPs and buffers using QIAGEN PCR purification kit. The 5' NleH flank and Kan cassette PCR products were mixed (3:1 ratio) to provide template for a PCR reaction with NleH 5 primer and Kan cassette R (P2) primer. Similarly, 3' NleH flank and Kan cassette PCR products mixed with NleH 3 primer and Kan cassette F (P1) primer. These doublet PCR products were cleaned again and mixed together to construct the final product of Kan cassette flanked with NleH 5' and 3' flanking sequence.

### 2.7.3.3 Allelic exchange vectors

As constructs had been made previously with the Kan cassette flanked with the NleH 5' and 3' UTR sequence (NleHKanflank), this was sub-cloned into a temperature sensitive plasmid with a Sac cassette alone. The Kan cassette from pTOF24 (Kan<sup>R</sup>Chl<sup>R</sup>) was excised by PstI digest and religated to create pKO3b (Kan<sup>S</sup>Chl<sup>R</sup>; named as not original pKO3 (Link *et al.*, 1997)). The NleHKanflank sequence was amplified using the nest primers that sit within the flanking sequence, phosphates added to the ends using T4 polynucleotide kinase (NEB, UK) and sub-cloned into PstI digested pKO3b that had its overhang ends blunted using T4 Klenow (large) fragment (NEB, UK). This resulted in Kan<sup>R</sup>, Chl<sup>R</sup> and sucrose sensitive allelic exchange vectors: pKO3bH1 and pKO3bH2. These constructs were then transformed into the indicated *E. coli* O157:H7 strains and allelic replacement performed as described in Section 2.7.2.

## 2.8 Transfection of HEK293T cells

HEK293T cells were cultured in DMEM (21989-0342; GIBCO/Invitrogen, UK) supplemented with 2mM L-Glutamine, 10% foetal calf serum (FCS), 100 U/ml penicillin and 100 µg/ml streptomycin. Per well in 24 well plates, cells were seeded at a density of  $5 \times 10^4$ , incubated at 37°C/5% CO<sub>2</sub> for 24 hours to reach 70-90% confluence, and transfected with 0.4 µg of control/expression plasmid (Table 2-7), 0.4 µg NF-κB luciferase plasmid and 0.1 µg β-galactosidase plasmid. GeneJuice (Merck, UK) transfection reagent was used as per manufacturer's instructions for transfecting 1 µg DNA. 40 hours after transfection, one half of the plate was stimulated by adding TNF-α (25 ng/ml). Following 24 hours stimulation, cells were washed twice with PBS before adding 250 µl lysis buffer from Dual-Light® System (Applied Biosystems). 20 µl of lysate from each well was assayed in duplicate for luciferase and, 60 minutes later, β galactosidase using a Lumat single tube Luminometer LB9507 (Titertek-berthold, Germany). Luciferase activity was determined and normalized to β galactosidase activity as described (Philpott *et al.*, 2000). Each experimental condition was performed in triplicate, and repeated three times.

**Table 2-7 Plasmids used for NF-κB assay in HEK293T cells**

Plasmid	Description	Source
<i>lacZ</i>	B-galactosidase enzyme constitutively produced by mammalian expression vector	Stratagene
NF-κB <i>luc</i>	Firefly luciferase gene under the control of canonical NF-κB promoter	Stratagene
pCMVTag3A	N-terminal myc tagging mammalian expression vector	Stratagene
pCMV-NleH1	NleH1 ORF cloned into PstI + HindIII digested pCMVTag3A	Prof Tom Evans
pCMV-NleH2	NleH2 ORF cloned into PstI + HindIII digested pCMVTag3A	Prof Tom Evans
pCMV-NleH1(D258)	Site directed mutant (SDM) of NleH1 residue D258 to alanine (A)	Prof Tom Evans
pCMV-NleH1(E173)	SDM of NleH1 residue E173 to alanine (A)	Prof Tom Evans
pCMV-NleH1(K159A)	SDM of NleH1 residue K159 to alanine (A)	Prof Tom Evans
pJ201-OspG	OspG ORF with PstI + HindIII sites	DNA2.0
pCMV-OspG	OspG ORF cloned into PstI + HindIII digested pCMVTag3A.	AH This study

## 2.9 2-D Fluorescence Difference Gel Electrophoresis (2-D DIGE)

2-D DiGE was carried out in collaboration with Professor Richard Burchmore and Mr Alan Scott at the Sir Henry Wellcome Functional Genomics Facility (SHWFGF) in order to try and elucidate the human protein target of NleH1 kinase activity.

HEK193T cells were seeded into four 6-well tissue culture plates (Costar, UK) at a density of  $1 \times 10^6$  cells/well. After 24 hours incubation, each well of cells were transfected with GeneJuice (Merck, UK) and 4  $\mu$ g DNA; 12 wells with pCMV-NleH1 and the other with kinase dead mutant, pCMV-NleH1(K159A). After 16 hours incubation at 37°C, 5% CO<sub>2</sub>, cells were stimulated with 1.5ml TNF- $\alpha$  (25 ng/ml) for 20 minutes prior to harvesting. Cells were washed gently in pre-warmed PBS, 0.5ml trypsin added to each well, the plate incubated at 37°C for 5 minutes to allow the cells to detach. The cells were transferred to a 15ml falcon tube (Corning) including a PBS wash of the wells to ensure all cells were harvested. The cells were centrifuged (1500xg, 3 minutes) and resuspended in culture media to inactivate the trypsin. The cells were washed in pre-warmed PBS 3 times, with as much of the PBS removed as possible for the cell pellet to be then frozen at -80°C for DiGE sample preparation.

The DiGE sample preparation, gel casting, electrophoresis and scanning were all carried out with Alan Scott. The cell samples were defrosted on ice, resuspended in 1ml ice-cold lysis buffer (6M urea, 2M thiourea, 4% CHAPS, 25mM tris base) supplemented with 100  $\mu$ g/ml Dnase, 5 mM MgCl<sub>2</sub> and protease inhibitor cocktail (P9599; Sigma, UK), sonicated briefly for 1-2 seconds on, 1 minute off; for 3 cycles on ice. After 10 minute incubation at room temperature with gentle mixing, the sample was centrifuged at 13,000xg for 10 minutes to pellet any insoluble material. The proteins from the supernatant were acetone precipitated at -20°C overnight. The precipitated proteins were then washed in 80% acetone and dried before resuspending in DiGE lysis buffer. The proteins were then Cy<sup>TM</sup> labelled; 10  $\mu$ l NleH sample (50  $\mu$ g) was labelled with Cy3 and 10  $\mu$ l K159A sample (50  $\mu$ g) with Cy5. Once the two samples are thoroughly mixed together, 500  $\mu$ l rehydration buffer (6M urea, 2M thiourea, 4% CHAPS, 0.5% IPG buffer, 65 mM dithiothreitol (DTT), trace bromophenol blue) was added before

being applied to an IPG strip, pH4-7. Isoelectric focusing is performed by applying the IPG strip with sample on an IPGphor system (Amersham, UK) and proteins separated at 8000V applied in a stepwise manner; 10-15 hours at 30 V (IPG strip rehydration step), 2 hours at 300 V, 2 hours gradient to 600 V, 2 hours gradient to 1000 V, 3 hours gradient to 8000 V, 8 hours at 8000 V. The strip equilibrated with SDS and is then applied to the top of a 12% SDS-PAGE gel and run overnight to separate the proteins based on their molecular weight. The 2D-gel is scanned on Typhoon 9400 (GE Healthcare Life Sciences, UK) which exposes the gel to the appropriate wavelengths to excite each of the CyDye labels and an image captured. These images were first cropped by Imagequant software and then loaded into DeCyder 5 software (GE Healthcare Life Sciences, UK) for analysis, and this DIGE analysis was carried out with Prof Richard Burchmore.

## 2.10 Yeast-two hybrid analysis

Yeast-two hybrid (Y2H) was first described as a method to detect protein-protein interactions in 1989 (Fields & Song, 1989). This system takes advantage of the Gal4 transcription factor from *Saccharomyces cerevisiae* which consists of two separate but equally essential functional domains; the DNA binding domain (DBD) which binds the promoter and an activation domain (AD) which recruits the transcription complex. By genetically fusing protein X to the DBD (bait) and protein Y to the AD (prey), protein-protein interaction can be determined by the transcription of a reporter gene which can only occur when the DBD and AD are restored to close proximity.

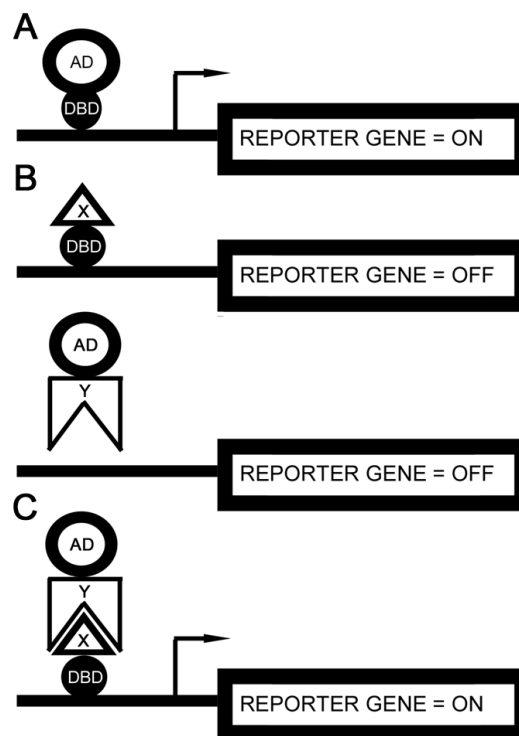


**Figure 2-4** The yeast-two hybrid system

**A.** Transcription factors consist of two functional domains, the DNA binding domain (DBD) and activation domain (AD), which act together to activate transcription of genes, **B.** as individual protein hybrids (X:DBD or Y:AD) these domains cannot induce transcription. **C.** When the domains are brought to close proximity through hybrid (X+Y) protein-protein interactions, transcriptional activity is restored. Figure is based upon (Fields & Song, 1989).

To identify the eukaryotic protein(s) which interact with NleH1 or NleH2, yeast-two hybrid analysis was carried out in collaboration with Prof Jurgen Haas, University of Edinburgh, Dr Peter Uetz and Dr Thorsten Stellberger at the Institute of Toxicology and Genetics, Karlsruhe, Germany, where they have a high-throughput robot-assisted Y2H assay in 96- well plate format (Uetz *et al.*,

2000; Rajagopala *et al.*, 2007; Stellberger *et al.*, 2010). The system uses the Gateway® cloning system to create expression vectors of either bait (DBD) or prey (AD) (Stellberger *et al.*, 2010). Gateway® entry clones of *E. coli* O157:H7 NleH1 and NleH2 were constructed as follows. NleH1 and NleH2 ORF were PCR amplified from pAHE27 and pAHE28 respectively and then a second round of PCR was carried out to add the full attB recombination sites to 5' and 3' of the PCR sequence. The primers used are detailed in Table 2-8. The NleH-attB flanked PCR product was then cloned into pDONR207 using BP Clonase II™ as per manufacturer instructions (Invitrogen, Scotland). This Gateway®-NleH entry clone was then electroporated into DH<sub>10</sub>B *E. coli* and 250 µl SOC media added for recovery at 37°C for 1 hour, shaking at 180rpm. 25 µl and 100 µl of culture was plated on LB+Gent plates and incubated at 37°C overnight. Gentamycin resistant colonies were picked and plasmid DNA purified as described previously, and plasmid confirmed for presence of correct insert by restriction digest analysis. The NleH entry clones were then sent to University of Edinburgh, to introduce the NleH1 and NleH2 genes into the yeast-two hybrid Gateway® expression clone pGBKT7-DEST (bait), via an LR recombination reaction (Stellberger *et al.*, 2010). The bait clones are transformed into yeast strain AH109 and screened against an array of yeast strain Y187 transformed with human cDNA prey (pGADT7-DEST) clones, in a high throughput approach previously described (Uetz *et al.*, 2000).

**Table 2-8 Primers used to create Y2H entry clones**

Primer	Sequence (5' → 3')
NleH1 Y2H F	AAAAAGCAGGCTCCGCCATGTTATCGCCATATTC
NleH1 Y2H R	AGAAAGCTGGGTCTTACTTAATACCACAC
NleH2 Y2H F	AAAAAGCAGGCTCCGCCATGTTATCGCCCTC
NleH2 Y2H R	A GAA AGC TGG GTC TTA
attB1 F	GGGGACAAGTTTGTACAAAAAAGCAGGCT
attB2 R	GGGGACCACTTTGTACAAGAAAGCTGGGT

## 2.11 *S. pneumoniae* codon-optimised constructs

### 2.11.1 *Fluorescent proteins and pneumolysin*

The coding sequences of monomeric GFP, YFP and RFP from Evrogen and pneumolysin from TIGR4 were codon-optimised and synthesised by DNA2.0 into pUC-based vectors. Also included in the design was the introduction of His, FLAG and Lumio (FLaSH) tags at the N-terminus of the sequence, an NdeI restriction site at the ATG start codon and an AgeI restriction site before the stop codon of the fluorescent proteins or the start methionine of pneumolysin. The pneumococcal *ami* promoter was chosen to control transcription of the codon-optimised protein as it has been shown to be constitutive in the pneumococcus (Claverys *et al.*, 1995). The constructs received from DNA2.0 are listed in Table 2-9. As the constructs could only be propagated in *E. coli*, the designed inserts were subcloned into an *E. coli-Streptococci* shuttle vector, pAL2YI. The inserts from pAHE1-5 were liberated by Aval digest, and pAHE6 by NcoI and AclI digest, then subcloned into pAL2YI. The NdeI and AgeI sites were used to create a construct with rfp gene alone, whereby the rfp gene was digested out of pAHE6, subcloned into the backbone of pAHE5 to provide the stop codon before a final subclone step into the shuttle vector. This strategy was repeated to create a number of constructs with pneumolysin genetically fused to a fluorescent protein at its N-terminus, Table 2-9.

**Table 2-9 Pneumolysin and fluorescent protein constructs**

Construct	Description (3 tags = His, FLAG, Lumio)	Source
pAHE1	3 tags: Domains 1, 2 and 3 pneumolysin (TIGR4)	DNA2.0
pAHE2	3 tags: Domain 4 pneumolysin (TIGR4)	DNA2.0
pAHE3	3 tags: Pneumolysin (TIGR4)	DNA2.0
pAHE4	3 tags: Green Fluorescent Protein	DNA2.0
pAHE5	3 tags: Yellow Fluorescent Protein	DNA2.0
pAHE6	3 tags: Red Fluorescent Protein: Pneumolysin (TIGR4)	DNA2.0
pAL2YI	Shuttle vector; derivative of pVA838 (Macrina <i>et al.</i> , 1982)	(Ibrahim <i>et al.</i> , 2004)
pAHE11	3tags: GFP-Ply [AgeI+NotI digest pAHE4 to give GFP:3tags insert, ligated into pAHE3 to tag Ply]	AH
pAHE12	3 tags: YFP-Ply[AgeI+NotI digest pAHE5 to give YFP:3tags insert, ligated into pAHE3 to tag Ply]	AH
pAHE13	3 tags: Red Fluorescent Protein [AgeI+NotI digest pAHE6 to give RFP:3tags insert, ligated into pAHE5]	AH

pAHE14	3 tags: GFP-Domain4 [Agel+NotI digest pAHE4 to give GFP:3tags insert, ligated into pAHE2 to tag Ply Domain 4]	AH
pAHE15	3 tags: YFP-Domain4 [Agel+NotI digest pAHE5 to give YFP:3tags insert, ligated into pAHE2 to tag Ply Domain 4]	AH
pAHE16	3 tags: RFP-Domain4 [Agel+NotI digest pAHE6 to give RFP:3tags insert, ligated into pAHE2 to tag Ply Domain 4]	AH
pAHE24	3tags: GFP-Domains123 [Agel+NotI digest pAHE4 to give GFP:3tags insert, ligated into pAHE1 to tag Ply Domain 123]	AH
pAHE25	3 tags: YFP-Domains123 [Agel+NotI digest pAHE5 to give YFP:3tags insert, ligated into pAHE1 to tag Ply Domain 123]	AH
pAHE26	3 tags: RFP-Domains123 [Agel+NotI digest pAHE6 to give RFP:3tags insert, ligated into pAHE1 to tag Ply Domain 123]	AH
pAHS1	Ply Domain 1-3; 3 tags [Aval digest from pAHE1 cloned into pAL2YI]	AH
pAHS2	Ply Domain 4; 3 tags [Aval digest from pAHE2 cloned into pAL2YI]	AH
pAHS3	Ply; 3 tags [Aval digest from pAHE3 cloned into pAL2YI]	AH
pAHS4	gfp++; 3 tags [Aval digest from pAHE4 cloned into pAL2YI]	AH
pAHS5	yfp++; 3 tags [Aval digest from pAHE5 cloned into pAL2YI]	AH
pAHS6	rfp-Ply; 3 tags [AclI + NcoI digest from pAHE6 cloned into pAL2YI]	AH
pAHS7	gfp-Ply Domain 4; 3 tags [Aval digest from pAHE14 cloned into pAL2YI]	AH
pAHS8	rfp++; 3 tags [Aval digest from pAHE13 cloned into pAL2YI]	AH
pAHS9	YFP-Ply Domain 4; 3 tags [Aval digest from pAHE15 cloned into pAL2YI]	AH
pAHS11	GFP-Ply Domain 1-3; 3 tags [Aval digest from pAHE24 cloned into pAL2YI]	AH

### **2.11.2 *Transcriptional reporter construct***

To assess the application of the fluorescent proteins as a transcriptional reporter, a shuttle vector had to first be constructed with a promoterless YFP gene. The cloning strategy was designed to PCR amplify YFP introducing restriction enzyme sites at its 5' and 3' ends to subclone into pAL2YI in a

suitable position where there was an additional restriction site available upstream to enable subsequent subcloning of putative promoters for testing. pAL2YI has *Stu*I, *Nco*I and *Acl*I sites in close proximity to allow the strategy, Figure 2-5.

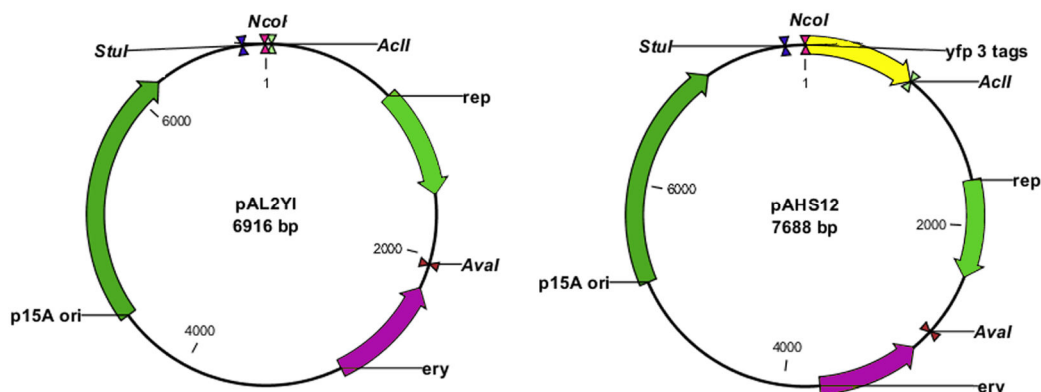


**Figure 2-5 Promoterless YFP construct pAHS12**

The molecular biology to create pAHS12 was carried out by Sultan Al-Sharif, a Masters student at the time. To assess the efficacy of the expression vector, three putative promoters of *NanA* (Camara *et al.*, 1994) were cloned into pAHS12, Figure 2-6, to control expression of YFP. Primers used are detailed in Table 2-10.

**Table 2-10 Primers used for transcriptional reporter constructs**

Primer	Sequence	Construct
YFP <i>Nco</i> I 5'	CGCCCTTGAACGTTTTAACCGG	pAHS12
YFP <i>Acl</i> I 3'	GGATAACCCATGGCTAATAAACATC	pAHS12
<i>NanA</i> promoter <i>Stu</i> I 5'	GTTTCGATAGGCCTTGAGCAGGAAG	-246/-291/-405 <i>NanA</i> pAHS12
-246 <i>NanA</i> <i>Nco</i> I 3'	GAAATAAGCCATGGACTCCAGAAAATGC	-246 <i>NanA</i> pAHS12
-291 <i>NanA</i> <i>Nco</i> I 3'	CTCCGATCCATGGTGATCCTCTC	-291 <i>NanA</i> pAHS12
-405 <i>NanA</i> <i>Nco</i> I 3'	GCCCCTTCCATGGCTAAAACAGGAG	-405 <i>NanA</i> pAHS12



**Figure 2-6 Putative promoter sequences of *NanA* cloned upstream of YFP**

## **2.12 Transformation of *S. pneumoniae***

*S. pneumoniae* were grown in 10ml BHI with 1mM CaCl<sub>2</sub> until an OD<sub>600nm</sub> of 0.1 was reached. Aliquots of 1ml of the culture were prepared, and 100 ng/ml competence stimulating peptide 1 (CSP-1, Sigma-Aldrich, UK) for type 2 pneumococci, or CSP-2 for type 4, was added to induce uptake of extracellular DNA. Samples were then incubated at 37°C for 15 min before addition of 500ng DNA and a further incubation at 37°C for 75 min. Samples were then plated on BAB + 5% horse blood and Ery or Chl where required.

## **2.13 Characterisation of codon-optimised proteins**

### **2.13.1 *Preparation of samples***

Strains were grown statically at 37°C in 15ml BHI until OD<sub>600nm</sub> = 0.6, centrifuged at 4,000xg for 15 minutes, 4°C in a 4K15 centrifuge (Sigma, UK). The supernatant was discarded and the pellet resuspended in 1ml PBS, and the sample sonicated at 10 microns for 30sec with 30sec rest on ice, for 3 cycles, using a Soniprep 150 sonicator (MSE, UK). The sonicated pellet was centrifuged at 13,000rpm for 1 min to pellet membranes and insoluble proteins.

The protein concentration of pneumococcal lysates was measured using Qubit<sup>®</sup> Protein Assay kit and fluorimeter (Invitrogen, Scotland) as per manufacturer's instructions.

### **2.13.2 *SDS-PAGE and western blotting***

Samples were mixed 3:1 in NuPAGE sample buffer (x4; Invitrogen) and boiled at 72°C for 12 minutes before loading 10 µl onto gel. Gels used were either a NuPAGE 4-12% Bis-Tris pre-cast SDS-PAGE gel (Invitrogen) or 10% polyacrylamide gel, where indicated. SeeBlue+2 (Invitrogen, UK) marker was used throughout. SDS-PAGE gels were stained overnight in Coomassie stain (500ml dH<sub>2</sub>O, 400ml

methanol, 100ml acetic acid, 0.5g Coomassie blue R250), and destained with destain solution (500ml dH<sub>2</sub>O, 400ml methanol, 100ml acetic acid) until clear.

For western blot, proteins were transferred using Sure-Lock Cell Blotting Module (Invitrogen) onto PVDF membrane at 30V for 75 minutes, then blocked in 3% skimmed milk (Marvel, UK) in Tris NaCl, pH 7.4 (10mM Tris, 150mM NaCl, 8mM HCl). Primary antibody was applied for 2-3 hours at 37°C diluted in 3% skimmed milk in Tris NaCl, pH7.4; α-FLAG® (#200471; Stratagene, UK) at 1:5000 dilution, α-Ply at 1:1000 dilution, α-GroEL (ADI-SPS-875; Enzo Life Sciences, UK) at 1:2000 dilution. After washing the membrane four times for 5 minutes in 100ml Tris NaCl, pH7.4 + 0.08% (v/v) Tween-20 (Sigma, UK), secondary horseradish-peroxidase (HRP) conjugate antibody, donkey α-rabbit IgG (Amersham Biosciences, UK) or goat α-mouse IgG (Promega, UK), was added to the membrane at 1:40000 dilution and incubated for 45 minutes, 37°C. After four 10 minute washes, the membrane was developed with Immobilon® Western HRP Chemiluminescent substrate (Millipore, UK).

### **2.13.3 Haemolytic assay**

The haemolytic activity of Ply in culture lysates was measured using a haemolytic assay previously described (Walker *et al.*, 1987), with modifications.

Briefly, doubling dilutions of 50 µl culture lysates were made in PBS in duplicate in a round-bottomed 96-well plate (Costar, UK). A control double dilution of a 1:1000 dilution of purified Ply (0.7 mg/ml) (Mitchell *et al.*, 1989) was included in duplicate. PBS was included as a negative control. 50 µl of 10mM DTT (Sigma-Aldrich, UK) was added to each well, to act as a reducing agent for any Ply oxidised in the lysate. The plate was then incubated at 37°C for 15 min with a lid to prevent evaporation. A 2% (vol/vol) solution of sheep erythrocytes (E&O Laboratories, Scotland) was prepared and 50 µl was added to each well. The plate was then incubated at 37°C for 30 min before addition of a further 50 µl PBS, and centrifugation at 500xg for 1 minute in a 4K15 centrifuge (Sigma-Aldrich, UK) to pellet the intact erythrocytes.

The haemolytic titre of a sample was calculated from the reciprocal of the last dilution to give 100% lysis as described previously (Benton *et al.*, 1997b).

## **2.13.4 Analysis of *S. pneumoniae* fluorescence**

### **2.13.4.1 Population based assay**

20ml of prewarmed BHI with Ery where appropriate, was inoculated with  $5 \times 10^5$  cfu/ml *S. pneumoniae*. At regular time points, 1ml of culture was removed, OD<sub>600nm</sub> measured, and centrifuged at 5,000 rpm for 2 minutes. The BHI supernatant was removed and the pellet resuspended in sterile PBS. 200 µl of this suspension was aliquoted in triplicate in a 96 well flat bottom plate (Costar, UK) then analysed in a FLUOstar Optima plate reader (BMG Labtech, UK). 20 µl of the suspension was also used for viable count. Untransformed *S. pneumoniae* or strain transformed with pAHS12 provided background fluorescence levels. Data was normalised and analysed as described previously in Section 2.5.3.

### **2.13.4.2 Single cell analysis**

Pneumococcal cells expressing fluorescent proteins were grown to OD<sub>600nm</sub> = 0.6, washed in PBS three times prior to mixing 1:1 (v/v) with 4% paraformaldehyde to fix the cells. After 20 minutes incubation at room temperature, 20 µl of fixed cells were spotted onto a microscope slide and dried. A coverslip was mounted after the application of fluorescence mounting media (Dako, USA).

Images were captured on a Zeiss M1 Axioskopp microscope as described previously in Section 2.5.3.2.

## 2.14 Fluorescence microscopy of pneumococci

### 2.14.1 Immunofluorescence

*S. pneumoniae* strains were grown in BHI at 37°C until  $OD_{600nm} = 0.6$ , and 1ml of culture was centrifuged for 2 minutes at 13,000rpm. The cell pellet was washed three times and suspended in 1ml sterile PBS and 100  $\mu$ l mixed 1:1 with 4% (w/v) paraformaldehyde. After 20 minutes incubation at room temperature, 1  $\mu$ l of the fixed cells were spotted with 20  $\mu$ l PBS onto a 12 spot microscope slide. Once the spots dried, the slide was washed twice with PBS. 20  $\mu$ l of primary antibody was added per spot,  $\alpha$ -Ply (1:500),  $\alpha$ -FLAG (1:500) or  $\alpha$ -capsule (1:1000), and incubated for an hour at room temperature. The slide is washed three times with PBS + 0.1% BSA before the application of secondary antibody,  $\alpha$ -rabbit IgG AlexaFluor conjugate (Invitrogen) or  $\alpha$ -mouse IgG Northern Lights at 1:1000 dilution. After 45 minutes incubation in the dark, the slide is washed four times with PBS + 0.1% BSA, dried and a cover slip mounted with Dako fluorescent mounting media. Images were captured on a Zeiss M1 Axioskopp microscope as described previously in Section 2.5.3.3.

### 2.14.2 Lumio™ fluorescence

*S. pneumoniae* strains were grown in BHI at 37°C until  $OD_{600nm} = 0.6-0.7$ , and 1ml of culture was centrifuged for 2 minutes at 13,000rpm. The cell pellet was washed three times with sterile PBS and finally suspended in 100  $\mu$ l PBS + 0.15  $\mu$ l Lumio™ Green reagent (Invitrogen). After 15 minutes incubation in the dark, the cells were washed with PBS to remove any excess reagent and 2  $\mu$ l of cells spotted onto a microscope slide and a coverslip applied; the wet mounts were immediately viewed using a Zeiss AxioImager M1 microscope. Images were captured as described previously in Section 2.5.3.3.

## 2.15 Construction of LytA-Ply fusion in TIGR4NO1

The A45 LytA-Ply fusion was introduced into TIGR4 through homologous recombination. The LytA-Ply fusion gene with 1kb of upstream and downstream sequence was amplified from A45 using LytA forward and 27R primers. This PCR product had phosphates added to its ends using T4 polynucleotide kinase to allow it to be ligated into a Klenow treated EcoRI linearised pUC18, to create pUCLytA27R. There is a natural BamHI restriction enzyme recognition site within the fusion gene and this was exploited to introduce a Cat cassette to allow selection of successful recombinants. The Cat cassette, with *ami* promoter (Iannelli *et al.*, 2004), was amplified from FP28 gDNA using CatF and CatR primers and this was treated with T4 polynucleotide kinase and ligated into Klenow treated BamHI linearised pUCLytA27R, to create pUCLytA27R::Chl. This final construct was transformed into *S. pneumoniae* strain TIGR4NO1, as described in Section 2.12. The plasmid cannot replicate in the pneumococcus as it has an *E. coli* origin of replication, therefore TIGR4 transformants which are Chl resistant can only arise from a recombination event.

**Table 2-11 Primers for LytA-Ply fusion**

Primer	Sequence
27R	CTTGGCTACGATATTGGC
LytA upstream	CCATTTCTCTAGTGAACATCG
Cat F	CTGAAAATTTGTTTGATTTTTAATGG
Cat R	GTTTATAAAAAGCCAGTCATTAG
52Q	ATTTCTGTAACAGCTACCAACGA
52R	GAATTCCCTGTCTTTTCAAAGTC
W99F	TTGGGGGCGGTTGGAATGC
W99R	TGGTAGAGGACTTGATTCA

## 2.16 Characterisation of TIGR4NO1 $\Delta$ LytA-Ply::Chl

### 2.16.1 Confirmation of successful mutation

The successful introduction of the autolysin-pneumolysin fusion (LytA-Ply) in TIGR4NO1, resulting in no production of pneumolysin or autolysin, was confirmed by PCR, sequencing, haemolytic assay, western blotting, all as described previously, and Gram staining.

#### 2.16.1.1 Gram staining of bacteria

For Gram stain, 5  $\mu$ l of broth culture was smeared onto a microscope slide and passed through a Bunsen flame to heat-fix; an *E. coli* sample was included on each slide as a Gram negative control. The slide was flooded with crystal violet for 1 minute, rinsed with water before flooding with iodine solution for 30 seconds. This forms an insoluble complex within the bacterial cells, staining them all purple. After rinsing with water, alcohol/acetone was added for 2-3 seconds to dehydrate the cells, which traps the crystal violet stain in the Gram positive cells due to the thick peptidoglycan cell wall and decolorises the thin-walled Gram negative cells as the stain complex can escape. The slide was flushed with water and flooded finally with safranin for 1 minute to counterstain the decolorised cells pink. When Gram staining *S. pneumoniae*, a smear of *E. coli* is always included as a staining control to ensure efficient counterstaining, thus a differential stain.

## 2.17 Fractionation of *S. pneumoniae*

Pneumococcal cells were separated into cellular fractions using a fractionation protocol previously described (Price & Camilli, 2009), with modifications.

In short, strains were grown statically at 37°C in 35-50ml BHI, until OD<sub>600nm</sub> = 0.6, then 24-25ml of culture was transferred to a centrifuge tube (Beckman Instruments, CA, USA) and centrifuged at 14,100xg for 6 minutes at 4°C in 4K15 centrifuge (Sigma-Aldrich, UK) with a 12172 rotor. The broth supernatant was

carefully removed, where indicated passed through a 0.2 µm syringe filter (Sartorius Stedim Biotech, Germany), and 6% (v/v) trichloroacetic acid and 4 µg/ml BSA (Sigma, UK) added, to precipitate proteins overnight at 4°C. BSA acts as a co-precipitate and can provide an indication of equivalent preparation and loading between samples. This was then centrifuged at 4,000xg for 30 minutes at 4°C to pellet the precipitated proteins and resuspended in 70 µl 50mM Tris-HCl, pH 7.5; giving the supernatant fraction. The pneumococcal cell pellet was washed once in sterile PBS before being resuspended in 70 µl cell wall digestion buffer (10mM Tris-HCl, 30% sucrose, 1 x protease inhibitor cocktail (Roche), 1 mg/ml lysozyme, 300U mutanolysin) and incubated at 37°C for 3 hours with gentle rocking. The sample was then centrifuged 14,100xg for 10 minutes at 4°C. If the sample did not pellet well, it was transferred to a 1.5ml Eppendorf tube and centrifuged in a 1K15 centrifuge (Sigma, UK) at 14,100xg for 10 minutes at 4°C. The supernatant was removed, giving the digested cell wall fraction; and the pellet was resuspended in 70 µl 50mM Tris-HCl, pH 7.5, giving the protoplast fraction.

### **2.17.1 Cell wall digestion buffer**

It was first reported in 1975 that pneumococcal cells spontaneously form protoplasts when incubated in hypertonic solutions (Lacks & Neuberger, 1975). This technique has been used in other studies (Vijayakumar & Morrison, 1986; Neef *et al.*, 2011) but incubation temperatures and times vary. *S. pneumoniae* D39 cells were resuspended in protoplast inducing buffer (100mM Tris-HCl pH7.5, 2mM MgCl<sub>2</sub>, 1 x protease inhibitor (Roche) and 30% sucrose) and separated into 3 aliquots to test different incubation times and temperatures; 25°C for 30 minutes, 37°C for 30 minutes and 30°C for 60 minutes. After incubation, 2 µl of pneumococcal cells, treated and untreated, and 2 µl of an overnight culture of *E. coli* were heat fixed onto a microscope slide and Gram stained to detect pneumococcal cells with reduced cell wall thickness.

## 3 Expression and regulation of Non-LEE encoded effectors (Nle) H1 and H2

### 3.1 Summary

Non-LEE encoded effectors H1 and H2 were identified through a bioinformatic screen searching for homologues to over 300 known T3SS effectors in animal and plant pathogens and symbionts; shown to be secreted into the extracellular media by a *sepL* hypersecretor mutant in EHEC O157:H7, and translocated into eukaryotic cells under inducing conditions (Tobe *et al.*, 2006). The aim of this chapter was to determine whether both *E. coli* O157:H7 NleH1 and NleH2 were expressed under T3SS secretion permissive conditions when under the control of their native promoters, and if this expression was in co-ordination with the LEE. LEE expression in EHEC O157 is complex as expression of the translocon of the T3SS (EspABD) has been shown to be heterogenous and regulated at the post-transcriptional level (Roe *et al.*, 2003; Roe *et al.*, 2004). Translational fusions to *gfp* were used to assess NleH expression in the population, at the single-cell level in co-ordination with the production of EspA filaments and upon contact with host cells. The translational fusions were also tested in LEE-encoded or endogenous regulator knockout strains to assess their impact upon NleH-GFP expression.

### 3.2 Expression of NleH in different media types

Previous work has shown that the media that *E. coli* O157:H7 is grown in can affect the expression of the LEE and genes which are co-regulated with the PAI. It has been reported that T3SS proteins EspD and Tir are secreted 5-10 fold higher in MEM media compared to DMEM (Roe *et al.*, 2007). These conditions were used to identify differentially regulated genes in *E. coli* O157:H7 and genes regulated in coordination with the O157 LEE PAI. From these data (GEO accession no. GSE6296), NleH expression was shown to be differentially expressed when grown in MEM compared to DMEM, indicating it was indeed

expressed and also that it was subject to regulation. In order to determine how the two alleles are expressed and regulated, translational fusions of NleH1 and NleH2 to GFP were constructed and their expression measured under different conditions.

### **3.2.1 Expression of GFP translational fusions**

Upon closer assessment of the sequence of NleH1 and NleH2 5' untranslated regions (5' UTR) from *E. coli* O157:H7 strain EDL933, it was evident that the sequences became more divergent further upstream from the ATG start codon. The upstream sequences share 70% identity to -120bp which decreases to 60% for 290bp and finally to 53% for 655bp, when the sequences are aligned using ClustalW, Figure 3-1. The length of 5' UTR cloned upstream of the translational fusion *nleH1/2::gfp* was varied to investigate if this had any effect upon NleH-GFP expression.

The constructs (pAHE8, pAHE18-22) were transformed into *E. coli* O157:H7 strain ZAP193 and the expression of NleH-GFP assessed during growth in MEM and DMEM as described. ZAP193 is a Shiga-like toxin-negative strain and there is a panel of mutants available in this background. The trend of expression of NleH1 and NleH2 in MEM media is that expression increases as the population increases. The trend seen in DMEM differs in that once the population reaches  $OD_{600nm} = 1.2$ , expression begins to decline and does not reach the same levels as seen in MEM. Expression of NleH1 and NleH2 at  $OD_{600} = 1.2$ , is ~4-fold greater in MEM compared to DMEM (Figure 3-2) which correlates with a previous report showing greater expression of NleA and NleB in this media (Roe *et al.*, 2007).



controlling expression. NleH1-GFP with 283bp 5' UTR (pAHE19) expression is 70%, and 120bp 5' UTR (pAHE18) expression is 30%, relative fluorescence units (RFU) of 531bp 5' UTR (pAHE8), at  $OD_{600} = 1.2$ . The difference in NleH1-GFP fluorescence from 531bp 5'UTR compared to 120bp 5' UTR is significant (One-way ANOVA with Bonferroni's multiple comparison test,  $p < 0.0001$ ), but not compared to 283bp 5' UTR (Student's t test,  $p = 0.063$ ). These trends in NleH1-GFP expression is not observed in DMEM, likely due to the largely reduced levels of expression of the GFP fusions in this media. Similarly, previous work has shown that expression of the LEE and non-LEE encoded effectors NleA-E is induced to greater levels in MEM compared to DMEM (Roe *et al.*, 2007). Comparing the formulations of MEM (M7278) with DMEM (D5671), they are both based upon Eagle's Basal Medium (EBM) but have the following differences. DMEM has no HEPES buffer; four times the concentration of vitamins; double the concentration of amino acids; and double the concentration of glucose compared with MEM+0.1% glucose. The greater LEE induction observed when *E. coli* O157:H7 are cultured in MEM cannot be attributed to a particular component present in the media (Dr Andrew Roe; personal communication) and therefore remains to be elucidated.

This stepwise increase in NleH1-GFP expression during the stationary phase of growth in MEM with increase in 5' UTR length indicates that an activator of transcription may bind between -283bp and -531bp; the secondary structure of the upstream DNA may influence transcription of NleH1; there may be competition between a repressor that binds close to the ORF of NleH1 and an activator that competes for a similar site but also requires an upstream sequence for binding. Expression of NleH2-GFP is dependent upon the 113 nucleotides upstream of the start of the open reading frame.

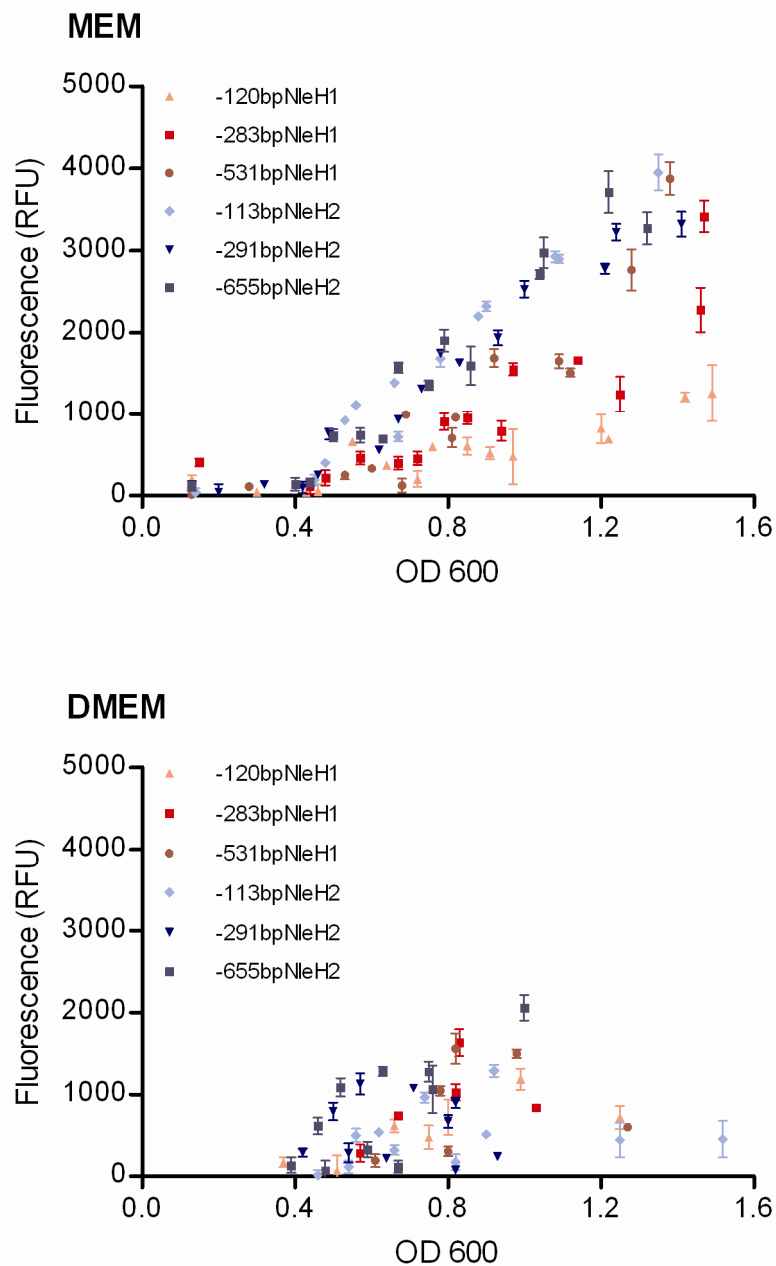


**Figure 3-2 Expression of NleH-GFP constructs in *E. coli* O157:H7 grown in minimal media** Constructs NleH1 with 120bp (pAHE18), 283bp (pAHE19) or 531 bp (pAHE8), and NleH2 with 113bp (pAHE20), 291bp (pAHE21) or 655bp (pAHE22), 5' UTR cloned upstream of *gfp* were transformed into ZAP193 and grown in MEM (A) or DMEM (B) and fluorescence measured during growth as described in Materials and Methods. All values were corrected for background by subtracting the value of a promoterless *gfp* (pAJR70) control measured at the same optical density, with the mean+SEM plotted. Graphs represent the measurements from three biological repeats performed on different days.

### 3.3 Expression of NleH in defined regulatory deletions

In order to try to ascertain what influences NleH expression in *E. coli* O157:H7, the translational fusions (pAHE8 and pAHE22) were assessed in a number of gene knockouts to test their affect on NleH expression. NleH-GFP expression in a K-12 *E. coli* background was investigated to determine whether expression is dependent upon endogenous or EHEC specific factors.

#### 3.3.1 Expression in stationary phase regulator knockouts

As expression of NleH-GFP is greatest towards the stationary phase of growth and therefore high population density, this raised the question whether quorum sensing or alternative sigma factors affect *nleH* gene transcription. Quorum sensing has been shown to regulate T3SS expression (Sperandio *et al.*, 1999) and QseC is the sensor kinase in the signalling pathway (Clarke & Sperandio, 2005a). The alternative sigma factor RpoS has also been shown to have an effect on the regulation of horizontally acquired elements, such as the LEE (Sperandio *et al.*, 1999; Dong & Schellhorn, 2009).

To test this, pAHE8 (-531bp\_*nleH1::gfp*) and pAHE22 (-655bp\_*nleH2::gfp*) were transformed into an *E. coli* K-12 $\Delta$ *qseC* and  $\Delta$ *rpoS* mutants, alongside their isogenic parent strain and expression monitored during growth in MEM. The construct pAJR132 (*tir::gfp*) was included to act as a LEE encoded effector control in the expression assay. The expression profiles of NleH-GFP differ between K-12 strains, which may be attributed to the transformation of data from subtracting the background fluorescence from strains containing promoterless *gfp* plasmid pAJR70. NleH-GFP expression is negligible in *E. coli* K-12 strain BW25113 and reduced at least 8-fold in strain MC1000 (Figure 3-3 A and C). NleH1-GFP fusion protein expression slightly greater than NleH2-GFP, opposite to what was observed from the same constructs in *E. coli* O157:H7 ZAP193; Tir-GFP fusion protein expression is reduced ~60-fold in BW25113 and ~120-fold in MC1000. In BW25113 $\Delta$ *rpoS* (Figure 3-3 B), NleH-GFP is only detected in the lag phase of growth, H1 until OD<sub>600</sub> = 0.15 and H2 until OD<sub>600</sub> = 0.3. Expression of NleH1-GFP fusion protein in VS184 (MC1000 $\Delta$ *qseC*; Figure 3-3

D) is only detected between  $OD_{600} = 0.35$  and  $0.95$ , and NleH2-GFP fusion protein expression is not detected in this strain.

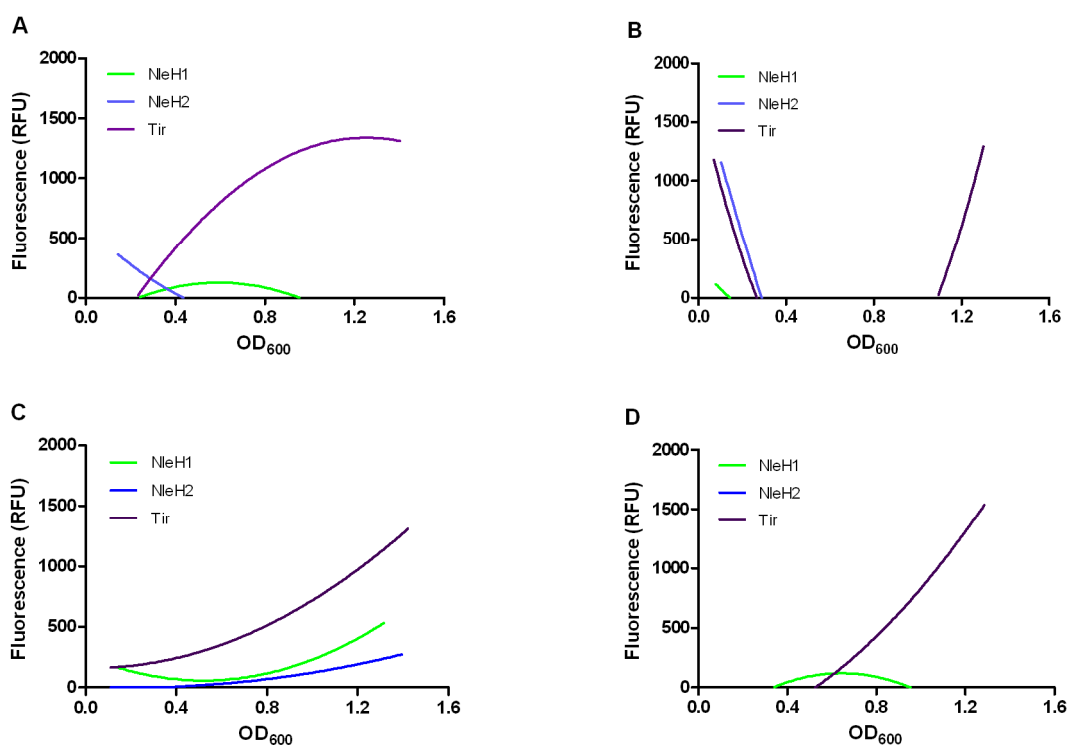


**Figure 3-3** Expression of NleH-GFP and Tir-GFP in *E. coli* K-12,  $\Delta rpoS$  and  $\Delta qseC$  mutants NleH1-GFP (pAHE8), NleH2-GFP (pAHE22) and Tir-GFP (pAJR132) expression was analysed when transformed into *E. coli* K-12 strain BW25113 (A), BW25113 $\Delta rpoS$  (B), MC1000 (C) and VS184 (D) as described in Materials and Methods. Lines represent the average of two biological repeats.

These results therefore indicate that the presence of *E. coli* O157:H7 specific factors are central to *nleH* expression. Tir expression is also reduced in an *E. coli* K-12 background and these effectors are all upregulated in LEE inducing conditions. Owing to this, *nleH::gfp* expression was tested in LEE regulator knockouts.

### 3.3.2 Expression in LEE regulator knockouts

As it has been indicated from previous experiments that the expression of *nleH* is dependent on *E. coli* O157:H7 specific regulators and upregulated alongside the LEE; pAHE8 and pAHE22 were transformed into *E. coli* O157:H7 ZAP193 isogenic mutants of *ler* and *glaA*, two characterised LEE encoded regulators. Ler has

been shown not only to positively regulate the transcription of LEE encoded effectors, but also non-LEE encoded effectors, such as *nleA* (Elliott *et al.*, 2000; Roe *et al.*, 2007; Schwidder *et al.*, 2011) and *tccP/espF<sub>v</sub>* (Abe *et al.*, 2008). Transcription of the *ler* gene can be self-regulated (Berdichevsky *et al.*, 2005) and positively regulated by GrlA (Deng *et al.*, 2004; Huang & Syu, 2008). Transcription of the *grlA* gene is regulated by Ler, through its ability to alleviate H-NS repression, thereby forming a positive feedback loop (Barba *et al.*, 2005); indirectly and positively regulated by QseA (Russell *et al.*, 2007); indirectly and negatively regulated by RpoS (Dong & Schellhorn, 2009); and post-transcriptionally regulated by Hfq (Hansen & Kaper, 2009; Shakhnovich *et al.*, 2009). GrlA protein activity is regulated through binding with GrlR (Jobichen *et al.*, 2007). GrlA can also exert an effect of transcription of genes outwith the LEE, such as the flagellar genes (Iyoda *et al.*, 2006) and the enterohaemolysin operon (Saitoh *et al.*, 2008).

NleH1-GFP expression, at OD<sub>600</sub> = 1.2 (intermediate level of expression), is reduced in ZAP193Δ*ler* and ZAP193Δ*grlA* by ~45% and ~65% respectively, Figure 3-4 A; NleH2-GFP expression is reduced in Δ*ler* and Δ*grlA* by ~40% and ~75% respectively, Figure 3-4 B. Tir-GFP (pAJR132) was included as a control as its expression has been shown to be dependent upon both Ler and GrlA (Elliott *et al.*, 2000; Deng *et al.*, 2004), which is reflected in the results, Figure 3-4 C. Tir-GFP expression at OD<sub>600</sub> = 1.0 (near maximum level of expression), is reduced by ~85% in the absence of Ler and by ~50% in the absence of GrlA. Tir expression is 15-fold that of NleH. Ler has a more significant effect on the expression of Tir-GFP compared to GrlA, as Ler has been shown to directly bind the promoter region of *tir*. This suggests that the result seen for ZAP193Δ*grlA*/pAJR132 is likely to be an indirect effect due to the reduction in the transcription of *ler* in the absence of GrlA. An opposite trend is seen with NleH-GFP expression in these regulator mutants, with the expression of NleH-GFP reduced more in the absence of GrlA than in the absence of Ler. This also implies that these regulators have an indirect effect upon *nleH* gene transcription.

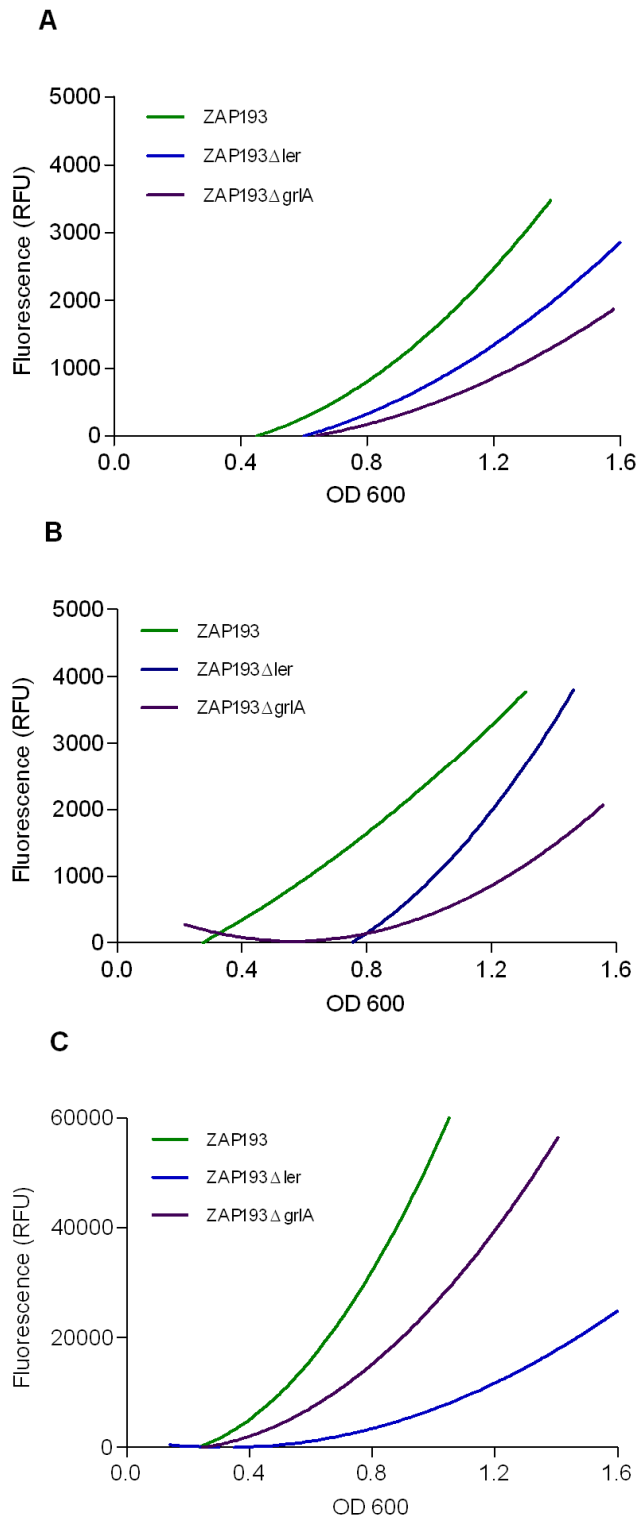


**Figure 3-4 Expression of NleH-GFP and Tir-GFP in *E. coli* O157:H7 defined LEE regulator mutants**  
*E. coli* O157:H7 ZAP193, ZAP193 $\Delta$ ler and ZAP193 $\Delta$ grIA were transformed with constructs expressing NleH1-GFP (pAHE8; A), NleH2-GFP (pAHE22; B) and Tir-GFP (pAJR132; C). GFP expression was monitored during growth of the transformants in MEM media, with a promoterless gfp construct (pAJR70) as a background control. Lines represent the average of three biological repeats.

Although reporter plasmids are frequently used to assess gene transcription and translation in bacteria, often the results observed should be supported by other techniques, such as RT-PCR or single chromosomal insertions. This is due to the possible implications from the use of plasmid reporter systems, such as difference in DNA topology compared to the chromosome (Parsot & Mekalanos, 1992); the fitness cost of heterologous (GFP) expression (Knodler *et al.*, 2005) and/or plasmid maintenance (Clark *et al.*, 2009); and amplification of expression levels due to the presence of multiple copies of the gene/promoter of interest. Therefore, to further quantify the effects of Ler and GrlA on the transcription of NleH1 and NleH2, quantitative PCR (Q-PCR) was performed on RNA harvested from strains grown in MEM to  $OD_{600} = 1.2$ , as described in Materials and Methods. The *nleH* transcripts were normalised between samples using 16S RNA as a control. Transcription of *nleH* in the mutants was compared to wild-type expression to give a fold-change. The Q-PCR results show that the NleH transcripts are reduced in the  $\Delta ler$  and  $\Delta grlA$  strains, Figure 3-5. NleH1 transcript levels are reduced 13- and 14-fold in ZAP193 $\Delta ler$  and ZAP193 $\Delta grlA$ , respectively. Similarly, NleH2 is reduced 22- and 17-fold in the same mutants. These results indicate a strong influence of Ler and GrlA in NleH transcription, confirming the results obtained with the translational fusions to *gfp*.

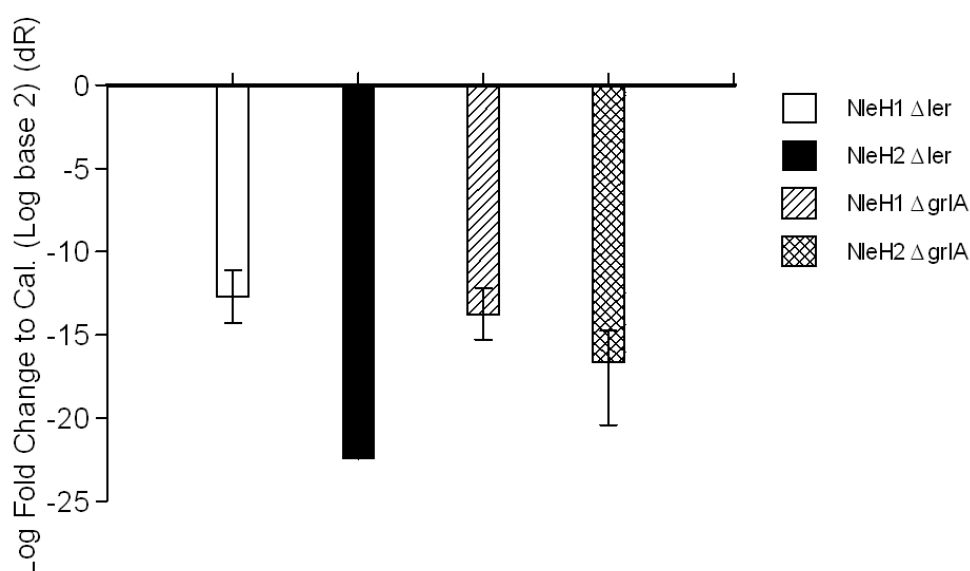


**Figure 3-5 Quantitative PCR of NleH transcripts in LEE regulator knockouts**  
 RNA was collected from ZAP193 strains WT,  $\Delta ler$  and  $\Delta grlA$  grown to  $OD_{600} = 1.2$  in MEM and cDNA prepared. NleH1, NleH2 and 16S RNA transcript was then quantified by q-PCR, NleH values normalised to that of 16S RNA, and the fold change calculated comparing mutant to wild-type. Bars represent the average of three biological samples.

Expression of the T3SS apparatus, specifically the EspA filaments, has been shown to be heterogenous in a population as LEE4 is posttranscriptionally regulated (Roe *et al.*, 2003; Roe *et al.*, 2004). NleH has been shown to be secreted via the T3SS (Tobe *et al.*, 2006; Garcia-Angulo *et al.*, 2008; Gao *et al.*, 2009), the GFP translational fusions were assessed by fluorescence microscopy to ascertain whether expression of NleH in a population is homo- or heterogenous in ZAP193, its isogenic *ler* and *grlA* mutants, and whether this expression is coordinated with the T3S apparatus. Maximal expression of EspA occurs at  $OD_{600nm} = 0.8$  (Roe *et al.*, 2004), therefore this optical density was chosen to investigate if NleH expression is co-ordinated with the LEE translocon.

NleH is not strictly co-ordinately expressed with EspA filaments, as there is approximately 18-20% of the population expressing NleH-GFP without EspA filaments, and therefore T3SS apparatus, Figure 3-6 A. Quantification of the mean GFP fluorescence (RFU) per voxel, in at least 100 individual bacteria from 3 separate fields shows that NleH2 is expressed at ~2 fold greater levels than NleH1, Figure 3-6 D and E, correlating with the results from the population studies at the same optical density. NleH2-GFP expression is also heterogenous as there is a sub-population (14%) which are 'hyperexpressors', where they are expressing GFP approximately 5-fold greater levels (average RFU = 234 units) than the rest of the population (RFU = 49 units), Figure 3-6 A and E. Analysis of these 'hyperexpressors' separate from the rest of the population show that they maintain the same percentage (18-20%) of cells not expressing EspA filaments, therefore there is no correlation between the hyperexpression of NleH2-GFP with the presence of EspA filaments.

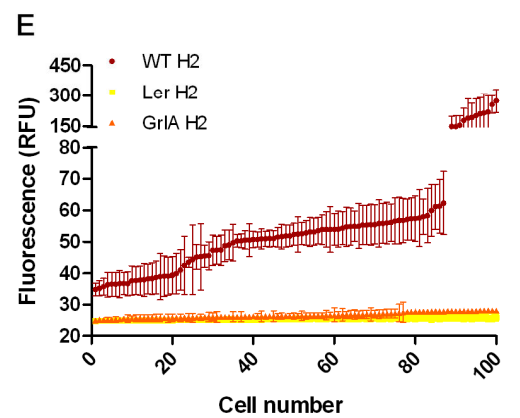
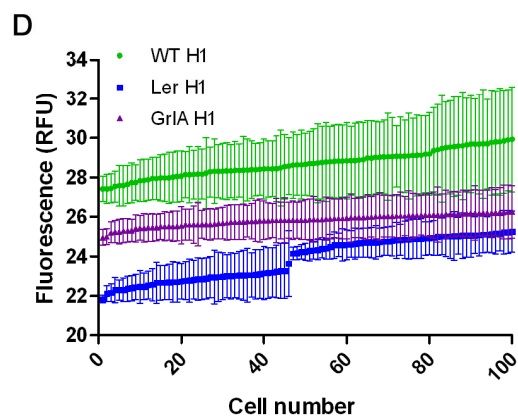
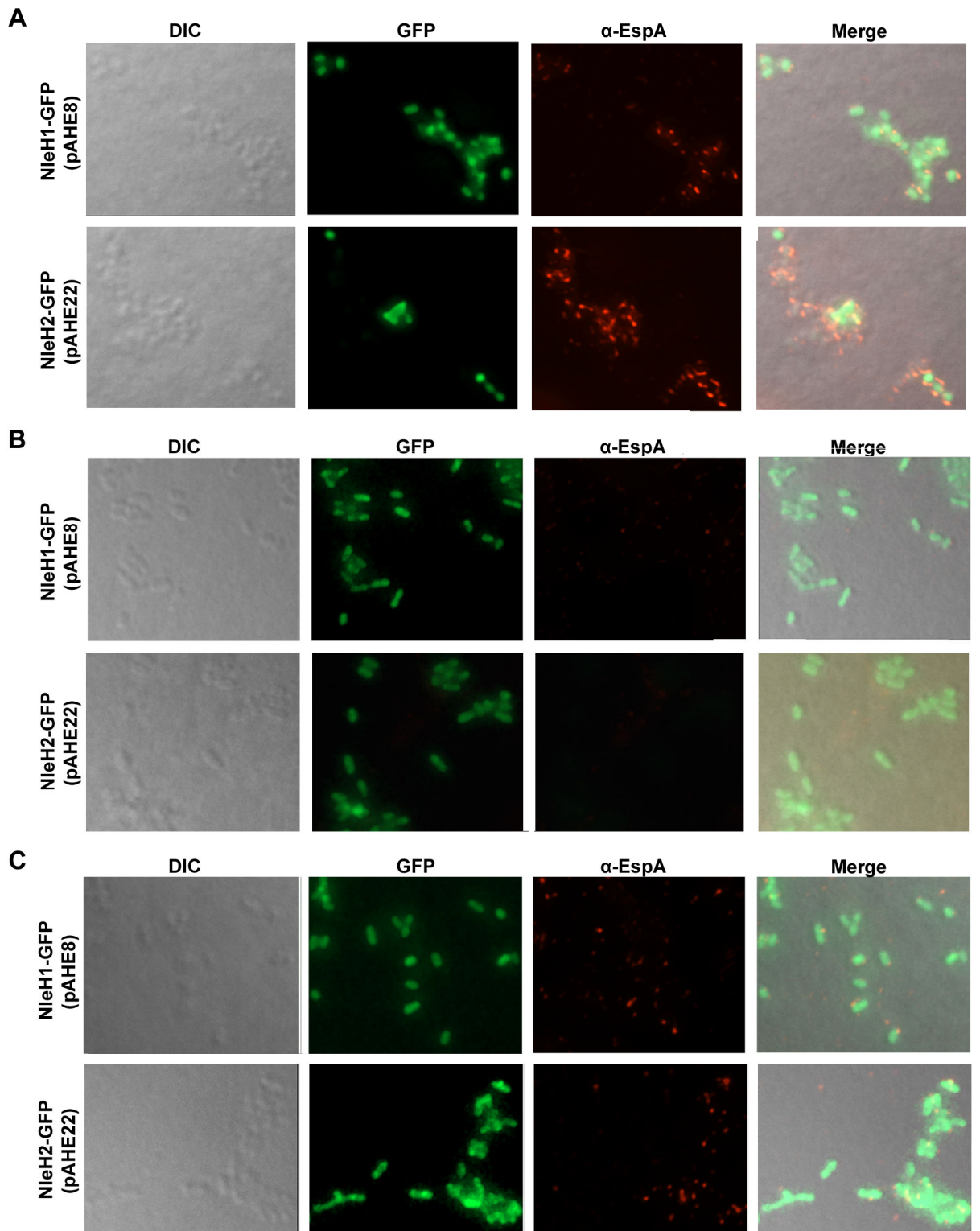


**Figure 3-6 Fluorescence microscopy of NleH-GFP**  
pAHE8 (NleH1-GFP) and pAHE22 (NleH2-GFP) were transformed in ZAP193 (A), ZAP193 $\Delta$ ler (B) and ZAP193 $\Delta$ grlA (C) and at OD<sub>600</sub> = 0.8 fixed onto a microscope slide, stained for EspA filaments and z-stacks taken as described in Materials and Methods. Using Volocity quantification software, the average GFP fluorescence per voxel of 100 individual bacteria of each strain was measured and plotted for NleH1 (D) and NleH2 (E). Error bars represent the standard deviation.

EspA filaments are not detected in a *ler* negative background and are reduced in the *grlA* mutant. The expression of NleH-GFP in both mutants is reduced, and the heterogeneity seen with NleH2-GFP is lost. NleH1-GFP expression is reduced from a mean RFU value of 29 in wildtype to 24 and 26 RFU in a  $\Delta$ ler and  $\Delta$ grlA mutant respectively; NleH2-GFP from an overall average of 78 RFU to 25 and 27 RFU. The difference in NleH-GFP expression between the two mutants is not great at this optical density; the difference may be more apparent if the sample was taken from a later point as it can be seen from the population analysis that the difference increases during the stationary phase of growth, Figure 3-4. However, assessment of the presence of EspA filaments cannot occur at OD<sub>600nm</sub> = 1.2 as EspA expression is rapidly reduced upon entry into stationary phase (Roe *et al.*, 2003).

### **3.3.3 Expression in *nleH* knockouts**

#### **3.3.3.1 Construction of *E. coli* O157:H7 $\Delta$ *nleH* mutants**

*E. coli* O157:H7 strain TUV93-0 is a non Shiga-like toxin-producing derivative of the genome sequenced strain EDL933 (Perna *et al.*, 2001), with the sequence publically available on coliBASE (<http://www.xbase.ac.uk/genome/escherichia-coli-o157h7-edl933>). The availability of the sequence allows confident primer design and to create defined *nleH* deletions in this strain. The first approach to generate mutants was to use lambda red-mediated gene replacement and this technique was chosen because it is a one-step process. First, In-Fusion cloning was used to construct a plasmid containing a Kan cassette flanked with 500bp of sequence homologous to NleH1 5' and 3' UTRs (pAHE17). This product was PCR amplified and purified for recombination into the chromosome. Three separate

Lambda Red-mediated recombination events were attempted to replace the *NleH1* gene with the Kan cassette in the TUV93-0 chromosome. Although possible recombinants with the kanamycin resistant phenotype were generated, the replacement of *NleH1* by the Kan cassette could not be confirmed by PCR. On other occasions, the recombinants would remain ampicillin resistant indicating that pKM201 had not been lost. Overexpression of the *red* and *gam* genes, present on pKM201, are mutagenic to *E. coli* O157:H7 therefore recombinants must not retain this plasmid in order to ensure that any phenotype seen is solely due to the engineered deletion (Murphy & Campellone, 2003). Owing to this an alternative strategy, allelic exchange, was undertaken to create *nleH* mutants and allelic exchange vectors pK03bH1 and pK03bH2 were constructed. *NleH1* was successfully replaced with a kanamycin cassette in TUV93-0, and subsequently the cassette excised by Flp recombinase expressed from pCP20, which was confirmed by PCR using primers which bind upstream and downstream of *NleH1*, at a position outwith the flanking regions used for allelic exchange. Figure 3-7 shows that the PCR product is increased from 2090bp in the TUV wildtype to ~2500bp in TUV $\Delta$ *nleH1*::Kan due to the replacement of the *NleH1* gene (882bp) with the kanamycin cassette (1400bp). The PCR product from TUV $\Delta$ *nleH1* is 1200bp due to the deletion of *nleH1*.

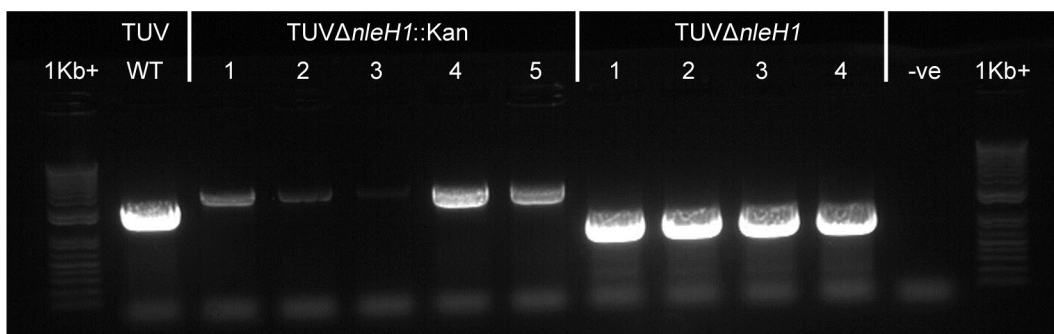


**Figure 3-7 PCR to confirm replacement or deletion of *NleH1* in EHEC strain TUV93-0**  
 EHEC O157:H7 strain TUV93-0 was transformed with allelic exchange vector pK03bH1 to create TUV $\Delta$ *nleH1*::Kan, which was then transformed with pCP20 to excise the antibiotic cassette to create TUV $\Delta$ *nleH1*. Genomic DNA was extracted from each variant, with numbers denoting different mutant clones, and PCR performed with primers *NleH1*.ext.F and *NleH1*.ext.R to amplify across the *NleH1* gene.

TUV93-0 and TUV $\Delta$ *nleH1* were transformed with pK03bH2 to exchange *NleH2* with a kanamycin cassette; unfortunately a successful recombinant could not be resolved after three individual attempts for each strain. Therefore, due to time

constraints, an NleH double mutant and its parent *E. coli* O157:H7 strain 85-170 was requested from Prof Gad Frankel (Hemrajani *et al.*, 2008). Single allele mutants were not available therefore 85-170 was transformed with pKO3bH1 or pKO3bH2 for allelic exchange. 85-170 $\Delta$ nleH1 was successfully made and although recombination with pKO3bH2 was unsuccessful, a single allele mutant in NleH1 may still provide interesting results. PCR was performed to amplify across the NleH1 or NleH2 genes on 85-170 wild-type, 85-170 $\Delta$ nleH1H2 and 85-170 $\Delta$ nleH1 to confirm replacement or deletion. Wild-type 85-170 nleH1 and nleH2 generates a PCR product of 2090bp and 2120bp respectively, Figure 3-8. 85-170 $\Delta$ nleH1H2 produces PCR products greater (~3000bp) and smaller (~1400bp) than wild-type for nleH1 and nleH2 respectively; this shows a replacement of NleH1 and deletion of NleH2 in this strain. The PCR product from 85-170 $\Delta$ nleH1 is 1200bp, showing the successful deletion of the nleH1 gene.

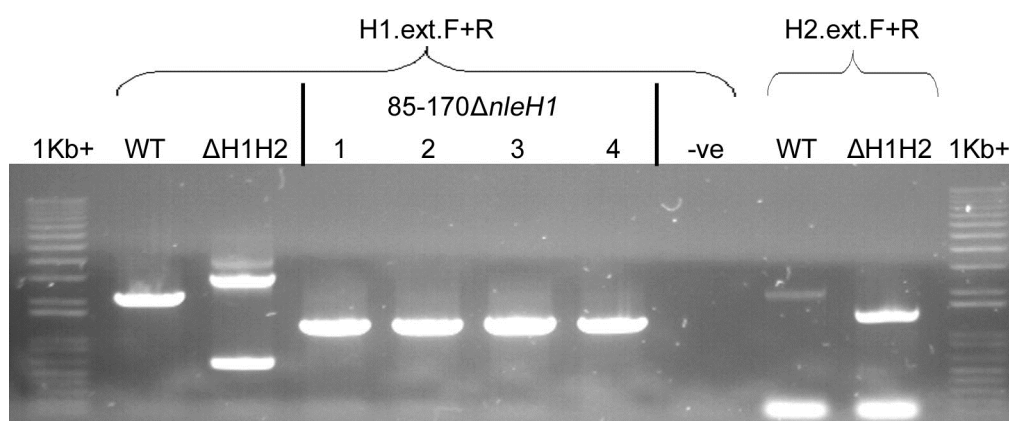


**Figure 3-8** PCR to confirm NleH1 and NleH2 replacement or deletion in EHEC strain 85-170. EHEC strain 85-170 and 85-170 $\Delta$ nleH1H2 were received from Prof Gad Frankel; 85-170 was transformed with pKO3bH1 and pCP20 to generate single NleH1 mutant. Genomic DNA was extracted from each variant, with numbers denoting different mutant clones, and PCR performed with primers H1.ext.F+R or H2.ext.F+R to amplify across the NleH1 or NleH2 gene respectively.

### 3.3.3.2 Expression of NleH-GFP

Once replacement or deletion of the *nleH* alleles was confirmed in the mutants, all three strains were transformed with pAHE8 and pAHE22 to assess NleH-GFP expression in these backgrounds. NleH-GFP expression is negligible in 85-170 wild-type (WT) and 85-170 $\Delta$ nleH1 ( $\Delta$ H1) (Figure 3-9); the expression levels are ~200-fold less than in ZAP193, Figure 3-2. Expression of NleH-GFP in the double mutant increases as the OD<sub>600</sub> increases; NleH1-GFP is ~11-14 times, and NleH2-

GFP is ~8 times, that of wild-type. NleH1-GFP expression is double that of NleH2-GFP in 85-170 $\Delta$ nleH1H2 after OD<sub>600</sub> = 0.6. At OD<sub>600</sub> = 1.2, NleH1-GFP expression is ~4-fold less in 85-170 $\Delta$ nleH1H2 than ZAP193; NleH2-GFP is reduced ~8-fold.

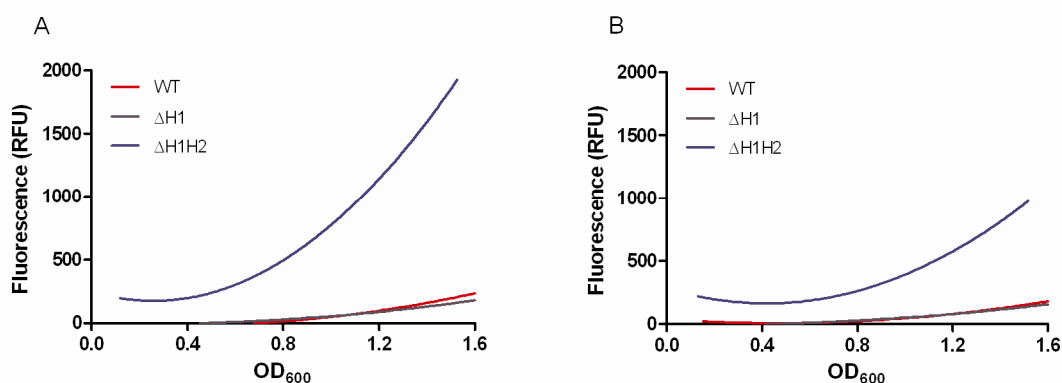


**Figure 3-9 NleH-GFP expression in NleH knockouts**  
pAHE8 (A) and pAHE22 (B) were transformed into 85-170, 85-170 $\Delta$ nleH1 and 85-170 $\Delta$ nleH1H2. Fluorescence was measured during growth in MEM as described in Materials and Methods.

Also, NleH1-GFP is expressed two times more than NleH2-GFP at OD<sub>600</sub> = 0.8; the converse is seen in ZAP193 at the same optical density. Growth of these strains in MEM media is comparable to that of ZAP193 as they reached similar optical density levels during the timecourse (8 hours maximum). Therefore, these results imply that there may be a different repertoire, or alternative action or expression, of regulators in 85-170 compared to ZAP193. For example, the alternative sigma factor *rpoS* can vary between strains/isolates, affecting phenotypes such as the GAD stress response (Bhagwat *et al.*, 2005), both of which are involved in LEE regulation, and can impact upon virulence. Also, it has previously been shown that EHEC strains differ in their expression of translocon proteins from the LEE (Roe *et al.*, 2003), therefore it can be possible to observe heterogeneity in expression of other horizontally acquired genes. NleH-GFP expression is greater in an 85-170 *nleH* double mutant compared to parent, and this may be attributed to less competition for binding to the Cest chaperone allowing NleH-GFP to be stabilised and protected from posttranslational degradation.

### 3.4 Expression of NleH upon host cell contact

Once the expression of NleH had been assessed in a population, the effect of host cell contact was tested by infecting embryonic bovine lung (EBL) epithelium cells with ZAP193 transformed with pAHE8, pAHE22 and pAJR145 (*rpsM::gfp*), a transcription reporter plasmid with the *rpsM* promoter cloned upstream of *gfp*, which constitutively expresses GFP (Roe *et al.*, 2004). Time 0 is determined as immediately after centrifugation of the bacteria upon the host cells at 1,000 xg for 5 minutes. At 5, 10, 30 and 180 minutes post infection, the media was removed, membrane stain applied then the cells were fixed in paraformaldehyde. The bacteria were stained by indirect immunofluorescence with  $\alpha$ -O157 and  $\alpha$ -rabbit AlexaFluor-555 conjugate antibodies.

Upon contact with host cells, the expression of NleH-GFP is reduced to below detectable levels at all time points tested, whereas the control, consisting of the constitutive *rpsM* promoter, was detected at all time points. This indicates that there are no experimental factors affecting GFP fluorescence during the course of the experiment. Also, it was previously mentioned that there can be a fitness cost inferred from the maintenance of GFP reporter plasmids which may result in a reduction in virulence, for example in *Salmonella* (Knodler *et al.*, 2005; Clark *et al.*, 2009). However, *E. coli* O157:H7 carrying the GFP reporter plasmids employed in this study can still form A/E lesions *in vitro* and within a similar time-scale to that of parent bacteria (results not shown; (Roe *et al.*, 2004).

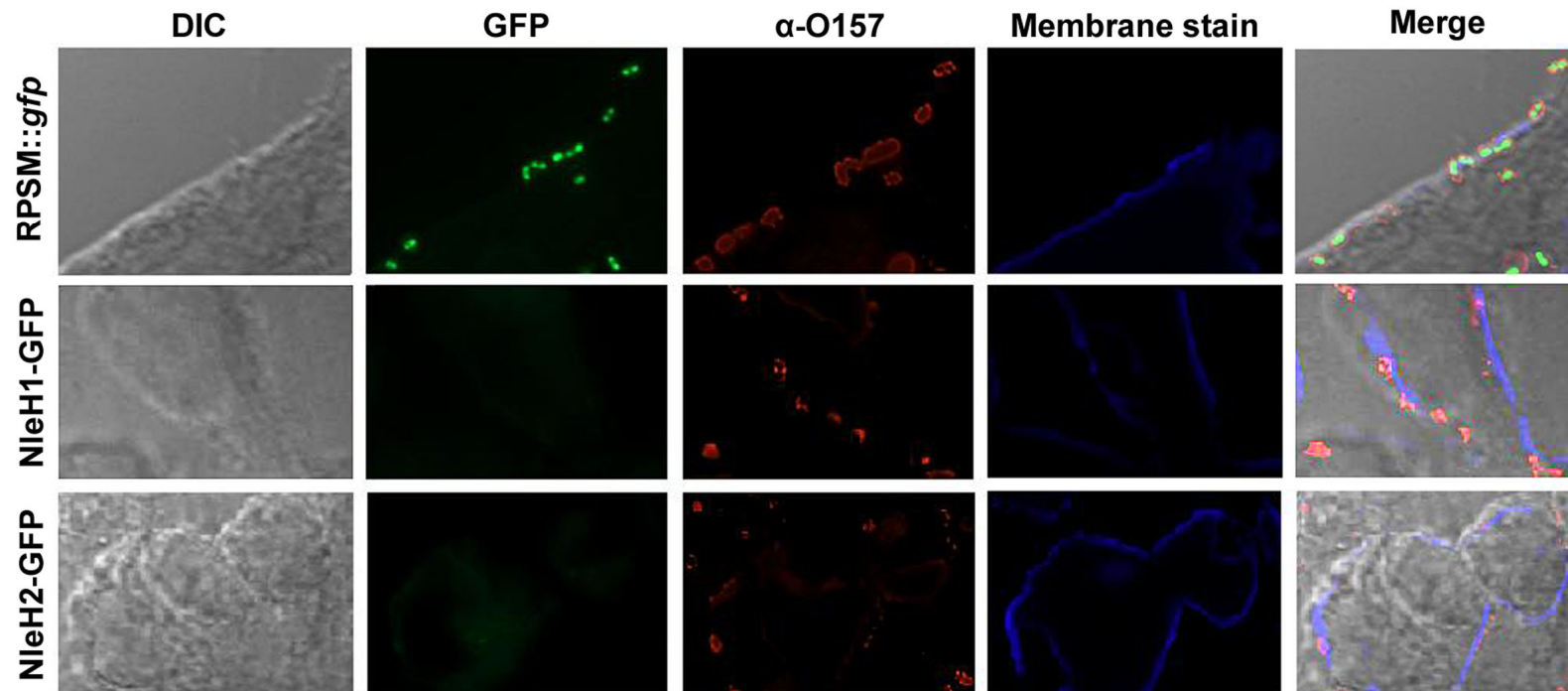


Figure 3-10 Expression of NleH-GFP upon *E. coli* O157:H7 ZAP193 contact with EBL cells  
 ZAP193 transformed with plasmids expressing GFP constitutively (pAJR145; *rpsm*::*gfp*) or translational fusions of *nleH* to *gfp* under the control of their native promoter (pAHE8; NleH1-GFP, pAHE22; NleH2-GFP) were added to EBL cells and incubated for 0, 5, 30 or 180 minutes at 37°C, 5% CO<sub>2</sub> before the removal of supernatant and fixation of cells. The panel of images was taken from 5 minutes post-infection but is representative of all time points tested.

### 3.5 Discussion

Non-LEE encoded effector H is a bacterial effector found in all A/E pathogens tested to date, and is translocated by the T3SS. It was first identified through a bioinformatic and proteomic approach, owing to its homology to *S. flexneri* effector OspG (Tobe *et al.*, 2006). There is only one *nleH* allele in the mouse A/E pathogen *C. rodentium* but there are two alleles present in *E. coli* O157:H7; each *nleH* allele is encoded on a prophage which also carries other *nle* effectors previously reported to be expressed and secreted. *NleH1* (z0989) is encoded on the same O-Island (OI-36) as *nleC* (z0986) and *nleD* (z0990) which are both transcribed in secretion permissive conditions, and *NleD* expression is reduced two-fold in a *ler* negative background (Roe *et al.*, 2007). *NleH2* (z6021) is encoded on the same O-Island (OI-71) as *nleA* (z6024), *nleF* (z6022) and *nleG* (z6030); *nleA* has been shown to be transcribed and its expression dependant upon *Ler* (Roe *et al.*, 2007; Schwidder *et al.*, 2011). *NleH* was a good candidate for further research due to preliminary data showing that its expression was upregulated in the same conditions which upregulated the LEE; also the presence of two alleles encoded on separate O-Islands raised questions as to whether they are each expressed under the same conditions, how their expression is regulated and if it is differential.

Upon comparison of the 5' UTR sequences of *E. coli* O157:H7 EDL933 *NleH1* and *NleH2*, it was apparent that the further from the ATG start codon of the ORF, the more diverse the sequence. This led to the hypothesis that transcription may vary between the two alleles depending upon the length of 5' UTR cloned upstream of a translational fusion of *nleH* to *gfp*. The length of 5' UTR did not vary the expression of *NleH2*-GFP, indicating a minimum of 113 nucleotides upstream of the start of the ORF is required for expression; it would have been interesting to test if the coding sequence of *NleH2* is also required for its expression with this length of 5' UTR by cloning the *NleH2* 5' UTR upstream of *NleH1*-GFP. However, *NleH1*-GFP expression in MEM is dependant upon the 5' UTR length, as after  $OD_{600nm} = 0.8$ , expression increases with an increase in 5' UTR length cloned. Research, published during this study, using ChIP-on-chip analysis demonstrated that the *E. coli* O157:H7 Per-C like homologue (Pch) regulator directly binds the *nleH1* promoter but binds further upstream in the

*nleH2* prophage in order to exert its control (Abe *et al.*, 2008). This study also determined that Pch does not have a general consensus binding site, as it has various numbers and positions of binding sites depending upon the target gene, thus regulating a broad range of genes. Therefore, the increase in NleH1-GFP expression with increase in 5' UTR cloned may be due to a direct effect of Pch binding to the area between -283 and -531bp, or an indirect effect of Pch modulating the secondary structure of *nleH1* and its 5' UTR, facilitating the action of another positive regulator, or displacing a repressor such as H-NS. Further experiments would have to be carried out to confirm that Pch binds to this region of the NleH1 5' UTR. NleH-GFP expression is greatest upon entry into stationary phase, nutrient depletion in this stage of growth increases the concentration of ppGpp, a signalling molecule which positively regulates the transcription of *ler* and *pch* via its interaction with RNA polymerase (Nakanishi *et al.*, 2006). Pch regulators are not present in K-12 strains, thus providing some explanation to the lack of expression of the NleH-GFP plasmids observed in this background. It can be concluded from the NleH-GFP expression in BW25113 $\Delta$ *rpoS* data, Figure 3-3 B, that RpoS is not a direct repressor of *nleH* expression. It would have been interesting to test NleH-GFP expression in an *E. coli* O157:H7  $\Delta$ *rpoS* background, as RpoS negatively regulates *pch* transcription (Iyoda & Watanabe, 2005), or to co-express Pch with NleH-GFP in *E. coli* K-12 $\Delta$ *rpoS*.

Previous work has shown that the LEE is upregulated when *E. coli* O157:H7 is cultured in MEM compared to DMEM, as well as non-LEE encoded effectors NleA-E (Roe *et al.*, 2007). Analysis of the expression of translational fusions of *nleH1* and *nleH2* to *gfp* under the control of their native promoters reveals that expression of NleH-GFP is 4-fold greater in MEM compared to DMEM, Figure 3-2. As discussed previously, it remains to be elucidated which component, or combination of nutrients, is responsible for the increased induction of gene expression in MEM compared to DMEM. It may be that the lower concentrations of amino acids and vitamins present in MEM provide a better representation of the conditions encountered by the bacterium *in vivo*. Previous studies have reported that EHEC *esp*::lacZ expression is detected in DMEM+HEPES but not in DMEM alone (Beltrametti *et al.*, 1999) and EHEC adherence *in vitro* is increased by the addition of bicarbonate ions, but not HEPES, to LB (Abe *et al.*, 2002). A

recent report has shown that adding butyrate to DMEM increases LEE expression and EHEC adherence to cells *in vitro* (Nakanishi *et al.*, 2009). It has also been reported in other bacterial species that small modifications of culture media can affect the expression of the T3SS. In *Yersinia*, the translocon of the T3SS is secreted in the presence of calcium ions, and when these ions are chelated from the media, secretion of the Yop effectors is induced (Nilles *et al.*, 1997; DeBord *et al.*, 2003; Edqvist *et al.*, 2003; Torruellas *et al.*, 2005). Similarly, the absence of magnesium in the media induces expression of the second T3SS SPI-2 in *Salmonella enterica* serovar typhimurium (Deiwick *et al.*, 1999). Also the SPI-1 system of *S. Typhimurium* is induced when in the presence of increased sodium chloride concentrations (Song *et al.*, 2004; Ibarra *et al.*, 2010). These results demonstrate that expression of the T3SS, and its effectors, can vary significantly depending upon the *in vitro* culture conditions.

Based on the hypothesis that effectors would be co-ordinately expressed with the apparatus that secretes them, NleH-GFP expression was assessed in LEE encoded regulator negative backgrounds. GFP expression *in vitro* from the translational fusions was reduced for NleH1 and NleH2 in *ler* and *grlA* negative strains. Q-PCR shows that *nleH1* and *nleH2* transcription, or mRNA stability, is dependant upon *ler* and *grlA*; however based upon the 5' UTR assay results and other published research, these regulators are likely to have an indirect effect on *nleH* expression. Pch has been shown to regulate expression of *nleH1* and *nleH2* independent of *Ler*, through microarray analysis and ChIP-on-chip (Abe *et al.*, 2008). Investigations published during the period of my study reported that *C. rodentium nleH* (CR*nleH*) transcription is reduced in a *ler* and *grlA* mutant background, in a similar trend to the results above with *E. coli* O157:H7 *nleH1* and *nleH2*, although not significantly in their CAT activity assay (Garcia-Angulo *et al.*, 2008). Further analysis with  $\Delta$ *ler*,  $\Delta$ *grlA*,  $\Delta$ *grlR* and  $\Delta$ *cesT* mutants transformed with a plasmid expressing CR*nleH*::HA under the control of an inducible promoter demonstrated that CRNleH-HA is regulated posttranslationally; with its stability dependant upon the presence of its chaperone CesT (Thomas *et al.*, 2005; Thomas *et al.*, 2007) and active secretion, its degradation is mediated by Lon, thereby regulating NleH in coordination with the LEE. GrlR was also shown to have a negative posttranscriptional and posttranslational effect on CRNleH expression, which may be in concert with the

indirect effect of *ler* and *grlA* on NleH expression, as they are all involved in the same regulatory loop (Barba *et al.*, 2005), with GrlR binding to GrlA thereby hindering its regulatory activity (Jobichen *et al.*, 2007; Huang & Syu, 2008).

Many *E. coli* O157:H7 virulence factors are expressed heterogeneously, such as *espA* (Roe *et al.*, 2003), *tir*, *map*, *intimin* (Roe *et al.*, 2004) and *nleA* (Roe *et al.*, 2007), in order to co-ordinate expression of the effectors with that of the T3S apparatus. Single cell imaging of NleH-GFP expressing *E. coli* O157:H7 showed that NleH-GFP is expressed by all cells, however the RFU of GFP measured per cell is homogenous in NleH1 and heterogeneous in NleH2. When cultured in MEM, only 80% of the population co-stained for EspA filaments, correlating with previous reports (Roe *et al.*, 2003) showing that only a sub-population of ZAP193 (40-80%) express EspA filaments when cultured in the same media, and this percentage was maintained in the 'hyperexpressor' population of NleH2. This shows that although NleH-GFP expression is induced by the same conditions as that for the LEE, it is not strictly co-ordinated. Expression of *nleA* is strictly co-ordinated with the LEE and its transcription has been shown to be directly regulated by *ler* (Roe *et al.*, 2007; Abe *et al.*, 2008; Schwidder *et al.*, 2011). NleA also plays an important role in the virulence of A/E pathogens (Gruenheid *et al.*, 2004; Thanabalasuriar *et al.*, 2010). These results suggest that the contribution of an effector to *E. coli* O157:H7 pathogenesis may reflect how the effector is regulated to be expressed in co-ordination with the LEE.

NleH-GFP expression cannot be detected upon contact with host cells under the conditions tested, and it has previously been reported that host cell contact results in a reduction in expression of non LEE genes (Dahan *et al.*, 2004; Roe *et al.*, 2007). The persistence of *E. coli* O157:H7 on host cells has been shown to be mediated through *gadE* (Tatsuno *et al.*, 2003; Tree *et al.*, 2011). GadE is a transcriptional regulator, part of the GAD acid stress response, which is also able to repress LEE2/3 thereby reducing LEE-encoded effector transcription. This induction of the GAD stress response and reciprocal repression of the LEE mediated by GadE is controlled by *psr* genes. There is a high association between non-LEE encoded effectors with *psr* and/or *pch* regulator genes encoded on the same horizontally acquired element, leading to the hypothesis that the Psr mediated induction of *gadE* transcription and subsequent repression

of LEE encoded effectors facilitates non-LEE encoded effector secretion (Tree *et al.*, 2011). It is also interesting to note that many nle effector proteins, including NleH, exhibit an important role in colonisation but not for A/E lesion production or pathogenesis (Dziva *et al.*, 2004; van Diemen *et al.*, 2005; Kelly *et al.*, 2006; Vlisidou *et al.*, 2006b; Wickham *et al.*, 2007; Echtenkamp *et al.*, 2008; Garcia-Angulo *et al.*, 2008; Hemrajani *et al.*, 2008).

In conclusion, NleH1 and NleH2 are expressed in *E. coli* O157:H7 ZAP193 under secretion permissive conditions and their transcription is dependant upon regulators specific to *E. coli* O157:H7. Although the 120bp sequence upstream of NleH1 and NleH2 is 70% homologous, expression of the two alleles is differential as this is enough for maximal NleH2 expression but NleH1 requires additional upstream sequence. Therefore, NleH1 expression is under the control of a regulator, possibly Pch, which binds between 531 and 283bp upstream of the ORF. LEE encoded regulators Ler and GrlA have an indirect effect on *nleH* transcription as NleH expression is not strictly co-ordinated with that of the T3S apparatus. NleH expression may be alternatively regulated in other *E. coli* O157:H7 strains as expression of the *nleH::gfp* translational fusions differed between two *E. coli* O157:H7 strains.

## 4 Function of Non-LEE encoded effector H (NleH)

### 4.1 Summary

During the course of this study, other laboratories have been investigating the function of NleH, and it has been found to play a role in modulating the host's response to infection through its interaction with ribosomal protein subunit 3 (RPS3), altering NF- $\kappa$ B activation (Gao *et al.*, 2009), and Bax inhibitor 1 (BI-1), inhibiting apoptosis (Hemrajani *et al.*, 2010). The aim of the work described in this chapter was to elucidate the function of *E. coli* O157:H7 NleH in the host cell by independently testing its effects on NF- $\kappa$ B activation, owing to its homology with OspG, and trying to determine its host target through 2D differential gel electrophoresis (DiGE) and a high throughput yeast two hybrid screen.

### 4.2 Bioinformatics

NleH1 and NleH2 are homologs of the OspG protein, an effector protein of *Shigella flexneri*, identified by a BLASTp query search (Tobe *et al.*, 2006). Using a yeast two hybrid screen, OspG was found to interact with E2 ubiquitin-conjugating enzymes, thereby inhibiting NF- $\kappa$ B activation and interfering with the host innate immune response (Kim *et al.*, 2005). An alignment of *E. coli* O157:H7 EDL933 NleH1, NleH2 and OspG primary sequences, using ClustalW (Figure 4-1), reveals that NleH1 and NleH2 share 87% identity and NleH1/2 and OspG share 14-15% identity. This indicates that the homology of NleH with OspG is largely because they share the key residues for kinase catalytic motifs (Hanks & Hunter, 1995); their C-terminal region shares 48% protein identity (Nobe *et al.*, 2009) and both effectors are able to autophosphorylate (Kim *et al.*, 2005; Gao *et al.*, 2009; Hemrajani *et al.*, 2010).



with those found in effectors, it is possible to highlight motifs specific to effectors that are not common in the proteome. If a non-proteome ELM is found within the sequence of a putative effector protein, this suggests that the ELM may contribute to the protein's function outwith the bacterium, i.e. within the mammalian cell. ELMs found in EPEC effectors include KEN box, PDZ\_1 ligand, SH3\_5 ligand, WW\_2 ligand and SUMO modification motifs (University of Glasgow Microbiology seminar 30/03/10, Dr Paul Dean). NleH1, NleH2 (from *E. coli* O157:H7 EDL933 sequence) and OspG were screened for the presence of ELMs; NleH1 has 36/153, NleH2 has 33/153 and OspG 21/153 possible ELMs. Three out of the five aforementioned ELMs common in EPEC effectors were identified in NleH1 and NleH2, Figure 4-1 (PDZ, SH3 and SUMO).

PDZ (PSD-95/Disk-large/ZO-1) domains have an important role in mediating protein-protein interactions within higher organisms and typically interact with proteins displaying a consensus sequence of X-S/T-X-H, where X is any amino acid and H is hydrophobic, at its C-terminal end. NleH1 binds Na<sup>+</sup>/H<sup>+</sup> exchanger regulatory factor 2 (NHERF2) via its PDZ motif (-SKI) (Martinez *et al.*, 2010); NHERF proteins are plasma membrane associated proteins which interact with multiple proteins, forming scaffolds, therefore influencing protein trafficking and localisation. NHERF2 binding to NleH1 modulates its trafficking to the endoplasmic reticulum and also subdues its anti-apoptotic function (Martinez *et al.*, 2010). The same study shows that the NHERF binding to effector proteins Map and NleA also affects their localisation and function within the host cell. The authors propose that NHERF binding of bacterial effectors provides an additional regulatory function to co-ordinate the localisation and timing of their function.

The SH3\_5 motif (PXXDY) is recognised by some Src Homology 3 (SH3) domains and SH3\_3 (XXXP/VXXP) is a more general SH3 recognition motif. This motif is also involved in protein-protein interactions and although common amongst bacterial effectors (Dean, 2011), a role for these motifs in protein function has only been described in two effectors, EspF and its homolog EspF<sub>U</sub>/TccP. EspF contains an SH3 binding motif in each of its proline rich repeats (PRR). A yeast two hybrid screen of EspF against cDNA prepared from HeLa cells determined that EspF interacts with sorting nexin 9 (SNX9), which is mediated by SNX9's SH3 domain (Marches *et al.*, 2006). Further studies using a phage library elucidated

the SH3 consensus sequence recognised by SNX9 (RXAPXXP), present in the N-terminal region of the PRRs in EspF (Alto *et al.*, 2007). EspF's role in membrane remodelling and rearranging the cytoskeleton is dependent upon this interaction, as it results in tubule formation by SNX9 allowing recruitment of N-WASP, another binding partner of EspF, to the tubules and subsequent actin polymerisation (Alto *et al.*, 2007).

SUMOs (Small Ubiquitin-related Modifiers) are ubiquitin-like proteins that can be reversibly and covalently conjugated onto lysine residues via E1, E2, E3-based system (like that used for NF- $\kappa$ B activation) (Hay, 2005). SUMO post-translational modification (aka sumoylation) is most common to nuclear proteins and can dramatically alter the subnuclear localisation of a modified protein (Wilson & Rangasamy, 2001). SUMO modification of a bacterial protein has not yet been described however this post-translational modification has been reported with viral proteins. The function of papillomavirus E1 protein, a DNA helicase, is dependent upon its localisation to the nucleus which is mediated by sumoylation (Rangasamy *et al.*, 2000). Human cytomegalovirus (CMV) protein IE1 is sumoylated (Spengler *et al.*, 2002), which promotes viral replication by increasing transcription of another CMV protein IE2 (Nevels *et al.*, 2004). Sumoylation of vaccinia virus protein A40R makes it soluble and controls its localisation, interestingly not to the host nucleus, but to the areas of viral replication in the cytoplasm termed by the authors as 'mini-nuclei' (Palacios *et al.*, 2005).

### **4.3 Investigating the effects of NleH on NF- $\kappa$ B signalling**

NleH is a predicted Ser/Thr protein kinase, and the C-terminal end of the protein shares sequence similarity with that of the *S. flexneri* effector OspG. OspG controls the host innate immune response by interfering with NF- $\kappa$ B activation. Therefore, NF- $\kappa$ B activation in the presence of *E. coli* O157:H7 NleH1 or NleH2 was tested *in vitro* to elucidate if NleH has the same effect as OspG. To facilitate the comparison, the OspG construct (pRK5myc-OspG) used in the OspG study (Kim *et al.*, 2005) was requested from the corresponding author,

Dr Claude Parsot, but unfortunately the request was refused. Owing to this, pCMV-OspG was constructed as described in Materials and Methods to allow a comparison between the effectors with the same assay. Shortly prior to conducting the experiment, it was reported that NleH1 inhibits and NleH2 stimulates NF- $\kappa$ B activation but they interact with the same host target (RPS3) (Gao *et al.*, 2009). These opposing, and possibly contradictory, results were surprising considering the high identity shared between the two proteins and consequently provided more reason to independently test the affect of NleH on NF- $\kappa$ B activation.

The impact of NleH on NF- $\kappa$ B activation in host cells was assessed by transfecting plasmids which expressed NleH variants, with pCMV (vector only) and OspG as controls, into HEK293T cells. Activation of NF- $\kappa$ B was stimulated by adding TNF- $\alpha$  (25 ng/ml) and quantified through a luciferase reporter. This work was carried out in collaboration with Prof Tom Evans, who provided the mammalian cell line and plasmids. Three site-directed mutants of NleH (K159A, E173A and D258A), Figure 4-1, were included to assess their affect on NF- $\kappa$ B activation. These residues are conserved in kinase domains, where the lysine (K159) residue is essential for activity, the glutamate (E173) stabilises ATP docking and the aspartate (D258) stabilises the catalytic loop (Hanks & Hunter, 1995). Prof Tom Evans performed an *in vitro* kinase assay and autoradiography to demonstrate autophosphorylation of recombinantly purified NleH1 protein and its kinase dead mutant K159A. This confirmed that NleH1 can autophosphorylate in the presence of radioactive labelled ATP and magnesium ions, an action shared with OspG (Kim *et al.*, 2005), and the loss of this kinase activity in the K159 mutant.

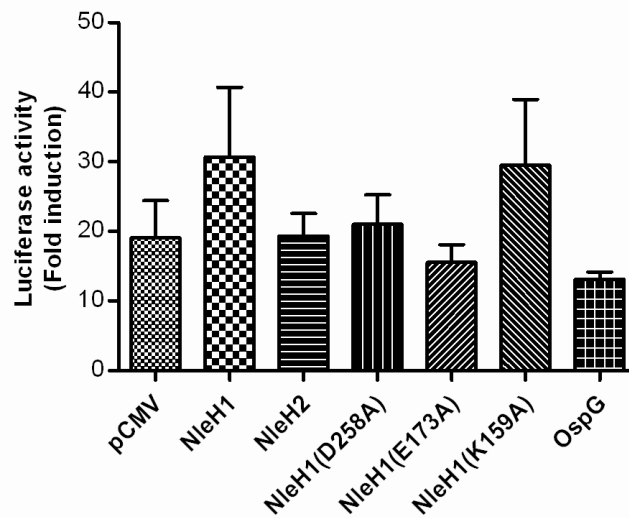


**Figure 4-2 NF- $\kappa$ B activation in the presence of NleH variants**

HEK293T cells were co-transfected with a luciferase reporter plasmid under the control of consensus  $\kappa$ B sites, a  $\beta$ -galactosidase and a control, NleH or OspG vector. After 40 hours, cells were stimulated by the addition of TNF- $\alpha$  (25 ng/ml; 24 hours). Statistical analysis with one-way ANOVA shows no significant difference compared with the pCMV control.

The luciferase assay results (Figure 4-2) indicate that NleH1 stimulates NF- $\kappa$ B activation by ~45% and this effect is not dependent upon its kinase activity, as kinase-dead mutant K159A demonstrates similar levels of NF- $\kappa$ B induction compared with the WT NleH1. NleH1 D258A reduces WT phenotype by ~35% and NleH1 E173A appears to abolish the WT phenotype as the NF- $\kappa$ B activity is similar to that of the control, pCMV. The effect of NleH2 on NF- $\kappa$ B is negligible, as there is no increase or decrease compared with the control, pCMV. OspG decreases NF- $\kappa$ B activation by ~17.5%, which is markedly lower compared to the 70% reduction previously reported (Kim *et al.*, 2005). Upon closer assessment of the experimental conditions employed in this study, the authors assayed transfections with increasing concentrations of OspG plasmid, and the 70% reduction in NF- $\kappa$ B activation is observed when there is 5 times more OspG (0.5  $\mu$ g) than the NF- $\kappa$ B reporter (0.1  $\mu$ g) transfected. In my assay, equivalent concentrations of effector and NF- $\kappa$ B reporter plasmids were transfected (0.4  $\mu$ g); the previous study reported a 30% decrease in NF- $\kappa$ B activation when equivalent concentrations of OspG and reporter plasmid were transfected. This provides explanation to the reduced effect of OspG on NF- $\kappa$ B activation in my results compared to those reported by Kim and authors (Kim *et al.*, 2005).

Therefore, these results suggest that NleH1 and NleH2 do not have the same effect upon NF- $\kappa$ B as its homolog OspG.

## **4.4 Elucidating the host protein targets of NleH**

NleH is regulated, expressed and secreted by *E. coli* O157:H7, has Ser/Thr protein kinase activity with the ability to autophosphorylate, and contains ELMs within its primary sequence. These characteristics suggest that NleH may have a function within the host cell. In order to identify potential host cell proteins which are modified by or interact with NleH, two dimensional differential gel electrophoresis (2D-DiGE) and yeast-two hybrid screening were used.

### **4.4.1 2D Differential Gel Electrophoresis**

2D-DiGE was first described in 1997 (Unlu *et al.*, 1997) and can be used to identify post-translational modifications (PTM) and differences in protein abundance by directly comparing the proteomes from two separate conditions, e.g. wild-type vs. mutant. The two samples are differentially labelled with CyDyes and co-separated on the same gel, and therefore the samples are both treated with the same handling conditions. This technique is two dimensional as it first separates proteins by their relative charge on the basis of their pI, using isoelectric focussing, then by molecular mass using SDS-PAGE. After separation, the gel is exposed to wavelengths of light that excite the chosen fluorophores, an image is taken for each sample and the images overlaid to determine any differential expression or PTM of the proteins.

2D-DiGE analysis of the proteome of HEK293T cells transfected with NleH1 was compared against that of HEK293T cells transfected with kinase-dead mutant NleH1 K159A. 16 hours after transfection, the cells were stimulated with TNF- $\alpha$  (25 ng/ml) for 20 minutes prior to harvesting, as described in Materials and Methods. The proteins from NleH1-1 WT transfected cells were labelled with Cy3 and those from NleH1-1 K159A transfected cells labelled with Cy5. These samples were mixed together and separated first by isoelectric focusing then by SDS-PAGE. The gel is scanned with a Typhoon scanner to excite the

fluorophores, first Cy3 (Ex/Em; 540 nm/590 nm) for the HEK293T+NleH1 sample then Cy5 (620 nm/680 nm) for HEK293T+K159A (Figure 4-3).

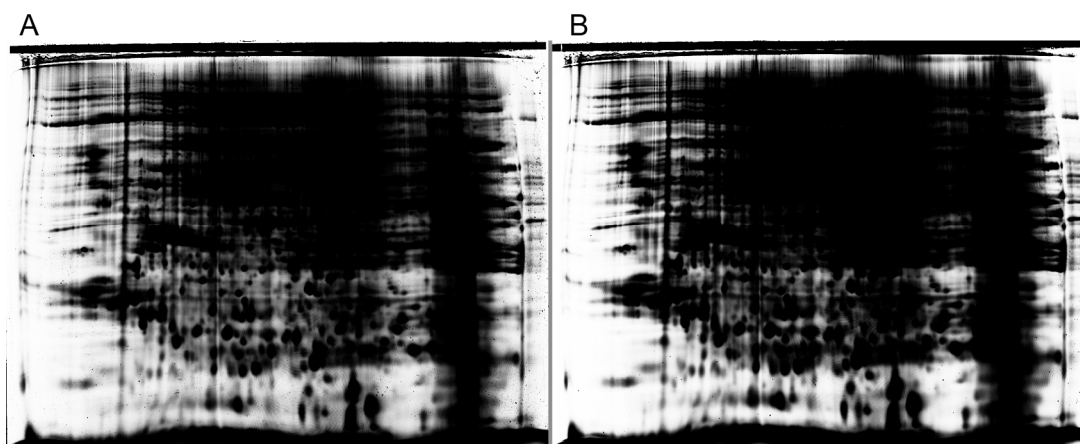


**Figure 4-3 Typhoon scans of NleH1 WT and K159A**  
HEK293T cells were transfected with NleH1 or its kinase dead mutant K159A, stimulated with TNF- $\alpha$  (25 ng/ml) for 20 minutes before harvesting and prepared for DiGE by labelling all the proteins from WT with Cy3 (A) and K159A with Cy5 (B). The proteins were then separated first by isoelectric focusing then by electrophoresis.

The 2D-DiGE gel was analysed using DeCyder analysis software. The DeCyder analysis software isolates each of the protein 'spots' on the gel and assesses differences between their positions and volumes/concentrations. Spots (Figure 4-4 A) which show any significant difference are labelled blue and areas of no change are labelled yellow. The threshold can be set to various stringency values, but even the most relaxed threshold did not resolve any significant differences between the two conditions (Figure 4-4 B).

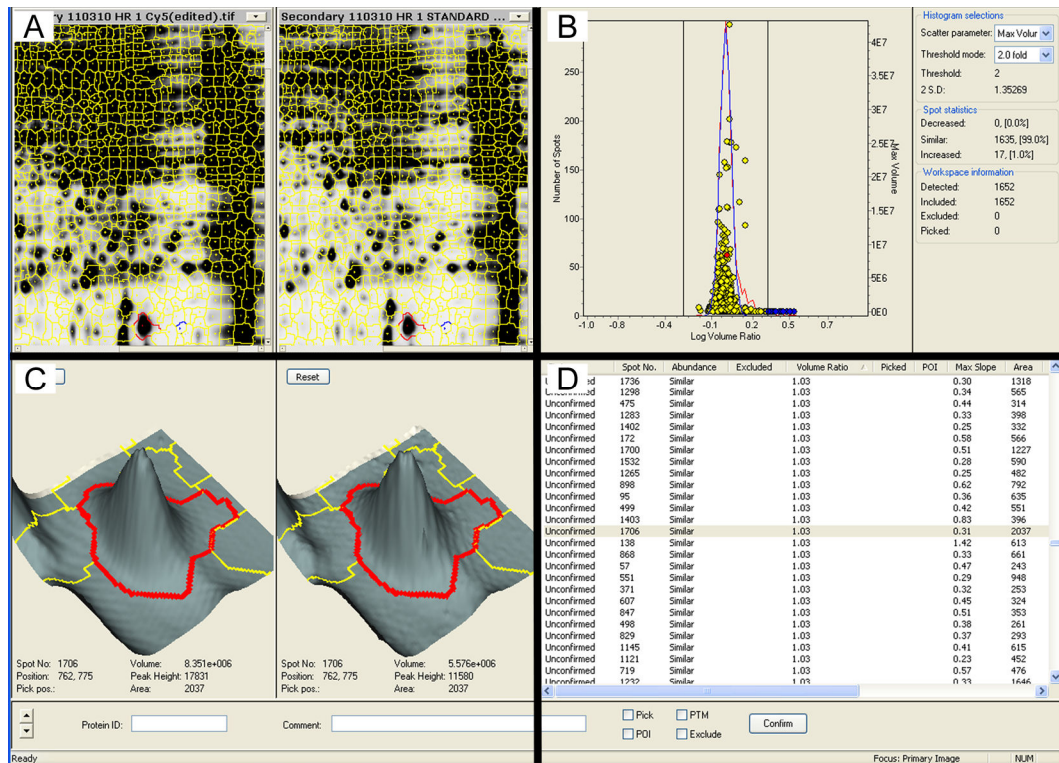


**Figure 4-4 Example view of DeCyder analysis software**

**A.** The Typhoon scans are loaded into the software which isolates each protein spot and the densitometry compared between the two samples; yellow indicates no change and blue indicates a significant difference between the gels. **B.** The graph plots the volume ratio for each spot with the vertical line each side representing the threshold chosen. **C.** A spot can be selected for individual analysis. **D.** Detailed analysis of each individual spot is provided in the table.

#### 4.4.2 Yeast-two hybrid screen

Yeast-two hybrid analysis can identify protein-protein interactions by the successful transcription of a reporter gene which can occur only when the DNA-binding domain of a transcription factor, e.g. Gal4, genetically fused to the protein of interest (X), is brought into close proximity with its activation domain, genetically fused to a protein (Y) which interacts with protein X (Fields & Song, 1989).

NleH1 and NleH2 ORF sequences from *E. coli* O157:H7 TUV93\_0 were cloned into Gateway™ vector pDONR207 (Invitrogen, Scotland) as described in Materials and Methods. These constructs were sent to Prof Jürgen Haas at University of Edinburgh for his laboratory to subclone NleH1 and NleH2 into their yeast two hybrid Gateway™ expression vector, pGBKT7-DEST, via an LR reaction (Stellberger *et al.*, 2010). They have access to an array-based yeast two hybrid

screening system allowing NleH1 and NleH2 to be screened, as bait, against a human cDNA (prey) library, comprising of about 100,000 targets, to test for protein-protein interactions.

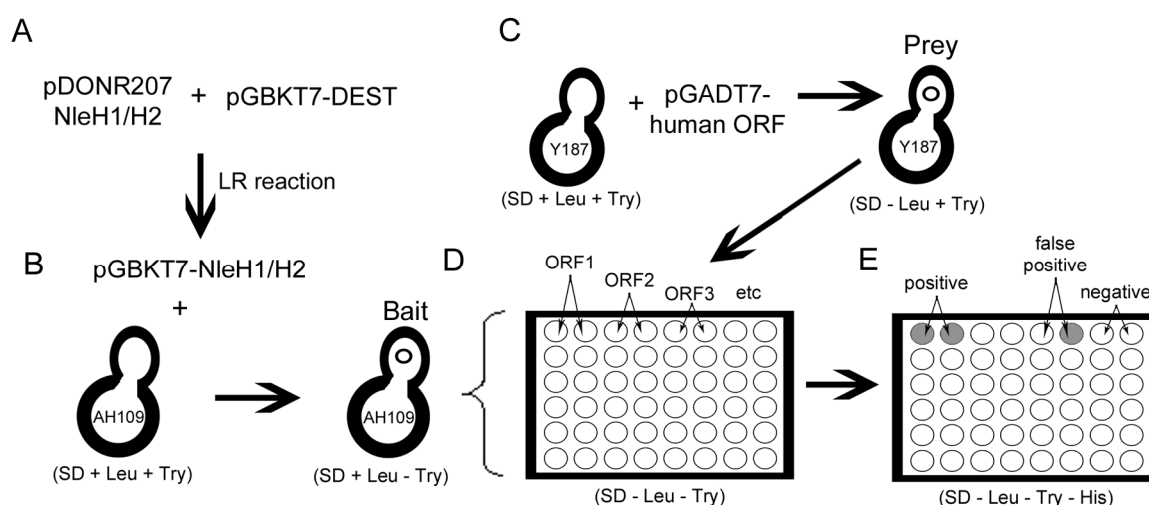


**Figure 4-5 Yeast-two hybrid screen with vectors described by (Stellberger *et al.*, 2010)**  
**A.** NleH1 and NleH2 ORFs are introduced into the Gateway<sup>®</sup> vector pGBKT7-DEST via an LR reaction to create vector pGBKT7-NleH1/H2 (Bait; Gal4 DNA binding domain). **B.** This bait vector is transformed into haploid AH109 (*gal4::his3*) yeast cells, and selected on media without the addition of tryptophan, to select for plasmid uptake. **C.** Haploid Y187 yeast cells are transformed with a library of human cDNA vectors, pGADT7-human ORF (Prey; Gal4 activation domain), and selected on media without the addition of leucine to select for plasmid uptake. **D.** Prey cells are plated, with each ORF represented in duplicate, in an array and mated with bait cells; diploid cells are selected by growth in media without both leucine and tryptophan to confirm mating. **E.** Diploid cells are then transferred for growth in media without leucine, tryptophan and histidine to select for protein-protein interactions. Growth (due to transcription of *gal4::his3*) in both wells indicates protein-protein interaction, growth in only one well indicates a false positive result, and no growth indicates that no interaction has occurred.

Each pairwise interaction is tested in duplicate to reduce the number of false positive interactions, which can occur due to overexpression of the hybrid proteins in the yeast. Three hits were found with NleH1 and two with NleH2 in this screen, unfortunately they were all false positives. It was anticipated that the screen would pick out the published NleH1 binding partners BI-1 and/or RPS3. A commercial human testes cDNA library from Clontech was used for the screen, so it cannot be known conclusively whether these proteins are represented in the screen. However, other published work demonstrates that both BI-1 (Walter *et al.*, 1995) and RPS3 (Schlecht *et al.*, 2004) are expressed in this tissue type; therefore these may be considered as false negatives within this screen.

## 4.5 Translocation reporter iLOV

In collaboration with Dr John Christie, University of Glasgow, we tested the application of iLOV (improved Light Oxygen Voltage sensor domain) as a reporter protein in *E. coli* O157:H7 (Chapman *et al.*, 2008). LOV domains are part of the photosensing Ser/Thr protein kinases (phototropins) in plants and when the domain was recombinantly expressed in *E. coli*, it fluoresced when exposed to UV light (Salomon *et al.*, 2000; Swartz *et al.*, 2001). The LOV domain was subjected to molecular evolution in order to improve its fluorescence and recovery after photobleaching to create iLOV (Chapman *et al.*, 2008). As proof-of-principle, iLOV was then shown to be successfully applied in the localisation of a viral protein *in planta*, overcoming the problems observed with GFP as a reporter (Chapman *et al.*, 2008). iLOV is less than half the size of GFP, Table 4-1, making it a suitable candidate to test as a reporter for T3S-mediated translocation.

**Table 4-1 Properties of GFP and iLOV**

Property	Fluorescent Protein	
	GFP	iLOV
Excitation/emission wavelength (nm)	488/509	450/495
Size (kDa)	26	10
Additional factors required for fluorescence	Oxygen	Flavin mononucleotide
Recovery after photobleaching	No	Yes

Preliminary data from our laboratory demonstrated that genetically fusing iLOV to the C-terminal end of Tir, a T3S effector of *E. coli* O157:H7, did not interfere with its secretion and translocation. We also found that a plasmid expressing Tir-iLOV can complement a ZAP193 $\Delta$ tir mutant and still function to form actin rich pedestals viewed with FAS staining. Therefore, translational fusions of NleH1 and NleH2 to iLOV, under the control of an IPTG inducible promoter, were constructed to provide further data in the characterisation of this protein as a reporter in *E. coli* O157:H7. The translocation and localisation of NleH in the host cell was investigated.

*E. coli* O157:H7 TUV93\_0 transformed with pJ284 (*ptac*::iLOV), pAHE27 (*ptac*::NleH1-iLOV) or pAHE28 (*ptac*::NleH2-iLOV) were added to EBL cells and incubated for 5, 10, 30 and 180 minutes before applying CellMask™ plasma membrane stain and fixing the cells with paraformaldehyde. *E. coli* were immunostained with  $\alpha$ -O157 antibodies raised in rabbits, followed by  $\alpha$ -rabbit IgG AlexaFluor-555 conjugate antibodies. Samples were viewed using a Zeiss AxioImager M1 and all z-stack images were acquired with the same acquisition protocol and excitation wavelength exposure times. Micrographs (Figure 4-6) show that iLOV from *ptac*::iLOV expressing cells, is within the  $\alpha$ -O157 labelled area indicating that it is contained within the bacterial cytoplasm. However, there is no green signal seen within the red labelled *E. coli* with NleH1-iLOV and NleH2-iLOV expressing cells, instead it is found within the blue outlines indicating NleH1- and NleH2-iLOV is within the mammalian cell. The green signal is not just diffuse within the cell, but appears localised to the cytoplasm, with some bright punctate areas visible. The boxed areas (Figure 4-6 Merge) were selected for additional analysis with Volocity 3D restoration software (PerkinElmer). These areas were viewed from above, side and below as shown in the diagram on the right-hand-side of Figure 4-7. From this, it can be seen that the bacteria are associated with the cell periphery, indicated by the blue stain. The side perspective shows that bacteria are either on or above the level of the membrane stain. This perspective also shows that the green signal from NleH1- and NleH2-iLOV is localised within the mammalian cell as it is found at a greater depth than the bacteria and mammalian membrane. This is also supported by the view from below, where NleH1-iLOV can be seen beneath the  $\alpha$ -O157 stain labelling the bacteria. The punctate areas of NleH-iLOV seem to be either near the plasma membrane or perinuclear.

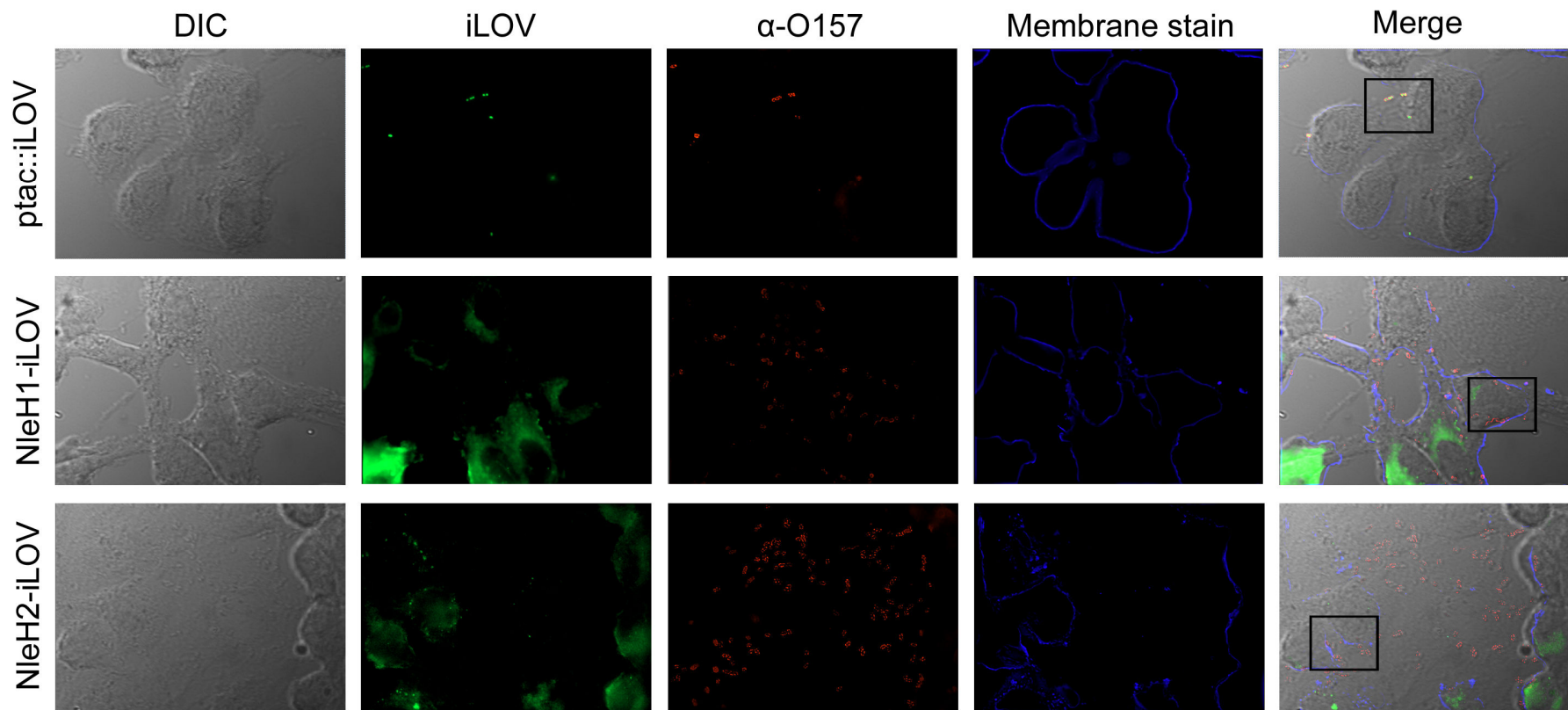


**Figure 4-6 Fluorescence microscopy of NleH-iLOV upon contact with EBL cells**

TUV93-0 were transformed with plasmids expressing iLOV (pJ284), NleH1-iLOV or NleH2-iLOV and grown in inducing conditions (MEM+Amp+IPTG) before adding to EBL cells and incubated at 37°C, 5% CO<sub>2</sub> before removing supernatant and fixing cells. The panel of images was taken from the 30 minute incubation but is representative of all time points tested. Boxed areas were analysed further using Volocity 3D restoration software (PerkinElmer).

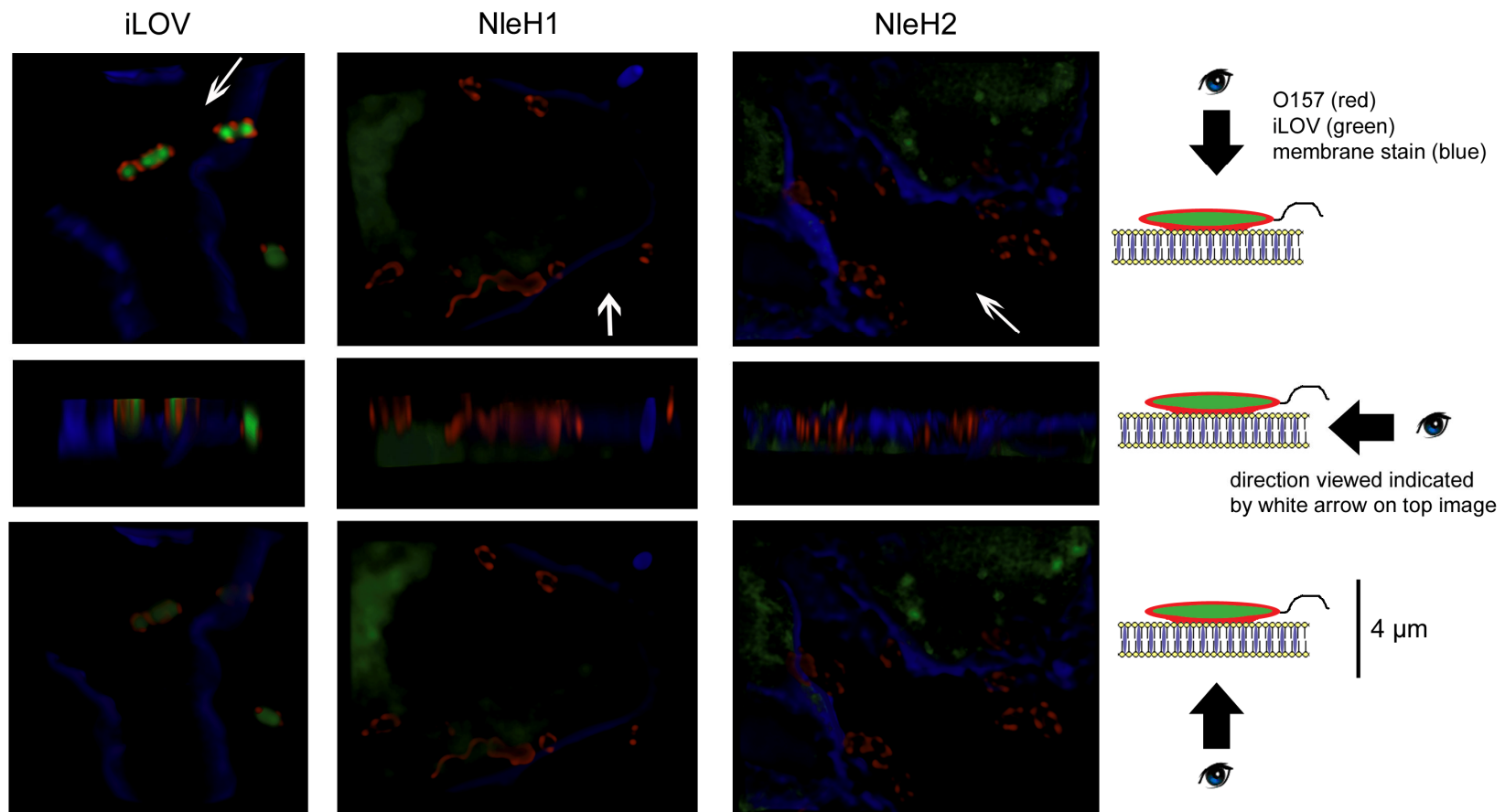


**Figure 4-7 Three dimensional viewing of bacteria adhering to EBL cells.** Boxed images from Figure 4-6 were analysed with 3D opacity Volocity software (PerkinElmer) to show the spatial localisation of membrane (membrane stain; blue), bacteria ( $\alpha$ -O157; red) and iLOV (green). The panel on the right describes the viewpoint of the adjacent micrographs.

## 4.6 Discussion

NleH1 and NleH2 are non-LEE encoded effectors which are translocated into the host cell via the T3SS (Tobe *et al.*, 2006; Garcia-Angulo *et al.*, 2008). When NleH1 and NleH2 were first identified, a BLASTp search found that it shared significant sequence identity with *S. flexneri* effector OspG (Tobe *et al.*, 2006). An alignment of the primary sequence of NleH1, NleH2 and OspG (Figure 4-1) shows that this similarity lies mainly within its conserved protein kinase domains. A study of enterohaemorrhagic *E. coli* serogroup O111 confirms that NleH is distantly related to OspG; *ospG* homologues, with >90% protein identity, are present in non-O157 serogroups and *Yersinia enterocolitica* (Nobe *et al.*, 2009). The *Y. enterocolitica* OspG homologue YspK was previously identified in a proteomic screen of effectors secreted via the Ysa T3S which is present only in *Y. enterocolitica* Biovar 1B (Matsumoto & Young, 2006).

NleH1 and NleH2 have 33 and 36 ELMs in their primary sequence, respectively, of which the PDZ binding domain has been characterised for NleH1 in EPEC (Martinez *et al.*, 2010). Although ELMs are present, they are not always used or modified. For example, in a study of neuronal proteins with SUMO modification motifs, only 14 of the 39 motifs were sumoylated *in vitro* (Wilkinson *et al.*, 2008). Regardless of this, assessing the ELMs present in a protein of interest provides areas of sequence which can be targeted by site-directed mutagenesis to investigate the function and/or localisation of the protein.

The effects of NleH on NF- $\kappa$ B activation were assessed *in vitro* with HEK293T transfections. The results (Figure 4-2) indicate that NleH1 activates NF- $\kappa$ B, which correlates with a previous report that *Citrobacter rodentium* NleH increases NF- $\kappa$ B activity *in vivo* (Hemrajani *et al.*, 2008). This was demonstrated through infection of NF- $\kappa$ B-*luc* reporter mice with *C. rodentium* or its isogenic  $\Delta$ nleH mutant and semiquantitative RT-PCR of TNF- $\alpha$  RNA transcript extracted from the infected colons (Hemrajani *et al.*, 2008). *E. coli* O157:H7 NleH1 shares protein identity with CRNleH, as they both lack the 10 amino acid indel sequence, which supports the shared effect upon NF- $\kappa$ B activation (Hemrajani *et*

*al.*, 2008). However, these results also contradict with a previous report that *E. coli* O157:H7 NleH1 inhibits and NleH2 stimulates NF- $\kappa$ B activation (Gao *et al.*, 2009). CRNleH tested under the same conditions inhibited NF- $\kappa$ B activation to similar levels as *E. coli* O157:H7 NleH1, which contradicts the activation observed *in vivo* in the previous study (Hemrajani *et al.*, 2008). Luciferase reporters were transfected into HEK293T cells in a manner similar to what was carried out in this study, however cells were stimulated with 4 times more TNF- $\alpha$  and analysed 1 hour post-stimulation. Similar to the OspG study (Kim *et al.*, 2005), the effector plasmid and the NF- $\kappa$ B reporter plasmid were transfected at a 4:1 ratio which appears to amplify the effect (to a similar degree) observed with equivalent concentrations of vectors (Gao *et al.*, 2009). Studies in EPEC have shown that both NleH1 and NleH2 reduce NF- $\kappa$ B activity, by interfering with IKK- $\beta$  induced NF- $\kappa$ B activation resulting in a suppression of I $\kappa$ B- $\alpha$  degradation (Royan *et al.*, 2010). This study also used transfection assays, but TNF- $\alpha$  was not used to stimulate NF- $\kappa$ B activation instead it was stimulated by the co-transfection of IKK- $\beta$  or p65 (Royan *et al.*, 2010). The conclusion that NleH interferes with IKK- $\beta$  induced activation of NF- $\kappa$ B was supported in part by further collaborative work with Philip Hardwidge and Michael Lenardo's groups investigating the role of RPS3 in NF- $\kappa$ B activation, where they show that *E. coli* O157:H7 NleH1 can inhibit the phosphorylation of RPS3 by IKK- $\beta$  (Wan *et al.*, 2011). Inhibiting the phosphorylation of RPS3 restricts its translocation into the nucleus, reducing transcription of RPS3 dependent  $\kappa$ B sites (Wan *et al.*, 2007; Gao *et al.*, 2009; Wan *et al.*, 2011). Regardless of this, transcription of genes controlled by non-RPS3 dependent  $\kappa$ B sites can still occur, providing some explanation as to why NleH1 and NleH2 did not significantly affect NF- $\kappa$ B activation in my assay. Royan and authors also report that EPEC NleH1 and NleH2 can inhibit ubiquitination of phosphorylated I $\kappa$ B $\alpha$ , which was observed alongside an OspG positive control, and this effect is dependent upon their intrinsic kinase activity (Royan *et al.*, 2010). Yet, it has not been shown that NleH specifically interact with E2 ubiquitin-conjugating enzymes like that of their OspG homolog.

2D-DiGE shows no significant changes in the proteomes of HEK293T cells transfected with NleH1 or its kinase-dead mutant K159A. This may be due to limitations in the technique in resolving proteins of low abundance. To improve

upon this, additional sample preparation steps could have been introduced to better resolve low abundance proteins, such as subcellular fractionation or phosphoprotein enrichment using immobilised metal-affinity chromatography (IMAC). Additional post-separation techniques include staining for phosphorylated proteins using Pro-Q Diamond stain (Molecular Probes) or immunoblotting with phosphomotif antibodies. Alternative results may be obtained by altering the incubation time between transfection and stimulation and/or the period during which the cells undergo stimulus. Another point to consider is that any affect of NleH on the host target protein may be transient and therefore the host target may be difficult to identify using this method.

NleH1 and NleH2 were assessed in an array based yeast-two hybrid screen to test for possible protein-protein interactions with human proteins, Figure 4-5. Only false positive hits were found, and as the proteins are recombinantly expressed in yeast, false negative results are possible. False negative results arise because heterologous protein expression in yeast does not guarantee that all the possible PTMs of a protein will be represented. NleH1 and NleH2 were shown to interact with Bax inhibitor 1 (BI-1) via a yeast-two hybrid screen (Hemrajani *et al.*, 2010), and with ribosomal protein subunit 3 (RPS3) via affinity purification with HeLa cell lysates and co-immunoprecipitation (Gao *et al.*, 2009). Based on these reports, these interactions may be considered as false negative results within our assay. The yeast two hybrid cDNA library used in this approach was constructed from one tissue type (testes), and although it provides a large range of possible targets for NleH interaction; the range of mRNA expressed, splice variants and post translational modifications can vary between different cell types. The yeast two hybrid assay may have provided positive interactions using a cDNA library constructed from a different tissue type, for example from human embryonic tissue, brain tissue or bovine tissue.

iLOV is a fluorescent protein which is less than half the molecular mass of GFP and is able to recover after photobleaching (Chapman *et al.*, 2008). A translational fusion of iLOV to the C-terminus of Tir can complement a Tir deficient strain of *E. coli* O157:H7 and form actin pedestals (K. Velentza, I. Houghton, A. Holmes and A. Roe; unpublished results). NleH-iLOV can be translocated into the host cell, as determined by fluorescence microscopy, Figure 4-6 and Figure 4-7. NleH-iLOV localises to the cytoplasm of the

mammalian cell, with bright punctate areas visible. These punctate areas near the plasma membrane may be where NleH localises when it is interacting with the NHERF2 scaffold protein (Martinez *et al.*, 2010). The possible perinuclear localisation of NleH-iLOV would have to be confirmed by nuclear staining, e.g. with DAPI, but this localisation correlates with the other host proteins which have been shown to interact with NleH, RPS3 (Gao *et al.*, 2009; Wan *et al.*, 2011) and BI-1 (Hemrajani *et al.*, 2010). These micrographs differ from what was observed with pAHE8 and pAHE22 (*nleH::gfp*) as GFP is too large to be translocated through the T3SS. It is interesting that NleH-iLOV is detected within the host cytoplasm soon after cell attachment. This may be because the bacteria were grown in T3SS inducing conditions (MEM) therefore the apparatus was already displayed when contact was made with the host cell. Also, NleH-iLOV expression is induced by the addition of IPTG suggesting that overexpression of an effector may 'override' the control mechanisms of the T3SS, such as the chaperones. It would have been interesting to test the translocation of NleH-iLOV under the control of its native promoter.

In conclusion, NleH1 and NleH2 are Ser/Thr protein kinases, with the ability to autophosphorylate. NleH-iLOV localises to the cytoplasm, plasma membrane and around the nucleus. DiGE analysis and yeast-two hybrid assays were not successful in trying to elucidate a human kinase target or interacting partner of NleH1 or NleH2. Other groups have shown that NleH1 interferes with RPS3-dependent transcription of NF- $\kappa$ B sites (Gao *et al.*, 2009) by inhibiting RPS3 phosphorylation by IKK- $\beta$ , retaining RPS3 in the cytoplasm (Wan *et al.*, 2011). The kinase activity of NleH1 is required to inhibit RPS3 phosphorylation by IKK- $\beta$  but it does not directly phosphorylate either protein. NleH in EPEC inhibits ubiquitination of phosphorylated I $\kappa$ B $\alpha$  *in vitro*, which is dependent upon its kinase activity. NleH also inhibits the pro-apoptotic pathway via its interaction with BI-1 (Hemrajani *et al.*, 2010). A phosphorylation target of NleH has yet to be elucidated. These results suggest that NleH is a multi-functional protein, which is not an uncommon trait of *E. coli* O157:H7 effector proteins, e.g. it has been described for EspF (Holmes *et al.*, 2010). iLOV can be genetically fused to T3S effectors without hindering their secretion, translocation or function. This newly developed fluorescent protein provides a useful tool for the study of T3S effectors.

## 5 Enhancing the fluorescent toolbox of *Streptococcus pneumoniae*

### 5.1 Summary

Green Fluorescent Protein (GFP) was first identified from the *Aequorea* species of bioluminescent jellyfish in 1979 by Osamu Shimomura, but the gene was not cloned until 1992 by Douglas Prasher (Prasher *et al.*, 1992). Over the years, the wild-type (WT) GFP has been modified to improve certain properties (such as brightness) and to produce variants emitting in the blue (BFP), cyan (CFP) and yellow (YFP) regions of the spectra. GFP has a  $\beta$ -barrel structure likened to that of the bacterial porins and the majority of amino acid mutations to produce the colour variants occur within the central alpha helix, where the chromophore (or fluorophore) is positioned. The chromophore is responsible for the protein's fluorescent properties and GFP does not require any additional co-factors from *Aequorea victoria*, for example aequorin needs calcium ions and luciferase requires ATP and other substrates in order to fluoresce. This was demonstrated by heterologous expression of GFP in *E. coli* and *C. elegans* (Chalfie *et al.*, 1994). However, GFP is dependent upon the availability of molecular oxygen for maturation of the chromophore after protein translation to form the fluorophore (Heim *et al.*, 1994). GFP is a weak dimer, but a monomeric form of GFP can be produced by replacing Alanine residue 260 with Lysine or Valine. Regardless of the numerous combinations of single mutations introduced, emission in the orange and red regions of the spectra was unachievable; until the discovery of DsRed. DsRed is a red fluorescent protein identified from the *Discosoma* species of non-bioluminescent red coral (Matz *et al.*, 1999). It is an obligate tetramer, and its monomer shares the  $\beta$ -barrel conformation of GFP. The excitement of the discovery of a red fluorescent protein (RFP) was short-lived due to problems with its application as a reporter protein. DsRed exhibits a slow maturation time (i.e. time to fold into a mature protein) and an intermediate green state (Jakobs *et al.*, 2000). Its tetrameric character results in a tendency to aggregate within the cytoplasm of the expressing cells, protein fusions can mislocalise or aggregates can be toxic to the host cell. Work in Roger Tsien's laboratory was paramount to the generation of monomeric RFP and coloured variants. Through

both direct mutagenesis, based on beneficial mutations found in GFP, and indirect mutagenesis with error-prone PCR, it was found that 33 mutations were required to make DsRed monomeric (Campbell *et al.*, 2002), creating mRFP1. The first and last 7 residues of GFP were added to the N- and C-terminus of DsRed, respectively, to enable the stable fusion of a protein to either terminus of the mRFP (Shaner *et al.*, 2004). In order to further improve the qualities and expand the emission spectra of mRFP1, single point mutations were introduced indirectly via somatic hypermutation (Wang *et al.*, 2004) and error-prone PCR (Shaner *et al.*, 2004), and mutants screened by fluorescence-activated cell sorting (FACS). The mutations involved in improving mRFP occur throughout the protein, and are not concentrated in the region of the chromophore like that for GFP. The emission spectrum variants of mRFP were called mFruits, so named due to the wide range of emission spectra covered by the different FP's and the 'm' denotes their monomeric property [reviewed in (Shaner *et al.*, 2007)].

The availability and development of fluorescent proteins has enabled the study of gene regulation, expression and protein localisation in all orders of organisms, from bacteria and fungi to higher eukaryotes. Fluorescent proteins have been exploited to prolific effect in labelling systems such as Brainbow (Livet *et al.*, 2007) and Fucci (fluorescent, ubiquitination-based cell cycle indicator) (Sakaue-Sawano *et al.*, 2008). Brainbow is a neuronal labelling system that has a number of different colour emitting fluorescent proteins encoded in tandem with *lox* recombination sites on a transgene. The addition of Cre recombinase results in shuffling of these tandem genes (by recombination or inversion), resulting in one of up to 90 different colour hues to be expressed, which was used to map the neuronal network architecture *in vitro* and *in vivo* (Livet *et al.*, 2007). The Fucci system expresses E3 ubiquitin ligase substrates Cdt1, which is expressed highest during G<sub>1</sub> phase, and Geminin, highest during S/G<sub>2</sub>/M phases, which have been genetically fused to red and green fluorescent proteins respectively, enabling tracking of the cell cycle progression from G<sub>1</sub> phase (red) to S/G<sub>2</sub>/M phases (green) *in vitro* and *in vivo* (Sakaue-Sawano *et al.*, 2008).

To date, fluorescent proteins have been used in a very limited number of pneumococcal studies; as a transcriptional reporter, as a live cell marker and for pneumococcal protein localisation. The expression of pneumococcal genes was investigated using differential fluorescence induction where a plasmid library

was created with random fragments of *S. pneumoniae* chromosomal DNA cloned upstream of a promoterless *gfp* gene (Bartilson *et al.*, 2001; Marra *et al.*, 2002). This library was cloned into *S. pneumoniae* D39 and the library clones subject to different growth conditions to assess pneumococcal gene induction evident by the expression of GFP. GFP expressing cells were selected by fluorescence activated cell sorting (FACS) and the differentially expressed genes identified through sequencing the selected clones. Growth conditions tested *in vitro* include the presence of competence stimulating peptide (CSP) (Bartilson *et al.*, 2001), carbon dioxide, high osmolarity, low iron, blood and change in temperature; gene expression during *in vivo* growth was also assessed (Marra *et al.*, 2002). One can only assume that the assessment of gene expression under different growth conditions was not continued using this technique due to the advances in, and cost reduction of, DNA microarray platforms.

*S. pneumoniae* transformed with a plasmid containing *gfp* under the control of an uncharacterised pneumococcal promoter was used to track the migration of whole pneumococcal cells in lung tissue *in vivo* (Kadioglu *et al.*, 2001). This study showed that GFP expressing pneumococci could be identified in murine lung histology samples, specifically within the broncho-epithelial cells 4 and 24 hours, after intranasal challenge. However, the GFP fluorescence exhibited by these pneumococci was not considered bright (personal communication, Prof Tim Mitchell). Upon closer assessment of the micrographs from this publication there is evidence of background fluorescence from the mammalian cells, which implies that a long exposure time was required in order to generate an adequate emission from the pneumococci expressing GFP. Whether this lack of brightness is due to poor GFP expression *in vivo*, the GFP allele chosen, or reduced activity of GFP due to insufficient fluorophore maturation, is unknown.

The localisation of proteins involved in *S. pneumoniae* choline metabolism, LicABCD, has been investigated using translational fusions to a fast-folding variant of GFP (Eberhardt *et al.*, 2009). The authors describe two plasmids which can integrate into the chromosome to create single copy genetic fusions to *gfp* at the 3' end, where the fusion is under the control of the native gene promoter due to integration of the plasmid at the native locus, or the 5' end where the fusion is under the control of a zinc-inducible promoter integrated at the non-essential *S. pneumoniae* *bgaA* gene locus. After proof-of-principle

experiments with these constructs successfully correlated the localisation of an already characterised protein, the localisation of GFP-LicABCD fusion proteins were assessed with fluorescence microscopy, where cytoplasmic and membrane localisation could clearly be distinguished.

The aim of the work reported in this chapter was to enhance the applications of fluorescent proteins in *Streptococcus pneumoniae*, by designing and characterising GFP, YFP and RFP, with their codon usage optimised for *S. pneumoniae* expression, as tools for future pneumococcal research.

## 5.2 Codon-optimised fluorescent proteins

The majority of the available genes for fluorescent proteins have a eukaryotic codon usage that can affect expression in prokaryotes. Codon usage can vary between different organisms; therefore a protein with heterologous prokaryotic codon usage may not be efficiently expressed due to underrepresentation of a particular tRNA. Therefore, the coding sequences for GFP, YFP and RFP were optimised to *S. pneumoniae* TIGR4 codon usage and synthesised by DNA2.0 (California, USA). DNA 2.0 uses the Codon Usage Database (<http://www.kazusa.or.jp/codon>) to optimise their products' codon usage to the species/strain specified. His, Lumio<sup>TM</sup> and FLAG tags were included in the gene design at the 5' end of the coding sequence. The constitutive promoter from the *S. pneumoniae* aminopterin resistance operon (*ami*) was included in the design to ensure transcription of the genes in the pneumococcus (Alloing *et al.*, 1990; Beard *et al.*, 2002), Figure 5-1. Therefore, if any problems arise with expressing the heterologous genes in the pneumococcus, they may be attributed to post-transcriptional or post-translational modifications of the gene product by the bacterium.



## **5.3 Characterisation of *S. pneumoniae* codon-optimised GFP, YFP and RFP**

### ***5.3.1 Expression of fluorescence during growth***

Once the plasmids were successfully transformed into D39, the levels of fluorescence were measured during the course of growth in BHI using a fluorescence plate reader. This tests if the proteins are being expressed constitutively, as expected being under the control of the *ami* promoter, and that the values are greater than that of any autofluorescence from the pneumococcus itself.

In a preliminary experiment, the fluorescence was measured directly from the culture in BHI, including a BHI only (blank) control, however it became apparent that this could not be continued in the protocol as the blank BHI control had similar fluorescence levels to that of the cultures. This phenomenon had been previously reported (Acebo *et al.*, 2000). To address the problem of BHI autofluorescence, instead of testing alternative media such as tryptone soy broth, the bacteria were pelleted from a 1ml sample and suspended in 1ml PBS before being analysed for fluorescence, thus giving a standard protocol that can be applied to any growth media. To account for the additional treatment viable counts were taken from the suspension in PBS, not from the BHI culture, to consider any potential cell loss. This potential cell loss can be considered as minimal, because the viable counts are reproducible from the biological replicates seen in Figure 5-2 D.

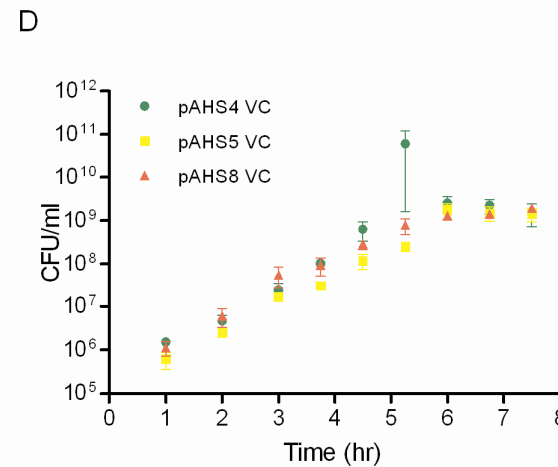
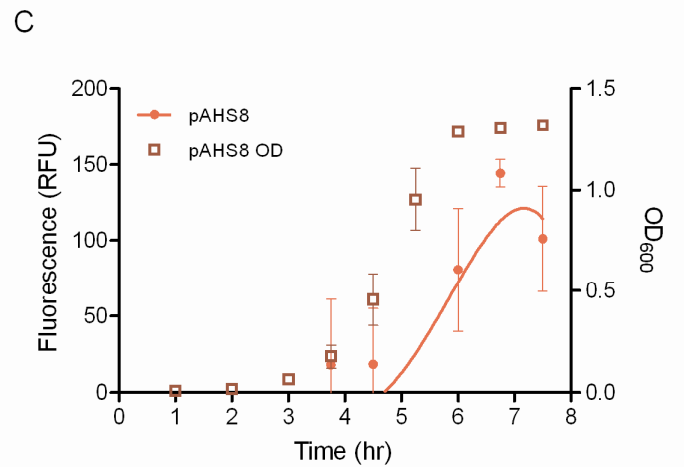
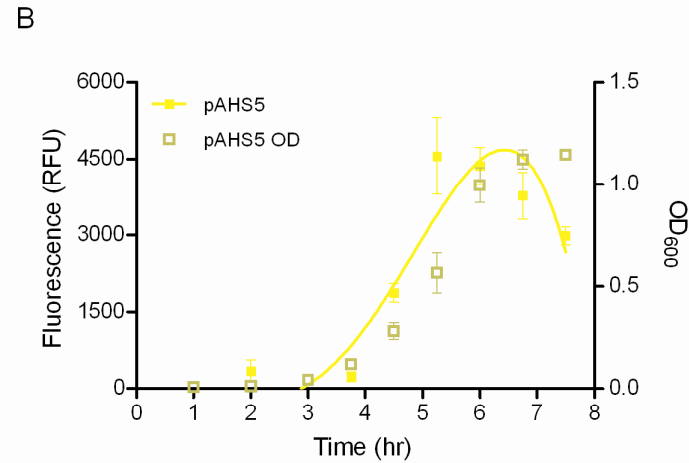
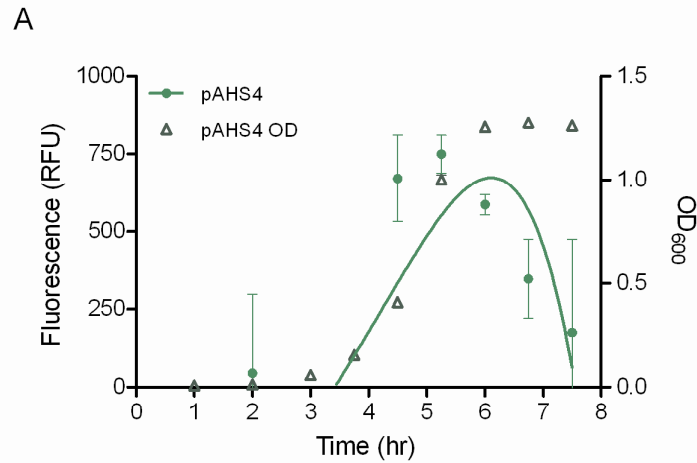


**Figure 5-2 Expression of fluorescent proteins during growth in *S. pneumoniae* D39**  
 20ml of BHI was inoculated with  $5 \times 10^5$  cfu/ml D39; D39 pAHS4 (A; green); D39 pAHS5 (A; yellow) and D39 pAHS8 (B; red). At regular intervals, 1ml of culture was removed and OD<sub>600</sub> measured (C); the remaining culture was incubated at 37°C. The 1ml sample was centrifuged and the bacterial pellet suspended in 1ml PBS; 200µl aliquots were analysed in triplicate for fluorescence (GFP/YFP = Ex. 485nm; Em. 520nm RFP = Ex. 544nm; Em. 620nm) in FLUOstar plate reader (BMG) and 20µl for viable count (C). D39 acted as a control for background fluorescence; fluorescence was plotted against OD<sub>600nm</sub> using Microsoft Excel software and a line of best fit obtained. Using this method, data were corrected for background fluorescence. The mean ± SEM of three biological repeats is plotted and lines represent the line of best fit for fluorescence.

The codon-optimised green, yellow and red fluorescent proteins are constitutively expressed as the increase in fluorescence follows a similar trend to that of the growth curve until the late stationary phase, where fluorescence begins to decline (Figure 5-2 A, B and C). The decline in fluorescence correlates with the decline in cell number due to autolysis (Figure 5-2 D), however at this stage of growth the pH of the culture media is likely to be acidic. Acidic conditions can inhibit fluorescent protein activity, which is optimum at pH 7 (Tsien, 1998). There was no obvious indication of plasmid burden upon the cells as the growth curves and viable counts are comparable to D39 alone (results not shown).

The greatest levels of GFP/YFP fluorescence are during late-exponential phase ( $\sim OD_{600} = 1$ ). YFP (pAHS5) gives a  $\sim 6$ -fold greater fluorescence than GFP (pAHS4), which may be attributed to the consensus that YFP is generally 'brighter' than GFP. Although expression of RFP follows the same trend as GFP/YFP; RFP fluorescence is first observed after 3 hours growth, an hour later than GFP and YFP. This lag cannot be attributed to reduced cell number, as the viable counts for all three cultures are similar throughout the growth curve (Figure 5-2 D). It may be that RFP has a longer maturation time than GFP/YFP or that more protein has to accumulate within the cell to overcome the background autofluorescence from the bacterial cell alone. Owing to this, RFP may not be suitable for use as a transcriptional or translational reporter.

### **5.3.2 Fluorescence microscopy**

Once fluorescence of a population was assessed during growth through measurement on a fluorescence plate reader, the transformed bacteria were assessed on a single cell basis by fluorescence microscopy.

*S. pneumoniae* D39 cells expressing GFP (pAHS4) and YFP (pAHS5) were grown to mid-exponential phase before fixing with paraformaldehyde and mounted onto microscope slides. Images were captured with the same acquisition protocol and cells were exposed to the excitation wavelength for the same period. The pneumococcal cells that are expressing YFP appear brighter than those

expressing GFP, Figure 5-3 A and B, which correlates with the previous results with the population assay. By comparing the DIC image with the fluorescent image, it can be seen that all the cells express GFP or YFP but RFP expression is not as consistent between cells.

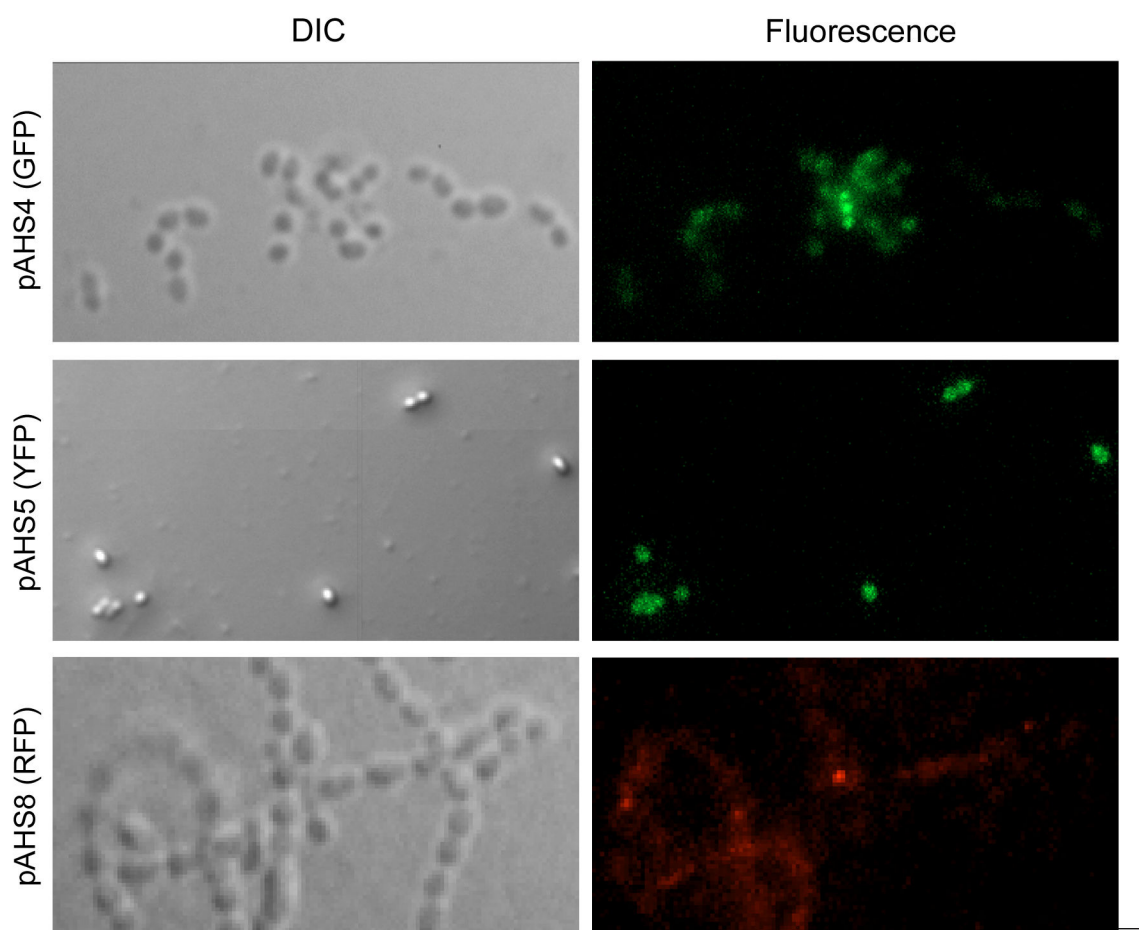


**Figure 5-3 Fluorescence microscopy of D39 pAHS4/5/8**  
*S. pneumoniae* strain D39 was transformed with pAHS4 (GFP), pAHS5 (YFP) or pAHS8 (RFP), grown in BHI to  $OD_{600} = 0.6$ , washed twice in PBS before fixing cells with paraformaldehyde. Cells were spotted onto a microscope slide and images captured with Zeiss AxioImager M1 microscope as described in Materials and Methods. GFP and YFP viewed with FITC filter, RFP with DsRed filter.

Once it was established that the pneumococci were indeed expressing the fluorescent proteins, immunofluorescence was used to show that the exterior of the pneumococcal cell could be distinguished from the interior, which is essential for future localisation studies. *S. pneumoniae* strain TIGR4 transformed with pAHS5 (YFP) was fixed onto a microscope slide and the capsule stained as described in Materials and Methods. The pneumococcal cells are all

expressing YFP, and the capsular stain is confined to the outer edges of the cell, with no obvious overlap between the two signals observed, Figure 5-4. This would account for a gap created by the cell wall between the plasma membrane, maintaining the cytoplasm stained green (YFP), and the capsule envelope, stained red ( $\alpha$ -Type 4).

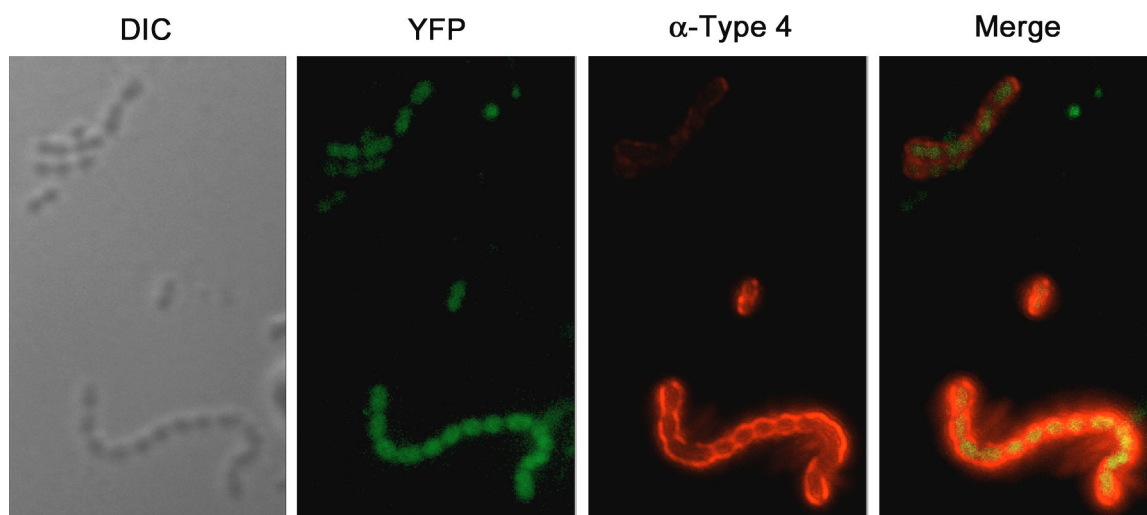


**Figure 5-4 Immunofluorescence microscopy with fluorescent pneumococci** TIGR4 was transformed with pAHS5 (YFP), grown in BHI to  $OD_{600}=0.6$ , washed twice in PBS before fixing cells with paraformaldehyde. Cells were spotted and dried onto a microscope slide and incubated with  $\alpha$ -capsule type 4 antibodies and  $\alpha$ -rabbit AlexaFluor 555 conjugate antibodies as described in Materials and Methods.

Turner and colleagues described a method of using the Cy labelling dyes (Amersham), which are traditionally used to label antibodies and nucleic acids, to stain bacteria (Turner *et al.*, 2000). As this could provide a tool to generally stain pneumococcal cells for colocalisation studies, without the need for additional antibodies, it was tested on TIGR4 expressing YFP (pAHS5). The pneumococcal cells were incubated with Cy5 dye for 15 minutes, washed with PBS and spotted onto a microscope slide. A z-stack of micrographs were taken using a Zeiss Axiolmager M1 microscope, as shown in Figure 5-5. It can be observed that the Cy5 dye localises to the outer surface of the cell, as initial images only detect YFP (green). The increase in z (height), moving left to right across the panel of images, begins to introduce some Cy signal (blue) at the periphery of the cell, gradually increasing across the upper outer surface of the cell. This occurs with the reduction of the detection of YFP in the internal space of the cell, until the view is out of focus above the top of the cell.

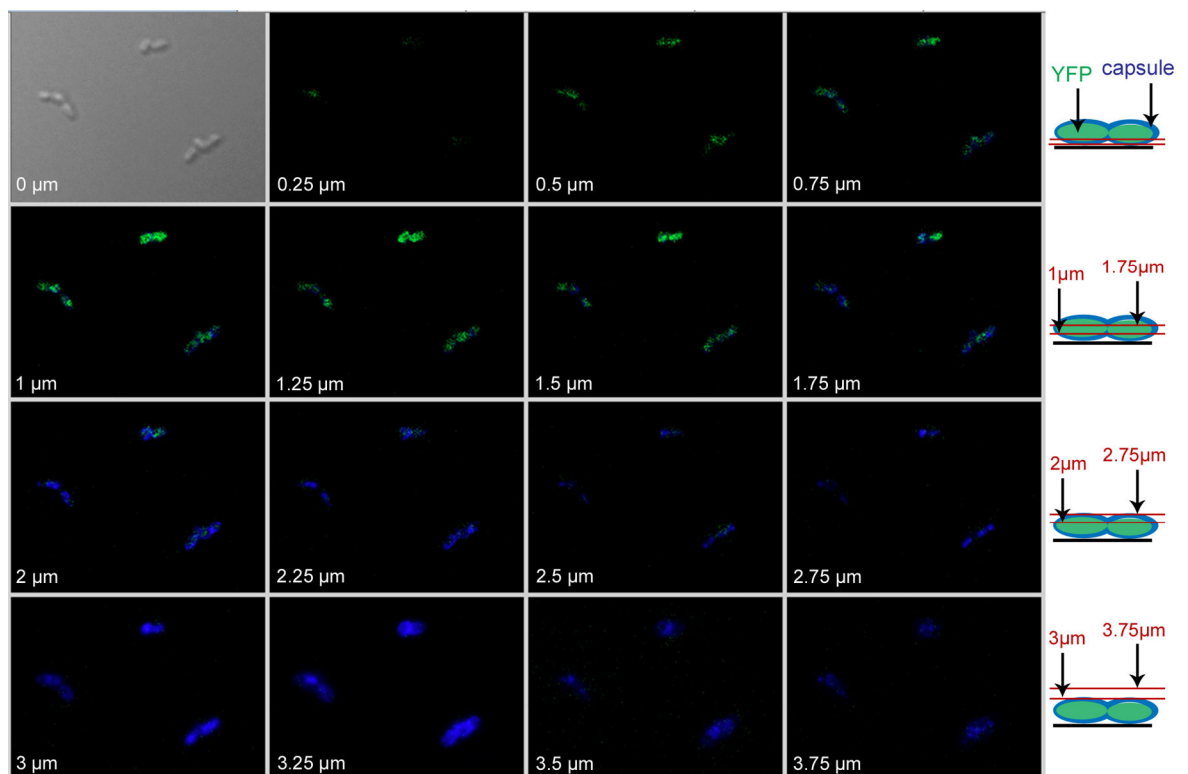


**Figure 5-5 Z-stack (thickness) of D39 pAHS5 labelled with Cy5**  
*S. pneumoniae* strain D39 was transformed with pAHS5 (YFP; green in image) and washed in PBS prior to being mixed with Cy5 dye (Amersham; blue in image), incubated, washed, and fixed with paraformaldehyde and applied to a microscope slide. The top left image is a DIC image of the bacterial cells and each fluorescence image from left to right is a 0.25 $\mu$ m increase in the z plane (height) of the lens up from the microscope slide, shown in the diagram on the far right.

### 5.3.3 Detection of Lumio<sup>TM</sup> and FLAG tags

As mentioned previously, each fluorescent protein has a His, Lumio<sup>TM</sup> and FLAG tag at its N-terminus. These tags were included to allow purification (His), immunodetection (FLAG) and substrate-dependent fluorescence (Lumio<sup>TM</sup>) of reporter fusions. The Lumio<sup>TM</sup> tag is a tetracysteine motif (CCPGCC) that binds a fluorescein arsenical binding hairpin (FLAsH<sup>TM</sup>) reagent (Griffin *et al.*, 1998), by forming covalent bonds between the arsenical molecules and the cysteine residues of the motif, unquenching the fluorescein and subsequently making it fluorescent when excited by the correct wavelength. The Lumio<sup>TM</sup> Green In-Gel detection kit (Invitrogen) can detect 1pmole of a Lumio fusion protein run on a SDS-PAGE gel, and detects the tag in all three fluorescent constructs from pneumococcal lysates, Figure 5-6.

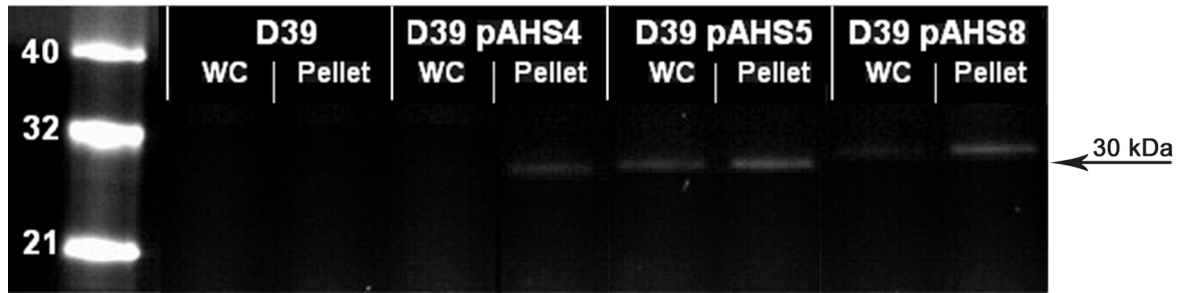


**Figure 5-6 In-Gel Lumio™ Tag Detection**

Pneumococcal lysates D39, D39/pAHS4 (GFP), D39/pAHS5 (YFP) and D39/pAHS8 (RFP) were separated into soluble (WC) and insoluble (Pellet) fractions. The samples were prepared using Lumio™ Green detection kit and proteins separated in NuPAGE 4-12% Bis-Tris SDS-PAGE gel (Invitrogen). Viewing the gel under UV transilluminator detects the fluorescence from the biarsenical-conjugated Lumio™ tag fused to the fluorescent proteins.

The FLAG epitope present at the N-terminus of the fluorescent proteins can be confidently detected by western blotting, Figure 5-7. Evidence of dimerisation is visible, which is most likely due to the Lumio™ tag because the SDS-PAGE gel was not reduced, the tetracysteine motif is unstable in oxidising conditions and as a result complexes with another motif to stabilise by forming disulphide bonds.

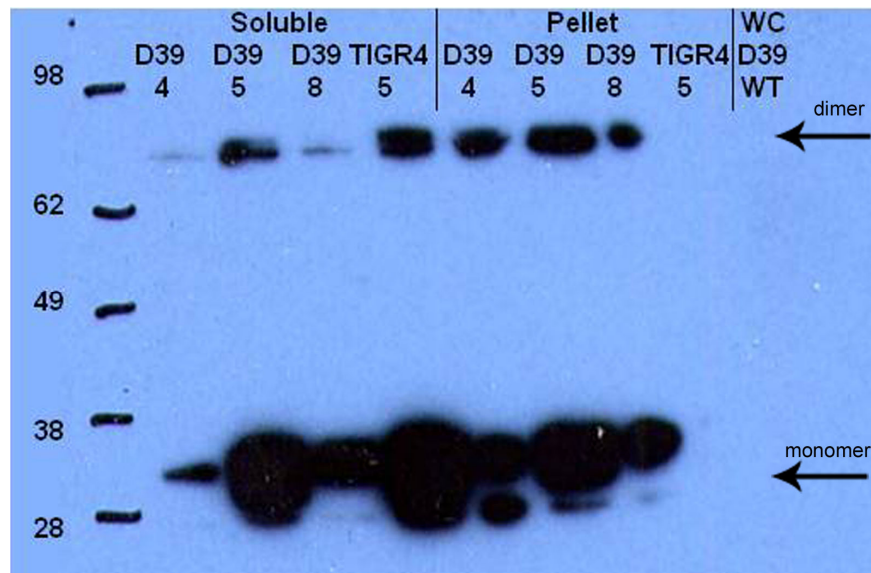


**Figure 5-7 Western detection of FLAG-Fluorescent protein – monoclonal  $\alpha$ -FLAG antibodies** Lysates, separated into soluble and insoluble (pellet) fractions, from pneumococcal strains D39 and TIGR4 transformed with plasmids expressing GFP/pAHS4 (4), YFP/pAHS5 (5) or RFP/pAHS8 (8) were probed with monoclonal antibody to FLAG (Stratagene) to detect expression of the fluorescent protein. Whole cell D39 lysate (WC D39 WT) was included as a FLAG negative control.

## 5.4 Application of fluorescent proteins for the pneumococcus

### 5.4.1 Transcriptional reporter

Fusions to reporter genes such as beta-galactosidase, chloramphenicol acetyltransferase (CAT), and fluorescent proteins have been used extensively to determine the expression of genes of interest in both bacterial and mammalian cell types. Fusions can be transcriptional or translational, where transcriptional fusions have the putative promoter region of a gene cloned upstream of a reporter and translational fusions also include the coding sequence of the gene of interest. The use of translational GFP fusions to investigate gene expression has been successful for NleH in *E. coli* O157:H7, therefore I wanted to test if this would be successful in the pneumococcus using the reagents developed.

An expression vector, pAHS12, was constructed where promoterless YFP was cloned into pAL2YI with two restriction sites upstream to permit any promoter of interest to be inserted. YFP was chosen as the reporter gene as it gave the highest levels of fluorescence when constitutively expressed. To assess the efficacy of the expression vector, the uncharacterised NanA promoter was tested. Analysis of the NanA sequence indicates that there are three putative promoters of NanA (Camara *et al.*, 1994), each of which were cloned upstream of YFP in pAHS12, detailed in Figure 5-8. NanA is a surface-anchored protein of *S. pneumoniae* which cleaves sialic acid from mucin in the secretions of the human nasopharynx. The presence of mucin in culture media as a carbon source as been shown to increase *nanA* transcription by ~24-fold, measured by RT-PCR (Yesilkaya *et al.*, 2008).

The transcriptional reporters were transformed into *S. pneumoniae* strain R6, which is the uncapsulated derivative of D39.

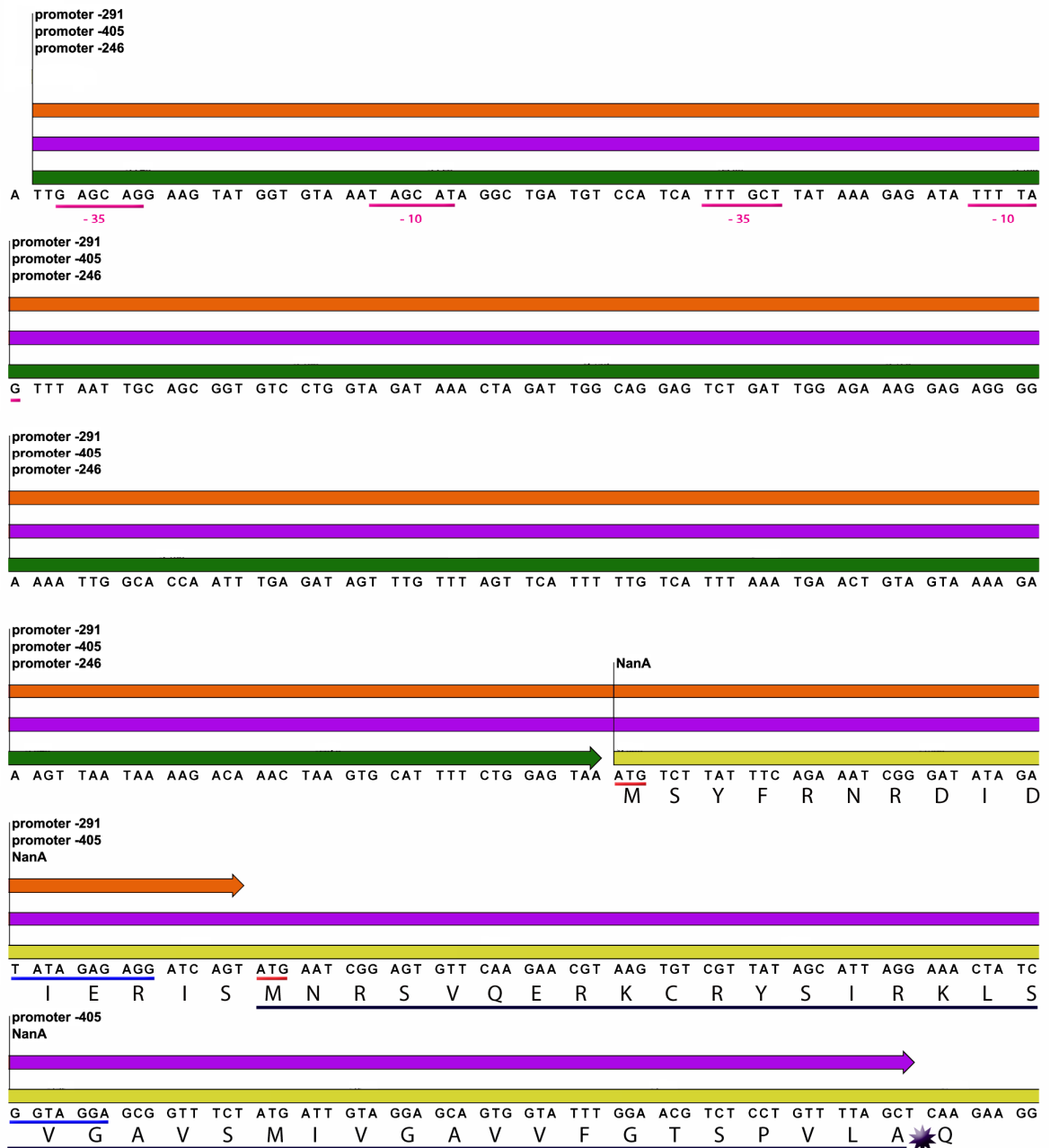


**Figure 5-8 Putative promoter sequences of NanA**

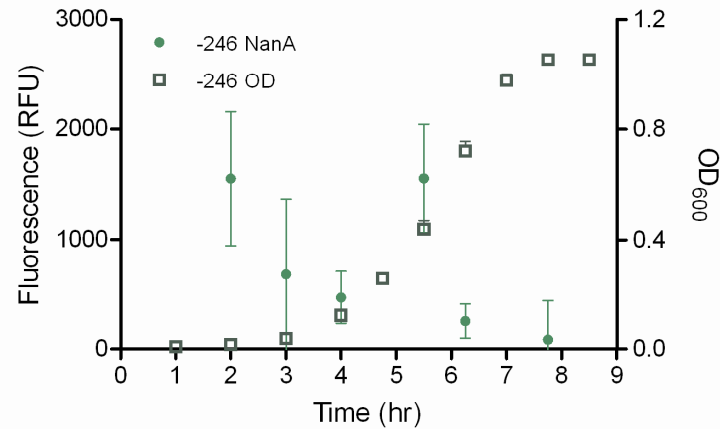
The nucleotide sequence of the sequences cloned upstream of YFP in pAHS12 are labelled promoter -246 (green); promoter -291 (orange) and promoter -405 (purple). The deduced amino acid sequence of NanA is included, with putative the two putative start (ATG) codons underlined in red. Two putative -35 and -10 promoter sequences are labelled and ribosome binding sites (Shine-Dalgarno sequences) are underlined in blue. The amino acid sequence underlined denotes a putative secretion signal sequence with a signal peptidase site indicated by a star. Figure is based on (Camara *et al.*, 1994)

YFP is expressed when under the control of the NanA promoters and is greatest during the early stages of growth (Figure 5-9 A, B, C). Unfortunately, due to the high levels of variance in the fluorescence readings between the constructs, a statistically significant conclusion cannot be made from the different lengths of

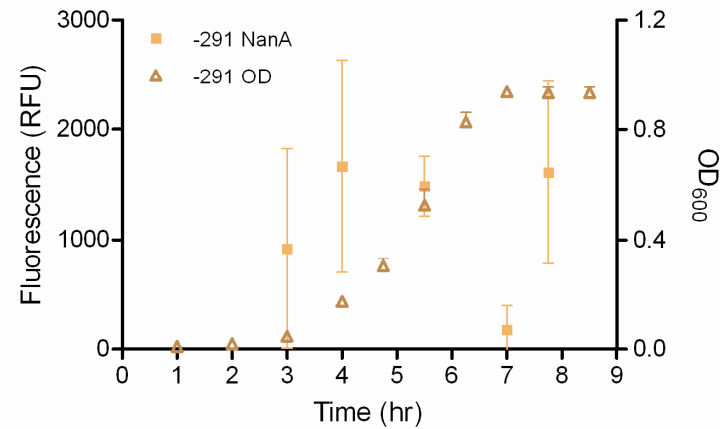
putative NanA promoter. To further validate the application of this construct as a transcriptional reporter, the results from this expression assay can be compared to transcriptomic data prepared from pneumococcal cells at  $OD_{600nm} = 0.6$ . The mRNA extraction, purification and cDNA synthesis experiments were carried out by Jiang Tao Ma and the sequencing data analysed by Jenny Herbert and Dr Andrea Mitchell. RPKM (reads per kilobase of exon model per million mapped reads) is a measure of transcript concentration, where the number of sequencing reads of a length of RNA transcript is normalised against the total number of reads in the sample. The RPKM value of the *ami* (SP\_1891) transcript is 385.67 and the *NanA* (SP\_1693) transcript is 8.87. The *NanA* transcriptional fusions are 2-fold less fluorescent compared to the *ami* fusion, which is supported by the difference seen in the transcriptomic data.

Although the transcriptional reporter is not sensitive enough to compare the putative promoters of *NanA*, the expression profile differs to that from the *ami* promoter (Figure 5-2 B). This demonstrates that the vector can be used to compare expression of different pneumococcal genes.

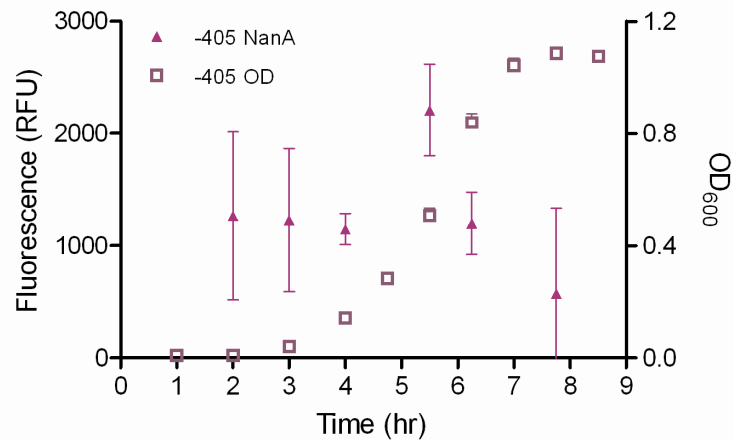
A



B



C



D

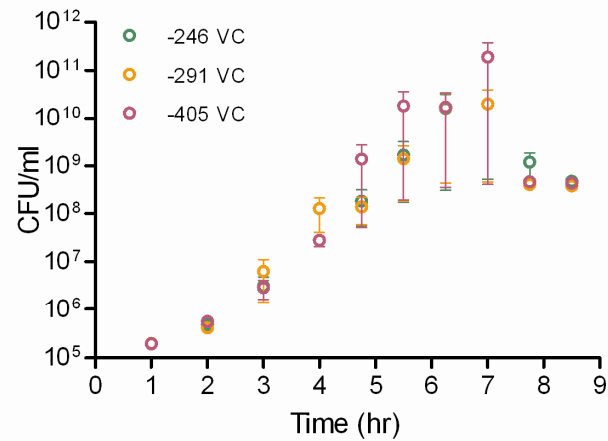


**Figure 5-9 Expression of NanA promoter reporter fusions in *S. pneumoniae* strain R6**  
 20ml of BHI was inoculated with  $1 \times 10^5$  cfu/ml R6 pAHS12; R6 -246NanA; R6 -291NanA; R6 -405NanA. At regular intervals, 1ml of culture was removed and OD<sub>600</sub> measured; the remaining culture was incubated at 37°C. The 1ml sample was centrifuged and the bacterial pellet suspended in 1ml PBS and 200 $\mu$ l aliquots were analysed in triplicate for fluorescence (YFP = Ex. 485nm; Em. 520nm) in FLUOstar plate reader (BMG) and 20 $\mu$ l used for viable count (graph B). R6 pAHS12, promoterless YFP plasmid, acted as a control for background fluorescence; fluorescence was plotted against OD<sub>600</sub> using Microsoft Excel software and a line of best fit obtained. Using this method, data were corrected for background fluorescence. The mean $\pm$ SEM of the three biological replicates are plotted.

## 5.5 Discussion

Since the gene encoding Green Fluorescent Protein was first cloned in 1992 and shown to be expressed in heterologous organisms in 1994, it has been used as a reporter of gene transcription, gene regulation and protein localisation in bacteria, fungi, plants and eukaryotes. However the applications of GFP, and its derivatives, as gene expression and protein localisation reporters do not appear to have been used extensively in previous pneumococcal research. Therefore constructs containing *S. pneumoniae* codon-optimised GFP, YFP or RFP, under the control of a pneumococcal promoter, were developed as tools for future pneumococcal research.

The fluorescent proteins are constitutively expressed in *S. pneumoniae*, as fluorescence intensity increases as the cell number increases in population assays, Figure 5-2. However, upon entry into the stationary phase of growth there is a sharp decline in fluorescence intensity. This decline may be attributed to the decrease in pH of the culture media which can inhibit fluorescent protein activity. Fluorescent proteins need to be post-translationally oxidised in order to mature into a functioning protein, and due to the microaerophilic nature of pneumococcal growth, the availability of oxygen will be reduced upon entry into the stationary phase, consequently reducing the amount of mature fluorescent protein to below detectable limits. Western blotting analysis of pneumococcal lysates from the later stages of growth ( $OD_{600nm} = 1-1.2$ ) would determine whether the decrease in fluorescence intensity is due to the reduced activity of the fluorescent protein or protein degradation. It would also be interesting to ascertain if this decline happens when the bacteria are cultured in buffered media, which would maintain the pH to optimum levels, or aerated before measuring fluorescence by introducing a plate shaking step in the FLUOStar plate reader. If these potential problems with their use in the stationary phase of growth cannot be alleviated, they can still be useful reagents for investigations during the dynamic exponential phase of growth.

The fluorescent proteins were characterised by fluorescence microscopy showing that expression was evident within the cell cytoplasm (Figure 5-3), which is

supported by labelling the pneumococcal surface by immunostaining the capsule polysaccharide (Figure 5-4) or CyDye labelling of free lysine residues (Figure 5-5). The inclusion of His, FLAG and Lumio tags allows the expression of the proteins to be assessed by In-Gel detection of the Lumio™ tag (Figure 5-6) and western blot detection of the FLAG epitope with monoclonal  $\alpha$ -FLAG antibodies (Figure 5-7).

To assess the application of YFP as a transcriptional reporter in the pneumococcus, a plasmid containing a promoterless YFP gene was created, pAHS12. Three putative *nanaA* promoter sequences, -246*nanaA*, -291*nanaA* and -405*nanaA*, were cloned upstream of the *yfp* gene in this plasmid and the expression of YFP monitored during growth in BHI (Figure 5-9). Due to the high variance in fluorescence levels from the NanA constructs, it cannot be concluded which promoter length is true for NanA expression; primer extension would define the NanA promoter. Another option could be to perform Q-PCR on the *yfp* transcript under the control of the various promoter lengths. Unfortunately the expression from *nanaA* promoters cannot be determined during stationary phase, as YFP fluorescence levels decline even when under the control of a known constitutive promoter. Additional experiments would have to be carried out to determine if the decline observed is attributed to the NanA promoter or the culture effects discussed previously. If not for time constraints, it would have been interesting to design and test an assay to utilise the Lumio tag included in the YFP sequence, to quantify the YFP present in each sample during stationary phase, once corrected for the pAHS12 promoterless YFP background control. Overall the results indicate that *nanaA* expression, and the regulation of its expression, in the pneumococcus is complex. To reiterate, the main objective of this experiment was not to define the *nanaA* promoter and *nanaA* expression, but to test the application of pAHS12 as a transcriptional reporter plasmid in the pneumococcus with an uncharacterised promoter sequence. The results confirm that pAHS12 can be used as a transcriptional reporter in *S. pneumoniae* as the YFP expression data can be corroborated with the transcriptomic data generated from another independent experiment.

This work demonstrates that codon-optimised fluorescent proteins can be expressed in *S. pneumoniae* and detected in pneumococcal lysates by western blotting. The fluorescent proteins can be viewed by fluorescence microscopy,

and a cytoplasmic distribution can be characterised with the addition of indirect immunofluorescence techniques, staining for the capsule, or indiscriminate labelling of the outer surface using CyDyes. The transcriptional reporter plasmid pAHS12 can be used to reveal the native expression of *S. pneumoniae* genes. Additional proof-of-principle work has to be completed in order to demonstrate the use of these reagents as tools for protein localisation studies within the pneumococcus.

## 6 Localisation of pneumolysin (Ply) within the pneumococcus

### 6.1 Summary

Ply is a well characterised toxin important for pneumococcal pathogenesis due to its toxicity to eukaryotic cells and its complement activating activity at sub-lytic concentrations. Ply is a cholesterol dependent cytolytic toxin which is mainly contained within the cytoplasm, as it does not possess a secretion signal sequence (Johnson, 1977; Walker *et al.*, 1987). There have been reports that it can localise to the cell wall (Price & Camilli, 2009) and be released without the action of autolysin (LytA) (Balachandran *et al.*, 2001). The aim of the work described in this chapter was to develop and characterise codon optimised versions of Ply and test their expression. Expression was tested by complementing a previously constructed Ply negative mutant of *S. pneumoniae* type 2 strain D39. These vectors were used to explore alternative methods to determine the localisation of Ply within/on the pneumococcal cell. A *S. pneumoniae* strain deficient in both autolysin and pneumolysin was created, by introducing a LytA-Ply gene fusion amplified from equine strain A45 into the chromosome of sequenced strain TIGR4. This mutant was used to determine if the genes immediately upstream of Ply and/or LytA are responsible for the cell wall localisation of Ply. The impact of the introduction of this LytA-Ply gene fusion upon TIGR4 virulence in a murine model of infection will also be tested. The potential implications of the cell wall localisation of Ply to pneumococcal pathogenesis are also discussed.

### 6.2 Ply constructs and expression analysis

Codon optimised Ply was synthesised with His, FLAG and Lumio (FLAsH) tags at the N-terminal end, so as not to interfere with its biological activity, and cloned into plasmids by DNA 2.0 (California, USA). DNA 2.0 uses the Codon Usage Database (<http://www.kazusa.or.jp/codon>) to optimise their products codon

usage to the species/strain specified. To ensure gene expression in the pneumococcus, the constitutive promoter from the aminopterin resistance operon (*ami*) (Alloing *et al.*, 1990) was cloned upstream of the gene in the plasmid and the fragment was subcloned into pAL2YI as described previously for the fluorescent protein constructs, producing vectors described in Table 6-1.

**Table 6-1 Ply vectors**

Construct	Description
pAHS1	Ply domains 123:3tags
pAHS2	Ply domain 4:3tags
pAHS3	Ply:3tags
pAHS6	RFP-Ply:3tags
pAHS7	GFP-PlyDomain4:3tags

3 tags = His, FLAG and Lumio

These vectors were transformed into *S. pneumoniae* Ply knockout strain (D39 $\Delta$ PlySTOP), created by Dr Calum Johnston through Janus mutagenesis (Sung *et al.*, 2001) of *S. pneumoniae* strain D39, introducing a single T nucleotide after the 6<sup>th</sup> base in Ply sequence generating a stop codon after the second amino acid. To test the episomal complement of the Ply mutant, the Ply expression from the constructs was characterised through western blotting, Lumio<sup>TM</sup> fluorescence and haemolytic assays.

### **6.2.1 Western blotting and Lumio<sup>TM</sup> analysis**

Western blotting with a pneumolysin polyclonal antibody, shows that D39 expresses wild-type protein with a predicted size of 53kDa, D39 $\Delta$ PlySTOP does not express any Ply protein unless complemented with pAHS1, expressing Ply Domains123 (43kDa), or pAHS3, expressing Ply:3tags (56kDa), Figure 6-1. D39 $\Delta$ PlySTOP pAHS2, expressing Ply Domain 4, did not resolve a band with the predicted size of 16kDa which may be due to the low sensitivity of the chloro-naphthol detection method used.

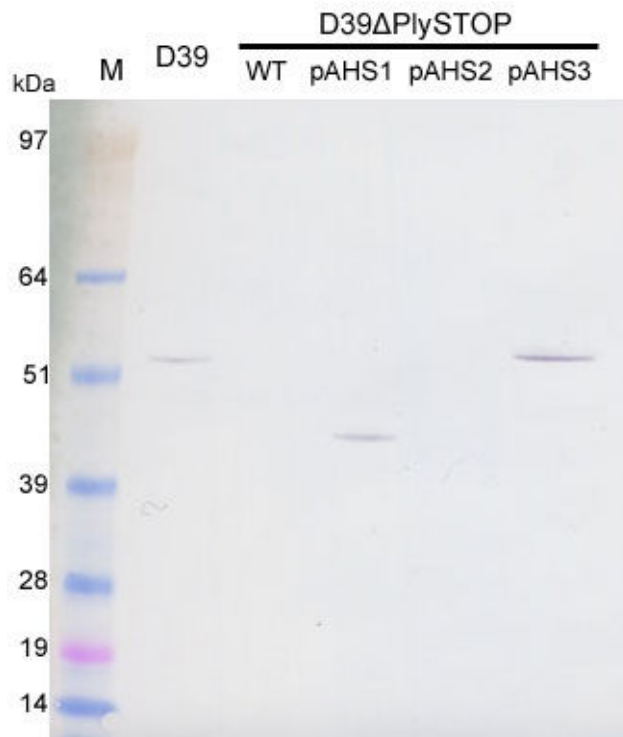


**Figure 6-1 Western blot analysis of pneumococcal lysates – polyclonal antibody**  
Pneumococcal lysates were probed against a polyclonal Ply antibody raised from rabbit. D39 is a positive Ply control; D39ΔPly-stop 'WT' is a negative Ply control. D39ΔPly-stop was transformed with Ply constructs pAHS1, pAHS2 and pAHS3.

The blot was repeated using monoclonal antibody (mAb PLY-5) specific for an epitope present in Ply Domain 4 and detection using chemiluminescent substrate to increase sensitivity. Due to overexposure of the film on the membrane, there are unspecific bands present on the blot which can be eliminated through comparison with the D39ΔPlySTOP Ply protein negative control (WT), Figure 6-2. The Ply protein products are highlighted by arrows, showing detection of Ply Domain 4 (2; 16kDa), GFP-Domain 4 (7; 43kDa), RFP-Ply (6; 83kDa) and purified Ply (Ply; 53kDa).

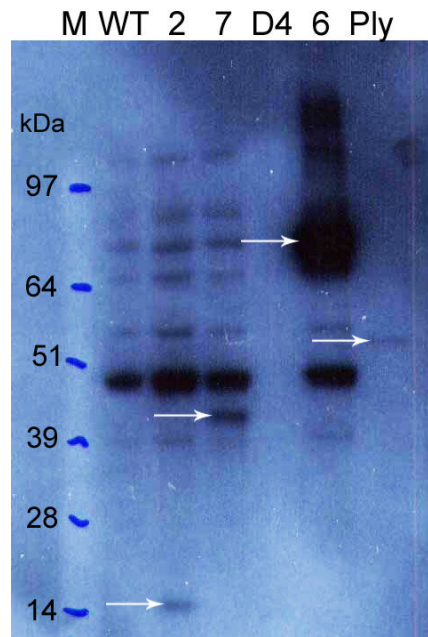


**Figure 6-2 Western blot analysis of pneumococcal lysates – monoclonal antibody**  
Pneumococcal lysates were probed with monoclonal Ply (mAb PLY-5) antibody.  
D39 $\Delta$ PlySTOP (WT) was transformed with Ply constructs pAHS2, pAHS6 and pAHS7.  
Purified Ply and Ply domain 4 (D4) were included as protein positive control.

As described previously, the Lumio tag allows substrate mediated fluorescence, which can be detected in SDS-PAGE gels by treating bacterial lysates containing the Lumio<sup>TM</sup> tagged protein with the Lumio<sup>TM</sup> Green Detection Reagent (Invitrogen). The arsenical treated lysates are separated on an SDS-PAGE gel, alongside a BenchMark<sup>TM</sup> fluorescent protein marker (Invitrogen), and viewed under a transilluminator to excite the fluorescein bound to the fusion protein. Figure 6-3 A shows that the Lumio<sup>TM</sup> fusion proteins, Domain 4 (2; 16kDa), Ply (3; 56kDa) and RFP-Ply (6; 83kDa), are expressed in the complemented mutant lysates, with no signal detected for D39 $\Delta$ PlySTOP (WT) alone with equivalent concentrations of proteins tested, seen by Coomassie Blue staining Figure 6-3 B.

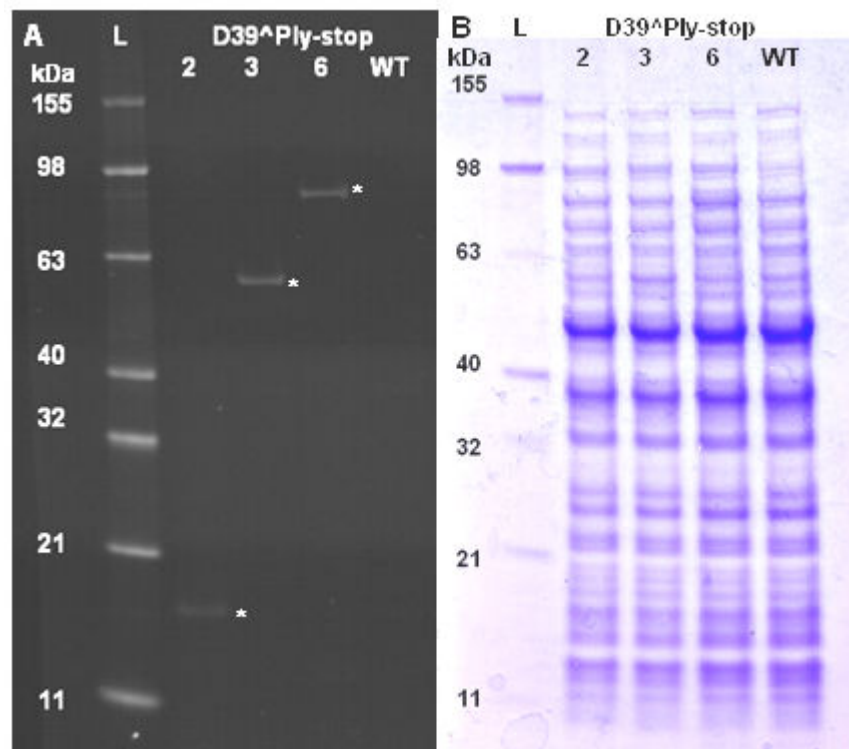


**Figure 6-3 Lumio™ tag detection of Ply complements in D39ΔPlySTOP**  
Pneumococcal lysates D39ΔPlySTOP WT, pAHS2, pAHS3 and pAHS6 were treated with Lumio Green Detection kit (Invitrogen) and subsequently run on NuPAGE 4-12% Bis-Tris SDS-PAGE gel (Invitrogen) for detection of fluorescent Lumio™ tagged fusion proteins (\*) under UV transilluminator (A) and the same gel was subsequently Coomassie stained (B).

### 6.2.2 Analysis of haemolytic activity

All Ply constructs were assessed for haemolytic activity with D39 lysates as a positive control and PBS as a negative control, Table 6-2. Lysates prepared from D39ΔPly-stop WT was also included as a control, to show that haemolysis could be attributed to the complementation of Ply from the plasmid and not due to another protein in the pneumococcal proteome. pAHS3 and pAHS6 complement the Ply knockout and pneumococcal whole cell lysates of these strains have a higher haemolytic activities compared to the D39 control, where the pAHS6 (RFP-Ply) titre is 8 times that of the D39 WT; pAHS3 (Ply) titre is 64 times. As expected, there is no haemolytic activity when D39ΔPlySTOP is complemented with Ply Domains123 (pAHS1), Domain 4 (pAHS2) or GFP-Domain 4 (pAHS7). Ply binding to membranes is mediated by Domain 4, but polymerisation and membrane insertion is mediated by Domains 123 (Gilbert *et al.*, 1999; Tilley *et*

*al.*, 2005) therefore Domain 4 can bind to membranes but cannot progress to form pores and Domains123 cannot interact with membranes at all.

**Table 6-2 Haemolytic activity of whole cell lysates from D39 $\Delta$ PlySTOP episomally complemented with Ply**

Strain	Haemolytic Activity (HU)
D39	40
D39 $\Delta$ Ply-stop	0
D39 $\Delta$ Ply-stop pAHS1 (Ply Domains123)	0
D39 $\Delta$ Ply-stop pAHS2 (Ply Domain 4)	0
D39 $\Delta$ Ply-stop pAHS3 (Ply)	2560
D39 $\Delta$ Ply-stop pAHS6 (RFP-Ply)	320
D39 $\Delta$ Ply-stop pAHS7 (GFP-Ply Domain 4)	0

### **6.2.3 Binding of RFP-Ply to erythrocytes.**

The ability of RFP-Ply to bind cholesterol containing membranes was confirmed by visualising sheep erythrocytes pre-incubated with D39 $\Delta$ PlySTOP pAHS6 lysate with fluorescence microscopy. It can be seen that cells treated with PBS alone are smooth and rounded and upon exposure to RFP-Ply, the cells become larger and irregular due to lysis when viewed under differential interference contrast (DIC) microscopy (Figure 6-4). Fluorescence microscopy (Figure 6-4, RFP) shows that no RFP is detected in PBS treated cells whereas the membranes from the erythrocyte ghosts, show punctate areas of RFP-Ply. These punctate areas of RFP are likely to be supramolecular structures (200-300nm) containing a mixture of RFP-Ply pores, pre-pores and arcs (incomplete pre-pores) (Dr Aspi Iliev; personal communication).

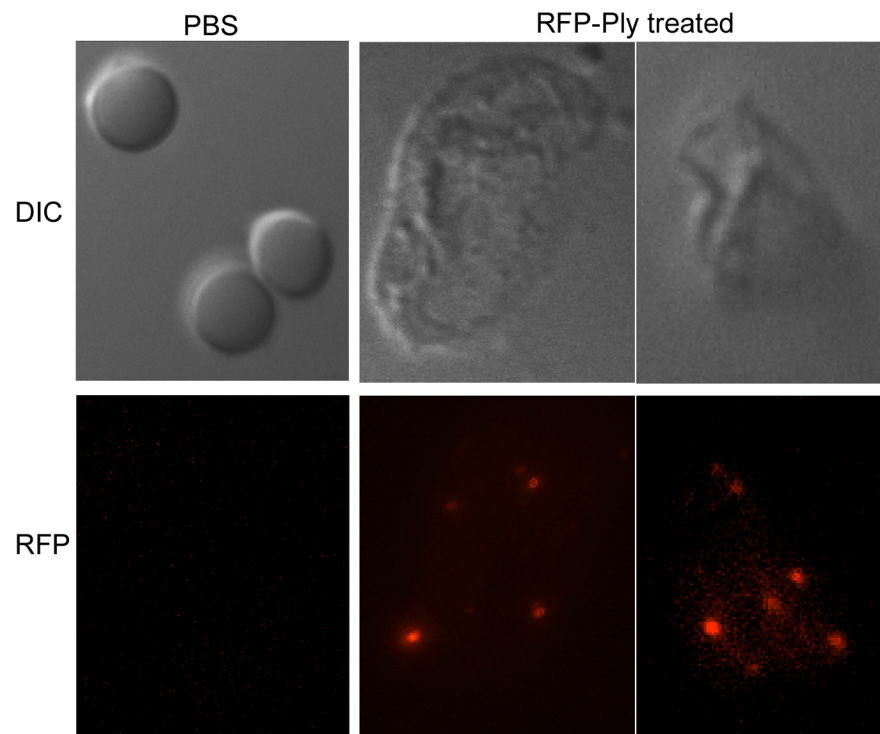


**Figure 6-4 Erythrocytes treated with PBS and D39ΔPlySTOP pAHS6 lysate**  
 Fluorescence microscopy, using x100 objective, of sheep erythrocytes incubated with 50μl PBS or 50μl D39ΔPlySTOP pAHS6 lysate, containing RFP-Ply. Images were magnified an additional 2.5 times.

## 6.3 Construction of isogenic mutant TIGR4ΔLytA-Ply::Chl

### 6.3.1 Rationale for construction of LytA-Ply fusion in TIGR4

The paradigm that Ply is intracellular until its release by cell lysis in the stationary phase was supported by a Ply localisation study (Johnson, 1977) which tested the haemolytic activity of pneumococcal fractions, showing that Ply is not linked to the membrane and therefore cytoplasmic; the lack of a secretion signal peptide within its primary sequence (Walker *et al.*, 1987); and the observations that haemolytic activity is not detected in the culture supernatant until late stationary phase. This paradigm is challenged by reports that in select strains Ply can be released before stationary phase (Benton *et al.*, 1997b) by an autolysin-independent mechanism (Balachandran *et al.*, 2001) and that fractionation of pneumococcal cells followed with detection of Ply protein by western blotting shows it can localise to the cell wall (Price & Camilli, 2009). The observations that Ply is released only in certain strains but can be found in

the cell wall fraction of many strains suggest that the secretion, cell wall localisation and/or release of Ply may be controlled by the presence of particular genes. It is possible that these genes are defective or missing in the strains which can release Ply prior to the stationary phase of growth. A Ply and LytA deficient strain of *S. pneumoniae* was created to further investigate the possible mechanisms behind the localisation and autolysin-independent release of Ply.

Upon assessment of the genetic location of Ply in the TIGR4 sequence, it can be seen that Ply (SP\_1923) and the genes downstream, SP\_1924, SP\_1925 and SP\_1926, are very close together and may be transcribed as a single mRNA, i.e. an operon, Figure 6-5.



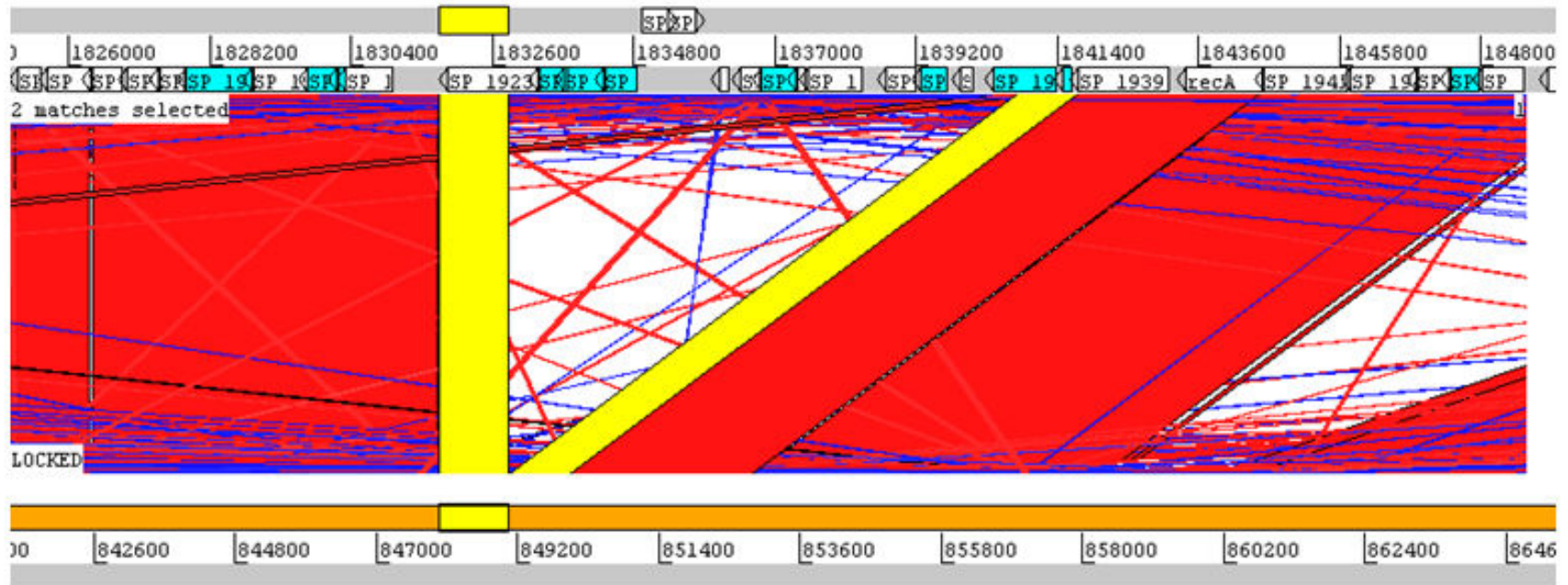
**Figure 6-5 Genes surrounding Ply in TIGR4 (SP\_1923; highlighted red) adapted from <http://www.ncbi.nlm.nih.gov/gene/931915>.**

From the aforementioned RNA-seq analysis of transcriptomic data generated by colleagues, Ply (SP\_1923) is transcribed within a polycistronic message including SP\_1926, SP\_1925, SP\_1924 and SP\_1922 (personal communication, Dr Andrea Mitchell). SP\_1924-26 ORFs encode hypothetical proteins of 136, 202 and 158 amino acids respectively, with no putative conserved domains found when submitted into a BLASTp search (<http://blast.ncbi.nlm.nih.gov/Blast.cgi>). The SP\_1922 ORF encodes a hypothetical protein, of 238 amino acids, consisting of a DUF28 domain, a domain of unknown function found in bacterial and some yeast proteins. These four ORFs are also all found in the sequenced strains of pneumococci, indicating that these genes are conserved with Ply. A poster was presented at the 7<sup>th</sup> International Symposium on Pneumococci and Pneumococcal Diseases (ISPPD) from Richard Malley's group in Boston, reporting results testing the hypothesis that SP\_1924 and SP\_1925 have a role in the localisation of Ply to the cell wall (Yadav, P., Thompson C., Lu Y.-J., Malley R.; Abstract No. 19). Through haemolytic assays and western blotting of cell wall and protoplast

fractions, testing a SP\_1924 and SP\_1925 double mutant with its TIGR4 isogenic parent, it was concluded that SP\_1924 and SP\_1925 'participate indirectly in the translocation of Ply to the cell surface'. Owing to this, I wanted to independently test if SP\_1924, SP\_1925 and SP\_1926 have a role in Ply localisation/secretion by investigating if Ply can still localise to the cell wall when expressed in a *S. pneumoniae* strain lacking these genes.

Naturally occurring LytA Ply deficient strains of pneumococci, isolated from horses, have been characterised (Whatmore *et al.*, 1999). Interestingly, only pneumococci with capsular serotype 3 are isolated from horses, which are commonly colonised by other species of Streptococci such as *S. zooepidemicus* and *S. equi* (Burrell *et al.*, 1986). A panel of serotype 3 pneumococcal isolates from horses were analysed and it was found that the LytA and Ply genes have been fused together by a recombination event (Whatmore *et al.*, 1999), resulting in the loss of the LytA and Ply functional proteins. Although these isolates lack two important virulence factors in murine models of infection (Berry *et al.*, 1989b; Berry *et al.*, 1992; Canvin *et al.*, 1995; Berry & Paton, 2000), Whatmore and authors note that the *S. equi* isolated from horses also do not encode a CDC toxin like streptolysin O, and postulate that the toxin genes were lost over time due to a selective disadvantage in the equine host. This natural mutant (Figure 6-6) has not only lost Ply and LytA but also the intervening genes, including SP\_1924-26, therefore this fusion was introduced into TIGR4 to generate a strain deficient in all these genes, TIGR4 $\Delta$ LytA-Ply.

TIGR4



A45

Figure 6-6 Artemis Comparison Tool (ACT) of TIGR4 at position SP\_1923 (Ply) and A45

This image demonstrates the natural 'fusion' of LytA and Ply seen in equine *S. pneumoniae* strain A45. Red bars denote homology between the two sequences, yellow bars highlight SP\_1923 (Ply) and SP\_1936 (LytA) which are ~7kB apart in TIGR4 but adjoined in A45.

This TIGR4 $\Delta$ LytA-Ply mutant was constructed to serve two purposes: to assess whether the genes upstream of Ply, and/or the action of autolysin, are involved in Ply secretion, localisation and/or release; and to compare the virulence of the LytA-Ply mutant to its isogenic parent to determine if this natural fusion alone contributes to the reduced virulence of equine serotype 3 strain A45 compared to other serotype 3 isolates. This mutation was made in serotype 4 strain TIGR4 because serotype 3 pneumococci are not amenable to *in vitro* transformation (Dr Andrea Mitchell; personal communication) and the murine pneumonia and bacteraemia model data is already available for TIGR4.

### **6.3.2 Confirmation of successful *lytA-ply* deletion in TIGR4**

The LytA-Ply fusion was introduced into the TIGR4 genome by PCR amplification of the sequence from *S. pneumoniae* (equine) strain A45 gDNA, cloning it into a pUC18 vector. A *cat* resistance cassette, under the control of the *ami* promoter, was introduced into the BamHI site present in the fusion gene to allow selection for recombinants, Figure 6-7 (1) and (2). This construct (pUCLytAPly::Chl) was transformed into TIGR4 and the success of the recombination event was confirmed by PCR, sequencing, gram staining, haemolytic activity and western blot using the polyclonal  $\alpha$ -Ply antibody.

Chl resistant clones generated from recombination of the *cat* cassette into the chromosome were selected and genomic DNA extracted to test for successful insertion of the fusion and the removal of the intervening 7kB DNA by PCR. Primers 52Q and 52R amplify a 350bp region of Ply, which is present in TIGR4 but not in A45; primers W99F and 52R amplify across the LytA-Ply fusion, which is present in A45 but not TIGR4. Chl resistant clones 3 and 4, Figure 6-8, are negative for 52Q/R PCR product and positive for the presence of the LytA-Ply fusion like A45, indicating successful recombination. Note the product of the LytA-Ply PCR product is larger than the A45 wild-type due to the presence of the *cat* resistance cassette.

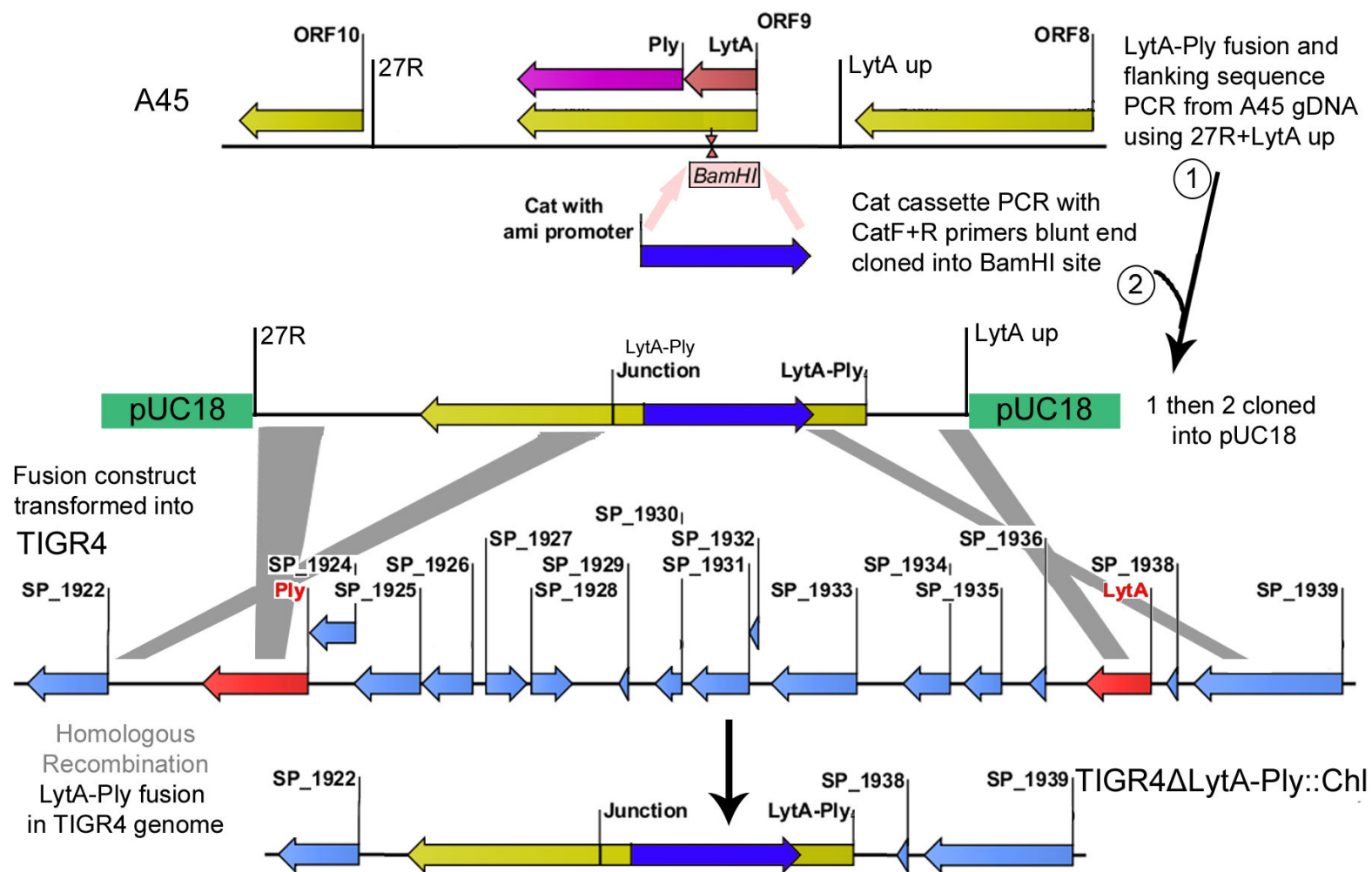


**Figure 6-7** Introducing the LytA-Ply genetic fusion from A45 into TIGR4 genome. The LytA-Ply fusion gene was PCR amplified with flanking sequence, homologous to TIGR4 sequence, using primers 27R and LytA up and the product cloned into pUC18. A Cat resistance cassette, with *ami* promoter, was PCR amplified from *S. pneumoniae* FP28 and cloned into the LytA-Ply pUC18 construct at the BamHI site present in the fusion gene to create pUCLytA-Ply::Chl. This construct was transformed into TIGR4 and homologous recombination (grey crosses) of the fusion gene into the TIGR4 chromosome was selected for through resistance to Chl, generating mutant TIGR4ΔLytA-Ply::Chl.

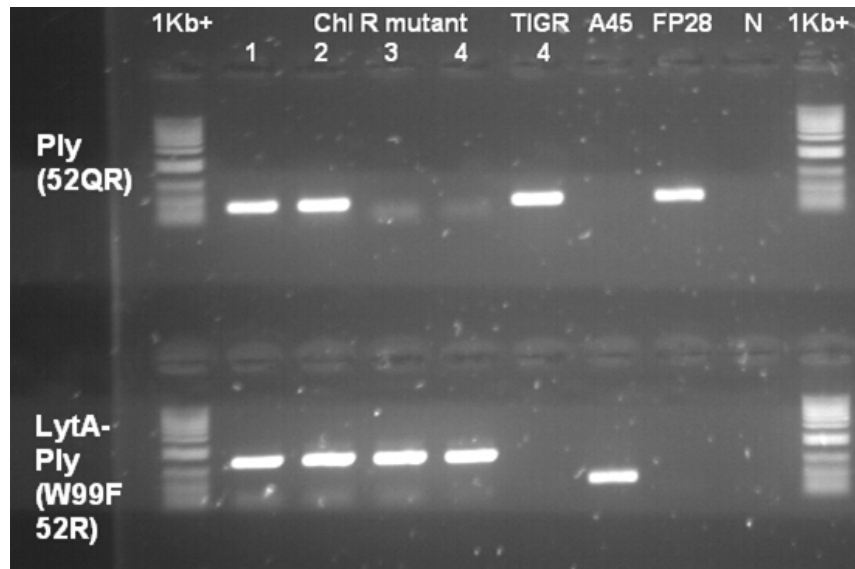


**Figure 6-8 Confirmation of successful deletion by PCR**

PCR of crude gDNA extract from Chl resistant clones to confirm recombination of LytA-Ply fusion into TIGR4 chromosome, with TIGR4 and A45 as controls. Primer pair 52QR amplifies a 350bp region of Ply and W99F52R amplifies across the LytA-Ply fusion; N denotes a no DNA PCR control for each primer pair. The Cat cassette was amplified from FP28, using CatF and CatR, PCR results not shown. Only clones 3 and 4 underwent successful recombination due to the absence of Ply (52QR) product.

Recombinants confirmed by PCR were selected and the region was amplified in 3 sections and sent for sequencing. The sequencing contigs were aligned against the A45 sequence, with the *cat* cassette inserted *in silico* at the appropriate position, to map the area where recombination has occurred between the plasmid insert and the TIGR4 genome. An alignment of A45 and TIGR4 sequences using CLC software, Figure 6-9, labels the single polynucleotide polymorphisms (SNPs) present in the A45 or TIGR4 sequence as 'conflicts'. By working across the consensus sequence, from left to right, the SNPs present in the TIGR4 $\Delta$ LytA-Ply sequence data should first represent those found in the TIGR4 genome (green) and then A45 (red) from the inserted sequence, returning to TIGR4 SNPs after the insert. Therefore, the left recombination area can be mapped between a TIGR4 and an A45 SNP, and the right recombination area between an A45 and a TIGR4 SNP, boxed conflicts on Figure 6-9. Due to the great sequence identity of this region of the genome, it is not possible to narrow the recombination region any further.



The disruption of the *LytA* gene in A45 leads to the formation of long chains of pneumococci compared to the diplococcus morphology characteristic of *S. pneumoniae*, reported by Whatmore and authors (Whatmore *et al.*, 1999). To characterise the mutant in TIGR4, a Gram stain was performed on TIGR4, A45 and TIGR4 $\Delta$ LytA-Ply::*Chl* as described in Materials and Methods. Figure 6-10 shows that A45 and TIGR4 $\Delta$ LytA-Ply form long chains of greater than 15 pneumococci, and TIGR4 is a mixture of diplococci and shorter chains of 5-8 pneumococci.

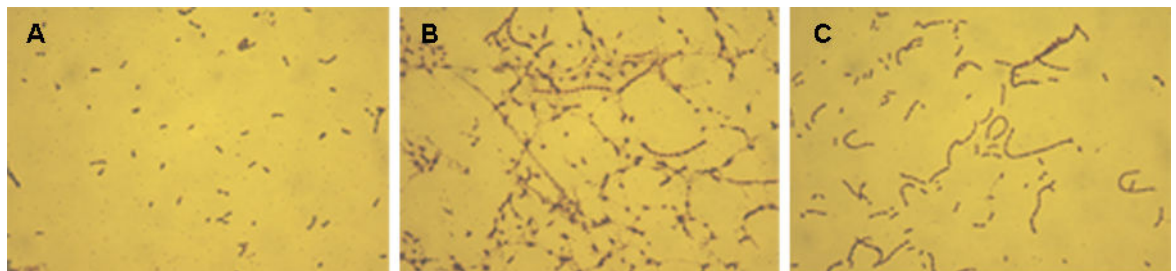


**Figure 6-10 Analysis of pneumococcal chain length**  
*S. pneumoniae* strains TIGR4 (A), A45 (B) and TIGR4 $\Delta$ LytA-Ply::*Chl* (C) were grown in BHI at 37°C until mid-exponential phase and 10 $\mu$ l heat fixed onto a microscope slide. Grams stain was applied before examining under x100 magnification on Zeiss Axioskop microscope.

Another phenotypic characteristic of A45 is the lack of haemolytic activity due to lack of pneumolysin production. The haemolytic activity of the isogenic parent TIGR4 was lost due the introduction of the fusion in TIGR4 $\Delta$ LytA-Ply and this could be restored through episomally produced pneumolysin from plasmid pAHS3, Figure 6-11. There is no haemolytic activity in extracts from TIGR4 $\Delta$ LytA-Ply transformed with pAHS1 (Ply Domain 4) or pAHS2 (Ply Domains123), as seen previously when expressed in D39 $\Delta$ PlySTOP in Section 6.2.2.

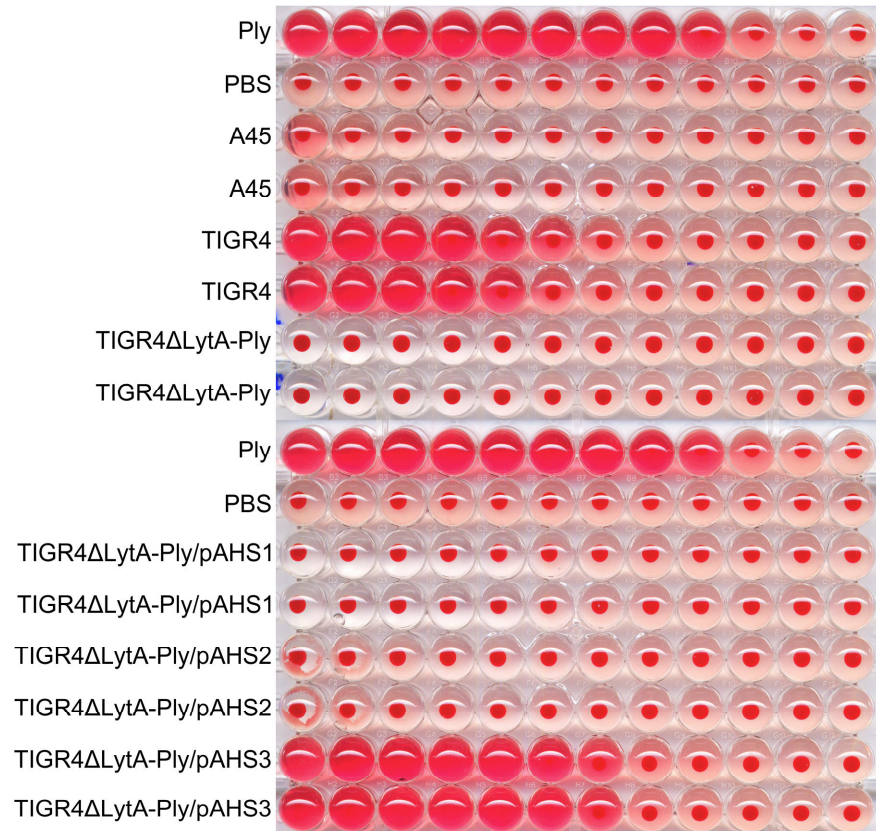


**Figure 6-11 Haemolytic assay of TIGR4ΔLytA-Ply, isogenic parent and episomal complement whole cell lysates.**

The loss of haemolytic activity was shown to be due to no production of Ply through western blotting using the polyclonal Ply antibody. The western blot (Figure 6-12) shows that Ply is produced by the wild-type TIGR4 but not A45 nor the TIGR4ΔLytA-Ply mutant (TdLP WT). Ply is detected in the complemented mutant with pAHS1 (Ply domains 123) and pAHS3 (Ply). The amount of Ply protein in the TdLP pAHS3 sample is greater than the parent strain as there are multiple copies of the Ply gene complementing the mutant; the plasmid has a copy number of 8 (Macrina *et al.*, 1982). No signal is detected for pAHS2 (Ply domain 4; not shown). Purified Ply was included as a positive control.

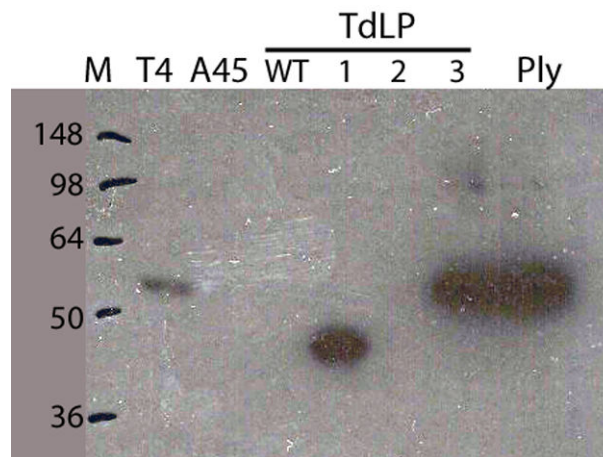


**Figure 6-12 Western blot of TIGR4ΔLytA-Ply – polyclonal α-Ply antibody**  
 Western blot of TIGR4ΔLytA-Ply (TdLP) mutant (WT) with plasmid complements pAHS1 (1), pAHS2 (2) and pAHS3 (3). TIGR4 (T4), A45 and purified Ply were included as controls.

## 6.4 Pneumococcal localisation of Ply.

Once the downstream genes of Ply, SP\_1924-26, and LytA were deleted in TIGR4 to create TIGR4ΔLytA-Ply, this mutant could now be used to elucidate whether the products of these genes have a role in the localisation and/or secretion of Ply from the pneumococcus. The mutant was complemented for Ply using the vector reagents, pAHS3 or pAHS6, developed and characterised previously. The localisation of Ply was assessed by pneumococcal cell fractionation with western blotting and immunofluorescence microscopy.

### 6.4.1 Fractionation analysis

The approach taken to determine the localisation of Ply within the pneumococcus was to separate a population of pneumococci into cellular fractions followed by Ply detection by western blotting. This provides a clearer indication of which fraction contains Ply compared to assaying each fraction for haemolytic activity (Johnson, 1977), as any fractioned Ply may not necessarily be functional or present at levels below the detection limit of the assay.

A number of fractionation experiments were carried out using D39 and its Ply negative mutant, D39 $\Delta$ PlySTOP, to optimise the fractionation protocol outlined by Katherine Price and Andrew Camilli (Price & Camilli, 2009). The first adjustment to the aforementioned protocol was to reduce the concentration of mutanolysin present in the cell wall digestion buffer from 300U/ $\mu$ l to 300U/70 $\mu$ l. The first fractionation experiment detected Ply in the cell wall fraction (results not shown), and upon further scrutiny of the protocol, a number of control steps were tested. The control steps were carried out in parallel to allow comparison between the protocols and included: washing the bacterial cell pellet with PBS and retaining the wash to test for the presence of Ply protein; passing the BHI culture supernatant through a 0.2 $\mu$ m syringe filter before TCA precipitation to remove any remaining intact cells; and adding Dnase I to the protoplast fraction. The wash samples tested did not contain any Ply protein as determined by western blotting. Before filtration, the D39 broth supernatant was haemolytic and after it was reduced to below the detection limit with no Ply protein detected by western blotting. The addition of Dnase I to the protoplast fraction facilitated sample loading (results not shown). Therefore these additional steps were added to the fractionation protocol, and applied to D39 and D39 $\Delta$ PlySTOP cultures. These samples were probed with  $\alpha$ -SecA antibodies raised in rabbit against purified *Bacillus subtilis* SecA (a kind gift from Prof Arnold Driessen, University of Groningen, Netherlands) as a cytoplasmic protein control, but no signal was detected (results not shown). Attempts to purify recombinant *S. pneumoniae* TIGR4 SecA, to generate antibodies in-house, were unsuccessful (results not shown) and  $\alpha$ -TrxA antibody (a kind gift from Dr Jetta Bijlsma, University of Groningen, Netherlands) was tested but unable to provide a reproducible result (results not shown). Therefore antibodies against GroEL, a commonly used cytoplasmic protein control, were tested against pneumococcal lysates and provided consistent results.

The localisation of Ply was assessed in TIGR4, the autolysin and pneumolysin negative mutant TIGR4 $\Delta$ LytA-Ply, and the mutant complemented for Ply with pAHS3. The cells were grown in BHI and fractionated using the optimised protocol.

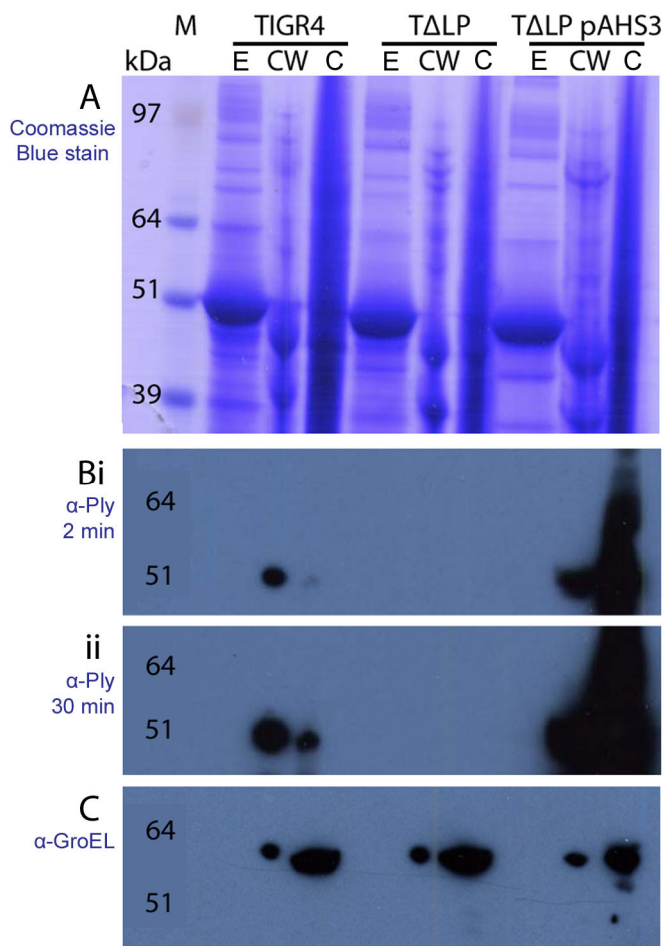


**Figure 6-13 Fractionation of TIGR4, TIGR4 $\Delta$ LytA-Ply (T $\Delta$ LP) and T $\Delta$ LP with pAHS3.** Fractionation was carried out as described in Materials and Methods, yielding extracellular (E), cell wall (CW) and cell (C) fractions. Samples were loaded onto 4-12% Bis-Tris precast NuPAGE gel (Invitrogen) and run at 75V for 25 mins, then 125V for 90 minutes. Proteins were stained for by coomassie blue (A) or transferred onto PVDF membrane to probe for Ply (B; i. for 2 min; ii. for 30 min) or GroEL (C).

Ply was detected in the cell wall and protoplast fractions, Figure 6-13, and not in the extracellular fraction from culture supernatant. However, GroEL is present in the cell wall fraction indicating pneumococcal cell lysis has occurred during the preparation of this fraction. Owing to this, the method of cell wall digestion was assessed to establish if the buffer could be adjusted to improve removal of the cell wall without inducing any stress or cell lysis.

The cell wall digestion buffer was adjusted by increasing the concentration of Tris buffer from 10mM to 100mM and increasing the ionic strength of the buffer by adding MgCl<sub>2</sub> (2mM), conditions which have previously been used to induce spontaneous protoplast formation in pneumococci without the additional action of murelytic enzymes (Lacks & Neuberger, 1975). Micrographs show that the cell

wall is removed when the sample is incubated at 37°C for 30 minutes or 30°C for 60 minutes, as there are cells present which are Gram stained pink, Figure 6-14 (see arrows), which indicates a reduction of cell wall thickness to retain the crystal violet-iodine complexes. Incubation of the sample at 25°C for 30 minutes does yield some pink stained pneumococci but not to the same proportion as that seen with the other incubation times. It also appears that some of the pneumococci in the 30°C and 37°C samples stain a lighter purple colour compared to the untreated control, implying some loss of cell wall thickness.

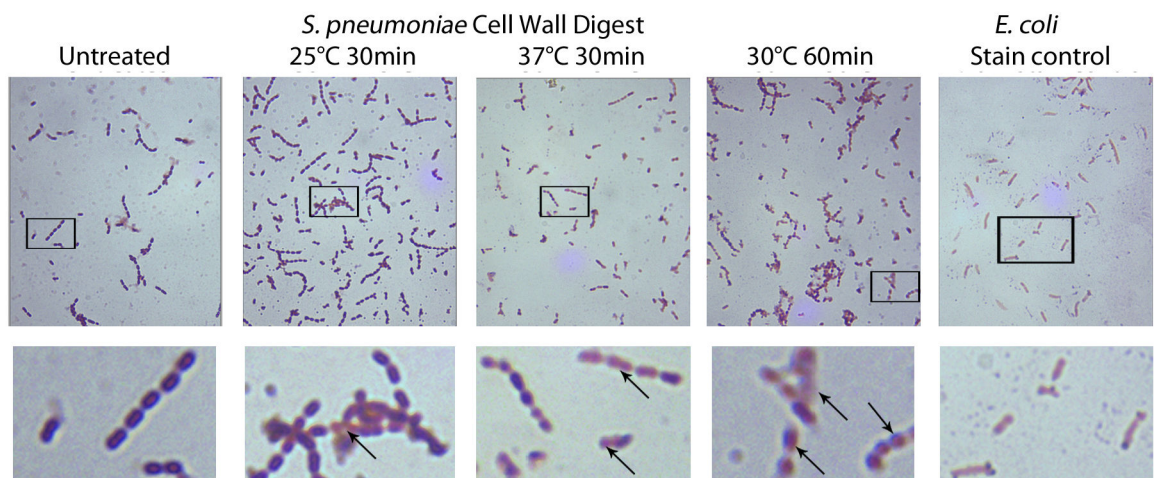


**Figure 6-14 Gram staining of pneumococci after cell wall digestion treatment** Pneumococcal strain D39 alone (untreated) or after incubation in cell wall digestion buffer (100mM Tris-HCl pH7.5, 2mM MgCl<sub>2</sub>, protease inhibitor and 30% sucrose) at 25°C or 37°C for 30 minutes or 30°C for 60 minutes was heat-fixed onto a microscope slide and Gram stained as outlined in Materials and Methods. Lower panel is close up of boxed areas. Arrows indicate pink (cell wall digested) *S. pneumoniae*. *E. coli* was included as a Gram negative stain control.

From the results, it was concluded that future cell wall digestion should be carried out by resuspending the bacterial pellet in 500µl of cell wall digestion buffer (100mM Tris-HCl pH7.5, 2mM MgCl<sub>2</sub>, 1 x protease inhibitor, 30% sucrose, 1mg/ml lysozyme, 600U/ml mutanolysin) and incubating at 30°C for 90 minutes. However, it should also be noted that although the cell wall fraction will contain cell wall fragments as there is evidence of cell wall digestion from whole cells, Figure 6-14, it cannot be conclusively said that the previously called protoplast fraction does not contain some cells with residual cell wall, therefore it will henceforth be referred to as the cell fraction.

TIGR4, TΔLP and TΔLP pAHS3 were grown to  $OD_{600} = 0.6$ , incubating at 25°C for 10 hours, then 37°C until the optical density was reached. The cultures were fractionated with the new cell wall digestion protocol, the proteins separated by SDS-PAGE, and western blotted for Ply and GroEL. GroEL (58kDa) was only detected in the cell fraction (Figure 6-15 C) showing that there was no whole cell carryover or lysis in the extracellular or cell wall fractions. Ply was detected in all three fractions; the extracellular supernatant, the cell wall and intracellular cell fraction. It is very interesting to note that Ply is detected in the extracellular fraction under these growth conditions, as it was not previously found when cultures were grown at 37°C from inoculation (Figure 6-13).

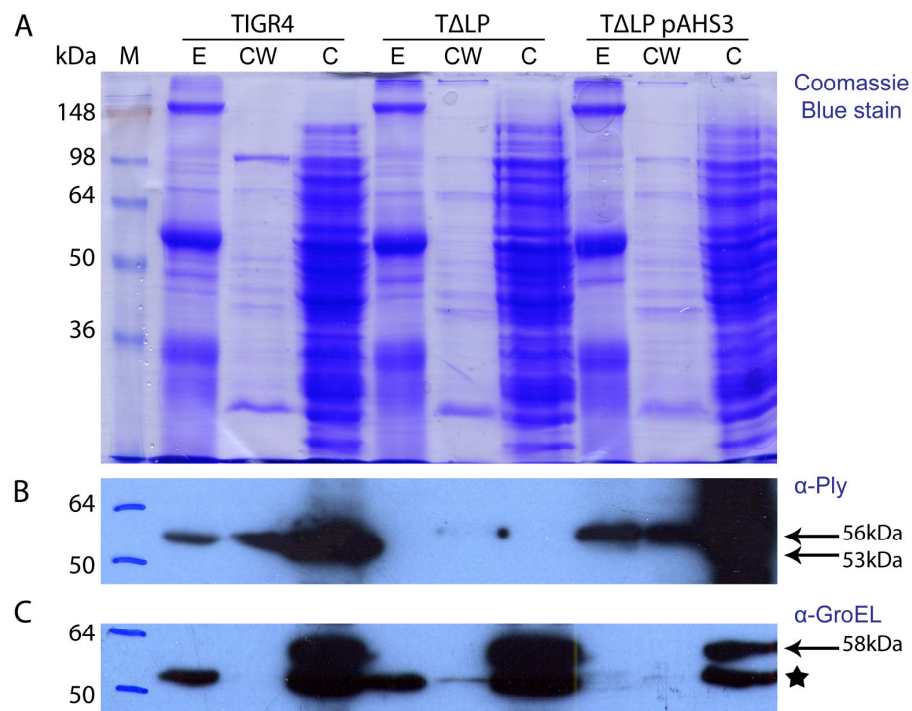


**Figure 6-15 Fractionation with alternative cell wall digestion buffer**  
TIGR4, TIGR4ΔLytA-Ply and TΔLP pAHS3 were grown to  $OD_{600nm} = 0.6$  and separated into extracellular (E), cell wall (CW) and cell (C) fractions as described in Materials and Methods. Pneumococcal cells were incubated in 0.5ml Cell wall digestion buffer (100mM Tris-HCl pH7.5, 2mM MgCl<sub>2</sub>, protease inhibitor cocktail, 30% sucrose, 600U/ml mutanolysin, 1mg/ml lysozyme) for 90 minutes. Samples were prepared and separated on 10% Bis-Tris SDS-PAGE, proteins stained with Coomassie Blue (A) or transferred onto PVDF membrane and probed for Ply (B) or GroEL (C). Ply has two sizes, wildtype TIGR4 is 53kDa or His, FLAG, Lumio tagged Ply from pAHS3 is 56kDa. GroEL is a cytoplasmic protein with a predicted size of 58kDa, and the western shows an unspecific band highlighted by star.

## **6.4.2 Fluorescence microscopy analysis**

It was interesting to not only detect Ply in the cell wall by fractionation and western blotting but to also to determine if Ply displays a particular distribution on the bacterial cell surface using the reagents developed. The localisation of Ply was assessed on *S. pneumoniae* strains D39, TIGR4 and their Ply deficient mutants complemented with plasmids expressing epitope and Lumio™ tagged Ply, pAHS3 or pAHS6. These reagents allow additional approaches to labelling Ply, either via indirect immunofluorescence using  $\alpha$ -FLAG antibodies or by the addition of Lumio™ substrate. If Ply localises to a distinct point on the pneumococcal surface, it may indicate that a specific interaction is occurring which could mediate its autolysin independent release.

### **6.4.2.1 Immunofluorescence**

A number of immunofluorescence experiments were carried out on paraformaldehyde fixed mid-exponential phase ( $OD_{600nm} = 0.6$ ) cultures of D39 and D39 $\Delta$ Ply-STOP using polyclonal  $\alpha$ -Ply antibodies and polyclonal  $\alpha$ -capsule type 2 antibodies, both raised in rabbits. Immunofluorescence with the  $\alpha$ -capsular antibody provided consistent results, with the outer edges of the pneumococcal cells labelled (Figure 6-16 B) showing that the conditions were optimum for this antibody. However, in-direct labelling of Ply was more difficult, whereby AlexaFluor 488 signal colocalised to pneumococcal cells at distinct points but this could not be conclusively attributed to Ply on D39 due to similar, albeit reduced in comparison, background fluorescence with the Ply negative mutant. Addition of BSA to PBS washes reduced the presence of this background signal in samples, and there is no AlexaFluor signal detected without prior incubation of the sample with primary  $\alpha$ -pneumococcal antibody. This indicates that the antibody concentration applied may not be optimum or there may be too many cells applied to the slide reducing the amount of antibody available to label Ply associated with each individual cell. Immunofluorescence labelling of D39 $\Delta$ PlySTOP and TIGR4 $\Delta$ LytA-Ply complemented with pAHS3 (Ply) was tested to utilise the FLAG epitope fused to Ply. Also, the monoclonal  $\alpha$ -

FLAG antibody was raised in mice which enabled double labelling (FLAG-Ply and capsule) of pneumococci to be trialed.

Results from immunofluorescence microscopy with a single antibody (Figure 6-16 A Merge) show that not all D39 $\Delta$ PlySTOP/pAHS3 and TIGR4 $\Delta$ LytA-Ply/pAHS3 cells are labelled with  $\alpha$ -FLAG antibodies and the cells which are labelled display a universal distribution of FLAG-Ply on the cell. The double-labelling experiment,  $\alpha$ -FLAG then  $\alpha$ -capsule primary antibodies, shows that the capsule is confidently stained (blue) with the highest levels of fluorescence distributed at the periphery of the cells for both strains (Figure 6-16 B  $\alpha$ -capsule). FLAG-Ply (green) appears stained for in majority of cells, again with a general distribution, and some punctate areas of signal are present a number of which colocalise with the edge of a pneumococcal cell (Figure 6-16 B  $\alpha$ -FLAG and Merge).

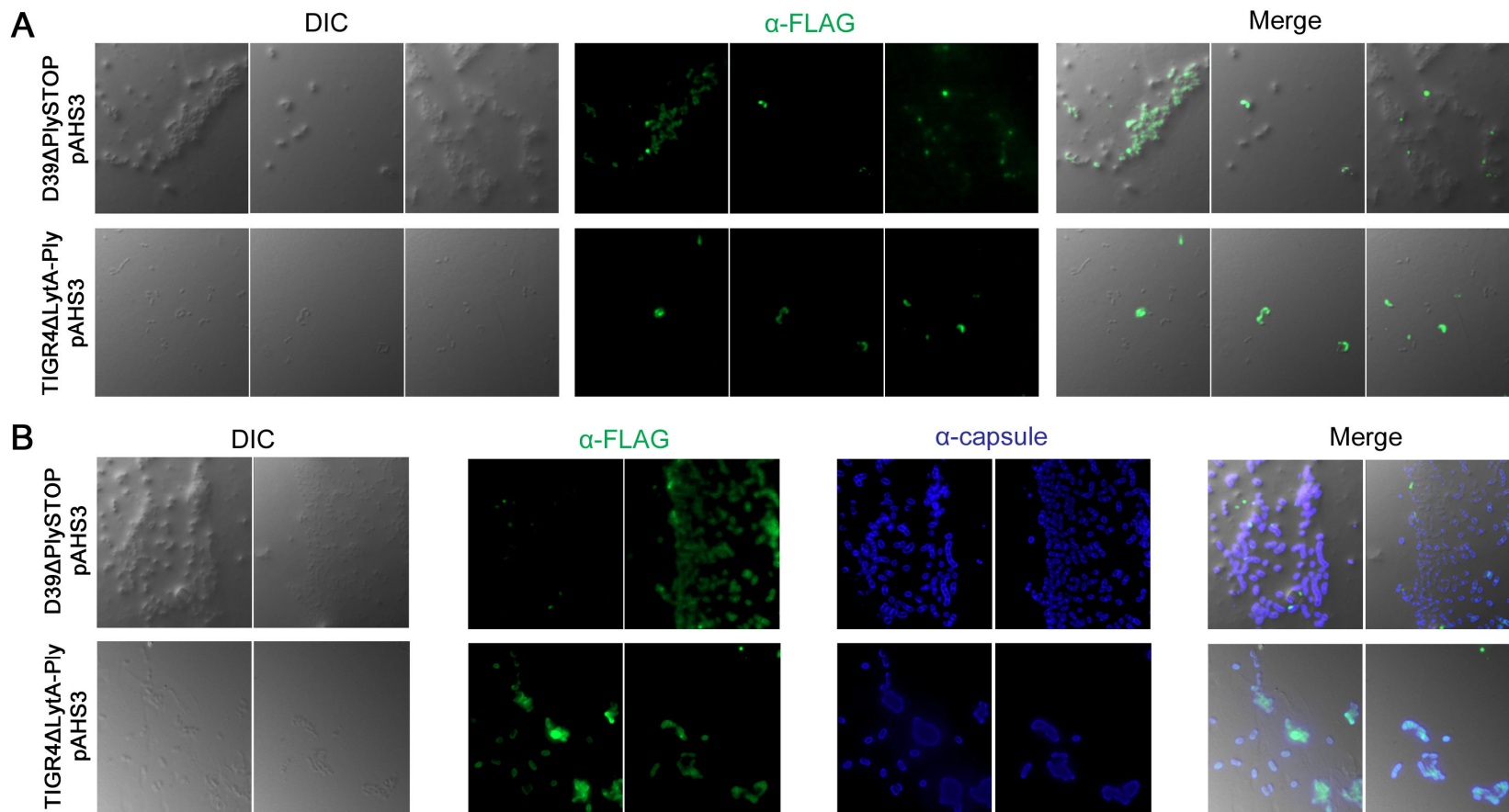


**Figure 6-16**  
**Immunofluorescence microscopy of D39 $\Delta$ PlySTOP/pAHS3 and TIGR4 $\Delta$ LytA-Ply/pAHS3.**  
 To ascertain the cellular localisation of Ply, pneumococci were grown to mid-exponential phase in BHI, the cells fixed then indirectly stained for (A) FLAG-Ply (green) with  $\alpha$ -FLAG and  $\alpha$ -mouse AlexaFluor 488, or (B) for both FLAG-Ply and the polysaccharide capsule ( $\alpha$ -capsule and  $\alpha$ -rabbit AlexaFluor 647; blue). Three (A) or two (B) separate fields of view are depicted for the samples.

#### 6.4.2.2 Lumio™ substrate dependent fluorescence

The localisation of Ply on the pneumococcal surface was assessed by adding Lumio™ reagent to live mid-exponential ( $OD_{600nm} = 0.6$ ) BHI cultures of D39ΔPly-STOP, D39ΔPlySTOP pAHS3 (Ply) and D39ΔPlySTOP pAHS6 (Ply) to label the introduced tetracysteine motif at the N-terminal end of Ply. The labelled cells, on poly-L-lysine coated microscope slides, were viewed using a Zeiss AxioImager M1 microscope and images captured as described in Materials and Methods. Lumio™ labelling of fusion proteins has not been previously described in Gram positive bacteria; reports were only available for Gram negative bacteria species such as *E. coli* (Ignatova & Gierasch, 2004), *Shigella* (Enninga et al., 2005) and *Salmonella* (Sciara et al., 2008). These studies used Lumio™ to study real-time protein production and aggregation, protein localisation and protein secretion/translocation respectively.

From the micrographs, it can be seen that there is some background fluorescence seen with the negative control, Lumio™ reagent treated D39ΔPly-STOP (Figure 6-17 A), however this background fluorescence is little in comparison to the fluorescence observed with D39ΔPlySTOP expressing tetracysteine tagged Ply (Figure 6-17 B and C). The Lumio™ fluorescence localises to the pneumococcal cell, although it can be seen for the right half of D39ΔPlySTOP/pAHS3 panel that there is some signal displaced, which is likely due to slight movement of the cell during the imaging protocol. The distribution of Lumio™ appears consistent across the cell (Figure 6-17 B) and from analysis of each individual z-slice this distribution continues through the cell (data not shown). This is expected as the reagent is membrane permeable therefore it is able to travel through the cell wall and membrane to label the intracellular pool of Ply. No fluorescence ‘displacement’ is seen with the cells expressing D39ΔPlySTOP/pAHS6, indicating that the cells have successfully been immobilised by the poly-L-lysine coating on the microscope slide. As these cells are expressing both Lumio™ and RFP tagged Ply, it is interesting to compare the distribution of these two signals (Figure 6-17 C). The RFP fluorescence imaged can be attributed solely to the production of RFP-Ply, as there is no RFP detected when the identical image acquisition protocol was applied to D39ΔPlySTOP/pAHS3 (results not shown). Areas that are yellow in colour indicate the presence of both Lumio™ (green) and RFP (red) fluorescence, seen

Figure 6-17 C (L+R). When observed with Volocity 3D restoration software (Figure 6-18), the Lumio™ signal surrounds the RFP signal with areas of yellow and pneumococcal cells which are more red than green/yellow in the micrographs in Figure 6-17 C is due to insufficient Lumio™ labelling.

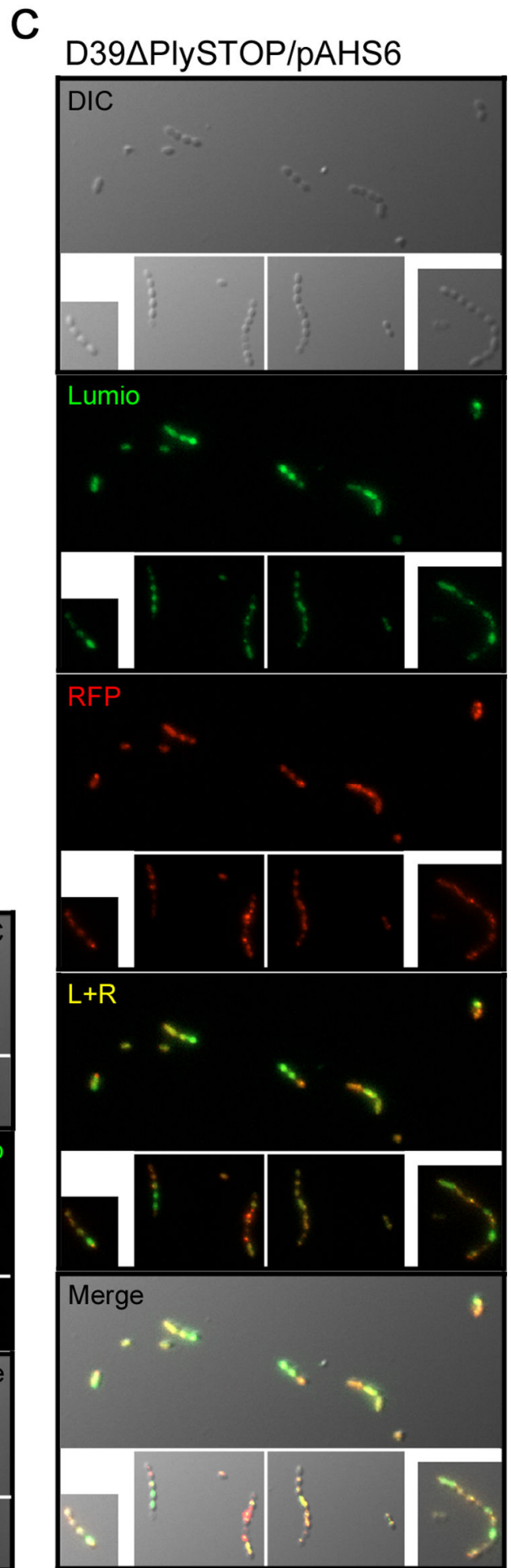
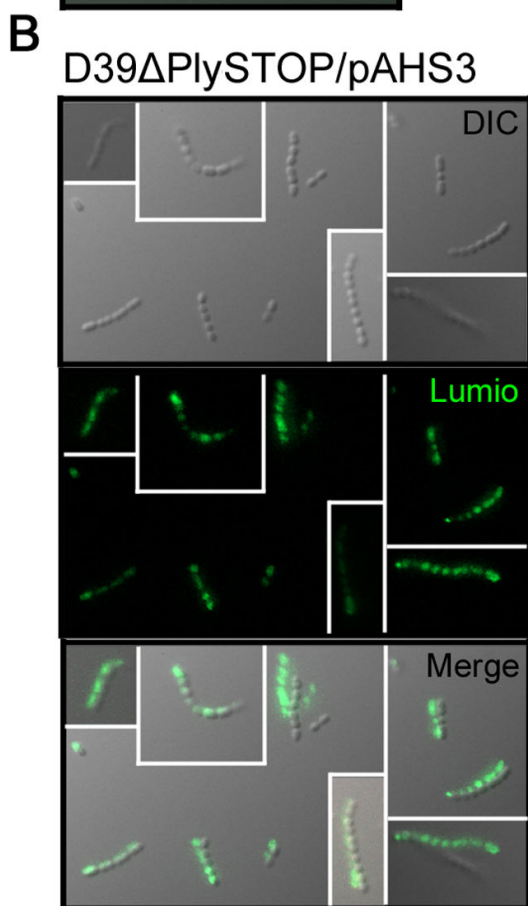
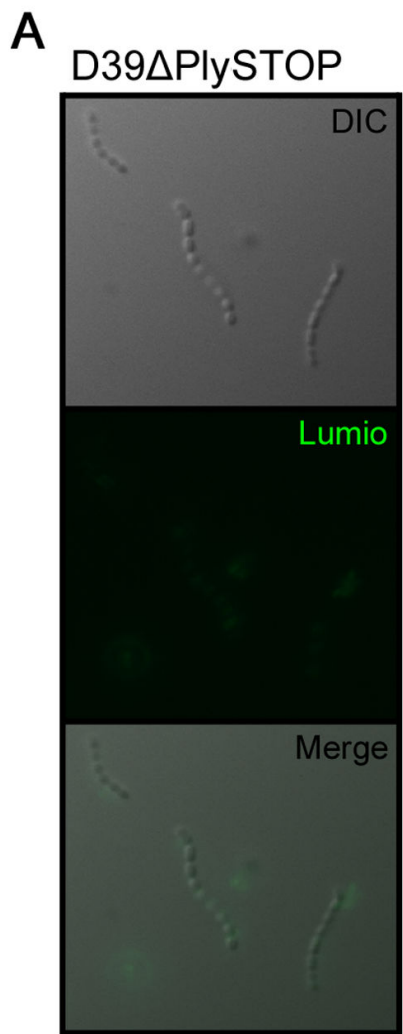


**Figure 6-17 Lumio™ labeling of D39ΔPlySTOP expressing tagged-Ply**  
*S. pneumoniae* D39ΔPlySTOP (A), D39ΔPlySTOP/pAHS3 (B; Ply) and D39ΔPlySTOP/pAHS6 (C; RFP-Ply) cells were incubated with Lumio™ reagent, washed and spotted onto a poly-L-lysine coated slide. Z-stacks with 0.2µm spacing were acquired with FITC (Lumio) and DsRed (RFP) filters.

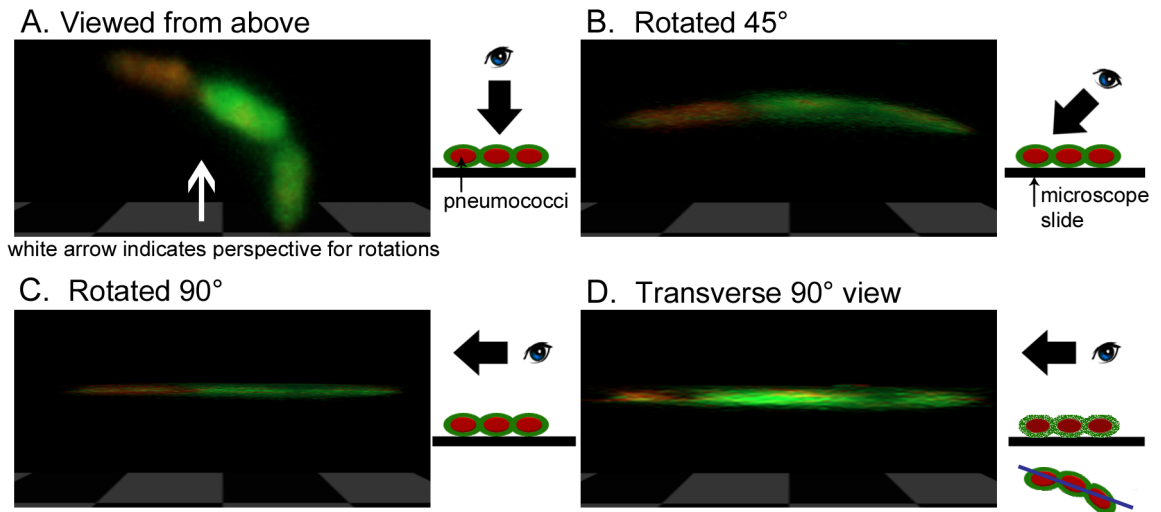


**Figure 6-18 3D analysis of D39ΔPlySTOP/pAHS6 with Lumio™ substrate**  
Pneumococci cells from Figure 6-17 were analysed with Volocity 3D restoration software (PerkinElmer) in order to determine the distribution of Lumio™ fluorescence in relation to RFP-Ply expressed by the cells. The cells were viewed from above (A), an elevated side view (B), and directly adjacent (C); images to the right describe the perspective viewed. A transverse view, indicated by the blue line in the bottom perspective diagram, was also observed to determine the distribution within the cell (D).

The localisation of Lumio™ tagged Ply was also assessed with TIGR4ΔLytA-Ply pAHS3 alongside a negative control and in comparison with D39ΔPlySTOP pAHS3, which was cultured and labelled in parallel. Again, background fluorescence is observed with the Ply negative controls (Figure 6-19 A and C) but this differs markedly from the cells expressing tetracysteine tagged Ply.

D39ΔPlySTOP/pAHS3 displays the same distribution of Lumio™ seen previously in Figure 6-17 B, which is a general distribution of Ply throughout the cell.

Lumio™-Ply is also detected throughout TIGR4ΔLytA-Ply/pAHS3 cells, however a brighter signal is observed surrounding the outer boundary of the cell than from the central area, Figure 6-20. This suggests that Lumio™-Ply localises to the periphery of TIGR4ΔLytA-Ply cells.

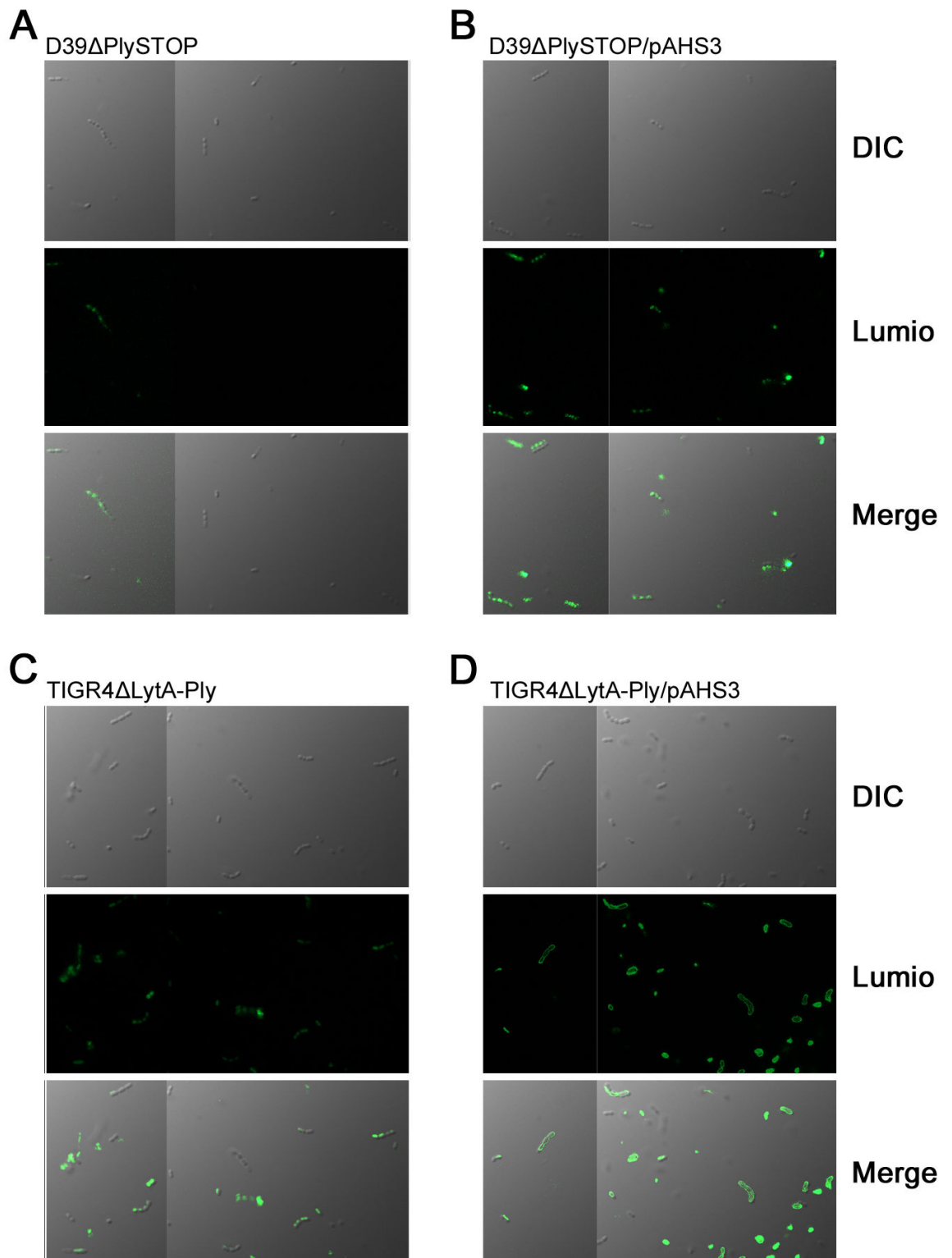


**Figure 6-19** Fluorescence microscopy of pneumococci incubated with Lumio™ reagent *S. pneumoniae* strains D39ΔPlySTOP (A), D39ΔPlySTOP/pAHS3 (B), TIGR4ΔLytA-Ply (C) and TIGR4ΔLytA-Ply/pAHS3 (D) were incubated with Lumio™ reagent, washed and spotted on a poly-L-lysine slide. Micrographs were acquired as described in Materials and Methods.

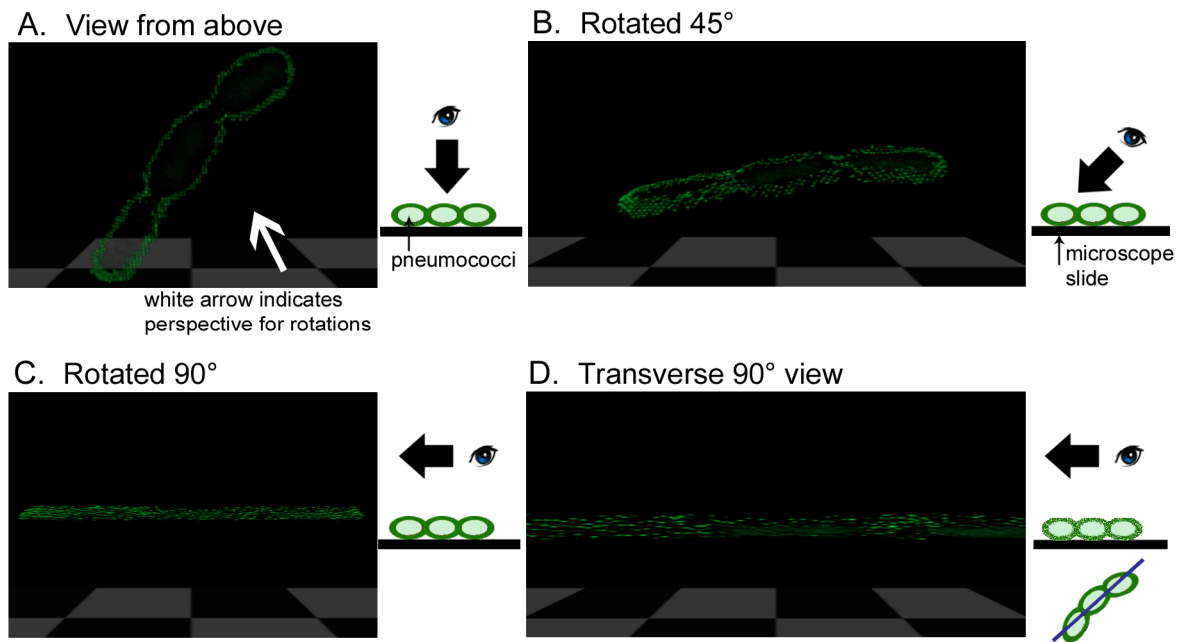


**Figure 6-20 3D analysis of TIGR4ΔLytA-Ply/pAHS3 with Lumio™ substrate**  
Pneumococci cells from Figure 6-19 were analysed with Volocity 3D restoration software (PerkinElmer) in order to determine the distribution of fluorescence from Lumio™ tag-Ply expressed by the cells. The cells were viewed from above (A), an elevated side view (B), and directly adjacent (C); images to the right describe the perspective viewed. A transverse view, indicated by the blue line in the bottom perspective diagram, was also observed to determine the distribution within the cell (D).

## 6.5 Virulence analysis of TIGR4ΔLytA-Ply::Chl

*S. pneumoniae* serotype 3 strain A45 has reduced virulence in our murine bacteraemia and pneumonia models compared to other serotype 3 (OXC141) pneumococci (Dr Andrea Mitchell, unpublished results). Therefore, assessing the virulence of TIGR4ΔLytA-Ply in our murine models of infection will determine whether this natural recombination event between LytA and Ply provides an explanation for the reduced virulence seen with A45. Whether Ply provides a selective advantage in the murine model of infection can also be tested by complementing the TIGR4ΔLytA-Ply mutant with episomally expressed Ply. For this study, a tagless version of codon-optimised Ply under the control of the *ami* promoter was introduced into pAL2YI to create pAHSTLPly. Animal experiments testing the survival of mice infected with TIGR4, TIGR4ΔLytA-Ply::Chl or TIGR4ΔLytA-Ply/pAHSTLPly are currently underway.

## 6.6 Discussion

Ply is a cholesterol dependent cytolysin of *S. pneumoniae*. It is the only CDC which does not have a typical Sec secretion signal and has been considered to be cytoplasmic (Johnson, 1977), and released upon cell lysis mediated by autolysin A (LytA). However, there have been reports that Ply can be released in a number of serotypes during early-stationary phase of growth (Benton *et al.*, 1997b), without the effect of LytA-dependent autolysis in a serotype 3 strain WU2 (Balachandran *et al.*, 2001) and can localise to the cell wall in a number of serotypes (Price & Camilli, 2009). Ply is not the only predicted cytoplasmic protein due to the absence of conserved signal and/or anchoring sequences, in the pneumococcal proteome, which is secreted and surface associated.

Examples include the plasmin(ogen) binding proteins enolase (Bergmann *et al.*, 2001; Bergmann *et al.*, 2003) and GAPDH (Bergmann *et al.*, 2004), PavA (Holmes *et al.*, 2001) and PcsB (Mills *et al.*, 2007). There is further evidence from other Gram positive organisms of predicted cytoplasmic proteins being secreted into the extracellular milieu without any evidence of cell lysis through what is being termed a non-classical secretion pathway, reviewed in (Bendtsen *et al.*, 2005). Enolase is also secreted from *B. subtilis* via a non-classical secretion pathway and it has recently been elucidated that an  $\alpha$ -helical membrane-embedding domain within its protein structure is required for its lysis-independent release from the cell (Yang *et al.*, 2011).

To further characterise the localisation and potential release of Ply from the pneumococcal cell, N-terminal tagged codon-optimised versions of Ply were developed as reagents. These reagents were episomally expressed in a Ply negative mutant of D39, D39 $\Delta$ PlySTOP, and detected through western blotting with  $\alpha$ -Ply antibodies, Lumio<sup>TM</sup> substrate mediated fluorescence and restored haemolytic activity. pAHS3 and pAHS6 complement the D39 Ply knockout and have a higher haemolytic output compared to the D39 control where the pAHS6 (RFP-Ply) titre is 8 times that of the D39 WT; pAHS3 titre is 64 times. The copy number of the shuttle vector is 8 (Macrina *et al.*, 1982), therefore this provides explanation as to why the RFP-Ply titre is 8 times that of D39 WT. However the pAHS3 titre is 8 times that of pAHS6 and as both Ply fusions are cloned into the same vector, under the control of the same promoter, this implies that the rfp+

tag may affect oligomerisation of the toxin molecules to form a pore, thereby reducing haemolytic activity. The addition of DTT to the assay eliminates the possibility of dimers being formed through disulphide bonds between tetracysteine residues in the Lumio<sup>TM</sup> motif, which was evident when characterising the fluorescent protein reagents in the previous chapter. Also, previous and current work by colleagues in the lab have demonstrated that the genetic fusion of Ply to a fluorescent protein (eGFP) does not affect its haemolytic activity (Douce *et al.*, 2010). Western analysis shows that pAHS6 is highly expressed to a comparable level of that shown by pAHS3 (Figure 6-3), therefore the reduced haemolytic activity is not likely due to RFP-Ply instability and degradation in the pneumococcus. Another explanation for the higher haemolytic titre of pAHS3 compared to pAHS6 may be a difference in cell number between the two samples, as although the protein concentrations were comparable, there may have been 8 times more D39 pAHS3 pneumococcal cells than D39 pAHS6 in the sample. In hindsight, a viable count of the cultures could have been measured before pelleting the cells for sample preparation to ensure comparable numbers of pneumococcal cells were sonicated.

The introduction of the LytA-Ply fusion mutation, naturally occurring in equine *S. pneumoniae* strains, into TIGR4 allows the investigation of whether episomally expressed N-terminally tagged Ply is released without the action of autolysin or the genes which are co-transcribed with Ply. Through an optimised fractionation protocol, results show that Ply is present in the cell wall fraction, even when N-terminally tagged, in both the TIGR4 parent and  $\Delta$ LytA-Ply mutant which supports the previous report (Price & Camilli, 2009). This also suggests that the cell wall localisation of Ply is not dependent upon the function of autolysin or the intervening gene products. Although GroEL was detected in the cell wall fraction for all strains (Figure 6-13), as western blotting is assaying a population, it can be seen particularly in the TIGR4 WT that the GroEL found in the cell wall fraction is less compared to the cell fraction. This indicates that it is a small proportion of cells which have lysed and yet a larger amount of Ply is found in this fraction compared to the cell fraction. The difference in proportions of GroEL to Ply implies that some of the Ply found in the cell wall fraction has been liberated from cell wall digestion and not just from cell lysis. This is supported by subsequent results (Figure 6-15) which show that Ply is present in the cell

wall fraction without any cell lysis, indicated by the detection of GroEL. A very interesting result arose the pneumococcal culture grown from a smaller inoculum and extended incubation time at a lower temperature, given that Ply was detected in the extracellular fraction without any indication of cell lysis, i.e. no GroEL was present in the fraction (Figure 6-15). There was no evidence of this release of Ply occurring when cultures were grown at 37°C from inoculation (Figure 6-13 and results not shown from D39 data). This suggests that this *in vitro* culture condition is required for Ply release into the extracellular milieu from the pneumococcus in an autolysin-independent mechanism. However, these results merit further research to determine if this is a common phenomenon due to the low incubation temperature, extended lag phase and/or low population density; if it is active or passive secretion of Ply; or if it is an artefact. It would have been interesting to have investigated if the Ply truncates, Domains 123 and Domain 4, can localise to the cell wall in both D39 $\Delta$ PlySTOP and TIGR4 $\Delta$ LytA-Ply strains.

There are many difficulties with fractionation, such as cell lysis during bacterial culture or experimental procedure, incomplete cell wall digestion, and whole cell contamination of early fractions. The addition of appropriate controls to the fractionation procedure can reduce the occurrence of cell lysis or cross contamination of fractions. Pneumococcal protoplast formation in previous studies was measured by the reduction in absorbance when the suspension is added to a hypotonic solution inducing lysis by osmotic shock (Lacks & Neuberger, 1975; Vijayakumar & Morrison, 1986). However, Gram negative bacterial cells would also be sensitive to osmotic shock in hypotonic solution and these cells still possess a thin peptidoglycan cell wall, therefore this method would not confirm complete cell wall removal from the cell. Similar reasoning applies to Gram staining of cells as Gram negative cells stain pink, as would Gram-positive cells with reduced cell wall thickness and bacterial protoplasts. Owing to this, it is possible to hypothesise that a pool of Ply may exist in the space between the cytoplasmic membrane and cell wall (periplasm). This hypothesis is challenged by published work, where Ply can be liberated from the pneumococcal surface by SDS and digested from the surface by proteinase K (Price & Camilli, 2009). However, there may have been incomplete cell wall digestion in this study, leading this pool of periplasmic Ply being considered as

intracellular as successful cell wall digestion was confirmed by blotting fractions with  $\alpha$ -RrgB, the major protein subunit of pneumococcal pili (LeMieux *et al.*, 2006). Blotting with this antibody showed that the high molecular weight complexes were mainly present in the cell wall fraction but there is a faint band visible in the protoplast fraction. Also, the presence of RrgB can only be confirmed in TIGR4 as D39 does not carry the pilus (rlr) pathogenicity island (Tettelin *et al.*, 2001; Price & Camilli, 2009). In fact, the sortase genes encoded on the rlr pathogenicity island are only present in approximately 17% (14/82) of pneumococcal clinical isolates (Paterson & Mitchell, 2006). This demonstrates the difficulty in choosing a suitable cell wall control protein to detect by western blotting in order to confirm complete cell wall digestion.

Immunofluorescence microscopy of D39 $\Delta$ PlySTOP/pAHS3 and TIGR4 $\Delta$ LytA-Ply/pAHS3 with  $\alpha$ -Ply and  $\alpha$ -FLAG antibodies will require further optimisation of experimental conditions, as FLAG-Ply was detected using  $\alpha$ -FLAG antibodies only on a number of cells, with a general distribution of FLAG-Ply on the surface of the cell (Figure 6-16). To further support the evidence for extracellular localisation of FLAG-Ply, the samples were co-stained for the capsule polysaccharide to label the outermost of the cell. FLAG-Ply was detected on most cells in this co-labelling experiment and the lack of FLAG-Ply seen in the D39 $\Delta$ PlySTOP/pAHS3 left-hand-side panel is likely due to insufficient antibody staining rather than all the cells in the other panels being labelled due to AlexaFluor647 signal bleed through in the FITC filter. This explanation is supported by the experimental procedure employed as the same image acquisition protocol was applied to all samples, and AlexaFluor 647 was chosen because its excitation and emission spectra has no overlap with that of AlexaFluor 488. The general extracellular distribution of Ply on the pneumococcal cell is further supported by the Lumio<sup>TM</sup> fluorescence microscopy data. Lumio<sup>TM</sup> fluorescence was largely detected on the periphery of D39 $\Delta$ PlySTOP/pAHS6 (Figure 6-17 C and Figure 6-18) and TIGR4 $\Delta$ LytA-Ply/pAHS3 (Figure 6-19 D and Figure 6-20). The peripheral localisation Lumio<sup>TM</sup>-Ply in D39 $\Delta$ PlySTOP/pAHS6 (Figure 6-18) may be due to insufficient substrate to label the intracellular pool or because the cells were imaged live, super-resolution microscopy would be needed to detect both signals within an individual voxel. Comparing the distribution of TIGR4 $\Delta$ LytA-Ply/pAHS3 (Figure 6-19 D) with

D39 $\Delta$ PlySTOP/pAHS3 (Figure 6-19 B), the peripheral signal is brighter in the complemented TIGR4 mutant than in the D39 mutant which suggests that there is more Lumio<sup>TM</sup>-Ply present on the surface. This implies that although the genes deleted in the TIGR4 mutant do not inhibit the localisation of Ply to the cell surface, they may play a role in controlling the amount of Ply which is present on the surface. The background fluorescence observed with cultures not expressing Lumio<sup>TM</sup> fusion proteins may be reduced by including  $\beta$ -mercaptoethanol in PBS washes (Langhorst *et al.*, 2006). Lumio<sup>TM</sup> binding to endogenous cysteine-rich proteins has previously been reported (Stroffekova *et al.*, 2001), yet the occurrence of this should be limited in these conditions as the Lumio<sup>TM</sup> reagent is pre-complexed with ethanedithiol (EDT) to ensure specific labelling. Nonetheless, additional control experiments still need to be carried out to confirm these results, which could not be done during the course of my study due to time constraints. Also, it would have been interesting to test the localisation of Ply, using immunofluorescence and/or Lumio<sup>TM</sup> labelling, on pneumococci grown in the *in vitro* conditions in which Ply was released into the extracellular milieu, as seen in the fractionation experiment (Figure 6-15).

Ply can localise to the cell wall during *in vitro* growth, and is broadly distributed on the cell surface. The cell wall localisation of Ply is not dependent upon autolysin (LytA) or the open reading frames present between Ply and LytA, as the phenotype is still observed by fractionation and fluorescence microscopy with TIGR4 $\Delta$ LytA-Ply. However, one (or more) of the deleted genes may control the amount of Ply displayed on the surface, as there appears to be more Ply present on TIGR4 $\Delta$ LytA-Ply/pAHS3 surface compared with D39 $\Delta$ PlySTOP/pAHS3. The production of Ply has been shown to be advantageous for continued growth of a Ply deficient type 2 mutant PLN-A *in vivo* during co-infection with D39 in a murine sepsis model of infection (Benton *et al.*, 1995), which suggests the presence of an extracellular pool of Ply during the early stages of bacterial growth in the blood to cause inflammation which promotes acute sepsis. The authors hypothesised that this extracellular Ply was from autolysin-dependent release of Ply *in vivo*, however the data from this study offers another hypothesis in that Ply may be released from the pneumococcal cell wall *in vivo*, potentially by a host dependent mechanism, before autolysis. Sublytic concentrations of Ply have been shown to activate complement (Mitchell *et al.*,

1991) and deposition of C3 is greater on strains deficient in Ply production compared to parent strains (Yuste *et al.*, 2005). In addition to this, sublytic concentrations (100 ng/ml) of Ply can also modulate the host cell cytoskeleton resulting in microtubule bundling and the formation of actin stress fibres, filopodia and lamellipodia contributing to the pathology caused pneumococcal meningitis (Iliev *et al.*, 2007; Iliev *et al.*, 2009; Förtsch *et al.*, 2011). This concentration of Ply can also mediate the uptake of peptidoglycan from competing colonising species, such as *Haemophilus influenzae*, by epithelial cells inducing a host immune response (via Nod1) against the co-colonising species (Ratner *et al.*, 2007). It would be advantageous if these activities were induced either by the Ply associated with the cell surface or Ply released by an autolysin-independent mechanism, as this could be considered to be a controlled approach compared to the large general Ply release from whole cell lysis. *S. pneumoniae* activates nitric oxide (NO) production by macrophages in a mechanism dependent on Ply, as there is little NO produced with the Ply deficient mutant, PLN-A (Braun *et al.*, 1999). The nitrite concentration produced by macrophages incubated with sublytic concentrations of recombinant Ply protein was 50-fold that found with pneumococcal cell wall extracts, which suggests that there is no cell wall localised Ply, otherwise a greater nitrite concentration would have been observed. This observation can be explained by the cell wall preparation protocol, whereby the extracts were treated with SDS, which has been shown to remove Ply from the cell wall fraction (Price & Camilli, 2009). Taking this into consideration, these results provides additional support for the cell wall localisation of Ply and possibly LytA-independent Ply release, as NO production is observed in cultures before late-stationary phase without cell lysis. It has recently been observed that Ply can be released from *S. pneumoniae* TIGR4 strain treated with lysozyme (LysM), which degrades peptidoglycan and is present on mucosal surfaces, and this was necessary for Nod2 stimulation, production of the chemokine CCL2 and monocyte/macrophage influx (Davis *et al.*, 2011). This study also provides a plausible *in vivo* mode of Ply release from the pneumococcal cell wall.

In conclusion, the codon-optimised Ply reagents developed can complement a Ply deficient *S. pneumoniae* strain and the full-length version retains its haemolytic activity. Autolysin and the genes co-transcribed with Ply are not

required for Ply secretion across the cytoplasmic membrane, for its cell wall localisation or its release from the cell wall; which is supported by the following results:

- The N-terminal tagged Ply can still localise to the cell wall, therefore the tag does not interfere with its secretion, suggesting its secretion across the cytoplasmic membrane is not by a classical pathway.
- Ply can localise to the cell wall in the TIGR4 $\Delta$ LytA-Ply mutant shown by cell fractionation (Figure 6-15) and Lumio<sup>TM</sup> fluorescence microscopy (Figure 6-19 and Figure 6-20).
- Ply is released from the wild-type (TIGR4) and mutant (TIGR4 $\Delta$ LytA-Ply) cell wall, without any evidence of cell lysis, when pneumococci are grown from a low inoculum at a low temperature (25°C) (Figure 6-15).

The quantity of Ply on the pneumococcal cell surface, observed by fluorescence microscopy (Figure 6-19), is greater on TIGR4 $\Delta$ LytA-Ply/pAHS3 than D39 $\Delta$ PlySTOP/pAHS3 which suggests that one (or more) of the deleted genes may play a role in limiting the amount of Ply displayed on the cell surface. Whether this gene(s) role is involved in the secretion of Ply across the cytoplasmic membrane or mediating the interaction of Ply with the cell wall remains to be elucidated. The release of Ply may be a more controlled and gradual process without the requirement that members of the population undergo lysis. This gradual release may assist the 'subtle' functions of Ply which include complement activation, rearrangement of the host cytoskeleton, nitric oxide production from macrophages and pneumococcal survival in the host via Nod1 and Nod2 sensing.

## 7 Final Discussion

The general aim of this project was to characterise conditions which may be conducive for protein translocation; for two *E. coli* O157:H7 non-LEE encoded T3S effector homologs and for a predicted cytoplasmic toxin of *S. pneumoniae*.

Regulation of the LEE PAI is complex as it not only regulates its own expression, but it is regulated by other horizontally acquired factors, such as *pch* or indirectly by *psr* genes. Upon assessment of the literature, the regulatory pathway of the LEE has also integrated into regulatory networks endogenous to *E. coli*, such as quorum sensing (*qseABCDEFG*), phosphorelay systems (*rcsABCDF*), and stress response pathways (*gadE* and *rpoS*). This complex regulatory network enables the LEE to be expressed at the most optimum time, i.e. upon detection of host factors (such as epinephrine) or cell contact. As expression of the T3SS apparatus, and the LEE-encoded effectors, is under the influence of so many factors, it is interesting to determine which factors influence the expression of non-LEE encoded effectors. NleH1 and NleH2 are carried on separate horizontally acquired O-Islands (OI-36 and OI-71 respectively) and share 87% protein identity. Analysis of the 5' UTR of both alleles revealed that the sequence similarity decreased further from the ORF, which implied that the genes may be differentially expressed or regulated. Assessment of translational fusions to *gfp*, in *E. coli* O157:H7 strain ZAP193, showed that expression of both NleH1 and NleH2 is enhanced when cultured under *in vitro* conditions which stimulate expression of the T3SS and that maximal expression of NleH1 required 531bp of the upstream untranslated region but NleH2 only required 113bp. This indicates that a regulatory factor binds the 5' UTR of NleH1 controlling its expression whereas NleH2 expression is not as strictly controlled. This observation was supported by results testing Pch regulation of the EDL933L genome, which predicted that Pch binds to the promoter of NleH1 but not NleH2 (Abe *et al.*, 2008). The LEE-encoded effectors Ler and GrlA are indirectly involved in the positive regulation of NleH1 and NleH2 *in vitro*, therefore providing a basal level of co-ordinate expression with the apparatus that translocates them. However, this co-ordinate expression is not strict as NleH is expressed in cells which do not have an assembled T3SS. This suggests that NleH

may be regulated at the post-transcriptional or post-translational level. This hypothesis is supported by research investigating the regulation of *C. rodentium* NleH, which is regulated post-translationally by LonP-mediated degradation in this background (Garcia-Angulo *et al.*, 2008). This 'loose' co-ordination of expression with the LEE may ensure that non-LEE encoded effectors are available for secretion by the T3SS, once the LEE encoded effectors have been translocated or if the transcription of the LEE effectors is repressed later in the infection process. Host cell binding repressed NleH expression and the timing, and level, of NleH expression during active *in vitro* infection of cells remains to be determined.

NleH proteins are predicted serine/threonine kinases and homologues of OspG, a T3SS effector of *S. flexneri*. Similar to its homolog, NleH1 can autophosphorylate in the presence of ATP and Mg<sup>++</sup>. OspG has been characterised as a modulator of the host immune response by interacting with E2 ubiquitin-conjugating enzymes resulting in the inhibition of NF-κB activation. Owing to this, the effect of NleH on NF-κB activation was tested, using luciferase reporter constructs, but its effects were not significant. This contradicts other reports where NleH has been shown to modulate NF-κB activation. However in most of these studies, NleH is highly overexpressed in comparison to the NF-κB reporter, which may be very different to the physiological scenario, potentially giving an incorrect assessment of NleH functionality. Another research group have reported that EPEC NleH can function as an anti-apoptotic factor which is dependent upon interaction with Bax-inhibitor 1 (BI-1) (Hemrajani *et al.*, 2010). This interaction with BI-1 is dependent upon the C-terminal end of NleH but not its kinase activity; this region of NleH shares high protein identity with OspG yet OspG does not interact with BI-1. This supports the hypothesis that NleH may have multiple functions within the host cell. The phosphorylation of a host protein has not been described for NleH therefore DiGE analysis was performed on lysates from HEK293T cells transfected with NleH or its kinase-dead mutant K159A. Unfortunately, no targets were identified and a yeast two hybrid screen of NleH1 and NleH2 also did not provide a potential eukaryotic binding partner. In conclusion, I feel there still remains some controversy regarding NleH function and it is very likely that further eukaryotic targets will be discovered for this

effector although this may require using more appropriate tools such as bovine based Y2H screens.

LOV domains are part of the photosensing Ser/Thr protein kinases (phototropins) in plants and when the domain was recombinantly expressed in *E. coli*, it fluoresced when exposed to UV light (Salomon *et al.*, 2000; Swartz *et al.*, 2001). The LOV domain was subjected to molecular evolution in order to improve its fluorescence and recovery after photobleaching to create iLOV (Chapman *et al.*, 2008). iLOV is less than half the size of GFP, making it a suitable candidate to test as a reporter for T3S-mediated translocation. A translational fusion of iLOV to the C-terminus of Tir can complement a Tir deficient strain of *E. coli* O157:H7 and form actin pedestals (K. Velentza, I. Houghton, A. Holmes and A. Roe; unpublished results). NleH-iLOV can be translocated into the host cell, as determined by fluorescence microscopy, and its distribution correlates with previous reports (Gao *et al.*, 2009; Hemrajani *et al.*, 2010; Martinez *et al.*, 2010; Wan *et al.*, 2011). In conclusion, iLOV can be genetically fused to T3S effectors without hindering their secretion, translocation or function. This newly developed fluorescent protein provides a useful tool for the study of T3S effectors.

Codon-optimised fluorescent proteins were developed as reagents for future pneumococcal research as they have not been used extensively, in comparison to the Gram positive organism *B. subtilis*, in past studies. Fluorescent proteins as reporter genes can be useful for gene expression studies, like the NleH study, and assessment of protein localisation. These proteins were successfully expressed to detectable levels, determined by fluorimeter measurement and fluorescence microscopy, in the pneumococcus from lag phase to early stationary phase of growth. Fluorescence levels decreased during the stationary phase which may be due to lack of oxygen, which is required for protein maturation. The inclusion of His, FLAG and Lumio™ tags at the N-terminus of the proteins provide the possibility of additional approaches to be employed to assess protein localisation, such as immunofluorescence and substrate (Lumio™) mediated fluorescence. The pneumococcal transcriptional reporter pAHS12 was constructed and can be successfully used to characterise gene expression *in vitro*, which was exemplified by testing the *nanA* promoter. Although transcriptional fluorescent reporters may not be as sensitive as other

techniques, such as Q-PCR, it can be a valuable tool for preliminary tests and to track gene expression during growth *in vitro*.

The predicted cytoplasmic toxin of *S. pneumoniae*, Ply, was found to be detected in the extracellular environment prior to entry into the stationary phase in certain strains, when the intracellular pool of Ply is first detected (Benton *et al.*, 1997b). This may suggest that these strains of *S. pneumoniae* which can 'secrete' Ply have additional genes in their genome to provide this phenotype. However Ply is detected in the cell wall in all strains tested to date (Price & Camilli, 2009), which contradicts the hypothesis that Ply 'secretory' strains have additional genes in their genomes to control Ply secretion from the cell. Therefore the hypothesis that particular genes may contribute to the secretion, cell wall localisation and/or release of Ply was tested by constructing the mutant TIGR4 $\Delta$ LytA-Ply. This mutant has a LytA-Ply fusion gene, which is naturally present in equine pneumococcal strains, inserted in the genome which results in the deletion of the intervening sequence and loss of Ply and LytA expression. Fractionation and immunofluorescence studies of this mutant complemented with labelled Ply suggest that the quantity of Ply present on the cell surface may be controlled by a product encoded between Ply (SP\_1923) and LytA (SP\_1937). However, none of these genes are required for Ply secretion across the cytoplasmic membrane, cell wall localisation or even cell wall release as these processes were not affected in TIGR4 $\Delta$ LytA-Ply. Secretion of predicted cytoplasmic proteins has been previously described in the pneumococcus (Bergmann *et al.*, 2001; Holmes *et al.*, 2001; Bergmann *et al.*, 2003; Bergmann *et al.*, 2004; Mills *et al.*, 2007). Enolase can be secreted from *B. subtilis* and its secretion does not require accessory gene products but it does depend upon a particular domain within the enolase structure (Yang *et al.*, 2011). This suggests that Ply secretion across the cytoplasmic membrane may occur via the non-classical secretion pathway and controlled by the structure of the protein. The presence of a protein domain in Ply which confers the ability to be secreted has not been investigated in this study. Ply was released from cells grown in particular culture conditions, of low cell density and incubation at low temperature (25°C). Whether these conditions are required for the expression of a gene which is required for Ply release from the cell wall or induces the function of a protein which catalyses the release of Ply remains to be

elucidated. By discovering these 'secretion' inducing conditions it suggests that all pneumococcal strains which can localise Ply to their cell wall may also have the potential to release it into the extracellular milieu. The ability to release Ply into the environment without the need for cell lysis implies that Ply can be released in a controlled manner from the cell during earlier stages of population growth. The cell wall localisation and potential for controlled release of Ply has major implications on this toxin's contribution to pneumococcal pathogenesis. Many recent publications have determined functions of Ply present at sub-lytic or physiological concentrations. Such functions include host cytoskeleton rearrangements contributing to disease pathology (Iliev *et al.*, 2007; Iliev *et al.*, 2009; Förtsch *et al.*, 2011) and activating the complement pathway. An interesting consequence of the cell wall localisation of Ply is during colonisation of the mucosal surfaces with other species such as *H. influenzae*. Lysozyme is present on the host mucosal surface which is an enzyme that degrades the peptidoglycan in bacterial cell walls. This degradation results in release of Ply from the pneumococcus (Davis *et al.*, 2011) which can induce an immune response against competing Gram negative colonising species by Ply dependent delivery of their peptidoglycan products into the epithelial cell (Ratner *et al.*, 2007).

In conclusion, Ply is secreted from the pneumococcus via a non-classical system, displayed on the cell surface and can be released into the extracellular environment. Ply secretion, localisation and release mechanisms are not controlled by genes which are encoded between Ply and LytA in the TIGR4 genome however there is evidence that the quantity of Ply displayed on the cell surface may be controlled by one or more of these genes. The gene(s) involved in the quantity control of surface-localised Ply may be characterised by assessing systematic gene complements of the mutant for the restoration of the wild-type phenotype.

## Publications

Holmes, A., Lindestam Arlehamn C. S., Wang, D., Mitchell, T. J., Evans, T. J. & Roe, A. J. (2012) Expression and Regulation of the *Escherichia coli* O157:H7 Effector Proteins NleH1 and NleH2. *PLoS One* 7(3):e33408

- Attached in Appendix

Witzenrath, M., Pache, F., Lorenz, D. Koppe, U., Gutbier, B., Tabeling, C., Reppe, K., Meixenberger, K., Dorhoi, A., Ma, J., Holmes, A., Trendelenburg, G., Heimesaat, M. M., Bereswill, S., van der Linden, M., Tschopp, J., Mitchell, T. J., Suttorp, N. & Opitz, B. (2011) The NLRP3 Inflammasome Is Differentially Activated by Pneumolysin Variants and Contributes to Host Defense in Pneumococcal Pneumonia. *J Immunol* 187, 434-440.

Holmes, A., Muhlen, S., Roe, A. J. & Dean, P. (2010) The EspF Effector, a Bacterial Pathogen's Swiss Army Knife. *Infection & Immunity* 78(11):4445.

## Conference contributions

September 2010 Society of General Microbiology Meeting, Nottingham.

- Oral Presentation 'Dissecting virulence of the pneumococcus'.
  - Holmes, A., Mitchell, A. M. & Mitchell, T. J

May 2010 American Society of General Microbiology General Meeting, San Diego.

- Poster Presentation 'Characterisation of *Escherichia coli* O157 Non-Locus of effacement Encoded (Nle) effectors NleH1-1 and NleH1-2: regulation of expression and activity in the host cell'.
  - Holmes, A., Evans, T. J., Lindestam Arlehamn, C. S., Mitchell, T.J. & Roe, A.J.

June 2009 EuroPneumo (European Meeting on the Molecular Biology of the Pneumococcus), Bern, Switzerland.

- Oral and Poster Presentation 'Enhancing the fluorescent toolbox for *Streptococcus pneumoniae*'.
  - Holmes, A., Roe, A. J. & Mitchell, T. J.

## List of References

- Aaberge, I. S., Eng, J., Lermark, G. & Lovik, M. (1995). Virulence of *Streptococcus pneumoniae* in mice: a standardized method for preparation and frozen storage of the experimental bacterial inoculum. *Microb Pathog* **18**, 141-152.
- Abdallah, A. M., Gey van Pittius, N. C., Champion, P. A., Cox, J., Luirink, J., Vandenbroucke-Grauls, C. M., Appelmelk, B. J. & Bitter, W. (2007). Type VII secretion--mycobacteria show the way. *Nat Rev Microbiol* **5**, 883-891.
- Abe, H., Tatsuno, I., Tobe, T., Okutani, A. & Sasakawa, C. (2002). Bicarbonate ion stimulates the expression of locus of enterocyte effacement-encoded genes in enterohemorrhagic *Escherichia coli* O157:H7. *Infect Immun* **70**, 3500-3509.
- Abe, H., Miyahara, A., Oshima, T., Tashiro, K., Ogura, Y., Kuhara, S., Ogasawara, N., Hayashi, T. & Tobe, T. (2008). Global regulation by horizontally transferred regulators establishes the pathogenicity of *Escherichia coli*. *DNA Res* **15**, 25-38.
- Abeyta, M., Hardy, G. G. & Yother, J. (2003). Genetic alteration of capsule type but not PspA type affects accessibility of surface-bound complement and surface antigens of *Streptococcus pneumoniae*. *Infect Immun* **71**, 218-225.
- Acebo, P., Nieto, C., Corrales, M. A., Espinosa, M. & Lopez, P. (2000). Quantitative detection of *Streptococcus pneumoniae* cells harbouring single or multiple copies of the gene encoding the green fluorescent protein. *Microbiology-Sgm* **146**, 1267-1273.
- Agarwal, S., Kulshreshtha, P., Bambah Mukku, D. & Bhatnagar, R. (2008). alpha-Enolase binds to human plasminogen on the surface of *Bacillus anthracis*. *Biochim Biophys Acta* **1784**, 986-994.
- Akira, S., Takeda, K. & Kaisho, T. (2001). Toll-like receptors: critical proteins linking innate and acquired immunity. *Nat Immunol* **2**, 675-680.
- Alcantara, R. B., Preheim, L. C. & Gentry, M. J. (1999). Role of Pneumolysin's complement-activating activity during pneumococcal bacteremia in cirrhotic rats. *Infect Immun* **67**, 2862-2866.
- Alcantara, R. B., Preheim, L. C. & Gentry-Nielsen, M. J. (2001). Pneumolysin-induced complement depletion during experimental pneumococcal bacteremia. *Infect Immun* **69**, 3569-3575.
- Alloing, G., Trombe, M. C. & Claverys, J. P. (1990). The *ami* locus of the gram-positive bacterium *Streptococcus pneumoniae* is similar to binding protein-dependent transport operons of gram-negative bacteria. *Mol Microbiol* **4**, 633-644.

Alto, N. M., Weflen, A. W., Rardin, M. J. & other authors (2007). The type III effector EspF coordinates membrane trafficking by the spatiotemporal activation of two eukaryotic signaling pathways. *J Cell Biol* **178**, 1265-1278.

Arbeloa, A., Bulgin, R. R., MacKenzie, G., Shaw, R. K., Pallen, M. J., Crepin, V. F., Berger, C. N. & Frankel, G. (2008). Subversion of actin dynamics by EspM effectors of attaching and effacing bacterial pathogens. *Cell Microbiol* **10**, 1429-1441.

Arbeloa, A., Garnett, J., Lillington, J., Bulgin, R. R., Berger, C. N., Lea, S. M., Matthews, S. & Frankel, G. (2010). EspM2 is a RhoA guanine nucleotide exchange factor. *Cell Microbiol* **12**, 654-664.

Arbeloa, A., Oates, C. V., Marches, O., Hartland, E. L. & Frankel, G. (2011). Enteropathogenic and enterohemorrhagic *Escherichia coli* type III secretion effector EspV induces radical morphological changes in eukaryotic cells. *Infect Immun* **79**, 1067-1076.

Arbibe, L., Kim, D. W., Batsche, E., Pedron, T., Mateescu, B., Muchardt, C., Parsot, C. & Sansonetti, P. J. (2007). An injected bacterial effector targets chromatin access for transcription factor NF-kappaB to alter transcription of host genes involved in immune responses. *Nat Immunol* **8**, 47-56.

Avery, O. T., Macleod, C. M. & McCarty, M. (1944). Studies on the Chemical Nature of the Substance Inducing Transformation of Pneumococcal Types : Induction of Transformation by a Desoxyribonucleic Acid Fraction Isolated from Pneumococcus Type III. *J Exp Med* **79**, 137-158.

Baba, H., Kawamura, I., Kohda, C., Nomura, T., Ito, Y., Kimoto, T., Watanabe, I., Ichiyama, S. & Mitsuyama, M. (2001). Essential role of domain 4 of pneumolysin from *Streptococcus pneumoniae* in cytolytic activity as determined by truncated proteins. *Biochem Biophys Res Commun* **281**, 37-44.

Baba, H., Kawamura, I., Kohda, C., Nomura, T., Ito, Y., Kimoto, T., Watanabe, I., Ichiyama, S. & Mitsuyama, M. (2002). Induction of gamma interferon and nitric oxide by truncated pneumolysin that lacks pore-forming activity. *Infect Immun* **70**, 107-113.

Baba, T., Ara, T., Hasegawa, M. & other authors (2006). Construction of *Escherichia coli* K-12 in-frame, single-gene knockout mutants: the Keio collection. *Mol Syst Biol* **2**, 2006 0008.

Bagnoli, F., Moschioni, M., Donati, C. & other authors (2008). A second pilus type in *Streptococcus pneumoniae* is prevalent in emerging serotypes and mediates adhesion to host cells. *J Bacteriol* **190**, 5480-5492.

Balachandran, P., Hollingshead, S. K., Paton, J. C. & Briles, D. E. (2001). The autolytic enzyme LytA of *Streptococcus pneumoniae* is not responsible for releasing pneumolysin. *J Bacteriol* **183**, 3108-3116.

Barba, J., Bustamante, V. H., Flores-Valdez, M. A., Deng, W., Finlay, B. B. & Puente, J. L. (2005). A positive regulatory loop controls expression of the locus

of enterocyte effacement-encoded regulators Ler and GrlA. *J Bacteriol* **187**, 7918-7930.

Barocchi, M. A., Ries, J., Zogaj, X. & other authors (2006). A pneumococcal pilus influences virulence and host inflammatory responses. *Proc Natl Acad Sci U S A* **103**, 2857-2862.

Bartilson, M., Marra, A., Christine, J., Asundi, J. S., Schneider, W. P. & Hromockyj, A. E. (2001). Differential fluorescence induction reveals *Streptococcus pneumoniae* loci regulated by competence stimulatory peptide. *Mol Microbiol* **39**, 126-135.

Baruch, K., Gur-Arie, L., Nadler, C. & other authors (2011). Metalloprotease type III effectors that specifically cleave JNK and NF-kappaB. *Embo J* **30**, 221-231.

Beard, S. J., Salisbury, V., Lewis, R. J., Sharpe, J. A. & MacGowan, A. P. (2002). Expression of *lux* genes in a clinical isolate of *Streptococcus pneumoniae*: using bioluminescence to monitor gemifloxacin activity. *Antimicrob Agents Chemother* **46**, 538-542.

Beghetto, E., Gargano, N., Ricci, S., Garufi, G., Peppoloni, S., Montagnani, F., Oggioni, M., Pozzi, G. & Felici, F. (2006). Discovery of novel *Streptococcus pneumoniae* antigens by screening a whole-genome lambda-display library. *FEMS Microbiol Lett* **262**, 14-21.

Beltrametti, F., Kresse, A. U. & Guzman, C. A. (1999). Transcriptional regulation of the *esp* genes of enterohemorrhagic *Escherichia coli*. *J Bacteriol* **181**, 3409-3418.

Bendtsen, J. D., Kiemer, L., Fausboll, A. & Brunak, S. (2005). Non-classical protein secretion in bacteria. *BMC Microbiol* **5**, 58.

Bensing, B. A. & Sullam, P. M. (2002). An accessory *sec* locus of *Streptococcus gordonii* is required for export of the surface protein GspB and for normal levels of binding to human platelets. *Mol Microbiol* **44**, 1081-1094.

Bensing, B. A., Siboo, I. R. & Sullam, P. M. (2007). Glycine residues in the hydrophobic core of the GspB signal sequence route export toward the accessory Sec pathway. *J Bacteriol* **189**, 3846-3854.

Bensing, B. A. & Sullam, P. M. (2010). Transport of preproteins by the accessory Sec system requires a specific domain adjacent to the signal peptide. *J Bacteriol* **192**, 4223-4232.

Benton, K. A., Everson, M. P. & Briles, D. E. (1995). A pneumolysin-negative mutant of *Streptococcus pneumoniae* causes chronic bacteremia rather than acute sepsis in mice. *Infect Immun* **63**, 448-455.

Benton, K. A., Paton, J. C. & Briles, D. E. (1997a). The hemolytic and complement-activating properties of pneumolysin do not contribute individually to virulence in a pneumococcal bacteremia model. *Microb Pathog* **23**, 201-209.

Benton, K. A., Paton, J. C. & Briles, D. E. (1997b). Differences in virulence for mice among *Streptococcus pneumoniae* strains of capsular types 2, 3, 4, 5, and 6 are not attributable to differences in pneumolysin production. *Infect Immun* **65**, 1237-1244.

Berdichevsky, T., Friedberg, D., Nadler, C., Rokney, A., Oppenheim, A. & Rosenshine, I. (2005). Ler is a negative autoregulator of the LEE1 operon in enteropathogenic *Escherichia coli*. *J Bacteriol* **187**, 349-357.

Bergmann, S., Rohde, M., Chhatwal, G. S. & Hammerschmidt, S. (2001). alpha-Enolase of *Streptococcus pneumoniae* is a plasmin(ogen)-binding protein displayed on the bacterial cell surface. *Mol Microbiol* **40**, 1273-1287.

Bergmann, S., Wild, D., Diekmann, O., Frank, R., Bracht, D., Chhatwal, G. S. & Hammerschmidt, S. (2003). Identification of a novel plasmin(ogen)-binding motif in surface displayed alpha-enolase of *Streptococcus pneumoniae*. *Mol Microbiol* **49**, 411-423.

Bergmann, S., Rohde, M. & Hammerschmidt, S. (2004). Glyceraldehyde-3-phosphate dehydrogenase of *Streptococcus pneumoniae* is a surface-displayed plasminogen-binding protein. *Infect Immun* **72**, 2416-2419.

Berry, A. M., Lock, R. A., Hansman, D. & Paton, J. C. (1989a). Contribution of autolysin to virulence of *Streptococcus pneumoniae*. *Infect Immun* **57**, 2324-2330.

Berry, A. M., Yother, J., Briles, D. E., Hansman, D. & Paton, J. C. (1989b). Reduced virulence of a defined pneumolysin-negative mutant of *Streptococcus pneumoniae*. *Infect Immun* **57**, 2037-2042.

Berry, A. M., Paton, J. C. & Hansman, D. (1992). Effect of insertional inactivation of the genes encoding pneumolysin and autolysin on the virulence of *Streptococcus pneumoniae* type 3. *Microb Pathog* **12**, 87-93.

Berry, A. M. & Paton, J. C. (1996). Sequence heterogeneity of PsaA, a 37-kilodalton putative adhesin essential for virulence of *Streptococcus pneumoniae*. *Infect Immun* **64**, 5255-5262.

Berry, A. M. & Paton, J. C. (2000). Additive attenuation of virulence of *Streptococcus pneumoniae* by mutation of the genes encoding pneumolysin and other putative pneumococcal virulence proteins. *Infect Immun* **68**, 133-140.

Beurg, M., Hafidi, A., Skinner, L., Cowan, G., Hondarrague, Y., Mitchell, T. J. & Dulon, D. (2005). The mechanism of pneumolysin-induced cochlear hair cell death in the rat. *J Physiol* **568**, 211-227.

Bhagwat, A. A., Chan, L., Han, R., Tan, J., Kothary, M., Jean-Gilles, J. & Tall, B. D. (2005). Characterization of enterohemorrhagic *Escherichia coli* strains based on acid resistance phenotypes. *Infect Immun* **73**, 4993-5003.

Biemans-Oldehinkel, E., Sal-Man, N., Deng, W., Foster, L. J. & Finlay, B. B. (2011). Quantitative Proteomic Analysis Reveals Formation of an EscL-EscQ-EscN Type III Complex in Enteropathogenic *E. coli*. *J Bacteriol*.

- Bingle, L. E., Bailey, C. M. & Pallen, M. J. (2008). Type VI secretion: a beginner's guide. *Curr Opin Microbiol* 11, 3-8.
- Blue, C. E., Paterson, G. K., Kerr, A. R., Berge, M., Claverys, J. P. & Mitchell, T. J. (2003). ZmpB, a novel virulence factor of *Streptococcus pneumoniae* that induces tumor necrosis factor alpha production in the respiratory tract. *Infect Immun* 71, 4925-4935.
- Bogaert, D., De Groot, R. & Hermans, P. W. (2004). *Streptococcus pneumoniae* colonisation: the key to pneumococcal disease. *Lancet Infect Dis* 4, 144-154.
- Borczyk, A. A., Karmali, M. A., Lior, H. & Duncan, L. M. (1987). Bovine reservoir for verotoxin-producing *Escherichia coli* O157:H7. *Lancet* 1, 98.
- Brandon, L. D., Goehring, N., Janakiraman, A., Yan, A. W., Wu, T., Beckwith, J. & Goldberg, M. B. (2003). IcsA, a polarly localized autotransporter with an atypical signal peptide, uses the Sec apparatus for secretion, although the Sec apparatus is circumferentially distributed. *Mol Microbiol* 50, 45-60.
- Braun, J. S., Novak, R., Gao, G., Murray, P. J. & Shenep, J. L. (1999). Pneumolysin, a protein toxin of *Streptococcus pneumoniae*, induces nitric oxide production from macrophages. *Infect Immun* 67, 3750-3756.
- Braun, J. S., Sublett, J. E., Freyer, D., Mitchell, T. J., Cleveland, J. L., Tuomanen, E. I. & Weber, J. R. (2002). Pneumococcal pneumolysin and H(2)O(2) mediate brain cell apoptosis during meningitis. *J Clin Invest* 109, 19-27.
- Braun, J. S., Hoffmann, O., Schickhaus, M., Freyer, D., Dagand, E., Bermpohl, D., Mitchell, T. J., Bechmann, I. & Weber, J. R. (2007). Pneumolysin causes neuronal cell death through mitochondrial damage. *Infect Immun* 75, 4245-4254.
- Briles, D. E., Hollingshead, S. K., Paton, J. C., Ades, E. W., Novak, L., van Ginkel, F. W. & Benjamin, W. H., Jr. (2003). Immunizations with pneumococcal surface protein A and pneumolysin are protective against pneumonia in a murine model of pulmonary infection with *Streptococcus pneumoniae*. *J Infect Dis* 188, 339-348.
- Burrell, M. H., Mackintosh, M. E. & Taylor, C. E. (1986). Isolation of *Streptococcus pneumoniae* from the respiratory tract of horses. *Equine Vet J* 18, 183-186.
- Bustamante, V. H., Santana, F. J., Calva, E. & Puente, J. L. (2001). Transcriptional regulation of type III secretion genes in enteropathogenic *Escherichia coli*: Ler antagonizes H-NS-dependent repression. *Mol Microbiol* 39, 664-678.
- Calix, J. J. & Nahm, M. H. (2010). A new pneumococcal serotype, 11E, has a variably inactivated wcjE gene. *J Infect Dis* 202, 29-38.

- Camara, M., Boulnois, G. J., Andrew, P. W. & Mitchell, T. J. (1994). A neuraminidase from *Streptococcus pneumoniae* has the features of a surface protein. *Infect Immun* **62**, 3688-3695.
- Campbell, R. E., Tour, O., Palmer, A. E., Steinbach, P. A., Baird, G. S., Zacharias, D. A. & Tsien, R. Y. (2002). A monomeric red fluorescent protein. *Proc Natl Acad Sci U S A* **99**, 7877-7882.
- Campellone, K. G., Giese, A., Tipper, D. J. & Leong, J. M. (2002). A tyrosine-phosphorylated 12-amino-acid sequence of enteropathogenic *Escherichia coli* Tir binds the host adaptor protein Nck and is required for Nck localization to actin pedestals. *Mol Microbiol* **43**, 1227-1241.
- Campellone, K. G., Robbins, D. & Leong, J. M. (2004). EspF(U) is a translocated EHEC effector that interacts with Tir and N-WASP and promotes nck-independent actin assembly. *Dev Cell* **7**, 217-228.
- Campo, N., Tjalsma, H., Buist, G. & other authors (2004). Subcellular sites for bacterial protein export. *Mol Microbiol* **53**, 1583-1599.
- Canvin, J. R., Marvin, A. P., Sivakumaran, M., Paton, J. C., Boulnois, G. J., Andrew, P. W. & Mitchell, T. J. (1995). The Role of Pneumolysin and Autolysin in the Pathology of Pneumonia and Septicemia in Mice Infected with a Type-2 Pneumococcus. *Journal of Infectious Diseases* **172**, 119-123.
- Cardozo, D. M., Nascimento-Carvalho, C. M., Andrade, A. L., Silvany-Neto, A. M., Daltro, C. H., Brandao, M. A., Brandao, A. P. & Brandileone, M. C. (2008). Prevalence and risk factors for nasopharyngeal carriage of *Streptococcus pneumoniae* among adolescents. *J Med Microbiol* **57**, 185-189.
- Carneiro, C. R., Postol, E., Nomizo, R., Reis, L. F. & Brentani, R. R. (2004). Identification of enolase as a laminin-binding protein on the surface of *Staphylococcus aureus*. *Microbes Infect* **6**, 604-608.
- Casadaban, M. J. & Cohen, S. N. (1980). Analysis of gene control signals by DNA fusion and cloning in *Escherichia coli*. *J Mol Biol* **138**, 179-207.
- Cascales, E. & Christie, P. J. (2003). The versatile bacterial type IV secretion systems. *Nat Rev Microbiol* **1**, 137-149.
- Chalfie, M., Tu, Y., Euskirchen, G., Ward, W. W. & Prasher, D. C. (1994). Green fluorescent protein as a marker for gene expression. *Science* **263**, 802-805.
- Chapman, P. A., Siddons, C. A. & Harkin, M. A. (1996). Sheep as a potential source of verocytotoxin-producing *Escherichia coli* O157. *Vet Rec* **138**, 23-24.
- Chapman, S., Faulkner, C., Kaiserli, E., Garcia-Mata, C., Savenkov, E. I., Roberts, A. G., Oparka, K. J. & Christie, J. M. (2008). The photoreversible fluorescent protein iLOV outperforms GFP as a reporter of plant virus infection. *Proc Natl Acad Sci U S A* **105**, 20038-20043.

- Charpentier, X. & Oswald, E. (2004). Identification of the secretion and translocation domain of the enteropathogenic and enterohemorrhagic *Escherichia coli* effector Cif, using TEM-1 beta-lactamase as a new fluorescence-based reporter. *Journal of Bacteriology* **186**, 5486-5495.
- Chen, L. F. & Greene, W. C. (2004). Shaping the nuclear action of NF-kappaB. *Nat Rev Mol Cell Biol* **5**, 392-401.
- Chen, S., Paterson, G. K., Tong, H. H., Mitchell, T. J. & DeMaria, T. F. (2005). Sortase A contributes to pneumococcal nasopharyngeal colonization in the chinchilla model. *FEMS Microbiol Lett* **253**, 151-154.
- Cho, B. K., Barrett, C. L., Knight, E. M., Park, Y. S. & Palsson, B. O. (2008). Genome-scale reconstruction of the Lrp regulatory network in *Escherichia coli*. *Proc Natl Acad Sci U S A* **105**, 19462-19467.
- Clark, L., Martinez-Argudo, I., Humphrey, T. J. & Jepson, M. A. (2009). GFP plasmid-induced defects in Salmonella invasion depend on plasmid architecture, not protein expression. *Microbiology* **155**, 461-467.
- Clarke, M. B. & Sperandio, V. (2005a). Transcriptional autoregulation by quorum sensing *Escherichia coli* regulators B and C (QseBC) in enterohaemorrhagic *E. coli* (EHEC). *Mol Microbiol* **58**, 441-455.
- Clarke, M. B. & Sperandio, V. (2005b). Transcriptional regulation of *flhDC* by QseBC and sigma (FlhA) in enterohaemorrhagic *Escherichia coli*. *Mol Microbiol* **57**, 1734-1749.
- Clarke, M. B., Hughes, D. T., Zhu, C., Boedeker, E. C. & Sperandio, V. (2006). The QseC sensor kinase: a bacterial adrenergic receptor. *Proc Natl Acad Sci U S A* **103**, 10420-10425.
- Claverys, J. P., Dintilhac, A., Pestova, E. V., Martin, B. & Morrison, D. A. (1995). Construction and evaluation of new drug-resistance cassettes for gene disruption mutagenesis in *Streptococcus pneumoniae*, using an ami test platform. *Gene* **164**, 123-128.
- Collier-Hyams, L. S., Zeng, H., Sun, J., Tomlinson, A. D., Bao, Z. Q., Chen, H., Madara, J. L., Orth, K. & Neish, A. S. (2002). Cutting edge: *Salmonella* AvrA effector inhibits the key proinflammatory, anti-apoptotic NF-kappa B pathway. *J Immunol* **169**, 2846-2850.
- Cornelis, G. R. (2006). The type III secretion injectisome. *Nat Rev Microbiol* **4**, 811-825.
- Coulthurst, S. J. & Palmer, T. (2008). A new way out: protein localization on the bacterial cell surface via Tat and a novel Type II secretion system. *Mol Microbiol* **69**, 1331-1335.
- Crepin, V. F., Prasannan, S., Shaw, R. K., Wilson, R. K., Creasey, E., Abe, C. M., Knutton, S., Frankel, G. & Matthews, S. (2005). Structural and functional studies of the enteropathogenic *Escherichia coli* type III needle complex protein EscJ. *Mol Microbiol* **55**, 1658-1670.

Creuzburg, K., Recktenwald, J., Kuhle, V., Herold, S., Hensel, M. & Schmidt, H. (2005). The Shiga toxin 1-converting bacteriophage BP-4795 encodes an NleA-like type III effector protein. *J Bacteriol* **187**, 8494-8498.

Cron, L. E., Bootsma, H. J., Noske, N., Burghout, P., Hammerschmidt, S. & Hermans, P. W. (2009). Surface-associated lipoprotein PpmA of *Streptococcus pneumoniae* is involved in colonization in a strain-specific manner. *Microbiology* **155**, 2401-2410.

Cui, J., Yao, Q., Li, S. & other authors (2010). Glutamine deamidation and dysfunction of ubiquitin/NEDD8 induced by a bacterial effector family. *Science* **329**, 1215-1218.

Dahan, S., Knutton, S., Shaw, R. K., Crepin, V. F., Dougan, G. & Frankel, G. (2004). Transcriptome of enterohemorrhagic *Escherichia coli* O157 adhering to eukaryotic plasma membranes. *Infect Immun* **72**, 5452-5459.

Dahan, S., Wiles, S., La Ragione, R. M. & other authors (2005). EspJ is a prophage-carried type III effector protein of attaching and effacing pathogens that modulates infection dynamics. *Infect Immun* **73**, 679-686.

Daniell, S. J., Delahay, R. M., Shaw, R. K., Hartland, E. L., Pallen, M. J., Booy, F., Ebel, F., Knutton, S. & Frankel, G. (2001). Coiled-coil domain of enteropathogenic *Escherichia coli* type III secreted protein EspD is involved in EspA filament-mediated cell attachment and hemolysis. *Infection and Immunity* **69**, 4055-4064.

Datsenko, K. A. & Wanner, B. L. (2000). One-step inactivation of chromosomal genes in *Escherichia coli* K-12 using PCR products. *Proc Natl Acad Sci U S A* **97**, 6640-6645.

Dave, S., Brooks-Walter, A., Pangburn, M. K. & McDaniel, L. S. (2001). PspC, a pneumococcal surface protein, binds human factor H. *Infect Immun* **69**, 3435-3437.

Davis, K. M., Nakamura, S. & Weiser, J. N. (2011). Nod2 sensing of lysozyme-digested peptidoglycan promotes macrophage recruitment and clearance of *S. pneumoniae* colonization in mice. *J Clin Invest* **121**, 3666-3676.

Dean, P. & Kenny, B. (2004). Intestinal barrier dysfunction by enteropathogenic *Escherichia coli* is mediated by two effector molecules and a bacterial surface protein. *Mol Microbiol* **54**, 665-675.

Dean, P., Maresca, M., Schuller, S., Phillips, A. D. & Kenny, B. (2006). Potent diarrheagenic mechanism mediated by the cooperative action of three enteropathogenic *Escherichia coli*-injected effector proteins. *Proc Natl Acad Sci U S A* **103**, 1876-1881.

Dean, P., Muhlen, S., Quitard, S. & Kenny, B. (2010a). The bacterial effectors EspG and EspG2 induce a destructive calpain activity that is kept in check by the co-delivered Tir effector. *Cell Microbiol* **12**, 1308-1321.

- Dean, P., Scott, J. A., Knox, A. A., Quitard, S., Watkins, N. J. & Kenny, B. (2010b). The enteropathogenic *E. coli* effector EspF targets and disrupts the nucleolus by a process regulated by mitochondrial dysfunction. *PLoS Pathog* **6**, e1000961.
- Dean, P. (2011). Functional domains and motifs of bacterial type III effector proteins and their roles in infection. *FEMS Microbiol Rev*.
- DeBord, K. L., Galanopoulos, N. S. & Schneewind, O. (2003). The *ttsA* gene is required for low-calcium-induced type III secretion of Yop proteins and virulence of *Yersinia enterocolitica* W22703. *J Bacteriol* **185**, 3499-3507.
- Deiwick, J., Nikolaus, T., Erdogan, S. & Hensel, M. (1999). Environmental regulation of *Salmonella* pathogenicity island 2 gene expression. *Mol Microbiol* **31**, 1759-1773.
- Delahay, R. M., Knutton, S., Shaw, R. K., Hartland, E. L., Pallen, M. J. & Frankel, G. (2005). The coiled-coil domain of EspA is essential for the assembly of the type III secretion translocon on the surface of enteropathogenic *Escherichia coli* (vol 274, pg 35969, 1999). *Journal of Biological Chemistry* **280**, 19436-19436.
- den Blaauwen, T. & Driessen, A. J. (1996). Sec-dependent preprotein translocation in bacteria. *Arch Microbiol* **165**, 1-8.
- Deng, W., Li, Y., Hardwidge, P. R. & other authors (2005). Regulation of type III secretion hierarchy of translocators and effectors in attaching and effacing bacterial pathogens. *Infect Immun* **73**, 2135-2146.
- Deng, W. Y., Puente, J. L., Gruenheid, S. & other authors (2004). Dissecting virulence: Systematic and functional analyses of a pathogenicity island. *Proceedings of the National Academy of Sciences of the United States of America* **101**, 3597-3602.
- Desvaux, M. & Hebraud, M. (2006). The protein secretion systems in *Listeria*: inside out bacterial virulence. *FEMS Microbiol Rev* **30**, 774-805.
- Deville, K., Gold, V. A., Robson, A., Whitehouse, S., Sessions, R. B., Baldwin, S. A., Radford, S. E. & Collinson, I. (2011). The oligomeric state and arrangement of the active bacterial translocon. *J Biol Chem* **286**, 4659-4669.
- DeVinney, R., Stein, M., Reinscheid, D., Abe, A., Ruschkowski, S. & Finlay, B. B. (1999). Enterohemorrhagic *Escherichia coli* O157:H7 produces Tir, which is translocated to the host cell membrane but is not tyrosine phosphorylated. *Infect Immun* **67**, 2389-2398.
- DeVinney, R., Puente, J. L., Gauthier, A., Goosney, D. & Finlay, B. B. (2001). Enterohaemorrhagic and enteropathogenic *Escherichia coli* use a different Tir-based mechanism for pedestal formation. *Mol Microbiol* **41**, 1445-1458.
- Dintilhac, A., Alloing, G., Granadel, C. & Claverys, J. P. (1997). Competence and virulence of *Streptococcus pneumoniae*: Adc and PsaA mutants exhibit a

requirement for Zn and Mn resulting from inactivation of putative ABC metal permeases. *Mol Microbiol* **25**, 727-739.

Dockrell, D. H., Marriott, H. M., Prince, L. R., Ridger, V. C., Ince, P. G., Hellewell, P. G. & Whyte, M. K. (2003). Alveolar macrophage apoptosis contributes to pneumococcal clearance in a resolving model of pulmonary infection. *J Immunol* **171**, 5380-5388.

Donati, C., Hiller, N. L., Tettelin, H. & other authors (2010). Structure and dynamics of the pan-genome of *Streptococcus pneumoniae* and closely related species. *Genome Biol* **11**, R107.

Dong, N., Liu, L. & Shao, F. (2010). A bacterial effector targets host DH-PH domain RhoGEFs and antagonizes macrophage phagocytosis. *Embo J* **29**, 1363-1376.

Dong, T. & Schellhorn, H. E. (2009). Global effect of RpoS on gene expression in pathogenic *Escherichia coli* O157:H7 strain EDL933. *BMC Genomics* **10**, 349.

Dorman, C. J. & Deighan, P. (2003). Regulation of gene expression by histone-like proteins in bacteria. *Curr Opin Genet Dev* **13**, 179-184.

Douce, G., Ross, K., Cowan, G., Ma, J. & Mitchell, T. J. (2010). Novel mucosal vaccines generated by genetic conjugation of heterologous proteins to pneumolysin (PLY) from *Streptococcus pneumoniae*. *Vaccine* **28**, 3231-3237.

Driessen, A. J. (1992). Precursor protein translocation by the *Escherichia coli* translocase is directed by the protonmotive force. *Embo J* **11**, 847-853.

Driessen, A. J., Fekkes, P. & van der Wolk, J. P. (1998). The Sec system. *Curr Opin Microbiol* **1**, 216-222.

Dziva, F., van Diemen, P. M., Stevens, M. P., Smith, A. J. & Wallis, T. S. (2004). Identification of *Escherichia coli* O157 : H7 genes influencing colonization of the bovine gastrointestinal tract using signature-tagged mutagenesis. *Microbiology* **150**, 3631-3645.

Ebel, F., Podzadel, T., Rohde, M., Kresse, A. U., Kramer, S., Deibel, C., Guzman, C. A. & Chakraborty, T. (1998). Initial binding of Shiga toxin-producing *Escherichia coli* to host cells and subsequent induction of actin rearrangements depend on filamentous EspA-containing surface appendages. *Mol Microbiol* **30**, 147-161.

Eberhardt, A., Wu, L. J., Errington, J., Vollmer, W. & Veening, J. W. (2009). Cellular localization of choline-utilization proteins in *Streptococcus pneumoniae* using novel fluorescent reporter systems. *Mol Microbiol* **74**, 395-408.

Echtenkamp, F., Deng, W., Wickham, M. E., Vazquez, A., Puente, J. L., Thanabalasuriar, A., Gruenheid, S., Finlay, B. B. & Hardwidge, P. R. (2008). Characterization of the NleF effector protein from attaching and effacing bacterial pathogens. *FEMS Microbiol Lett* **281**, 98-107.

- Economou, A. (1998).** Bacterial preprotein translocase: mechanism and conformational dynamics of a processive enzyme. *Mol Microbiol* **27**, 511-518.
- Economou, A. (2002).** Bacterial secretome: the assembly manual and operating instructions (Review). *Mol Membr Biol* **19**, 159-169.
- Edqvist, P. J., Olsson, J., Lavander, M., Sundberg, L., Forsberg, A., Wolf-Watz, H. & Lloyd, S. A. (2003).** YscP and YscU regulate substrate specificity of the *Yersinia* type III secretion system. *J Bacteriol* **185**, 2259-2266.
- Elliott, S. J., Sperandio, V., Giron, J. A., Shin, S., Mellies, J. L., Wainwright, L., Hutcheson, S. W., McDaniel, T. K. & Kaper, J. B. (2000).** The locus of enterocyte effacement (LEE)-encoded regulator controls expression of both LEE- and non-LEE-encoded virulence factors in enteropathogenic and enterohemorrhagic *Escherichia coli*. *Infect Immun* **68**, 6115-6126.
- Elliott, S. J., O'Connell, C. B., Koutsouris, A., Brinkley, C., Donnenberg, M. S., Hecht, G. & Kaper, J. B. (2002).** A gene from the locus of enterocyte effacement that is required for enteropathogenic *Escherichia coli* to increase tight-junction permeability encodes a chaperone for EspF. *Infect Immun* **70**, 2271-2277.
- Emmerson, J. R., Gally, D. L. & Roe, A. J. (2006).** Generation of gene deletions and gene replacements in *Escherichia coli* O157:H7 using a temperature sensitive allelic exchange system. *Biol Proced Online* **8**, 153-162.
- Endo, Y., Tsurugi, K., Yutsudo, T., Takeda, Y., Ogasawara, T. & Igarashi, K. (1988).** Site of action of a Vero toxin (VT2) from *Escherichia coli* O157:H7 and of Shiga toxin on eukaryotic ribosomes. RNA N-glycosidase activity of the toxins. *Eur J Biochem* **171**, 45-50.
- Enninga, J., Mounier, J., Sansonetti, P. & Tran Van Nhieu, G. (2005).** Secretion of type III effectors into host cells in real time. *Nat Methods* **2**, 959-965.
- Esgleas, M., Li, Y., Hancock, M. A., Harel, J., Dubreuil, J. D. & Gottschalk, M. (2008).** Isolation and characterization of alpha-enolase, a novel fibronectin-binding protein from *Streptococcus suis*. *Microbiology* **154**, 2668-2679.
- Feldman, C., Mitchell, T. J., Andrew, P. W., Boulnois, G. J., Read, R. C., Todd, H. C., Cole, P. J. & Wilson, R. (1990).** The effect of *Streptococcus pneumoniae* pneumolysin on human respiratory epithelium *in vitro*. *Microb Pathog* **9**, 275-284.
- Ferrandez, Y. & Condemine, G. (2008).** Novel mechanism of outer membrane targeting of proteins in Gram-negative bacteria. *Mol Microbiol* **69**, 1349-1357.
- Fields, S. & Song, O. (1989).** A novel genetic system to detect protein-protein interactions. *Nature* **340**, 245-246.
- Filloux, A., Hachani, A. & Bleves, S. (2008).** The bacterial type VI secretion machine: yet another player for protein transport across membranes. *Microbiology* **154**, 1570-1583.

- Finlay, B. B. & Falkow, S. (1997). Common themes in microbial pathogenicity revisited. *Microbiol Mol Biol Rev* 61, 136-169.
- Förtsch, C., Hupp, S., Ma, J., Mitchell, T. J., Maier, E., Benz, R. & Iliev, A. I. (2011). Changes in Astrocyte Shape Induced by Sublytic Concentrations of the Cholesterol-Dependent Cytolysin Pneumolysin Still Require Pore-Forming Capacity. *Toxins* 3, 43-62.
- Francez-Charlot, A., Laugel, B., Van Gemert, A., Dubarry, N., Wiorowski, F., Castanie-Cornet, M. P., Gutierrez, C. & Cam, K. (2003). RcsCDB His-Asp phosphorelay system negatively regulates the *flhDC* operon in *Escherichia coli*. *Mol Microbiol* 49, 823-832.
- Friedberg, D., Umanski, T., Fang, Y. & Rosenshine, I. (1999). Hierarchy in the expression of the locus of enterocyte effacement genes of enteropathogenic *Escherichia coli*. *Mol Microbiol* 34, 941-952.
- Frolet, C., Beniazza, M., Roux, L., Gallet, B., Noirclerc-Savoie, M., Vernet, T. & Di Guilmi, A. M. (2010). New adhesin functions of surface-exposed pneumococcal proteins. *BMC Microbiol* 10, 190.
- Galan, J. E. & Collmer, A. (1999). Type III secretion machines: bacterial devices for protein delivery into host cells. *Science* 284, 1322-1328.
- Gao, X., Wan, F., Mateo, K. & other authors (2009). Bacterial effector binding to ribosomal protein s3 subverts NF-kappaB function. *PLoS Pathog* 5, e1000708.
- Garcia-Angulo, V. A., Deng, W., Thomas, N. A., Finlay, B. B. & Puente, J. L. (2008). Regulation of expression and secretion of NleH, a new non-locus of enterocyte effacement-encoded effector in *Citrobacter rodentium*. *J Bacteriol* 190, 2388-2399.
- Garcia-Gomez, E., Espinosa, N., de la Mora, J., Dreyfus, G. & Gonzalez-Pedrajo, B. (2011). The muramidase EtgA from enteropathogenic *Escherichia coli* is required for efficient type III secretion. *Microbiology*.
- Garcia-Suarez Mdel, M., Cima-Cabal, M. D., Florez, N., Garcia, P., Cernuda-Cernuda, R., Astudillo, A., Vazquez, F., De los Toyos, J. R. & Mendez, F. J. (2004). Protection against pneumococcal pneumonia in mice by monoclonal antibodies to pneumolysin. *Infect Immun* 72, 4534-4540.
- Garcia-Suarez Mdel, M., Florez, N., Astudillo, A., Vazquez, F., Villaverde, R., Fabrizio, K., Pirofski, L. A. & Mendez, F. J. (2007). The role of pneumolysin in mediating lung damage in a lethal pneumococcal pneumonia murine model. *Respir Res* 8, 3.
- Garmendia, J., Phillips, A. D., Carlier, M. F. & other authors (2004). TccP is an enterohaemorrhagic *Escherichia coli* O157:H7 type III effector protein that couples Tir to the actin-cytoskeleton. *Cell Microbiol* 6, 1167-1183.

- Garmendia, J., Frankel, G. & Crepin, V. F. (2005). Enteropathogenic and enterohemorrhagic *Escherichia coli* infections: translocation, translocation, translocation. *Infect Immun* **73**, 2573-2585.
- Gauthier, A. & Finlay, B. B. (2003). Translocated intimin receptor and its chaperone interact with ATPase of the type III secretion apparatus of enteropathogenic *Escherichia coli*. *J Bacteriol* **185**, 6747-6755.
- Gauthier, A., Puente, J. L. & Finlay, B. B. (2003). Secretin of the enteropathogenic *Escherichia coli* type III secretion system requires components of the type III apparatus for assembly and localization. *Infect Immun* **71**, 3310-3319.
- Ge, J., Catt, D. M. & Gregory, R. L. (2004). *Streptococcus mutans* surface alpha-enolase binds salivary mucin MG2 and human plasminogen. *Infect Immun* **72**, 6748-6752.
- Giddings, K. S., Zhao, J., Sims, P. J. & Tweten, R. K. (2004). Human CD59 is a receptor for the cholesterol-dependent cytolysin intermedilysin. *Nat Struct Mol Biol* **11**, 1173-1178.
- Gilbert, R. J., Jimenez, J. L., Chen, S., Tickle, I. J., Rossjohn, J., Parker, M., Andrew, P. W. & Saibil, H. R. (1999). Two structural transitions in membrane pore formation by pneumolysin, the pore-forming toxin of *Streptococcus pneumoniae*. *Cell* **97**, 647-655.
- Gilbert, R. J. (2002). Pore-forming toxins. *Cell Mol Life Sci* **59**, 832-844.
- Gilbert, R. J. C., Rossjohn, J., Parker, M. W. & other authors (1998). Self-interaction of pneumolysin, the pore-forming protein toxin of *Streptococcus pneumoniae*. *Journal of Molecular Biology* **284**, 1223-1237.
- Gohlke, U., Pullan, L., McDevitt, C. A., Porcelli, I., de Leeuw, E., Palmer, T., Saibil, H. R. & Berks, B. C. (2005). The TatA component of the twin-arginine protein transport system forms channel complexes of variable diameter. *Proc Natl Acad Sci U S A* **102**, 10482-10486.
- Gold, V. A., Robson, A., Bao, H., Romantsov, T., Duong, F. & Collinson, I. (2010). The action of cardiolipin on the bacterial translocon. *Proc Natl Acad Sci U S A* **107**, 10044-10049.
- Goosney, D. L., DeVinney, R. & Finlay, B. B. (2001). Recruitment of cytoskeletal and signaling proteins to enteropathogenic and enterohemorrhagic *Escherichia coli* pedestals. *Infect Immun* **69**, 3315-3322.
- Gosink, K. K., Mann, E. R., Guglielmo, C., Tuomanen, E. I. & Masure, H. R. (2000). Role of novel choline binding proteins in virulence of *Streptococcus pneumoniae*. *Infect Immun* **68**, 5690-5695.
- Gould, C. M., Diella, F., Via, A. & other authors (2010). ELM: the status of the 2010 eukaryotic linear motif resource. *Nucleic Acids Res* **38**, D167-180.

Greenberg, D., Givon-Lavi, N., Broides, A., Blancovich, I., Peled, N. & Dagan, R. (2006). The contribution of smoking and exposure to tobacco smoke to *Streptococcus pneumoniae* and *Haemophilus influenzae* carriage in children and their mothers. *Clin Infect Dis* 42, 897-903.

Griffin, B. A., Adams, S. R. & Tsien, R. Y. (1998). Specific covalent labeling of recombinant protein molecules inside live cells. *Science* 281, 269-272.

Gruenheid, S., DeVinney, R., Bladt, F., Goosney, D., Gelkop, S., Gish, G. D., Pawson, T. & Finlay, B. B. (2001). Enteropathogenic *E. coli* Tir binds Nck to initiate actin pedestal formation in host cells. *Nat Cell Biol* 3, 856-859.

Gruenheid, S., Sekirov, I., Thomas, N. A. & other authors (2004). Identification and characterization of NleA, a non-LEE-encoded type III translocated virulence factor of enterohaemorrhagic *Escherichia coli* O157:H7. *Mol Microbiol* 51, 1233-1249.

Guttman, J. A., Li, Y., Wickham, M. E., Deng, W., Vogl, A. W. & Finlay, B. B. (2006). Attaching and effacing pathogen-induced tight junction disruption *in vivo*. *Cell Microbiol* 8, 634-645.

Haack, K. R., Robinson, C. L., Miller, K. J., Fowlkes, J. W. & Mellies, J. L. (2003). Interaction of Ler at the LEE5 (tir) operon of enteropathogenic *Escherichia coli*. *Infect Immun* 71, 384-392.

Hamaguchi, M., Hamada, D., Suzuki, K. N., Sakata, I. & Yanagihara, I. (2008). Molecular basis of actin reorganization promoted by binding of enterohaemorrhagic *Escherichia coli* EspB to alpha-catenin. *Febs J* 275, 6260-6267.

Hamilton, M. D., Nuara, A. A., Gammon, D. B., Buller, R. M. & Evans, D. H. (2007). Duplex strand joining reactions catalyzed by vaccinia virus DNA polymerase. *Nucleic Acids Res* 35, 143-151.

Hanks, S. K. & Hunter, T. (1995). Protein kinases 6. The eukaryotic protein kinase superfamily: kinase (catalytic) domain structure and classification. *Faseb J* 9, 576-596.

Hansen, A. M. & Kaper, J. B. (2009). Hfq affects the expression of the LEE pathogenicity island in enterohaemorrhagic *Escherichia coli*. *Mol Microbiol* 73, 446-465.

Hardwidge, P. R., Deng, W., Vallance, B. A., Rodriguez-Escudero, I., Cid, V. J., Molina, M. & Finlay, B. B. (2005). Modulation of host cytoskeleton function by the enteropathogenic *Escherichia coli* and *Citrobacter rodentium* effector protein EspG. *Infect Immun* 73, 2586-2594.

Hartlein, M., Schiessl, S., Wagner, W., Rdest, U., Kreft, J. & Goebel, W. (1983). Transport of hemolysin by *Escherichia coli*. *J Cell Biochem* 22, 87-97.

Hava, D. L. & Camilli, A. (2002). Large-scale identification of serotype 4 *Streptococcus pneumoniae* virulence factors. *Mol Microbiol* 45, 1389-1406.

- Hay, R. T. (2005). SUMO: a history of modification. *Mol Cell* **18**, 1-12.
- Hayden, M. S. & Ghosh, S. (2004). Signaling to NF-kappaB. *Genes Dev* **18**, 2195-2224.
- Heim, R., Prasher, D. C. & Tsien, R. Y. (1994). Wavelength mutations and posttranslational autoxidation of green fluorescent protein. *Proc Natl Acad Sci U S A* **91**, 12501-12504.
- Hemrajani, C., Marches, O., Wiles, S. & other authors (2008). Role of NleH, a type III secreted effector from attaching and effacing pathogens, in colonization of the bovine, ovine and murine gut. *Infect Immun*.
- Hemrajani, C., Berger, C. N., Robinson, K. S., Marches, O., Mousnier, A. & Frankel, G. (2010). NleH effectors interact with Bax inhibitor-1 to block apoptosis during enteropathogenic *Escherichia coli* infection. *Proc Natl Acad Sci U S A* **107**, 3129-3134.
- Henderson, I. R., Navarro-Garcia, F., Desvaux, M., Fernandez, R. C. & Ala'Aldeen, D. (2004). Type V protein secretion pathway: the autotransporter story. *Microbiol Mol Biol Rev* **68**, 692-744.
- Henrichsen, J. (1995). Six newly recognized types of *Streptococcus pneumoniae*. *J Clin Microbiol* **33**, 2759-2762.
- Hill, J., Andrew, P. W. & Mitchell, T. J. (1994). Amino acids in pneumolysin important for hemolytic activity identified by random mutagenesis. *Infect Immun* **62**, 757-758.
- Hiller, N. L., Janto, B., Hogg, J. S. & other authors (2007). Comparative genomic analyses of seventeen *Streptococcus pneumoniae* strains: insights into the pneumococcal supragenome. *J Bacteriol* **189**, 8186-8195.
- Hilleringmann, M., Giusti, F., Baudner, B. C., Maignani, V., Covacci, A., Rappuoli, R., Barocchi, M. A. & Ferlenghi, I. (2008). Pneumococcal pili are composed of protofilaments exposing adhesive clusters of Rrg A. *PLoS Pathog* **4**, e1000026.
- Hirst, R. A., Sikand, K. S., Rutman, A., Mitchell, T. J., Andrew, P. W. & O'Callaghan, C. (2000). Relative roles of pneumolysin and hydrogen peroxide from *Streptococcus pneumoniae* in inhibition of ependymal ciliary beat frequency. *Infect Immun* **68**, 1557-1562.
- Hirst, R. A., Gosai, B., Rutman, A., Guerin, C. J., Nicotera, P., Andrew, P. W. & O'Callaghan, C. (2008). *Streptococcus pneumoniae* deficient in pneumolysin or autolysin has reduced virulence in meningitis. *J Infect Dis* **197**, 744-751.
- Hoge, C. W., Reichler, M. R., Dominguez, E. A. & other authors (1994). An epidemic of pneumococcal disease in an overcrowded, inadequately ventilated jail. *N Engl J Med* **331**, 643-648.

- Holland, I. B., Schmitt, L. & Young, J. (2005). Type 1 protein secretion in bacteria, the ABC-transporter dependent pathway (review). *Mol Membr Biol* **22**, 29-39.
- Holmes, A., Muhlen, S., Roe, A. J. & Dean, P. (2010). The EspF effector, a bacterial pathogen's Swiss army knife. *Infect Immun* **78**, 4445-4453.
- Holmes, A. R., McNab, R., Millsap, K. W., Rohde, M., Hammerschmidt, S., Mawdsley, J. L. & Jenkinson, H. F. (2001). The pavA gene of *Streptococcus pneumoniae* encodes a fibronectin-binding protein that is essential for virulence. *Mol Microbiol* **41**, 1395-1408.
- Honda, N., Iyoda, S., Yamamoto, S., Terajima, J. & Watanabe, H. (2009). LrhA positively controls the expression of the locus of enterocyte effacement genes in enterohemorrhagic *Escherichia coli* by differential regulation of their master regulators PchA and PchB. *Mol Microbiol* **74**, 1393-1341.
- Hoskins, J., Alborn, W. E., Jr., Arnold, J. & other authors (2001). Genome of the bacterium *Streptococcus pneumoniae* strain R6. *J Bacteriol* **183**, 5709-5717.
- Hotze, E. M., Wilson-Kubalek, E. M., Rossjohn, J., Parker, M. W., Johnson, A. E. & Tweten, R. K. (2001). Arresting pore formation of a cholesterol-dependent cytolysin by disulfide trapping synchronizes the insertion of the transmembrane beta-sheet from a prepore intermediate. *J Biol Chem* **276**, 8261-8268.
- Hotze, E. M., Heuck, A. P., Czajkowsky, D. M., Shao, Z., Johnson, A. E. & Tweten, R. K. (2002). Monomer-monomer interactions drive the prepore to pore conversion of a beta-barrel-forming cholesterol-dependent cytolysin. *J Biol Chem* **277**, 11597-11605.
- Howard, L. V. & Gooder, H. (1974). Specificity of the autolysin of *Streptococcus (Diplococcus) pneumoniae*. *J Bacteriol* **117**, 796-804.
- Hu, P., Bian, Z., Fan, M., Huang, M. & Zhang, P. (2008). Sec translocase and sortase A are colocalised in a locus in the cytoplasmic membrane of *Streptococcus mutans*. *Arch Oral Biol* **53**, 150-154.
- Huang, L. H. & Syu, W. J. (2008). GrlA of enterohemorrhagic *Escherichia coli* O157:H7 activates LEE1 by binding to the promoter region. *J Microbiol Immunol Infect* **41**, 9-16.
- Iannelli, F., Chiavolini, D., Ricci, S., Oggioni, M. R. & Pozzi, G. (2004). Pneumococcal surface protein C contributes to sepsis caused by *Streptococcus pneumoniae* in mice. *Infect Immun* **72**, 3077-3080.
- Ibarra, J. A., Knodler, L. A., Sturdevant, D. E., Virtaneva, K., Carmody, A. B., Fischer, E. R., Porcella, S. F. & Steele-Mortimer, O. (2010). Induction of *Salmonella* pathogenicity island 1 under different growth conditions can affect *Salmonella*-host cell interactions *in vitro*. *Microbiology* **156**, 1120-1133.
- Ibrahim, Y. M., Kerr, A. R., McCluskey, J. & Mitchell, T. J. (2004). Control of virulence by the two-component system CiaR/H is mediated via HtrA, a major virulence factor of *Streptococcus pneumoniae*. *J Bacteriol* **186**, 5258-5266.

- Ide, T., Laarmann, S., Greune, L., Schillers, H., Oberleithner, H. & Schmidt, M. A. (2001). Characterization of translocation pores inserted into plasma membranes by type III-secreted Esp proteins of enteropathogenic *Escherichia coli*. *Cell Microbiol* **3**, 669-679.
- Ignatova, Z. & Gierasch, L. M. (2004). Monitoring protein stability and aggregation in vivo by real-time fluorescent labeling. *Proc Natl Acad Sci U S A* **101**, 523-528.
- Iliev, A. I., Djannatian, J. R., Nau, R., Mitchell, T. J. & Wouters, F. S. (2007). Cholesterol-dependent actin remodeling via RhoA and Rac1 activation by the *Streptococcus pneumoniae* toxin pneumolysin. *Proc Natl Acad Sci U S A* **104**, 2897-2902.
- Iliev, A. I., Djannatian, J. R., Opazo, F., Gerber, J., Nau, R., Mitchell, T. J. & Wouters, F. S. (2009). Rapid microtubule bundling and stabilization by the *Streptococcus pneumoniae* neurotoxin pneumolysin in a cholesterol-dependent, non-lytic and Src-kinase dependent manner inhibits intracellular trafficking. *Mol Microbiol* **71**, 461-477.
- Iyoda, S. & Watanabe, H. (2004). Positive effects of multiple *pch* genes on expression of the locus of enterocyte effacement genes and adherence of enterohaemorrhagic *Escherichia coli* O157 : H7 to HEp-2 cells. *Microbiology* **150**, 2357-2571.
- Iyoda, S. & Watanabe, H. (2005). ClpXP protease controls expression of the type III protein secretion system through regulation of RpoS and GrlR levels in enterohemorrhagic *Escherichia coli*. *J Bacteriol* **187**, 4086-4094.
- Iyoda, S., Koizumi, N., Satou, H., Lu, Y., Saitoh, T., Ohnishi, M. & Watanabe, H. (2006). The GrlR-GrlA regulatory system coordinately controls the expression of flagellar and LEE-encoded type III protein secretion systems in enterohemorrhagic *Escherichia coli*. *J Bacteriol* **188**, 5682-5692.
- Izore, T., Contreras-Martel, C., El Mortaji, L., Manzano, C., Terrasse, R., Vernet, T., Di Guilmi, A. M. & Dessen, A. (2010). Structural basis of host cell recognition by the pilus adhesin from *Streptococcus pneumoniae*. *Structure* **18**, 106-115.
- Jacobs, T., Cima-Cabal, M. D., Darji, A. & other authors (1999). The conserved undecapeptide shared by thiol-activated cytolysins is involved in membrane binding. *FEBS Lett* **459**, 463-466.
- Jakobs, S., Subramaniam, V., Schonle, A., Jovin, T. M. & Hell, S. W. (2000). EFGP and DsRed expressing cultures of *Escherichia coli* imaged by confocal, two-photon and fluorescence lifetime microscopy. *FEBS Lett* **479**, 131-135.
- Jedrzejewski, M. J. (2001). Pneumococcal virulence factors: structure and function. *Microbiol Mol Biol Rev* **65**, 187-207 ; first page, table of contents.
- Jeffery, C. J. (1999). Moonlighting proteins. *Trends Biochem Sci* **24**, 8-11.

- Jin, P., Kong, F., Xiao, M., Oftadeh, S., Zhou, F., Liu, C., Russell, F. & Gilbert, G. L. (2009). First report of putative *Streptococcus pneumoniae* serotype 6D among nasopharyngeal isolates from Fijian children. *J Infect Dis* **200**, 1375-1380.
- Jobichen, C., Li, M., Yerushalmi, G., Tan, Y. W., Mok, Y. K., Rosenshine, I., Leung, K. Y. & Sivaraman, J. (2007). Structure of GrlR and the implication of its EDED motif in mediating the regulation of type III secretion system in EHEC. *PLoS Pathog* **3**, e69.
- Johnson, M. K. (1977). Cellular Location of Pneumolysin. *Fems Microbiology Letters* **2**, 243-245.
- Johnson, M. K., Geoffroy, C. & Alouf, J. E. (1980). Binding of Cholesterol by Sulphydryl-Activated Cytolysins. *Infection and Immunity* **27**, 97-101.
- Johnson, S. E., Dykes, J. K., Jue, D. L., Sampson, J. S., Carlone, G. M. & Ades, E. W. (2002). Inhibition of pneumococcal carriage in mice by subcutaneous immunization with peptides from the common surface protein pneumococcal surface adhesin a. *J Infect Dis* **185**, 489-496.
- Jounblat, R., Kadioglu, A., Mitchell, T. J. & Andrew, P. W. (2003). Pneumococcal behavior and host responses during bronchopneumonia are affected differently by the cytolytic and complement-activating activities of pneumolysin. *Infect Immun* **71**, 1813-1819.
- Jubelin, G., Taieb, F., Duda, D. M. & other authors (2010). Pathogenic bacteria target NEDD8-conjugated cullins to hijack host-cell signaling pathways. *PLoS Pathog* **6**.
- Kadioglu, A., Sharpe, J. A., Lazou, I., Svanborg, C., Ockleford, C., Mitchell, T. J. & Andrew, P. W. (2001). Use of green fluorescent protein in visualisation of pneumococcal invasion of broncho-epithelial cells in vivo. *Fems Microbiology Letters* **194**, 105-110.
- Kaper, J. B., Nataro, J. P. & Mobley, H. L. (2004). Pathogenic *Escherichia coli*. *Nat Rev Microbiol* **2**, 123-140.
- Karmali, M. A., Petric, M., Lim, C., Fleming, P. C. & Steele, B. T. (1983). *Escherichia coli* cytotoxin, haemolytic-uraemic syndrome, and haemorrhagic colitis. *Lancet* **2**, 1299-1300.
- Kedrov, A., Kusters, I., Krasnikov, V. V. & Driessen, A. J. (2011). A single copy of SecYEG is sufficient for preprotein translocation. *Embo J*.
- Keenan, K. P., Sharpnack, D. D., Collins, H., Formal, S. B. & O'Brien, A. D. (1986). Morphologic evaluation of the effects of Shiga toxin and *E coli* Shiga-like toxin on the rabbit intestine. *Am J Pathol* **125**, 69-80.
- Keenan, R. J., Freymann, D. M., Stroud, R. M. & Walter, P. (2001). The signal recognition particle. *Annu Rev Biochem* **70**, 755-775.

- Kelly, M., Hart, E., Mundy, R. & other authors (2006). Essential role of the type III secretion system effector NleB in colonization of mice by *Citrobacter rodentium*. *Infect Immun* **74**, 2328-2337.
- Kendall, M. M., Rasko, D. A. & Sperandio, V. (2010). The LysR-type regulator QseA regulates both characterized and putative virulence genes in enterohaemorrhagic *Escherichia coli* O157:H7. *Mol Microbiol* **76**, 1306-1321.
- Kenny, B., DeVinney, R., Stein, M., Reinscheid, D. J., Frey, E. A. & Finlay, B. B. (1997). Enteropathogenic *E. coli* (EPEC) transfers its receptor for intimate adherence into mammalian cells. *Cell* **91**, 511-520.
- Kenny, B. (1999). Phosphorylation of tyrosine 474 of the enteropathogenic *Escherichia coli* (EPEC) Tir receptor molecule is essential for actin nucleating activity and is preceded by additional host modifications. *Mol Microbiol* **31**, 1229-1241.
- Kenny, B. & Jepson, M. (2000). Targeting of an enteropathogenic *Escherichia coli* (EPEC) effector protein to host mitochondria. *Cell Microbiol* **2**, 579-590.
- Kenny, B. (2001). The enterohaemorrhagic *Escherichia coli* (serotype O157:H7) Tir molecule is not functionally interchangeable for its enteropathogenic *E. coli* (serotype O127:H6) homologue. *Cell Microbiol* **3**, 499-510.
- Kenny, B., Ellis, S., Leard, A. D., Warawa, J., Mellor, H. & Jepson, M. A. (2002). Co-ordinate regulation of distinct host cell signalling pathways by multifunctional enteropathogenic *Escherichia coli* effector molecules. *Mol Microbiol* **44**, 1095-1107.
- Kerr, A. R., Paterson, G. K., McCluskey, J., Iannelli, F., Oggioni, M. R., Pozzi, G. & Mitchell, T. J. (2006). The contribution of PspC to pneumococcal virulence varies between strains and is accomplished by both complement evasion and complement-independent mechanisms. *Infect Immun* **74**, 5319-5324.
- Kim, D. W., Lenzen, G., Page, A. L., Legrain, P., Sansonetti, P. J. & Parsot, C. (2005). The *Shigella flexneri* effector OspG interferes with innate immune responses by targeting ubiquitin-conjugating enzymes. *Proceedings of the National Academy of Sciences of the United States of America* **102**, 14046-14051.
- Kim, J., Thanabalasuriar, A., Chaworth-Musters, T. & other authors (2007). The bacterial virulence factor NleA inhibits cellular protein secretion by disrupting mammalian COPII function. *Cell Host Microbe* **2**, 160-171.
- Kirkham, L. A., Jefferies, J. M., Kerr, A. R., Jing, Y., Clarke, S. C., Smith, A. & Mitchell, T. J. (2006). Identification of invasive serotype 1 pneumococcal isolates that express nonhemolytic pneumolysin. *J Clin Microbiol* **44**, 151-159.
- Kline, K. A., Kau, A. L., Chen, S. L. & other authors (2009). Mechanism for sortase localization and the role of sortase localization in efficient pilus assembly in *Enterococcus faecalis*. *J Bacteriol* **191**, 3237-3247.

Knoblauch, N. T., Rudiger, S., Schonfeld, H. J., Driessen, A. J., Schneider-Mergener, J. & Bukau, B. (1999). Substrate specificity of the SecB chaperone. *J Biol Chem* 274, 34219-34225.

Knodler, L. A., Bestor, A., Ma, C., Hansen-Wester, I., Hensel, M., Vallance, B. A. & Steele-Mortimer, O. (2005). Cloning vectors and fluorescent proteins can significantly inhibit *Salmonella enterica* virulence in both epithelial cells and macrophages: implications for bacterial pathogenesis studies. *Infect Immun* 73, 7027-7031.

Knowles, T. J., Scott-Tucker, A., Overduin, M. & Henderson, I. R. (2009). Membrane protein architects: the role of the BAM complex in outer membrane protein assembly. *Nat Rev Microbiol* 7, 206-214.

Knutton, S., Lloyd, D. R. & McNeish, A. S. (1987). Adhesion of enteropathogenic *Escherichia coli* to human intestinal enterocytes and cultured human intestinal mucosa. *Infect Immun* 55, 69-77.

Knutton, S., Baldwin, T., Williams, P. H. & McNeish, A. S. (1989). Actin accumulation at sites of bacterial adhesion to tissue culture cells: basis of a new diagnostic test for enteropathogenic and enterohemorrhagic *Escherichia coli*. *Infect Immun* 57, 1290-1298.

Knutton, S., Rosenshine, I., Pallen, M. J., Nisan, I., Neves, B. C., Bain, C., Wolff, C., Dougan, G. & Frankel, G. (1998). A novel EspA-associated surface organelle of enteropathogenic *Escherichia coli* involved in protein translocation into epithelial cells. *Embo J* 17, 2166-2176.

Kodama, T., Akeda, Y., Kono, G., Takahashi, A., Imura, K., Iida, T. & Honda, T. (2002). The EspB protein of enterohaemorrhagic *Escherichia coli* interacts directly with alpha-catenin. *Cell Microbiol* 4, 213-222.

Kostyukova, N. N., Volkova, M. O., Ivanova, V. V. & Kvetnaya, A. S. (1995). A study of pathogenic factors of *Streptococcus pneumoniae* strains causing meningitis. *FEMS Immunol Med Microbiol* 10, 133-137.

Kresse, A. U., Rohde, M. & Guzman, C. A. (1999). The EspD protein of enterohemorrhagic *Escherichia coli* is required for the formation of bacterial surface appendages and is incorporated in the cytoplasmic membranes of target cells. *Infect Immun* 67, 4834-4842.

Kurushima, J., Nagai, T., Nagamatsu, K. & Abe, A. (2010). EspJ effector in enterohemorrhagic *E. coli* translocates into host mitochondria via an atypical mitochondrial targeting signal. *Microbiol Immunol* 54, 371-379.

Laaberki, M. H., Janabi, N., Oswald, E. & Repoila, F. (2006). Concert of regulators to switch on LEE expression in enterohemorrhagic *Escherichia coli* O157:H7: interplay between Ler, GrlA, HNS and RpoS. *Int J Med Microbiol* 296, 197-210.

Lacks, S. & Neuberger, M. (1975). Membrane location of a deoxyribonuclease implicated in the genetic transformation of *Diplococcus pneumoniae*. *J Bacteriol* 124, 1321-1329.

- Lange, R. & Hengge-Aronis, R. (1991). Identification of a central regulator of stationary-phase gene expression in *Escherichia coli*. *Mol Microbiol* **5**, 49-59.
- Langhorst, M. F., Genisyuerek, S. & Stuermer, C. A. (2006). Accumulation of FLAsH/Lumio Green in active mitochondria can be reversed by beta-mercaptoethanol for specific staining of tetracysteine-tagged proteins. *Histochem Cell Biol* **125**, 743-747.
- Lanie, J. A., Ng, W. L., Kazmierczak, K. M., Andrzejewski, T. M., Davidsen, T. M., Wayne, K. J., Tettelin, H., Glass, J. I. & Winkler, M. E. (2007). Genome sequence of Avery's virulent serotype 2 strain D39 of *Streptococcus pneumoniae* and comparison with that of unencapsulated laboratory strain R6. *J Bacteriol* **189**, 38-51.
- Lau, G. W., Haataja, S., Lonetto, M., Kensit, S. E., Marra, A., Bryant, A. P., McDevitt, D., Morrison, D. A. & Holden, D. W. (2001). A functional genomic analysis of type 3 *Streptococcus pneumoniae* virulence. *Mol Microbiol* **40**, 555-571.
- Le Negrate, G., Faustin, B., Welsh, K. & other authors (2008). *Salmonella* secreted factor L deubiquitinase of *Salmonella typhimurium* inhibits NF-kappaB, suppresses I kappa B alpha ubiquitination and modulates innate immune responses. *J Immunol* **180**, 5045-5056.
- Lee, S. F., Kelly, M., McAlister, A., Luck, S. N., Garcia, E. L., Hall, R. A., Robins-Browne, R. M., Frankel, G. & Hartland, E. L. (2008). A C-terminal class I PDZ binding motif of EspI/NleA modulates the virulence of attaching and effacing *Escherichia coli* and *Citrobacter rodentium*. *Cell Microbiol* **10**, 499-513.
- Lee, V. T. & Schneewind, O. (2001). Protein secretion and the pathogenesis of bacterial infections. *Genes Dev* **15**, 1725-1752.
- Legarda, D., Klein-Patel, M. E., Yim, S., Yuk, M. H. & Diamond, G. (2005). Suppression of NF-kappaB-mediated beta-defensin gene expression in the mammalian airway by the *Bordetella* type III secretion system. *Cell Microbiol* **7**, 489-497.
- Lehnen, D., Blumer, C., Polen, T., Wackwitz, B., Wendisch, V. F. & Uden, G. (2002). LrhA as a new transcriptional key regulator of flagella, motility and chemotaxis genes in *Escherichia coli*. *Mol Microbiol* **45**, 521-532.
- LeMessurier, K. S., Ogunniyi, A. D. & Paton, J. C. (2006). Differential expression of key pneumococcal virulence genes in vivo. *Microbiology* **152**, 305-311.
- LeMieux, J., Hava, D. L., Basset, A. & Camilli, A. (2006). RrgA and RrgB are components of a multisubunit pilus encoded by the *Streptococcus pneumoniae* rlrA pathogenicity islet. *Infect Immun* **74**, 2453-2456.
- Li, M., Rosenshine, I., Yu, H. B., Nadler, C., Mills, E., Hew, C. L. & Leung, K. Y. (2006). Identification and characterization of NleI, a new non-LEE-encoded

effector of enteropathogenic *Escherichia coli* (EPEC). *Microbes Infect* **8**, 2890-2898.

Lill, R., Dowhan, W. & Wickner, W. (1990). The ATPase activity of SecA is regulated by acidic phospholipids, SecY, and the leader and mature domains of precursor proteins. *Cell* **60**, 271-280.

Link, A. J., Phillips, D. & Church, G. M. (1997). Methods for generating precise deletions and insertions in the genome of wild-type *Escherichia coli*: application to open reading frame characterization. *J Bacteriol* **179**, 6228-6237.

Littmann, M., Albiger, B., Frentzen, A., Normark, S., Henriques-Normark, B. & Plant, L. (2009). *Streptococcus pneumoniae* evades human dendritic cell surveillance by pneumolysin expression. *EMBO Mol Med* **1**, 211-222.

Livet, J., Weissman, T. A., Kang, H., Draft, R. W., Lu, J., Bennis, R. A., Sanes, J. R. & Lichtman, J. W. (2007). Transgenic strategies for combinatorial expression of fluorescent proteins in the nervous system. *Nature* **450**, 56-62.

Lock, R. A., Hansman, D. & Paton, J. C. (1992). Comparative Efficacy of Autolysin and Pneumolysin as Immunogens Protecting Mice against Infection by *Streptococcus pneumoniae*. *Microbial Pathogenesis* **12**, 137-143.

Lock, R. A., Zhang, Q. Y., Berry, A. M. & Paton, J. C. (1996). Sequence variation in the *Streptococcus pneumoniae* pneumolysin gene affecting haemolytic activity and electrophoretic mobility of the toxin. *Microbial Pathogenesis* **21**, 71-83.

Low, J. C., McKendrick, I. J., McKechnie, C., Fenlon, D., Naylor, S. W., Currie, C., Smith, D. G., Allison, L. & Gally, D. L. (2005). Rectal carriage of enterohemorrhagic *Escherichia coli* O157 in slaughtered cattle. *Appl Environ Microbiol* **71**, 93-97.

Macrina, F. L., Tobian, J. A., Jones, K. R., Evans, R. P. & Clewell, D. B. (1982). A cloning vector able to replicate in *Escherichia coli* and *Streptococcus sanguis*. *Gene* **19**, 345-353.

Madigan, M. T., Martinko, J. M. & Parker, M. (2003). *Brock Biology of Microorganisms*, 10 edn: Prentice Hall/Pearson Education, Inc.

Malley, R., Henneke, P., Morse, S. C. & other authors (2003). Recognition of pneumolysin by Toll-like receptor 4 confers resistance to pneumococcal infection. *Proc Natl Acad Sci U S A* **100**, 1966-1971.

Manco, S., Hernon, F., Yesilkaya, H., Paton, J. C., Andrew, P. W. & Kadioglu, A. (2006). Pneumococcal neuraminidases A and B both have essential roles during infection of the respiratory tract and sepsis. *Infect Immun* **74**, 4014-4020.

Manting, E. H., van Der Does, C., Remigy, H., Engel, A. & Driessen, A. J. (2000). SecYEG assembles into a tetramer to form the active protein translocation channel. *Embo J* **19**, 852-861.

- Marches, O., Ledger, T. N., Boury, M. & other authors (2003). Enteropathogenic and enterohaemorrhagic *Escherichia coli* deliver a novel effector called Cif, which blocks cell cycle G2/M transition. *Mol Microbiol* **50**, 1553-1567.
- Marches, O., Wiles, S., Dziva, F. & other authors (2005). Characterization of two non-locus of enterocyte effacement-encoded type III-translocated effectors, NleC and NleD, in attaching and effacing pathogens. *Infect Immun* **73**, 8411-8417.
- Marches, O., Batchelor, M., Shaw, R. K. & other authors (2006). EspF of enteropathogenic *Escherichia coli* binds sorting nexin 9. *J Bacteriol* **188**, 3110-3115.
- Marches, O., Covarelli, V., Dahan, S., Cougoule, C., Bhatta, P., Frankel, G. & Caron, E. (2008). EspJ of enteropathogenic and enterohaemorrhagic *Escherichia coli* inhibits opsono-phagocytosis. *Cell Microbiol* **10**, 1104-1115.
- Marra, A., Asundi, J., Bartilson, M. & other authors (2002). Differential fluorescence induction analysis of *Streptococcus pneumoniae* identifies genes involved in pathogenesis. *Infect Immun* **70**, 1422-1433.
- Marriott, H. M., Ali, F., Read, R. C., Mitchell, T. J., Whyte, M. K. & Dockrell, D. H. (2004). Nitric oxide levels regulate macrophage commitment to apoptosis or necrosis during pneumococcal infection. *Faseb J* **18**, 1126-1128.
- Martinez, E., Schroeder, G. N., Berger, C. N. & other authors (2010). Binding to Na(+)/H(+) exchanger regulatory factor 2 (NHERF2) affects trafficking and function of the enteropathogenic *Escherichia coli* type III secretion system effectors Map, EspI and NleH. *Cell Microbiol* **12**, 1718-1731.
- Matsumoto, H. & Young, G. M. (2006). Proteomic and functional analysis of the suite of Ysp proteins exported by the Ysa type III secretion system of *Yersinia enterocolitica* Biovar 1B. *Mol Microbiol* **59**, 689-706.
- Matsuyama, S., Fujita, Y. & Mizushima, S. (1993). SecD is involved in the release of translocated secretory proteins from the cytoplasmic membrane of *Escherichia coli*. *Embo J* **12**, 265-270.
- Matsuzawa, T., Kuwae, A., Yoshida, S., Sasakawa, C. & Abe, A. (2004). Enteropathogenic *Escherichia coli* activates the RhoA signaling pathway via the stimulation of GEF-H1. *Embo J* **23**, 3570-3582.
- Matsuzawa, T., Kuwae, A. & Abe, A. (2005). Enteropathogenic *Escherichia coli* type III effectors EspG and EspG2 alter epithelial paracellular permeability. *Infect Immun* **73**, 6283-6289.
- Matz, M. V., Fradkov, A. F., Labas, Y. A., Savitsky, A. P., Zaraisky, A. G., Markelov, M. L. & Lukyanov, S. A. (1999). Fluorescent proteins from nonbioluminescent Anthozoa species. *Nat Biotechnol* **17**, 969-973.

- McDaniel, T. K., Jarvis, K. G., Donnenberg, M. S. & Kaper, J. B. (1995). A genetic locus of enterocyte effacement conserved among diverse enterobacterial pathogens. *Proc Natl Acad Sci U S A* **92**, 1664-1668.
- McNamara, B. P., Koutsouris, A., O'Connell, C. B., Nougayrede, J. P., Donnenberg, M. S. & Hecht, G. (2001). Translocated EspF protein from enteropathogenic *Escherichia coli* disrupts host intestinal barrier function. *J Clin Invest* **107**, 621-629.
- Mellies, J. L., Barron, A. M. & Carmona, A. M. (2007). Enteropathogenic and enterohemorrhagic *Escherichia coli* virulence gene regulation. *Infect Immun* **75**, 4199-4210.
- Mills, M. F., Marquart, M. E. & McDaniel, L. S. (2007). Localization of PcsB of *Streptococcus pneumoniae* and its differential expression in response to stress. *J Bacteriol* **189**, 4544-4546.
- Mitchell, T. J., Walker, J. A., Saunders, F. K., Andrew, P. W. & Boulnois, G. J. (1989). Expression of the pneumolysin gene in *Escherichia coli*: rapid purification and biological properties. *Biochim Biophys Acta* **1007**, 67-72.
- Mitchell, T. J., Andrew, P. W., Saunders, F. K., Smith, A. N. & Boulnois, G. J. (1991). Complement Activation and Antibody-Binding by Pneumolysin Via a Region of the Toxin Homologous to a Human Acute-Phase Protein. *Molecular Microbiology* **5**, 1883-1888.
- Mitchell, T. J., Andrew, P. W., Boulnois, G. J., Lee, C. J., Lock, R. A. & Paton, J. C. (1992). Molecular Studies of Pneumolysin the Thiol-Activated Toxin of *Streptococcus pneumoniae* as an Aid to Vaccine Design. In *Witholt, B, Et Al*, pp. 429-438.
- Mittal, R., Peak-Chew, S. Y. & McMahon, H. T. (2006). Acetylation of MEK2 and I kappa B kinase (IKK) activation loop residues by YopJ inhibits signaling. *Proc Natl Acad Sci U S A* **103**, 18574-18579.
- Mittal, R., Peak-Chew, S. Y., Sade, R. S., Vallis, Y. & McMahon, H. T. (2010). The acetyltransferase activity of the bacterial toxin YopJ of *Yersinia* is activated by eukaryotic host cell inositol hexakisphosphate. *J Biol Chem* **285**, 19927-19934.
- Mohammed, B. J., Mitchell, T. J., Andrew, P. W., Hirst, R. A. & O'Callaghan, C. (1999). The effect of the pneumococcal toxin, pneumolysin on brain ependymal cilia. *Microb Pathog* **27**, 303-309.
- Moon, H. W., Whipp, S. C., Argenzio, R. A., Levine, M. M. & Giannella, R. A. (1983). Attaching and effacing activities of rabbit and human enteropathogenic *Escherichia coli* in pig and rabbit intestines. *Infect Immun* **41**, 1340-1351.
- Morikawa, H., Kim, M., Mimuro, H., Punginelli, C., Koyama, T., Nagai, S., Miyawaki, A., Iwai, K. & Sasakawa, C. (2010). The bacterial effector Cif interferes with SCF ubiquitin ligase function by inhibiting deneddylation of Cullin1. *Biochem Biophys Res Commun* **401**, 268-274.

Mougous, J. D., Cuff, M. E., Raunser, S. & other authors (2006). A virulence locus of *Pseudomonas aeruginosa* encodes a protein secretion apparatus. *Science* **312**, 1526-1530.

Muhlen, S., Ruchaud-Sparagano, M. H. & Kenny, B. (2011). Proteasome-independent degradation of canonical NFkappaB complex components by the NleC protein of pathogenic *Escherichia coli*. *J Biol Chem* **286**, 5100-5107.

Mukherjee, S., Keitany, G., Li, Y., Wang, Y., Ball, H. L., Goldsmith, E. J. & Orth, K. (2006). *Yersinia* YopJ acetylates and inhibits kinase activation by blocking phosphorylation. *Science* **312**, 1211-1214.

Muller, J., Walter, F., van Dijl, J. M. & Behnke, D. (1992). Suppression of the growth and export defects of an *Escherichia coli* secA(Ts) mutant by a gene cloned from *Bacillus subtilis*. *Mol Gen Genet* **235**, 89-96.

Muller, J. P., Ozegowski, J., Vettermann, S., Swaving, J., Van Wely, K. H. & Driessen, A. J. (2000). Interaction of *Bacillus subtilis* CsaA with SecA and precursor proteins. *Biochem J* **348 Pt 2**, 367-373.

Mundy, R., Petrovska, L., Smollett, K. & other authors (2004). Identification of a novel *Citrobacter rodentium* type III secreted protein, Espl, and roles of this and other secreted proteins in infection. *Infect Immun* **72**, 2288-2302.

Murphy, K. C. & Campellone, K. G. (2003). Lambda Red-mediated recombinogenic engineering of enterohemorrhagic and enteropathogenic *E. coli*. *BMC Mol Biol* **4**, 11.

Musher, D. M., Phan, H. M. & Baughn, R. E. (2001). Protection against bacteremic pneumococcal infection by antibody to pneumolysin. *J Infect Dis* **183**, 827-830.

Nadler, C., Baruch, K., Kobi, S. & other authors (2010). The type III secretion effector NleE inhibits NF-kappaB activation. *PLoS Pathog* **6**, e1000743.

Nagamune, H., Ohnishi, C., Katsuura, A., Fushitani, K., Whiley, R. A., Tsuji, A. & Matsuda, Y. (1996). Intermedilysin, a novel cytotoxin specific for human cells secreted by *Streptococcus intermedius* UNS46 isolated from a human liver abscess. *Infect Immun* **64**, 3093-3100.

Nakamura, M., Sekino, N., Iwamoto, M. & Ohno-Iwashita, Y. (1995). Interaction of theta-toxin (perfringolysin O), a cholesterol-binding cytolysin, with liposomal membranes: change in the aromatic side chains upon binding and insertion. *Biochemistry* **34**, 6513-6520.

Nakanishi, N., Abe, H., Ogura, Y., Hayashi, T., Tashiro, K., Kuhara, S., Sugimoto, N. & Tobe, T. (2006). ppGpp with DksA controls gene expression in the locus of enterocyte effacement (LEE) pathogenicity island of enterohaemorrhagic *Escherichia coli* through activation of two virulence regulatory genes. *Mol Microbiol* **61**, 194-205.

- Nakanishi, N., Tashiro, K., Kuhara, S., Hayashi, T., Sugimoto, N. & Tobe, T. (2009). Regulation of virulence by butyrate sensing in enterohaemorrhagic *Escherichia coli*. *Microbiology* **155**, 521-530.
- Naylor, S. W., Low, J. C., Besser, T. E., Mahajan, A., Gunn, G. J., Pearce, M. C., McKendrick, I. J., Smith, D. G. & Gally, D. L. (2003). Lymphoid follicle-dense mucosa at the terminal rectum is the principal site of colonization of enterohemorrhagic *Escherichia coli* O157:H7 in the bovine host. *Infect Immun* **71**, 1505-1512.
- Neef, J., Andisi, V. F., Kim, K. S., Kuipers, O. P. & Bijlsma, J. J. (2011). Deletion of a Cation Transporter Promotes Lysis in *Streptococcus pneumoniae*. *Infect Immun* **79**, 2314-2323.
- Nelson, A. L., Ries, J., Bagnoli, F. & other authors (2007). RrgA is a pilus-associated adhesin in *Streptococcus pneumoniae*. *Mol Microbiol* **66**, 329-340.
- Nevels, M., Brune, W. & Shenk, T. (2004). SUMOylation of the human cytomegalovirus 72-kilodalton IE1 protein facilitates expression of the 86-kilodalton IE2 protein and promotes viral replication. *J Virol* **78**, 7803-7812.
- Newton, H. J., Pearson, J. S., Badea, L. & other authors (2010). The type III effectors NleE and NleB from enteropathogenic *E. coli* and OspZ from *Shigella* block nuclear translocation of NF-kappaB p65. *PLoS Pathog* **6**, e1000898.
- Nguyen, L., Paulsen, I. T., Tchieu, J., Hueck, C. J. & Saier, M. H., Jr. (2000). Phylogenetic analyses of the constituents of Type III protein secretion systems. *J Mol Microbiol Biotechnol* **2**, 125-144.
- Nilles, M. L., Williams, A. W., Skrzypek, E. & Straley, S. C. (1997). *Yersinia pestis* LcrV forms a stable complex with LcrG and may have a secretion-related regulatory role in the low-Ca<sup>2+</sup> response. *J Bacteriol* **179**, 1307-1316.
- Nishiyama, K., Fukuda, A., Morita, K. & Tokuda, H. (1999). Membrane deinsertion of SecA underlying proton motive force-dependent stimulation of protein translocation. *Embo J* **18**, 1049-1058.
- Nobe, R., Nougayrede, J. P., Taieb, F., Bardiau, M., Cassart, D., Navarro-Garcia, F., Mainil, J. G., Hayashi, T. & Oswald, E. (2009). Enterohaemorrhagic *Escherichia coli* serogroup O111 inhibits NF- $\kappa$ B-dependent innate responses in a manner independent of a type III secreted OspG orthologue. *Microbiology*.
- Nougayrede, J. P., Taieb, F., De Rycke, J. & Oswald, E. (2005). Cyclomodulins: bacterial effectors that modulate the eukaryotic cell cycle. *Trends Microbiol* **13**, 103-110.
- Nunn, D. (1999). Bacterial type II protein export and pilus biogenesis: more than just homologies? *Trends Cell Biol* **9**, 402-408.
- Obert, C., Sublett, J., Kaushal, D., Hinojosa, E., Barton, T., Tuomanen, E. I. & Orihuela, C. J. (2006). Identification of a Candidate *Streptococcus pneumoniae* core genome and regions of diversity correlated with invasive pneumococcal disease. *Infect Immun* **74**, 4766-4777.

- Ogunniyi, A. D., Grabowicz, M., Briles, D. E., Cook, J. & Paton, J. C. (2007a). Development of a vaccine against invasive pneumococcal disease based on combinations of virulence proteins of *Streptococcus pneumoniae*. *Infect Immun* **75**, 350-357.
- Ogunniyi, A. D., LeMessurier, K. S., Graham, R. M., Watt, J. M., Briles, D. E., Stroehrer, U. H. & Paton, J. C. (2007b). Contributions of pneumolysin, pneumococcal surface protein A (PspA), and PspC to pathogenicity of *Streptococcus pneumoniae* D39 in a mouse model. *Infect Immun* **75**, 1843-1851.
- Ogunniyi, A. D., Grabowicz, M., Mahdi, L. K., Cook, J., Gordon, D. L., Sadlon, T. A. & Paton, J. C. (2009). Pneumococcal histidine triad proteins are regulated by the Zn<sup>2+</sup>-dependent repressor AdcR and inhibit complement deposition through the recruitment of complement factor H. *FASEB J* **23**, 731-738.
- Orihuela, C. J., Gao, G., Francis, K. P., Yu, J. & Tuomanen, E. I. (2004a). Tissue-specific contributions of pneumococcal virulence factors to pathogenesis. *J Infect Dis* **190**, 1661-1669.
- Orihuela, C. J., Radin, J. N., Sublett, J. E., Gao, G., Kaushal, D. & Tuomanen, E. I. (2004b). Microarray analysis of pneumococcal gene expression during invasive disease. *Infect Immun* **72**, 5582-5596.
- Orskov, F., Orskov, I. & Villar, J. A. (1987). Cattle as reservoir of verotoxin-producing *Escherichia coli* O157:H7. *Lancet* **2**, 276.
- Orth, K. (2002). Function of the *Yersinia* effector YopJ. *Curr Opin Microbiol* **5**, 38-43.
- Overweg, K., Kerr, A., Sluijter, M., Jackson, M. H., Mitchell, T. J., de Jong, A. P., de Groot, R. & Hermans, P. W. (2000). The putative proteinase maturation protein A of *Streptococcus pneumoniae* is a conserved surface protein with potential to elicit protective immune responses. *Infect Immun* **68**, 4180-4188.
- Palacios, S., Perez, L. H., Welsch, S., Schleich, S., Chmielarska, K., Melchior, F. & Locker, J. K. (2005). Quantitative SUMO-1 modification of a vaccinia virus protein is required for its specific localization and prevents its self-association. *Mol Biol Cell* **16**, 2822-2835.
- Pallen, M. J., Beatson, S. A. & Bailey, C. M. (2005). Bioinformatics analysis of the locus for enterocyte effacement provides novel insights into type-III secretion. *Bmc Microbiology* **5**, -.
- Palmer, M., Harris, R., Freytag, C., Kehoe, M., Trantum-Jensen, J. & Bhakdi, S. (1998). Assembly mechanism of the oligomeric streptolysin O pore: the early membrane lesion is lined by a free edge of the lipid membrane and is extended gradually during oligomerization. *Embo J* **17**, 1598-1605.
- Pancholi, V. & Fischetti, V. A. (1998). alpha-enolase, a novel strong plasmin(ogen) binding protein on the surface of pathogenic streptococci. *Journal of Biological Chemistry* **273**, 14503-14515.

Park, I. H., Pritchard, D. G., Cartee, R., Brandao, A., Brandileone, M. C. & Nahm, M. H. (2007). Discovery of a new capsular serotype (6C) within serogroup 6 of *Streptococcus pneumoniae*. *J Clin Microbiol* **45**, 1225-1233.

Parsot, C. & Mekalanos, J. J. (1992). Structural analysis of the *acfA* and *acfD* genes of *Vibrio cholerae*: effects of DNA topology and transcriptional activators on expression. *J Bacteriol* **174**, 5211-5218.

Paterson, G. K. & Mitchell, T. J. (2006). The role of *Streptococcus pneumoniae* sortase A in colonisation and pathogenesis. *Microbes Infect* **8**, 145-153.

Paton, J. C., Rowan-Kelly, B. & Ferrante, A. (1984). Activation of human complement by the pneumococcal toxin pneumolysin. *Infect Immun* **43**, 1085-1087.

Paton, J. C., Andrew, P. W., Boulnois, G. J. & Mitchell, T. J. (1993). Molecular Analysis of the Pathogenicity of *Streptococcus pneumoniae* - the Role of Pneumococcal Proteins. *Annual Review of Microbiology* **47**, 89-115.

Pearson, J. S., Riedmaier, P., Marches, O., Frankel, G. & Hartland, E. L. (2011). A type III effector protease NleC from enteropathogenic *Escherichia coli* targets NF-kappaB for degradation. *Mol Microbiol* **80**, 219-230.

Peralta-Ramirez, J., Hernandez, J. M., Manning-Cela, R., Luna-Munoz, J., Garcia-Tovar, C., Nougayrede, J. P., Oswald, E. & Navarro-Garcia, F. (2008). EspF Interacts with nucleation-promoting factors to recruit junctional proteins into pedestals for pedestal maturation and disruption of paracellular permeability. *Infect Immun* **76**, 3854-3868.

Pericone, C. D., Overweg, K., Hermans, P. W. & Weiser, J. N. (2000). Inhibitory and bactericidal effects of hydrogen peroxide production by *Streptococcus pneumoniae* on other inhabitants of the upper respiratory tract. *Infect Immun* **68**, 3990-3997.

Perna, N. T., Plunkett, G., 3rd, Burland, V. & other authors (2001). Genome sequence of enterohaemorrhagic *Escherichia coli* O157:H7. *Nature* **409**, 529-533.

Peterson, C. N., Carabetta, V. J., Chowdhury, T. & Silhavy, T. J. (2006). LrhA regulates *rpoS* translation in response to the Rcs phosphorelay system in *Escherichia coli*. *J Bacteriol* **188**, 3175-3181.

Philpott, D. J., Yamaoka, S., Israel, A. & Sansonetti, P. J. (2000). Invasive *Shigella flexneri* activates NF-kappa B through a lipopolysaccharide-dependent innate intracellular response and leads to IL-8 expression in epithelial cells. *J Immunol* **165**, 903-914.

Piscatelli, H., Kotkar, S. A., McBee, M. E., Muthupalani, S., Schauer, D. B., Mandrell, R. E., Leong, J. M. & Zhou, D. (2011). The EHEC type III effector NleL is an E3 ubiquitin ligase that modulates pedestal formation. *PLoS One* **6**, e19331.

- Polekhina, G., Giddings, K. S., Tweten, R. K. & Parker, M. W. (2004). Crystallization and preliminary X-ray analysis of the human-specific toxin intermedilysin. *Acta Crystallogr D Biol Crystallogr* **60**, 347-349.
- Polissi, A., Pontiggia, A., Feger, G., Altieri, M., Mottl, H., Ferrari, L. & Simon, D. (1998). Large-scale identification of virulence genes from *Streptococcus pneumoniae*. *Infect Immun* **66**, 5620-5629.
- Polotsky, Y. E., Dragunskaya, E. M., Seliverstova, V. G. & other authors (1977). Pathogenic effect of enterotoxigenic *Escherichia coli* and *Escherichia coli* causing infantile diarrhoea. *Acta Microbiol Acad Sci Hung* **24**, 221-236.
- Porter, M. E., Mitchell, P., Free, A., Smith, D. G. & Gally, D. L. (2005). The LEE1 promoters from both enteropathogenic and enterohemorrhagic *Escherichia coli* can be activated by PerC-like proteins from either organism. *J Bacteriol* **187**, 458-472.
- Poulsen, K., Reinholdt, J. & Kilian, M. (1996). Characterization of the *Streptococcus pneumoniae* immunoglobulin A1 protease gene (iga) and its translation product. *Infect Immun* **64**, 3957-3966.
- Pradel, N., Ye, C., Livrelli, V., Xu, J., Joly, B. & Wu, L. F. (2003). Contribution of the twin arginine translocation system to the virulence of enterohemorrhagic *Escherichia coli* O157:H7. *Infect Immun* **71**, 4908-4916.
- Prasher, D. C., Eckenrode, V. K., Ward, W. W., Prendergast, F. G. & Cormier, M. J. (1992). Primary structure of the *Aequorea victoria* green-fluorescent protein. *Gene* **111**, 229-233.
- Price, K. E. & Camilli, A. (2009). Pneumolysin localizes to the cell wall of *Streptococcus pneumoniae*. *J Bacteriol* **191**, 2163-2168.
- Quin, L. R., Moore, Q. C., 3rd & McDaniel, L. S. (2007a). Pneumolysin, PspA, and PspC contribute to pneumococcal evasion of early innate immune responses during bacteremia in mice. *Infect Immun* **75**, 2067-2070.
- Quin, L. R., Onwubiko, C., Moore, Q. C., Mills, M. F., McDaniel, L. S. & Carmicle, S. (2007b). Factor H binding to PspC of *Streptococcus pneumoniae* increases adherence to human cell lines in vitro and enhances invasion of mouse lungs in vivo. *Infect Immun* **75**, 4082-4087.
- Quitard, S., Dean, P., Maresca, M. & Kenny, B. (2006). The enteropathogenic *Escherichia coli* EspF effector molecule inhibits PI-3 kinase-mediated uptake independently of mitochondrial targeting. *Cell Microbiol* **8**, 972-981.
- Rajagopala, S. V., Titz, B., Goll, J. & other authors (2007). The protein network of bacterial motility. *Mol Syst Biol* **3**, 128.
- Rambow-Larsen, A. A. & Weiss, A. A. (2004). Temporal expression of pertussis toxin and Ptl secretion proteins by *Bordetella pertussis*. *J Bacteriol* **186**, 43-50.

- Rangasamy, D., Woytek, K., Khan, S. A. & Wilson, V. G. (2000). SUMO-1 modification of bovine papillomavirus E1 protein is required for intranuclear accumulation. *J Biol Chem* **275**, 37999-38004.
- Ratner, A. J., Aguilar, J. L., Shchepetov, M., Lysenko, E. S. & Weiser, J. N. (2007). Nod1 mediates cytoplasmic sensing of combinations of extracellular bacteria. *Cell Microbiol* **9**, 1343-1351.
- Rayner, C. F., Jackson, A. D., Rutman, A., Dewar, A., Mitchell, T. J., Andrew, P. W., Cole, P. J. & Wilson, R. (1995). Interaction of pneumolysin-sufficient and -deficient isogenic variants of *Streptococcus pneumoniae* with human respiratory mucosa. *Infect Immun* **63**, 442-447.
- Reading, N. C., Torres, A. G., Kendall, M. M., Hughes, D. T., Yamamoto, K. & Sperandio, V. (2007). A novel two-component signaling system that activates transcription of an enterohemorrhagic *Escherichia coli* effector involved in remodeling of host actin. *J Bacteriol* **189**, 2468-2476.
- Reading, N. C., Rasko, D. A., Torres, A. G. & Sperandio, V. (2009). The two-component system QseEF and the membrane protein QseG link adrenergic and stress sensing to bacterial pathogenesis. *Proc Natl Acad Sci U S A* **106**, 5889-5894.
- Reading, N. C., Rasko, D., Torres, A. G. & Sperandio, V. (2010). A transcriptome study of the QseEF two-component system and the QseG membrane protein in enterohaemorrhagic *Escherichia coli* O157 : H7. *Microbiology* **156**, 1167-1175.
- Reid, S. D., Herbelin, C. J., Bumbaugh, A. C., Selander, R. K. & Whittam, T. S. (2000). Parallel evolution of virulence in pathogenic *Escherichia coli*. *Nature* **406**, 64-67.
- Richards, L., Ferreira, D. M., Miyaji, E. N., Andrew, P. W. & Kadioglu, A. (2010). The immunising effect of pneumococcal nasopharyngeal colonisation; protection against future colonisation and fatal invasive disease. *Immunobiology* **215**, 251-263.
- Rigel, N. W. & Braunstein, M. (2008). A new twist on an old pathway - accessory secretion systems. *Mol Microbiol* **69**, 291-302.
- Ritchie, J. M. & Waldor, M. K. (2005). The locus of enterocyte effacement-encoded effector proteins all promote enterohemorrhagic *Escherichia coli* pathogenicity in infant rabbits. *Infect Immun* **73**, 1466-1474.
- Roche, A., Heath, P. T., Sharland, M., Strachan, D., Breathnach, A., Haigh, J. & Young, Y. (2007). Prevalence of nasopharyngeal carriage of pneumococcus in preschool children attending day care in London. *Arch Dis Child* **92**, 1073-1076.
- Roe, A. J., Yull, H., Naylor, S. W., Woodward, M. J., Smith, D. G. & Gally, D. L. (2003). Heterogeneous surface expression of EspA translocon filaments by *Escherichia coli* O157:H7 is controlled at the posttranscriptional level. *Infect Immun* **71**, 5900-5909.

- Roe, A. J., Naylor, S. W., Spears, K. J. & other authors (2004). Co-ordinate single-cell expression of LEE4- and LEE5-encoded proteins of *Escherichia coli* O157:H7. *Mol Microbiol* **54**, 337-352.
- Roe, A. J., Tysall, L., Dransfield, T. & other authors (2007). Analysis of the expression, regulation and export of NleA-E in *Escherichia coli* O157 : H7. *Microbiology* **153**, 1350-1360.
- Rohde, H., Qin, J., Cui, Y. & other authors (2011). Open-source genomic analysis of Shiga-toxin-producing *E. coli* O104:H4. *N Engl J Med* **365**, 718-724.
- Rosch, J. & Caparon, M. (2004). A Microdomain for protein secretion in Gram-positive bacteria. *Science* **304**, 1513-1515.
- Rosch, J. W. & Caparon, M. G. (2005). The ExPortal: an organelle dedicated to the biogenesis of secreted proteins in *Streptococcus pyogenes*. *Mol Microbiol* **58**, 959-968.
- Rose, L., Shivshankar, P., Hinojosa, E., Rodriguez, A., Sanchez, C. J. & Orihuela, C. J. (2008). Antibodies against PsrP, a novel *Streptococcus pneumoniae* adhesin, block adhesion and protect mice against pneumococcal challenge. *J Infect Dis* **198**, 375-383.
- Rosenow, C., Ryan, P., Weiser, J. N., Johnson, S., Fontan, P., Ortqvist, A. & Masure, H. R. (1997). Contribution of novel choline-binding proteins to adherence, colonization and immunogenicity of *Streptococcus pneumoniae*. *Mol Microbiol* **25**, 819-829.
- Rossjohn, J., Feil, S. C., McKinstry, W. J., Tweten, R. K. & Parker, M. W. (1997). Structure of a cholesterol-binding, thiol-activated cytolysin and a model of its membrane form. *Cell* **89**, 685-692.
- Rothbaum, R., McAdams, A. J., Giannella, R. & Partin, J. C. (1982). A clinicopathologic study of enterocyte-adherent *Escherichia coli*: a cause of protracted diarrhea in infants. *Gastroenterology* **83**, 441-454.
- Royan, S. V., Jones, R. M., Koutsouris, A. & other authors (2010). Enteropathogenic *E. coli* non-LEE encoded effectors NleH1 and NleH2 attenuate NF-kappaB activation. *Mol Microbiol* **78**, 1232-1245.
- Rubins, J. B., Duane, P. G., Charboneau, D. & Janoff, E. N. (1992). Toxicity of pneumolysin to pulmonary endothelial cells *in vitro*. *Infect Immun* **60**, 1740-1746.
- Rubins, J. B., Duane, P. G., Clawson, D., Charboneau, D., Young, J. & Niewoehner, D. E. (1993). Toxicity of pneumolysin to pulmonary alveolar epithelial cells. *Infect Immun* **61**, 1352-1358.
- Rubins, J. B., Charboneau, D., Paton, J. C., Mitchell, T. J., Andrew, P. W. & Janoff, E. N. (1995). Dual function of pneumolysin in the early pathogenesis of murine pneumococcal pneumonia. *J Clin Invest* **95**, 142-150.

- Rubins, J. B., Charboneau, D., Fasching, C., Berry, A. M., Paton, J. C., Alexander, J. E., Andrew, P. W., Mitchell, T. J. & Janoff, E. N. (1996). Distinct roles for pneumolysin's cytotoxic and complement activities in the pathogenesis of pneumococcal pneumonia. *Am J Respir Crit Care Med* **153**, 1339-1346.
- Rubins, J. B., Paddock, A. H., Charboneau, D., Berry, A. M., Paton, J. C. & Janoff, E. N. (1998). Pneumolysin in pneumococcal adherence and colonization. *Microb Pathog* **25**, 337-342.
- Ruchaud-Sparagano, M. H., Maresca, M. & Kenny, B. (2007). Enteropathogenic *Escherichia coli* (EPEC) inactivate innate immune responses prior to compromising epithelial barrier function. *Cell Microbiol* **9**, 1909-1921.
- Russell, R. M., Sharp, F. C., Rasko, D. A. & Sperandio, V. (2007). QseA and GrlR/GrlA regulation of the locus of enterocyte effacement genes in enterohemorrhagic *Escherichia coli*. *J Bacteriol* **189**, 5387-5392.
- Saier, M. H., Jr. (2006). Protein secretion and membrane insertion systems in gram-negative bacteria. *J Membr Biol* **214**, 75-90.
- Saitoh, T., Iyoda, S., Yamamoto, S., Lu, Y., Shimuta, K., Ohnishi, M., Terajima, J. & Watanabe, H. (2008). Transcription of the *ehx* enterohemolysin gene is positively regulated by GrlA, a global regulator encoded within the locus of enterocyte effacement in enterohemorrhagic *Escherichia coli*. *J Bacteriol* **190**, 4822-4830.
- Sakaue-Sawano, A., Kurokawa, H., Morimura, T. & other authors (2008). Visualizing spatiotemporal dynamics of multicellular cell-cycle progression. *Cell* **132**, 487-498.
- Salomon, M., Christie, J. M., Knieb, E., Lempert, U. & Briggs, W. R. (2000). Photochemical and mutational analysis of the FMN-binding domains of the plant blue light receptor, phototropin. *Biochemistry* **39**, 9401-9410.
- Samba-Louaka, A., Nougayrede, J. P., Watrin, C., Jubelin, G., Oswald, E. & Taieb, F. (2008). Bacterial cyclomodulin Cif blocks the host cell cycle by stabilizing the cyclin-dependent kinase inhibitors p21 and p27. *Cell Microbiol* **10**, 2496-2508.
- Samba-Louaka, A., Nougayrede, J. P., Watrin, C., Oswald, E. & Taieb, F. (2009). The enteropathogenic *Escherichia coli* effector Cif induces delayed apoptosis in epithelial cells. *Infect Immun* **77**, 5471-5477.
- Sanchez, C. J., Shivshankar, P., Stol, K., Trakhtenbroit, S., Sullam, P. M., Sauer, K., Hermans, P. W. & Orihuela, C. J. (2010). The pneumococcal serine-rich repeat protein is an intra-species bacterial adhesin that promotes bacterial aggregation in vivo and in biofilms. *PLoS Pathog* **6**, e1001044.
- Sargent, F., Bogsch, E. G., Stanley, N. R., Wexler, M., Robinson, C., Berks, B. C. & Palmer, T. (1998). Overlapping functions of components of a bacterial Sec-independent protein export pathway. *Embo J* **17**, 3640-3650.

- Scanlon, K. L., Diven, W. F. & Glew, R. H. (1989). Purification and properties of *Streptococcus pneumoniae* neuraminidase. *Enzyme* 41, 143-150.
- Schaumburg, J., Diekmann, O., Hagendorff, P., Bergmann, S., Rohde, M., Hammerschmidt, S., Jansch, L., Wehland, J. & Karst, U. (2004). The cell wall subproteome of *Listeria monocytogenes*. *Proteomics* 4, 2991-3006.
- Schlecht, U., Demougin, P., Koch, R., Hermida, L., Wiederkehr, C., Descombes, P., Pineau, C., Jegou, B. & Primig, M. (2004). Expression profiling of mammalian male meiosis and gametogenesis identifies novel candidate genes for roles in the regulation of fertility. *Mol Biol Cell* 15, 1031-1043.
- Schwidder, M., Hensel, M. & Schmidt, H. (2011). Regulation of nleA in Shiga toxin-producing *Escherichia coli* O84:H4 strain 4795/97. *J Bacteriol* 193, 832-841.
- Sciara, M. I., Spagnuolo, C., Jares-Erijman, E. & Garcia Vescovi, E. (2008). Cytolocalization of the PhoP response regulator in *Salmonella enterica*: modulation by extracellular Mg<sup>2+</sup> and by the SCV environment. *Mol Microbiol* 70, 479-493.
- Scotland, S. M., Smith, H. R. & Rowe, B. (1985). Two distinct toxins active on Vero cells from *Escherichia coli* O157. *Lancet* 2, 885-886.
- Scotti, P. A., Urbanus, M. L., Brunner, J., de Gier, J. W., von Heijne, G., van der Does, C., Driessen, A. J., Oudega, B. & Luirink, J. (2000). YidC, the *Escherichia coli* homologue of mitochondrial Oxa1p, is a component of the Sec translocase. *Embo J* 19, 542-549.
- Shakhnovich, E. A., King, S. J. & Weiser, J. N. (2002). Neuraminidase expressed by *Streptococcus pneumoniae* desialylates the lipopolysaccharide of *Neisseria meningitidis* and *Haemophilus influenzae*: a paradigm for interbacterial competition among pathogens of the human respiratory tract. *Infect Immun* 70, 7161-7164.
- Shakhnovich, E. A., Davis, B. M. & Waldor, M. K. (2009). Hfq negatively regulates type III secretion in EHEC and several other pathogens. *Mol Microbiol* 74, 347-363.
- Sham, H. P., Shames, S. R., Croxen, M. A. & other authors (2011). The attaching/effacing bacterial effector NleC suppresses epithelial inflammatory responses by inhibiting NF- $\kappa$ B and p38-MAP Kinase activation. *Infect Immun*.
- Shames, S. R., Deng, W., Guttman, J. A. & other authors (2010). The pathogenic *E. coli* type III effector EspZ interacts with host CD98 and facilitates host cell pro-survival signalling. *Cell Microbiol* 12, 1322-1339.
- Shames, S. R., Bhavsar, A. P., Croxen, M. A. & other authors (2011). The pathogenic *Escherichia coli* type III secreted protease NleC degrades the host acetyltransferase p300. *Cell Microbiol*.

Shaner, N. C., Campbell, R. E., Steinbach, P. A., Giepmans, B. N., Palmer, A. E. & Tsien, R. Y. (2004). Improved monomeric red, orange and yellow fluorescent proteins derived from *Discosoma* sp. red fluorescent protein. *Nat Biotechnol* **22**, 1567-1572.

Shaner, N. C., Patterson, G. H. & Davidson, M. W. (2007). Advances in fluorescent protein technology. *J Cell Sci* **120**, 4247-4260.

Sharma, V. K. & Zuerner, R. L. (2004). Role of *hha* and *ler* in transcriptional regulation of the *esp* operon of enterohemorrhagic *Escherichia coli* O157:H7. *J Bacteriol* **186**, 7290-7301.

Sharp, F. C. & Sperandio, V. (2007). QseA directly activates transcription of *LEE1* in enterohemorrhagic *Escherichia coli*. *Infect Immun* **75**, 2432-2440.

Shaw, R. K., Smollett, K., Cleary, J., Garmendia, J., Straatman-Iwanowska, A., Frankel, G. & Knutton, S. (2005). Enteropathogenic *Escherichia coli* type III effectors EspG and EspG2 disrupt the microtubule network of intestinal epithelial cells. *Infect Immun* **73**, 4385-4390.

Shepard, L. A., Shatursky, O., Johnson, A. E. & Tweten, R. K. (2000). The mechanism of pore assembly for a cholesterol-dependent cytolysin: formation of a large prepore complex precedes the insertion of the transmembrane beta-hairpins. *Biochemistry* **39**, 10284-10293.

Shiomi, D., Yoshimoto, M., Homma, M. & Kawagishi, I. (2006). Helical distribution of the bacterial chemoreceptor via colocalization with the Sec protein translocation machinery. *Mol Microbiol* **60**, 894-906.

Shivshankar, P., Sanchez, C., Rose, L. F. & Orihuela, C. J. (2009). The *Streptococcus pneumoniae* adhesin PsrP binds to Keratin 10 on lung cells. *Mol Microbiol* **73**, 663-679.

Simovitch, M., Sason, H., Cohen, S., Zahavi, E. E., Melamed-Book, N., Weiss, A., Aroeti, B. & Rosenshine, I. (2010). EspM inhibits pedestal formation by enterohaemorrhagic *Escherichia coli* and enteropathogenic *E. coli* and disrupts the architecture of a polarized epithelial monolayer. *Cell Microbiol* **12**, 489-505.

Soltani, C. E., Hotze, E. M., Johnson, A. E. & Tweten, R. K. (2007). Specific protein-membrane contacts are required for prepore and pore assembly by a cholesterol-dependent cytolysin. *J Biol Chem* **282**, 15709-15716.

Song, M., Kim, H. J., Kim, E. Y. & other authors (2004). ppGpp-dependent stationary phase induction of genes on *Salmonella* pathogenicity island 1. *J Biol Chem* **279**, 34183-34190.

Spengler, M. L., Kurapatwinski, K., Black, A. R. & Azizkhan-Clifford, J. (2002). SUMO-1 modification of human cytomegalovirus IE1/IE72. *J Virol* **76**, 2990-2996.

Sperandio, V., Mellies, J. L., Nguyen, W., Shin, S. & Kaper, J. B. (1999). Quorum sensing controls expression of the type III secretion gene transcription

and protein secretion in enterohemorrhagic and enteropathogenic *Escherichia coli*. *Proc Natl Acad Sci U S A* **96**, 15196-15201.

Sperandio, V., Torres, A. G., Giron, J. A. & Kaper, J. B. (2001). Quorum sensing is a global regulatory mechanism in enterohemorrhagic *Escherichia coli* O157:H7. *J Bacteriol* **183**, 5187-5197.

Sperandio, V., Li, C. C. & Kaper, J. B. (2002a). Quorum-sensing *Escherichia coli* regulator A: a regulator of the LysR family involved in the regulation of the locus of enterocyte effacement pathogenicity island in enterohemorrhagic *E. coli*. *Infect Immun* **70**, 3085-3093.

Sperandio, V., Torres, A. G. & Kaper, J. B. (2002b). Quorum sensing *Escherichia coli* regulators B and C (QseBC): a novel two-component regulatory system involved in the regulation of flagella and motility by quorum sensing in *E. coli*. *Mol Microbiol* **43**, 809-821.

Srivastava, A., Henneke, P., Visintin, A. & other authors (2005). The apoptotic response to pneumolysin is Toll-like receptor 4 dependent and protects against pneumococcal disease. *Infect Immun* **73**, 6479-6487.

Steinfurt, C., Wilson, R., Mitchell, T. & other authors (1989). Effect of *Streptococcus pneumoniae* on human respiratory epithelium *in vitro*. *Infect Immun* **57**, 2006-2013.

Stellberger, T., Hauser, R., Baiker, A., Pothineni, V. R., Haas, J. & Uetz, P. (2010). Improving the yeast two-hybrid system with permuted fusions proteins: the Varicella Zoster Virus interactome. *Proteome Sci* **8**, 8.

Stroffekova, K., Proenza, C. & Beam, K. G. (2001). The protein-labeling reagent FLASH-EDT2 binds not only to CCXXCC motifs but also non-specifically to endogenous cysteine-rich proteins. *Pflugers Arch* **442**, 859-866.

Su, M. S., Kao, H. C., Lin, C. N. & Syu, W. J. (2008). Gene *l0017* encodes a second chaperone for EspA of enterohaemorrhagic *Escherichia coli* O157 : H7. *Microbiology* **154**, 1094-1103.

Sung, C. K., Li, H., Claverys, J. P. & Morrison, D. A. (2001). An *rpsL* cassette, janus, for gene replacement through negative selection in *Streptococcus pneumoniae*. *Appl Environ Microbiol* **67**, 5190-5196.

Swartz, T. E., Corchnoy, S. B., Christie, J. M., Lewis, J. W., Szundi, I., Briggs, W. R. & Bogomolni, R. A. (2001). The photocycle of a flavin-binding domain of the blue light photoreceptor phototropin. *J Biol Chem* **276**, 36493-36500.

Taieb, F., Nougayrede, J. P., Watrin, C., Samba-Louaka, A. & Oswald, E. (2006). *Escherichia coli* cyclomodulin Cif induces G2 arrest of the host cell cycle without activation of the DNA-damage checkpoint-signalling pathway. *Cell Microbiol* **8**, 1910-1921.

Tatsuno, I., Nagano, K., Taguchi, K., Rong, L., Mori, H. & Sasakawa, C. (2003). Increased adherence to Caco-2 cells caused by disruption of the *yhiE* and

*yhiF* genes in enterohemorrhagic *Escherichia coli* O157:H7. *Infect Immun* **71**, 2598-2606.

Taylor, K. A., Luther, P. W. & Donnenberg, M. S. (1999). Expression of the EspB protein of enteropathogenic *Escherichia coli* within HeLa cells affects stress fibers and cellular morphology. *Infect Immun* **67**, 120-125.

Tettelin, H., Nelson, K. E., Paulsen, I. T. & other authors (2001). Complete genome sequence of a virulent isolate of *Streptococcus pneumoniae*. *Science* **293**, 498-506.

Thanabalasuriar, A., Koutsouris, A., Weflen, A., Mimee, M., Hecht, G. & Gruenheid, S. (2010). The bacterial virulence factor NleA is required for the disruption of intestinal tight junctions by enteropathogenic *Escherichia coli*. *Cell Microbiol* **12**, 31-41.

Thomas, N. A., Deng, W., Puente, J. L., Frey, E. A., Yip, C. K., Strynadka, N. C. & Finlay, B. B. (2005). CesT is a multi-effector chaperone and recruitment factor required for the efficient type III secretion of both LEE- and non-LEE-encoded effectors of enteropathogenic *Escherichia coli*. *Mol Microbiol* **57**, 1762-1779.

Thomas, N. A., Deng, W., Baker, N., Puente, J. & Finlay, B. B. (2007). Hierarchical delivery of an essential host colonization factor in enteropathogenic *Escherichia coli*. *J Biol Chem* **282**, 29634-29645.

Tilley, S. J., Orlova, E. V., Gilbert, R. J., Andrew, P. W. & Saibil, H. R. (2005). Structural basis of pore formation by the bacterial toxin pneumolysin. *Cell* **121**, 247-256.

Tjalsma, H., Bolhuis, A., Jongbloed, J. D., Bron, S. & van Dijl, J. M. (2000). Signal peptide-dependent protein transport in *Bacillus subtilis*: a genome-based survey of the secretome. *Microbiol Mol Biol Rev* **64**, 515-547.

Tjalsma, H., Antelmann, H., Jongbloed, J. D. & other authors (2004). Proteomics of protein secretion by *Bacillus subtilis*: separating the "secrets" of the secretome. *Microbiol Mol Biol Rev* **68**, 207-233.

Tobe, T., Ando, H., Ishikawa, H., Abe, H., Tashiro, K., Hayashi, T., Kuhara, S. & Sugimoto, N. (2005). Dual regulatory pathways integrating the RcsC-RcsD-RcsB signalling system control enterohaemorrhagic *Escherichia coli* pathogenicity. *Mol Microbiol* **58**, 320-333.

Tobe, T., Beatson, S. A., Taniguchi, H. & other authors (2006). An extensive repertoire of type III secretion effectors in *Escherichia coli* O157 and the role of lambdoid phages in their dissemination. *Proceedings of the National Academy of Sciences of the United States of America* **103**, 14941-14946.

Tomson, F. L., Viswanathan, V. K., Kanack, K. J., Kanteti, R. P., Straub, K. V., Menet, M., Kaper, J. B. & Hecht, G. (2005). Enteropathogenic *Escherichia coli* EspG disrupts microtubules and in conjunction with Orf3 enhances perturbation of the tight junction barrier. *Mol Microbiol* **56**, 447-464.

- Torruellas, J., Jackson, M. W., Pennock, J. W. & Plano, G. V. (2005). The *Yersinia pestis* type III secretion needle plays a role in the regulation of Yop secretion. *Mol Microbiol* **57**, 1719-1733.
- Tree, J. J., Wolfson, E. B., Wang, D., Roe, A. J. & Gally, D. L. (2009). Controlling injection: regulation of type III secretion in enterohaemorrhagic *Escherichia coli*. *Trends Microbiol* **17**, 361-370.
- Tree, J. J., Roe, A. J., Flockhart, A. & other authors (2011). Transcriptional regulators of the GAD acid stress island are carried by effector protein-encoding prophages and indirectly control type III secretion in enterohemorrhagic *Escherichia coli* O157:H7. *Mol Microbiol* **80**, 1349-1365.
- Tsai, N. P., Wu, Y. C., Chen, J. W., Wu, C. F., Tzeng, C. M. & Syu, W. J. (2006). Multiple functions of *l0036* in the regulation of the pathogenicity island of enterohaemorrhagic *Escherichia coli* O157:H7. *Biochem J* **393**, 591-599.
- Tsien, R. Y. (1998). The green fluorescent protein. *Annu Rev Biochem* **67**, 509-544.
- Tu, X., Nisan, I., Yona, C., Hanski, E. & Rosenshine, I. (2003). EspH, a new cytoskeleton-modulating effector of enterohaemorrhagic and enteropathogenic *Escherichia coli*. *Mol Microbiol* **47**, 595-606.
- Turner, L., Ryu, W. S. & Berg, H. C. (2000). Real-time imaging of fluorescent flagellar filaments. *J Bacteriol* **182**, 2793-2801.
- Tzipori, S., Karch, H., Wachsmuth, K. I., Robins-Browne, R. M., O'Brien, A. D., Lior, H., Cohen, M. L., Smithers, J. & Levine, M. M. (1987). Role of a 60-megadalton plasmid and Shiga-like toxins in the pathogenesis of infection caused by enterohemorrhagic *Escherichia coli* O157:H7 in gnotobiotic piglets. *Infect Immun* **55**, 3117-3125.
- Uetz, P., Giot, L., Cagney, G. & other authors (2000). A comprehensive analysis of protein-protein interactions in *Saccharomyces cerevisiae*. *Nature* **403**, 623-627.
- Umanski, T., Rosenshine, I. & Friedberg, D. (2002). Thermoregulated expression of virulence genes in enteropathogenic *Escherichia coli*. *Microbiology* **148**, 2735-2744.
- Unlu, M., Morgan, M. E. & Minden, J. S. (1997). Difference gel electrophoresis: a single gel method for detecting changes in protein extracts. *Electrophoresis* **18**, 2071-2077.
- van Diemen, P. M., Dziva, F., Stevens, M. P. & Wallis, T. S. (2005). Identification of enterohemorrhagic *Escherichia coli* O26:H- genes required for intestinal colonization in calves. *Infect Immun* **73**, 1735-1743.
- van Rossum, A. M., Lysenko, E. S. & Weiser, J. N. (2005). Host and bacterial factors contributing to the clearance of colonization by *Streptococcus pneumoniae* in a murine model. *Infect Immun* **73**, 7718-7726.

- van Wely, K. H. M., Swaving, J., Freudl, R. & Driessen, A. J. M. (2001). Translocation of proteins across the cell envelope of Gram-positive bacteria. *Fems Microbiology Reviews* **25**, 437-454.
- Vijayakumar, M. N. & Morrison, D. A. (1986). Localization of competence-induced proteins in *Streptococcus pneumoniae*. *J Bacteriol* **165**, 689-695.
- Vingadassalom, D., Kazlauskas, A., Skehan, B., Cheng, H. C., Magoun, L., Robbins, D., Rosen, M. K., Saksela, K. & Leong, J. M. (2009). Insulin receptor tyrosine kinase substrate links the *E. coli* O157:H7 actin assembly effectors Tir and EspF(U) during pedestal formation. *Proc Natl Acad Sci U S A* **106**, 6754-6759.
- Viswanathan, V. K., Koutsouris, A., Lukic, S., Pilkinton, M., Simonovic, I., Simonovic, M. & Hecht, G. (2004). Comparative analysis of EspF from enteropathogenic and enterohemorrhagic *Escherichia coli* in alteration of epithelial barrier function. *Infect Immun* **72**, 3218-3227.
- Vlisidou, I., Dziva, F., La Ragione, R. M. & other authors (2006a). Role of intimin-tir interactions and the tir-cytoskeleton coupling protein in the colonization of calves and lambs by *Escherichia coli* O157:H7. *Infect Immun* **74**, 758-764.
- Vlisidou, I., Marches, O., Dziva, F., Mundy, R., Frankel, G. & Stevens, M. P. (2006b). Identification and characterization of EspK, a type III secreted effector protein of enterohaemorrhagic *Escherichia coli* O157:H7. *FEMS Microbiol Lett* **263**, 32-40.
- Vossenkamper, A., Marches, O., Fairclough, P. D. & other authors (2010). Inhibition of NF-kappaB signaling in human dendritic cells by the enteropathogenic *Escherichia coli* effector protein NleE. *J Immunol* **185**, 4118-4127.
- Walker, J. A., Allen, R. L., Falmagne, P., Johnson, M. K. & Boulnois, G. J. (1987). Molecular cloning, characterization, and complete nucleotide sequence of the gene for pneumolysin, the sulfhydryl-activated toxin of *Streptococcus pneumoniae*. *Infect Immun* **55**, 1184-1189.
- Walter, L., Marynen, P., Szpirer, J., Levan, G. & Gunther, E. (1995). Identification of a novel conserved human gene, TEGT. *Genomics* **28**, 301-304.
- Wan, F., Anderson, D. E., Barnitz, R. A. & other authors (2007). Ribosomal protein S3: a KH domain subunit in NF-kappaB complexes that mediates selective gene regulation. *Cell* **131**, 927-939.
- Wan, F., Weaver, A., Gao, X., Bern, M., Hardwidge, P. R. & Lenardo, M. J. (2011). IKKbeta phosphorylation regulates RPS3 nuclear translocation and NF-kappaB function during infection with *Escherichia coli* strain O157:H7. *Nat Immunol* **12**, 335-343.
- Wang, L., Jackson, W. C., Steinbach, P. A. & Tsien, R. Y. (2004). Evolution of new nonantibody proteins via iterative somatic hypermutation. *Proc Natl Acad Sci U S A* **101**, 16745-16749.

- Wani, J. H., Gilbert, J. V., Plaut, A. G. & Weiser, J. N. (1996). Identification, cloning, and sequencing of the immunoglobulin A1 protease gene of *Streptococcus pneumoniae*. *Infect Immun* **64**, 3967-3974.
- Weiser, J. N., Bae, D., Fasching, C., Scamurra, R. W., Ratner, A. J. & Janoff, E. N. (2003). Antibody-enhanced pneumococcal adherence requires IgA1 protease. *Proc Natl Acad Sci U S A* **100**, 4215-4220.
- Weiss, S. M., Ladwein, M., Schmidt, D. & other authors (2009). IRSp53 links the enterohemorrhagic *E. coli* effectors Tir and EspFU for actin pedestal formation. *Cell Host Microbe* **5**, 244-258.
- Wellmer, A., Zysk, G., Gerber, J., Kunst, T., Von Mering, M., Bunkowski, S., Eiffert, H. & Nau, R. (2002). Decreased virulence of a pneumolysin-deficient strain of *Streptococcus pneumoniae* in murine meningitis. *Infect Immun* **70**, 6504-6508.
- Whatmore, A. M., King, S. J., Doherty, N. C., Sturgeon, D., Chanter, N. & Dowson, C. G. (1999). Molecular characterization of equine isolates of *Streptococcus pneumoniae*: natural disruption of genes encoding the virulence factors pneumolysin and autolysin. *Infect Immun* **67**, 2776-2782.
- Wickham, M. E., Lupp, C., Vazquez, A. & other authors (2007). *Citrobacter rodentium* virulence in mice associates with bacterial load and the type III effector NleE. *Microbes Infect* **9**, 400-407.
- Wilkinson, K. A., Nishimune, A. & Henley, J. M. (2008). Analysis of SUMO-1 modification of neuronal proteins containing consensus SUMOylation motifs. *Neurosci Lett* **436**, 239-244.
- Wilson, R. K., Shaw, R. K., Daniell, S., Knutton, S. & Frankel, G. (2001). Role of EscF, a putative needle complex protein, in the type III protein translocation system of enteropathogenic *Escherichia coli*. *Cell Microbiol* **3**, 753-762.
- Wilson, V. G. & Rangasamy, D. (2001). Intracellular targeting of proteins by sumoylation. *Exp Cell Res* **271**, 57-65.
- Winston, J. T., Strack, P., Beer-Romero, P., Chu, C. Y., Elledge, S. J. & Harper, J. W. (1999). The SCFbeta-TRCP-ubiquitin ligase complex associates specifically with phosphorylated destruction motifs in I $\kappa$ B $\alpha$  and beta-catenin and stimulates I $\kappa$ B $\alpha$  ubiquitination *in vitro*. *Genes Dev* **13**, 270-283.
- Wu, B., Skarina, T., Yee, A. & other authors (2010). NleG Type 3 effectors from enterohaemorrhagic *Escherichia coli* are U-Box E3 ubiquitin ligases. *PLoS Pathog* **6**, e1000960.
- Yang, C. K., Ewis, H. E., Zhang, X., Lu, C. D., Hu, H. J., Pan, Y., Abdelal, A. T. & Tai, P. C. (2011). Non-classical protein secretion of *Bacillus subtilis* in the stationary phase is not due to cell lysis. *J Bacteriol*.

- Ye, Z., Petrof, E. O., Boone, D., Claud, E. C. & Sun, J. (2007). *Salmonella* effector AvrA regulation of colonic epithelial cell inflammation by deubiquitination. *Am J Pathol* **171**, 882-892.
- Yen, H., Ooka, T., Iguchi, A., Hayashi, T., Sugimoto, N. & Tobe, T. (2010). NleC, a type III secretion protease, compromises NF-kappaB activation by targeting p65/RelA. *PLoS Pathog* **6**, e1001231.
- Yesilkaya, H., Manco, S., Kadioglu, A., Terra, V. S. & Andrew, P. W. (2008). The ability to utilize mucin affects the regulation of virulence gene expression in *Streptococcus pneumoniae*. *FEMS Microbiology Letters* **278**, 231-235.
- Yona-Nadler, C., Umanski, T., Aizawa, S., Friedberg, D. & Rosenshine, I. (2003). Integration host factor (IHF) mediates repression of flagella in enteropathogenic and enterohaemorrhagic *Escherichia coli*. *Microbiology* **149**, 877-884.
- Younis, R., Bingle, L. E., Rollauer, S. & other authors (2010). SepL resembles an aberrant effector in binding to a class 1 type III secretion chaperone and carrying an N-terminal secretion signal. *J Bacteriol* **192**, 6093-6098.
- Yu, Y. C., Lin, C. N., Wang, S. H., Ng, S. C., Hu, W. S. & Syu, W. J. (2010). A putative lytic transglycosylase tightly regulated and critical for the EHEC type three secretion. *J Biomed Sci* **17**, 52.
- Yuk, M. H., Harvill, E. T., Cotter, P. A. & Miller, J. F. (2000). Modulation of host immune responses, induction of apoptosis and inhibition of NF-kappaB activation by the *Bordetella* type III secretion system. *Mol Microbiol* **35**, 991-1004.
- Yuste, J., Botto, M., Paton, J. C., Holden, D. W. & Brown, J. S. (2005). Additive inhibition of complement deposition by pneumolysin and PspA facilitates *Streptococcus pneumoniae* septicemia. *J Immunol* **175**, 1813-1819.
- Zhang, L., Chaudhuri, R. R., Constantinidou, C. & other authors (2004). Regulators encoded in the *Escherichia coli* type III secretion system 2 gene cluster influence expression of genes within the locus for enterocyte effacement in enterohemorrhagic *E. coli* O157:H7. *Infect Immun* **72**, 7282-7293.
- Zhou, H., Monack, D. M., Kayagaki, N., Wertz, I., Yin, J., Wolf, B. & Dixit, V. M. (2005). *Yersinia* virulence factor YopJ acts as a deubiquitinase to inhibit NF-kappa B activation. *J Exp Med* **202**, 1327-1332.
- Zhu, B., Cai, G., Hall, E. O. & Freeman, G. J. (2007). In-fusion assembly: seamless engineering of multidomain fusion proteins, modular vectors, and mutations. *Biotechniques* **43**, 354-359.
- Zurawski, D. V., Mumy, K. L., Faherty, C. S., McCormick, B. A. & Maurelli, A. T. (2009). *Shigella flexneri* type III secretion system effectors OspB and OspF target the nucleus to downregulate the host inflammatory response via interactions with retinoblastoma protein. *Mol Microbiol* **71**, 350-368.

Zysk, G., Bejo, L., Schneider-Wald, B. K., Nau, R. & Heinz, H. (2000). Induction of necrosis and apoptosis of neutrophil granulocytes by *Streptococcus pneumoniae*. *Clin Exp Immunol* 122, 61-66.

Zysk, G., Schneider-Wald, B. K., Hwang, J. H., Bejo, L., Kim, K. S., Mitchell, T. J., Hakenbeck, R. & Heinz, H. P. (2001). Pneumolysin is the main inducer of cytotoxicity to brain microvascular endothelial cells caused by *Streptococcus pneumoniae*. *Infection and Immunity* 69, 845-852.

# Appendix

# Expression and Regulation of the *Escherichia coli* O157:H7 Effector Proteins NleH1 and NleH2

Ashleigh Holmes, Cecilia S. Lindestam Arlehamn, Dai Wang, Tim J. Mitchell, Tom J. Evans, Andrew J. Roe\*

Institute of Infection, Immunity and Inflammation, College of Medical, Veterinary and Life Sciences, University of Glasgow, Glasgow, United Kingdom

## Abstract

**Background:** *E. coli* O157 carries two genes encoding the effector proteins NleH1 and NleH2 which are 87% identical. Despite the similarity between the proteins, the promoter regions upstream of the genes encoding the effectors are more divergent suggesting that the actual expression of the genes may be differentially regulated. This was tested by creating reporter fusions and examining their expression in different genetic backgrounds, media and on contact with host cells. The function of the proteins was also tested following transfection into host cells.

**Principal Findings:** Expression of both NleH1 and NleH2 was enhanced when cultured under conditions that stimulated expression of the Type Three Secretion System (T3SS) and was influenced by the regulators Ler and GrlA. Maximal expression of NleH1 required 531 bp of the upstream untranslated region but NleH2 required only 113 bp. Interestingly, contact with host cells strongly repressed expression of both NleH1 and NleH2. Following transfection, both proteins produced only minor effects on NF- $\kappa$ B activation when assessed using a NF- $\kappa$ B luciferase reporter assay, a result that is consistent with the recent report demonstrating the dependence on RPS3 for NleH1 modulation of NF- $\kappa$ B.

**Significance:** This study demonstrates the importance of considering gene regulation when studying bacterial effector proteins. Despite their sequence similarity, NleH1 and NleH2 are expressed differentially and may, therefore, be translocated at distinct times during an infection.

**Citation:** Holmes A, Lindestam Arlehamn CS, Wang D, Mitchell TJ, Evans TJ, et al. (2012) Expression and Regulation of the *Escherichia coli* O157:H7 Effector Proteins NleH1 and NleH2. PLoS ONE 7(3): e33408. doi:10.1371/journal.pone.0033408

**Editor:** Edward E. Schmidt, Montana State University, United States of America

**Received:** January 12, 2012; **Accepted:** February 13, 2012; **Published:** March 12, 2012

**Copyright:** © 2012 Holmes et al. This is an open-access article distributed under the terms of the Creative Commons Attribution License, which permits unrestricted use, distribution, and reproduction in any medium, provided the original author and source are credited.

**Funding:** AH was supported by a MRC studentship and AJR by grants (BB/G011389/1 and BB/H023518/1) from the BBSRC (Biotechnology and Biological Sciences Research Council). The funders had no role in study design, data collection and analysis, decision to publish, or preparation of the manuscript.

**Competing Interests:** The authors have read the journal's policy and have the following conflicts: AJR is a PLoS ONE editorial board member. This does not alter the authors' adherence to all PLoS ONE policies on sharing data and materials.

\* E-mail: Andrew.Roe@glasgow.ac.uk

## Introduction

Enteropathogenic *Escherichia coli* (EPEC) and enterohaemorrhagic *E. coli* (EHEC) are important causative agents of infectious diarrhoea worldwide. EPEC is the leading cause of prolonged watery diarrhoea in children living in developing countries [1]. EHEC causes sporadic outbreaks of haemorrhagic colitis and haemolytic uremic syndrome that have been widely reported in Europe, North America and Japan. EPEC and EHEC are extracellular pathogens that mediate an initial attachment via adhesins, such as their flagella [2,3], prior to a more intimate attachment. This intimate attachment is characterized as an attaching-and-effacing (A/E) lesion due to destruction of the brush-border microvilli and cytoskeletal rearrangements to form pedestals; this is dependent upon the expression of a Type Three Secretion System (T3SS).

The genes which encode the T3SS machinery, translocators, effectors, chaperones and its own regulators are within the Locus of Enterocyte Effacement (LEE) pathogenicity island (PAI). The T3SS apparatus not only translocates the 7 LEE-encoded effectors such as Tir [4], Map, and EspF but also other proteins encoded on prophage elements throughout the genome, which are termed non-LEE encoded effectors (Nle) [5,6,7,8,9].

Horizontally acquired genetic elements require appropriate regulation of expression that can be managed by both endogenous and exogenous elements. Currently, it is understood that expression of the LEE PAI is tightly regulated by an interplay of LEE-encoded, global and other horizontally-acquired regulators (reviewed in [10,11]). The LEE encodes three regulatory elements; LEE-encoded regulator (*Ler*), Global Regulator of the LEE Activator (*GlrA*) and *Grl* Repressor (*GlrR*). *Ler* is the first open reading frame of *LEE1* and belongs to the H-NS family of nucleoid-associated proteins which positively regulates transcription of both LEE and non-LEE genes [12,13]. *Ler* activates gene transcription by counteracting the effects of global regulator H-NS which silences transcription of genes by binding to curved AT-rich regions [14]. H-NS has been shown to repress the transcription of *ler* and *LEE4* [15,16]. *GlrA* and *GlrR* are encoded between *LEE1* and *LEE2*, are co-transcribed and transcription of these genes is dependent upon *Ler* [16,17]. *GlrA* can in turn positively regulate the expression of *Ler* through interacting with the *LEE1* promoter [18] forming a positive feedback loop [19]. *GlrR* directly interacts with *GlrA* and this interaction is proposed to act as a check-point to downregulate the feedback loop [18,19,20]. Additional horizontally acquired elements that regulate the LEE include

PerC (plasmid encoded regulator C) in EPEC or PerC-like homologues (Pch) in EHEC, of which there are seven present in the genome. PchABC can act globally by enhancing the transcription of *LEE1* (*ler*) and non-LEE encoded genes both dependent and independent of *Ler* [21,22,23].

Non-LEE encoded effector H (NleH) was identified as a homologue of the *Shigella flexneri* effector OspG [7], a serine-threonine protein kinase which subverts the host innate immune response [24]. NleH is conserved amongst the A/E pathogen family with *Citrobacter rodentium* encoding one allele and EPEC and EHEC encoding two alleles [7,25,26]. Despite the protein similarities of *E. coli* O157 NleH1 and NleH2 being greater than 80%, we found that their putative promoter sequences were more divergent and less well conserved, suggesting possible differences in their regulation and expression. The regulation of expression of *C. rodentium* NleH (CRODNleH) has been demonstrated to be largely post-translational, dependent upon the *Ler*/*GrlA* regulon [25]. However, as the upstream sequence of CRODNleH is only ~50% similar (see Table S1) to that of EHEC NleH1 (z0989) and NleH2 (z6021) we wished to investigate the control of NleH1 and NleH2 gene expression. We also investigated if EHEC NleH1 and NleH2 were under the regulatory control of *Ler* and/or *GrlA*.

## Results

### *In vitro* expression of *nleH1::gfp* and *nleH2::gfp* in *E. coli* O157:H7

Our previous work performed transcriptional profiling of the global changes associated with induction of the LEE, the genes that encode the *E. coli* O157:H7 T3SS. We have previously reported that MEM-HEPES media provides excellent conditions for expression of the LEE, even when compared to the widely used DMEM media. For example *escJ* and *escN*, which encode basal apparatus proteins, were both strongly induced in MEM-HEPES data. Analysis of the same transcriptomic data showed that *nleH1* showed a 6.4 fold ( $p = 0.008$ ) change in expression when cultured in MEM-HEPES when compared with DMEM (accession no. GSE6296). Therefore, *nleH1* was clearly expressed *in vitro* and subject to transcriptional regulation. We aimed to determine if *nleH1* and *nleH2* were expressed at the same time during growth in liquid media and following contact of *E. coli* O157 with host cells.

Upon assessment of the untranslated region (UTR) upstream of *nleH1* and *nleH2*, we noted that the first 100 bp were 70% identical, with this figure falling to 50% identity when extending this region to 500 bp upstream of the ATG start codon (Figure S1). To examine if these differences affected *nleH1* and *nleH2* expression and regulation, we generated a series of promoter fusions consisting of different lengths of the upstream UTR of the two genes fused to *gfp*. In each case, the complete *nleH1* or *nleH2* coding sequence was included in the fusion to create a “full-length” translational fusion. Each plasmid was transformed into *E. coli* O157:H7 and the amount of GFP produced monitored during growth in MEM-HEPES (Figure 1A) or DMEM media (Figure 1B). Highest expression of *nleH1::gfp* was achieved with the fusion containing the longest upstream UTR regions: 531 bp (pAHE8) (Figure 1). Expression of NleH2 was less dependent on promoter length, requiring only 113 bp (Figure 1A). When cultured in MEM-HEPES media, the *nleH1::gfp* and *nleH2::gfp* fusions showed markedly higher expression compared when cultured in DMEM: at an  $OD_{600} = 1.2$ , both fusions gave four-fold higher expression in MEM-HEPES compared to DMEM (Figure 1A and B). As the UTR was reduced in MEM-HEPES, *nleH1::gfp* showed a step-wise decrease in the amount of expression, with the fusion driven by the 120 bp UTR (pAHE18)

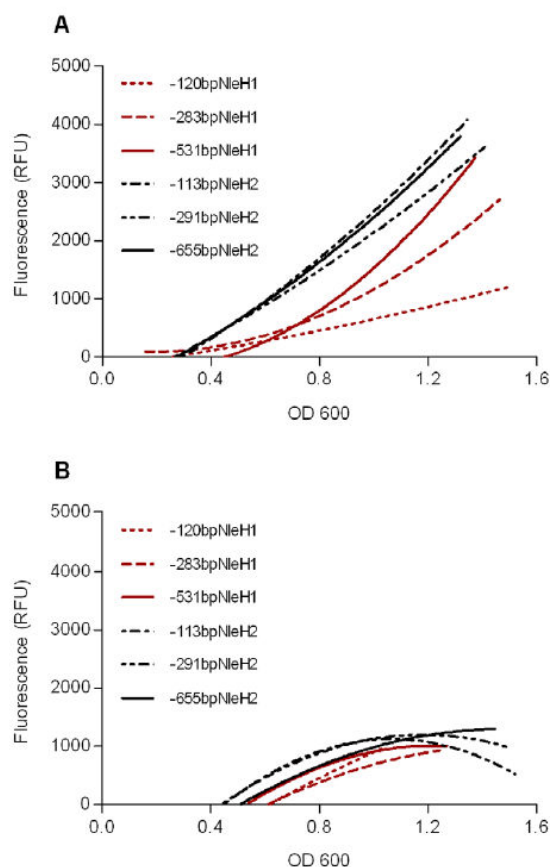


**Figure 1. Expression of NleH-GFP constructs in *E. coli* O157:H7 grown in defined media.** Constructs consisting of 120 bp (pAHE18), 283 bp (pAHE19) or 531 bp (pAHE8) of the NleH1 5' UTR and 113 bp (pAHE20), 291 bp (pAHE21) or 655 bp (pAHE22) of the NleH2 5' UTR cloned upstream of *gfp* were transformed into ZAP193, grown in MEM-HEPES (A) or DMEM (B) and GFP fluorescence measured during growth. All values were corrected for background from a promoter-less GFP (pAJR70) control measured at the same optical density. Graphs represent the average of three experimental repeats. doi:10.1371/journal.pone.0033408.g001

producing less than 25% of the GFP compared to the 531 bp UTR fusion (pAHE8; Figure 1A). In comparison, expression of *nleH2::gfp* was largely unaffected: reducing the length of the UTR to 113 bp (pAHE20) still produced 90% of the expression compared to the fusion containing the 655 bp UTR (Figure 1A). These results suggest that expression of *nleH1* is subject to stricter control through the influence of transcription factors and/or secondary DNA structure compared to *nleH2*, and that this control depends upon 120–531 bp of the 5' UTR.

### Expression in different genetic backgrounds

The data in Figure 1 showed maximal expression of *nleH1* and *nleH2* at high optical densities raising the possibility that either quorum sensing mechanisms or stationary phase sigma factors may contribute to their regulation. To test this, we transformed the *nleH1::gfp* and *nleH2::gfp* reporter plasmids, pAHE8 and pAHE22 into *E. coli* K12 and isogenic deletion strains of *spoS* and *gscC*.

Expression was tested in a number of K12 strains, including BW25113 and MC4100, but in all cases expression was negligible implying that an O157-specific regulator may be essential for their production (data not shown). We then assessed the importance of the LEE-associated regulators, Ler and GrlA for *nleH1* and *nleH2* expression. Plasmids pAHE8 and pAHE22 were transformed into *E. coli* O157:H7 strain ZAP193, an isogenic *ler* deletion strain and ZAP193 containing a mini-Tn5 cassette insertion in the *grlA* gene. Expression of *nleH1* and *nleH2* was markedly reduced by deletion of either *ler* and *grlA* (Figure 2A–B). At an OD<sub>600</sub> = 1.0, *nleH1* expression fell by 50% and 70% when *ler* or *grlA* were deleted respectively (Figure 2A). For *nleH2*, the reduction was 50% and 80% in the same backgrounds (Figure 2B). As a control, we also used a *tir::gfp* fusion, pAJR75 (Figure 2C) consisting of the *LEE5* promoter region. This fusion also showed *ler* and *grlA* dependence for full expression of *gfp* but was expressed at much greater levels than *nleH1* and *nleH2*, typically 15-fold higher.

To confirm the regulatory importance of *ler* and *grlA* on *nleH1* and *nleH2* expression, Q-PCR was used to assess levels of transcription directly. Strains were cultured in the same MEM-HEPES media as for the previous assays and cDNA prepared as described in Materials and Methods. Transcription of both *nleH1* and *nleH2* was markedly affected in the  $\Delta ler$  background, falling greater than ten-fold (Figure 3). Similarly, deletion of *grlA* reduced transcription of both *nleH1* and *nleH2*. The housekeeping gene, *gapA*, encoding glyceraldehyde-3-phosphate dehydrogenase showed only very minor changes in the different regulatory backgrounds (Figure 3). Expression of the gene encoding Tir, was found to be highly dependent on both Ler and GrlA confirming that both regulators are critical for expression of LEE-encoded effector proteins. Overall, these results confirm that *nleH* expression and transcription is dependent upon the presence of Ler and GrlA, as seen previously with the GFP reporter fusions (Figure 2A–B).

### Single cell expression

Previous work has demonstrated that several LEE-encoded and Nle effectors can be heterogeneously expressed within a population when assessed by either reporter fusions or by indirect immunofluorescent imaging. To determine if NleH1 and NleH2 expression was homo- or heterogeneous, bacteria transformed with pAHE8 and pAHE22 were examined using fluorescence microscopy and the expression of a minimum of 100 bacteria from at least three fields quantified using Velocity suite software (Perkin-Elmer). Expression of NleH1 was uniform, with the population expressing an average of 29 ( $\pm 1$ ) RFU (Figure 4A). In comparison, it was clear that NleH2 expression was more heterogeneous, with the majority of bacteria (86%) expressing an average of 49 $\pm$ 8 relative fluorescence units (RFU) but a small population (14%) expressing an average of 234 $\pm$ 55 RFU (Figure 4B). When expression was assessed in  $\Delta ler$  or  $\Delta grlA$  backgrounds, expression was lower for both NleH1 and NleH2 and the heterogeneity for NleH2 was no longer detectable. To ascertain whether NleH was expressed in co-ordination with the T3SS apparatus, the EspA filaments were immunostained as described previously [13]. The results show NleH expression is not strictly co-ordinated with the LEE as 18–20% of the population does not express EspA, but still express NleH (Figure S2A). Also, this percentage of EspA negative cells is maintained within the heterogenous population of NleH2-GFP expressing cells. As expected, EspA filaments are not detected in a *ler* negative background and are reduced in the *grlA* mutant (Figure S2B–C).

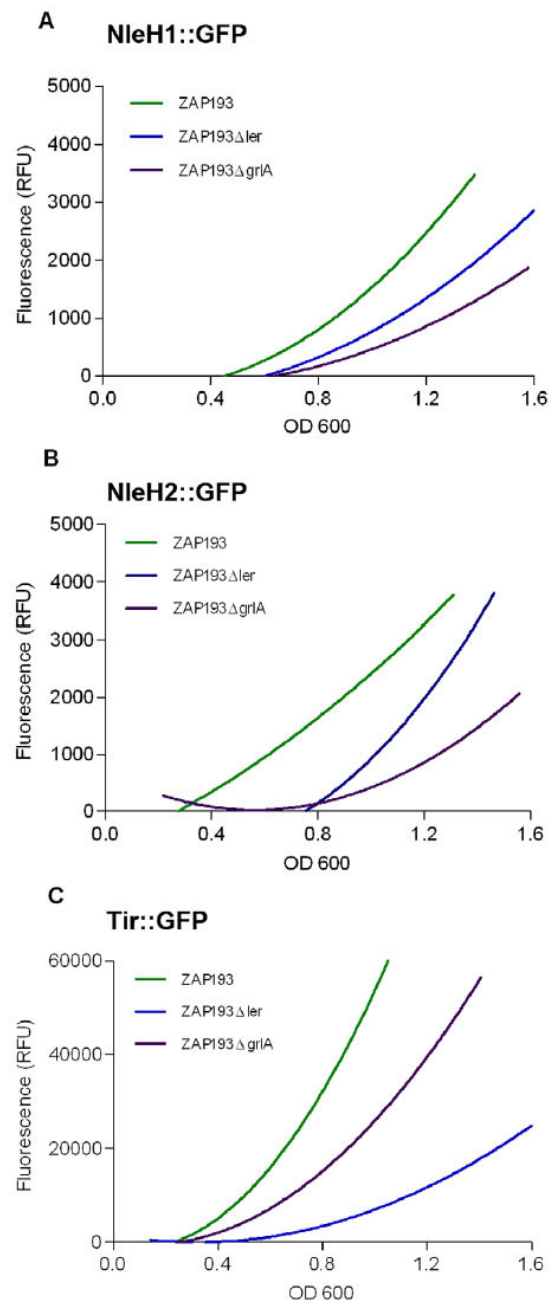


**Figure 2. Expression of NleH-GFP and Tir-GFP in *E. coli* O157:H7 defined LEE regulator mutants.** *E. coli* O157:H7 ZAP193, ZAP193 $\Delta ler$  and ZAP193 $\Delta grlA$  were transformed with constructs expressing NleH1-GFP (pAHE8; A), NleH2-GFP (pAHE22; B) and Tir-GFP (pAJR132; C). GFP expression was monitored during growth of the transformants in MEM media, with a promoterless GFP construct (pAJR70) as a background control. Fluorescence values were corrected for background and lines represent the average of three biological repeats. doi:10.1371/journal.pone.0033408.g002

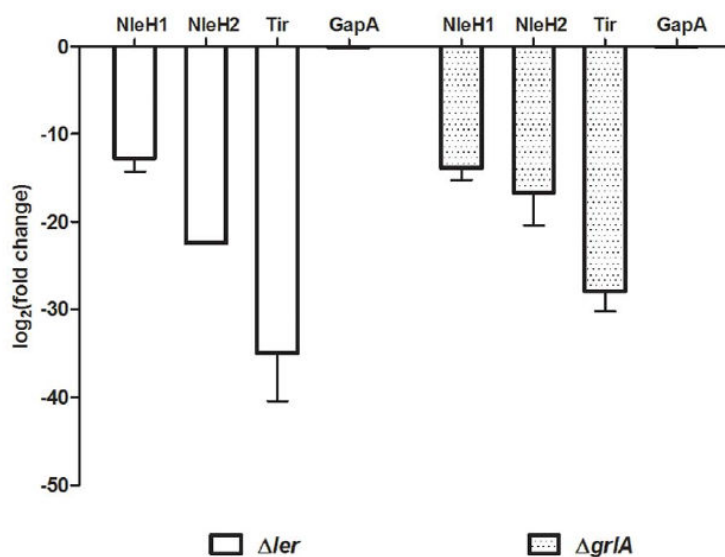


**Figure 3. Quantitative PCR of NleH transcripts in LEE regulator knockouts.** RNA was collected from ZAP193 strains WT,  $\Delta$ ler and  $\Delta$ grlA grown to  $OD_{600}=1.2$  in MEM and cDNA prepared. NleH1, NleH2, GapA, Tir and 16S RNA transcript was then quantified by q-PCR, NleH values normalised to that of 16S RNA, and the fold change calculated comparing mutant to wild-type. Bars represent the average of three biological samples. Error bars represent the standard error of the mean.  
doi:10.1371/journal.pone.0033408.g003

#### Expression of *nleH1::gfp* and *nleH2::gfp* in *E. coli* O157:H7 upon contact with host cells

The expression of effector proteins is subject to strict regulation thereby producing a discrete and carefully orchestrated pattern of protein injection into host cells. To test the regulation of *nleH1* and *nleH2* upon contact with host cells, we examined the expression of pAHE8 and pAHE22 during the interaction of *E. coli* O157:H7 with bovine epithelial cells (EBL). Bacteria were initially cultured to an  $OD_{600} = 0.6$  in MEM-HEPES media to promote expression of the T3SS before addition to the cell line at a multiplicity of infection of 200. When cultured in this media, we had previously seen rapid onset of GFP expression from these plasmids as optical density increased. Bacteria in contact with host cells were detected using an anti-O157 specific antibody and appropriate secondary conjugate. We examined expression at time points 5, 30, 60, 180 and 420 minutes after initial contact but no expression from *nleH1* or *nleH2* could be detected, suggesting marked repression of expression (Figure 5). In contrast, the control plasmid consisting of the promoter from the gene encoding the small ribosomal subunit (*rpsM*) fused to *gfp* (pAJR145) gave consistent and readily detectable expression throughout the course of the experiment. We also used a previously characterized *tir::gfp* fusion (pAJR75) and this gave rapid early expression during contact with the EBL cell line. Tir expression and was evident 60 mins after initial cell contact (Figure 5) but expression was reduced after that timepoint (data not shown).

#### Effect of NleH1 and NleH2 on host cell inflammatory response

The effect of NleH1 and NleH2 on host cell NF- $\kappa$ B modulation was then tested. Both proteins share a conserved domain with serine/threonine protein kinases including the Shigella effector protein OspG, which has been reported to strongly inhibit the activation of NF- $\kappa$ B [24]. To test the role of this kinase activity,

site directed mutants in three key residues were created. Specifically, lysine 159, aspartate 258, and glutamate 173 were substituted for alanine residues using site-directed mutagenesis. A K159A substitution results in loss of NleH1 kinase activity [27,28] and was confirmed by *in vitro* kinase assays with recombinant NleH1 protein (results not shown). Mutants D258A and E173A were created as these are highly conserved residues in Ser/Thr protein kinases and therefore may play important roles in their function. Each vector was transfected into a HEK293T cell line [29] alongside an NF- $\kappa$ B luciferase reporter plasmid and a constitutively expressed  $\beta$ -gal control plasmid. The  $\beta$ -gal activity was used to control for any variations in transfection efficiency and to normalize between replicates. Cells were stimulated using  $25 \text{ ng.ml}^{-1}$  TNF- $\alpha$  for 24 hours and the fold increase in NF- $\kappa$ B activity was determined using a luciferase reporter assay. The vector control gave a 20-fold stimulation of NF- $\kappa$ B activity upon addition of TNF- $\alpha$  demonstrating that the cells were responding as expected. Transfection with the vector expressing NleH1, NleH2, OspG or any of the site-directed variants produced no significant differences in the level of NF- $\kappa$ B activation as tested by one-way ANOVA (Figure 6). Although not statistically significant in our assay, OspG does show a trend towards repression of NF- $\kappa$ B activation, which was previously reported [24].

#### Discussion

Over the past ten years, the repertoire of *E. coli* O157 T3SS effector proteins has expanded greatly. This can be attributed to improvements in the sensitivity of mass spectrometry instruments and some excellent bioinformatics based studies, revealing a potential suite of over 50 effector proteins. Many of the identified Nle effector proteins can be grouped due to their high levels of identity, for example the EspG “family”. However, understanding the temporal expression and function for each of these effectors, in

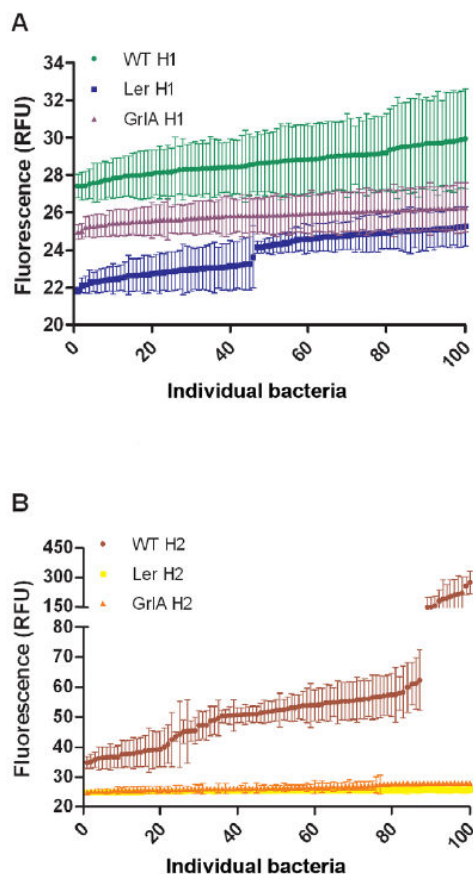


**Figure 4. Fluorescence microscopy of NleH-GFP.** pAHE8 (NleH1-GFP) and pAHE22 (NleH2-GFP) were transformed in ZAP193, ZAP193- $\Delta$ ler and ZAP193- $\Delta$ grIA and at OD<sub>600</sub>=0.8, dried onto a microscope slide in 4% PFA and stained for EspA filaments. Velocity quantification software was used to determine the average GFP fluorescence per voxel of 100 individual bacteria for NleH1 (A) and NleH2 (B). Each point represents the average GFP fluorescence from a composite from 16 z-slice images thus reducing planar effects. Error bars represent the standard deviation.

doi:10.1371/journal.pone.0033408.g004

addition to how they might function co-operatively or antagonistically, presents a daunting challenge for researchers.

In the current study, we examine the expression and regulation of *nleH1* and *nleH2* from *E. coli* O157:H7, which show a high level of similarity but greater diversity in their upstream UTRs, providing the potential for differential gene expression. Our previous work demonstrated that *nleA*, *nleB*, *nleD*, and *nleE* are transcribed in *E. coli* O157:H7 under secretion-permissive conditions [13]. Using GFP fusions, Q-PCR analysis and through interrogation of existing microarray data, we found that both *nleH1* and *nleH2* were expressed when grown in tissue culture medium. Maximal expression of *gfp* reporter fusion to *nleH1* required the longest upstream UTR region consisting of 531 bp. *nleH1* expression was more dependent on UTR length compared to *nleH2*. One interpretation of these data is that a transcriptional activator may bind strongly in a region further upstream of the

-283 bp 5' UTR of *nleH1*, and potentially at a similar site for *nleH2*, albeit much more weakly. Using ChIP-on-chip analyses, recent work demonstrated that the EHEC O157 Per-C like homologue (Pch) regulator directly binds the *nleH1* promoter but binds further upstream in the *nleH2* prophage in order to exert its control [21]. This study also determined that Pch does not have a consensus binding site, as it has various numbers and positions of binding sites depending upon the target gene, thus regulating a broad range of genes. Therefore, the increase in NleH1-GFP expression with increase in 5' UTR may be due to a direct effect of Pch binding to the area between -283 and -531 bp or an indirect effect of Pch modulating the promoter's secondary structure. This in turn may facilitate the action of another positive regulator or displace a repressor such as H-NS.

Assessment of the translational fusions in LEE-encoded regulator, Ler and GrIA deletion strains of *E. coli* O157:H7 ZAP193 indicated that expression of NleH1 and NleH2 requires these regulators. Expression was reduced greater in the absence of GrIA compared to Ler. These data are interesting to compare with a previous study investigating NleH regulation in *C. rodentium* [25]. This study also reported reduced expression of the NleH fusion in *C. rodentium*  $\Delta$ grIA and  $\Delta$ ler mutants compared to wild-type, albeit not significantly in this organism. In the current study, both *nleH1* and *nleH2* were subject to transcriptional regulation as demonstrated by Q-PCR analyses that showed that *nleH1* and *nleH2* transcripts were reduced approximately four-fold in the absence of *ler* or *grIA*. Therefore Ler and GrIA both influence *nleH1* and *nleH2* expression in both *E. coli* O157 and *C. rodentium*, but to markedly different extents. Further work needs to be performed to elucidate whether these LEE encoded regulators directly interact with the UTR of *nleH1* and *nleH2* or indirectly influence expression via other transcription factors.

Many *E. coli* O157:H7 virulence factors are expressed heterogeneously, such as EspA [30], Tir, Map, intimin [31] and NleA [13], in order to co-ordinate expression of the effectors with that of the T3S apparatus. Single cell imaging of NleH-GFP expressing *E. coli* O157:H7 showed that NleH-GFP is expressed by all cells in the population. However, the fluorescence of GFP measured on a per cell basis is homogenous in NleH1 but heterogeneous in NleH2. When cultured in MEM, only 80% of the population co-stained for EspA filaments, correlating with previous reports showing that only a subpopulation of ZAP193 (40–80%) express EspA filaments when cultured in the same media [32]. This percentage was maintained in the 'hyperexpressor' population of NleH2. This shows that although NleH-GFP expression is induced by the same conditions as that for the LEE, it is not strictly co-ordinated. In comparison, expression of *nleA* has been shown to be closely co-ordinated with the LEE and its transcription has been shown to be directly regulated by Ler [13,21,33]. NleA also plays an important role in the virulence of A/E pathogens [34,35].

The data show that both *nleH1* and *nleH2* are likely to be repressed during the early stages of A/E lesion formation and may be required later in the infection process. NleH-GFP expression was not detected upon contact with host cells under the conditions tested, and it has previously been reported that host cell contact results in a reduction in expression of many non-LEE encoded genes [13,36]. The persistence of *E. coli* O157:H7 on host cells has been shown to be mediated through the transcriptional regulator GadE [11,37]. The induction of the GAD stress response and reciprocal repression of the LEE mediated by GadE is, in turn, controlled by the *psr* genes. It has been reported that there is a high association between non-LEE encoded effectors with *psr* and/or *pch* regulated genes encoded on the same horizontally acquired

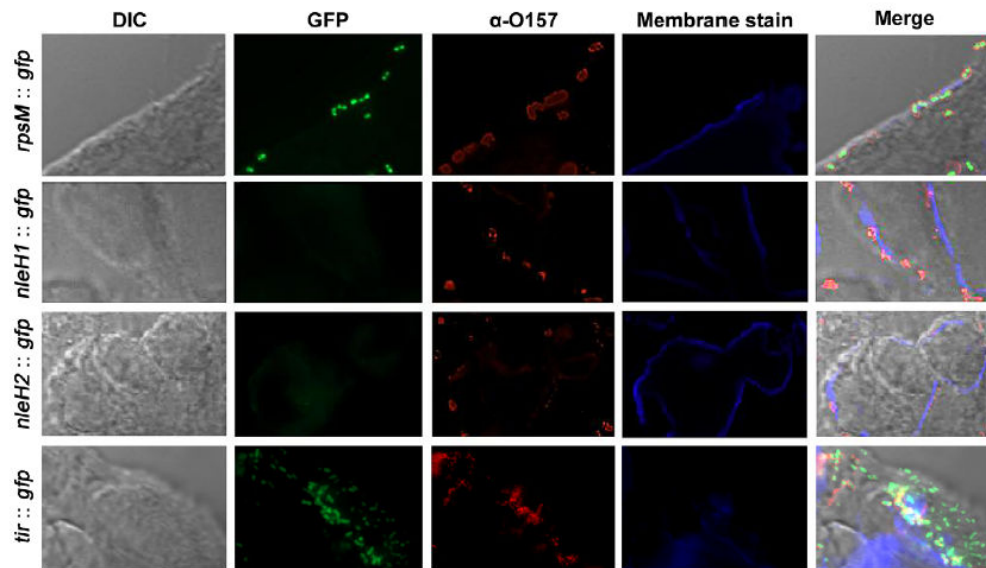


**Figure 5. Expression of NleH-GFP upon *E. coli* O157:H7 ZAP193 contact with EBL cells.** ZAP193 transformed with plasmids expressing GFP constitutively (pAJR145; *rpsM::gfp*) or translational fusions of *nleH* or *tir* to *gfp* under the control of their native promoter (pAHE8; NleH1-GFP, pAHE22; NleH2-GFP, pAJR75; Tir-GFP) were added to EBL cells and incubated for 0, 5, 30, 60 or 180 minutes at 37°C, 5% CO<sub>2</sub> before the removal of supernatant and fixation of cells with 4% paraformaldehyde. The panel of images is representative of all time points tested, apart from Tir-GFP, that showed strong early expression during cell contact but was markedly reduced at 180 minutes.  
doi:10.1371/journal.pone.0033408.g005

element [11]. This association led to the hypothesis that the Psr mediated induction of *gadE* transcription and subsequent repression of LEE encoded effectors facilitates non-LEE encoded effector secretion [11]. It is interesting to note that many Nle effector proteins, including NleH, exhibit a role in colonisation

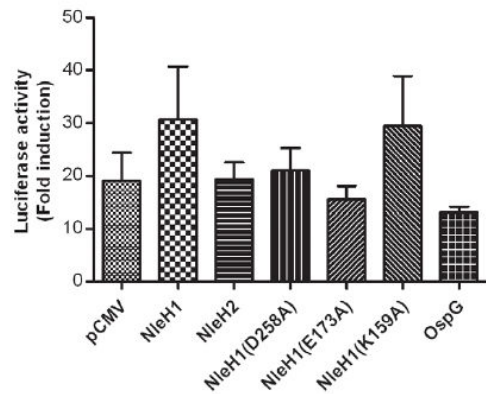


**Figure 6. NF-κB activity in the presence of NleH variants.** HEK293T cells were co-transfected with a luciferase reporter plasmid under the control of consensus κB sites, a β-galactosidase plasmid and a control (pCMV), NleH or OspG vector. After 40 hours, cells were stimulated by the addition of TNF-α (25 ng/ml; 24 hours). Results represent three biological replicates, where variants were tested in triplicate and assayed in duplicate. Statistical analysis with one-way ANOVA shows no significant difference compared with the pCMV control. Error bars represent the standard error of the mean.  
doi:10.1371/journal.pone.0033408.g006

rather than A/E lesion production or overt pathogenesis [25,26,38,39,40,41,42,43].

NleH is a predicted Ser/Thr protein kinase, and the C-terminal end of the protein shares sequence similarity with that of the *S. flexneri* effector OspG. OspG has been reported to modulate host innate immune responses by interfering with NF-κB activation [24] with a 70% reduction in NF-κB activation being observed when five times more OspG (0.5 μg) than the NF-κB reporter (0.1 μg) was transfected into HEK293T cells. This study reported a more modest 30% decrease in NF-κB activation when equivalent concentrations of OspG and reporter plasmid were used. This is broadly comparable to the level of NF-κB inhibition we observed (~17%) using OspG when equivalent concentrations of effector and NF-κB reporter plasmids were transfected (0.4 μg).

During the course of this study, it was reported that NleH1 inhibits NF-κB activation [27,44]. Luciferase reporters were transfected into HEK293T cells in a manner similar to that which was carried out in this study. However, cells were stimulated with four times more TNF-α and analysed 1 hour post-stimulation. Similar to the OspG study [24], the effector plasmid and the NF-κB reporter plasmid were transfected at a 4:1 ratio which appears to amplify the effect (to a similar degree) observed with equivalent concentrations of vectors [27]. Further work investigating the role of RPS3 in NF-κB activation led to the demonstration that *E. coli* O157:H7 NleH1 can inhibit RPS3 phosphorylation by IKK-β [45]. Inhibiting the phosphorylation of RPS3 restricts its translocation into the nucleus, reducing transcription of RPS3 dependant κB sites [27,45,46]. Regardless of this, transcription of genes controlled by non-RPS3 dependant κB sites can still occur, providing some additional reasoning as to why NleH1 and NleH2 did not significantly affect NF-κB activation in our assay. The kinase activity of NleH1 is required to inhibit RPS3 phosphory-

lation by IKK- $\beta$  but it does not directly phosphorylate either protein. NleH also inhibits the pro-apoptotic pathway via its interaction with Bax Inhibitor 1 (BI-1) [28]. This interaction with BI-1 is dependent upon the C-terminal end of NleH but not its kinase activity; this region of NleH shares high protein identity with OspG, yet OspG does not interact with BI-1. It has yet to be elucidated whether NleH phosphorylates proteins other than itself. Overall, NleH is a multi-functional protein, a common trait for *E. coli* O157:H7 effector proteins.

This study highlights the need to not only determine the function of putative effector proteins but also how their expression is regulated in relation to the apparatus that secretes them. We provide further evidence that *nleH1* and *nleH2* are expressed under the same conditions that promote LEE expression but this expression is not strictly co-ordinated *in vitro*. Both *nleH* alleles are transcriptionally regulated by Ler and GrlA in EHEC in comparison to the post-translational regulation by LonP protease for *C. rodentium*, highlighting the importance of independently investigating the regulation of similar genes in related pathogens.

## Materials and Methods

### Bacterial strains and media

Strains used in this study are described in Table 1. Luria-Bertani broth and two defined media were used, Minimal Essential Media with HEPES modification (MEM; Sigma M7278), and Dulbecco's Minimal Essential Media (DMEM; Sigma M5671). Glucose was added to the MEM to give a final concentration of 0.2%. Antibiotics were included where necessary at the following concentrations: 50  $\mu$ g/ml kanamycin (Kan), 12.5  $\mu$ g/ml chloramphenicol (Chl), 100  $\mu$ g/ml ampicillin (Amp), 15  $\mu$ g/ml gentamycin (Gent).

### Plasmid-based translational fusion construction and NleH expression constructs

Three promoter lengths and the entire coding sequence for NleH1 and NleH2 were amplified from strain TUV-930 and cloned into pAJR70 to create pAHE8, pAHE18-22 (Table 1). Figure S1 shows the putative promoter regions that were amplified and cloned to create the constructs.

**Table 1.** Bacterial strains and plasmids used in this study.

Strain	Description	Reference/Source
TUV 93-0	EHEC O157:H7 strain EDL933; <i>stx</i> <sup>-</sup> derivative	[49]
ZAP198	EHEC O157:H7 strain NCTC 12900 <i>stx</i> <sup>-</sup>	[50]
ZAP198 $\Delta$ ler	Unmarked <i>ler</i> deletion mutant in strain ZAP198	[50]
ZAP198 $\Delta$ grlA-Tn-Kan	<i>grlA</i> transposon mutant in EHEC strain ZAP198 (Tn5)	[51]
BW25113	<i>E. coli</i> K-12.	[52]
BW25113 <i>rpos</i> :Kan	BW25113 Keio mutant of <i>rpoS</i> .	[52]
MC1000	<i>araD139</i> $\Delta$ ( <i>araABC-leu</i> )7679 <i>galU galK</i> $\Delta$ ( <i>lac</i> )X74 <i>rpsL thi</i> .	[53]
VS184	MC1000 $\Delta$ qseC	[54]
XL1-Blue	<i>recA1 endA1 gyrA96 thi-1 hsdR17 supE44 relA1 lac</i> [F' <i>proAB lac</i> <sup>q</sup> ZAM15 Tn10 (Tet <sup>r</sup> )]	Stratagene
<b>Plasmid</b>		
pAJR70	pACYC eGFP	[30]
pAHE8	pAJR70 $\Omega$ [BamHI KpnI -531 bpNleH1_291::gfp]	This study
pAHE18	pAJR70 $\Omega$ [BamHI KpnI -120 bpNleH1_291::gfp]	This study
pAHE19	pAJR70 $\Omega$ [BamHI KpnI -283 bpNleH1_291::gfp]	This study
pAHE20	pAJR70 $\Omega$ [BamHI KpnI -113 bpNleH2_293::gfp]	This study
pAHE21	pAJR70 $\Omega$ [BamHI KpnI -291 bpNleH2_293::gfp]	This study
pAHE22	pAJR70 $\Omega$ [BamHI KpnI -655 bpNleH2_293::gfp]	This study
pAJR75	pAJR70 $\Omega$ [BamHI KpnI -442 bp including <i>LEE5</i> promoter cloned in frame 5' to <i>egfp</i>	Roe 2004
pAJR145	pACYC <i>rpsm</i> ::GFP+	Roe 2004
<i>pIacZ</i>	$\beta$ -galactosidase enzyme constitutively produced by mammalian expression vector	Stratagene
NF- $\kappa$ B <i>luc</i>	Firefly luciferase gene under the control of canonical NF- $\kappa$ B promoter	Stratagene
pCMVTag3A	N-terminal myc tagging mammalian expression vector	Stratagene
pCMV-NleH1	pCMVTag3A $\Omega$ [PstI HindIII - NleH1 ORF]	This study
pCMV-NleH2	pCMVTag3A $\Omega$ [PstI HindIII - NleH2 ORF]	This study
pCMV-NleH1(D258)	Site directed mutant (SDM) of NleH1 residue D258 to alanine (A)	This study
pCMV-NleH1(E173)	SDM of NleH1 residue E173 to alanine (A)	This study
pCMV-NleH1(K159A)	SDM of NleH1 residue K159 to alanine (A)	This study
pJ201-OspG	OspG ORF with PstI+HindIII sites	DNA2.0/this study
pCMV-OspG	pCMVTag3A $\Omega$ [PstI HindIII - OspG ORF]	This study

doi:10.1371/journal.pone.0033408.t001

Expression plasmids for NleH1 and NleH2 were made as shown in Table 1. Site directed mutants were made using the Quick Change 1 mutagenesis system (Stratagene).

### Analysis of bacterial fluorescence

Constructs pAHE8 and 18–22 were assessed by growing ZAP193, and mutant where indicated, transformants overnight in LB Chl then the next morning diluted to a final OD<sub>600</sub> of 0.08 into minimal media the next morning. Typically, 20 ml was cultured in Erlenmeyer flasks shaken at 180 rpm, 37°C. At regular intervals, 1 ml of culture was removed from the flask and 200 µl aliquots were analysed in triplicate with a fluorescent plate reader (Fluorostar Optima; BMG) at 37°C. For any strain and media combination, the promoterless *gfp* plasmid pAJR70 was included as a control. Fluorescence was plotted against OD<sub>600</sub> using Graphpad Prism 5 software and a line of best fit obtained. Using this method, data were corrected for background fluorescence. At least three biological replicates were carried out for each experiment. To measure single-cell expression by fluorescence microscopy, strains were grown in MEM and at OD<sub>600</sub> 0.8 a 100 µl aliquot was removed and diluted 1:1 in 4% paraformaldehyde. 20 µl was dried onto a microscope slide and EspA filaments stained as described previously [30]. The slides were examined by fluorescence microscopy on a Zeiss Axioskop M1 fluorescence microscope, using the appropriate filter sets and a Z-stack of 16 images was captured at a spacing of 0.15 µm using Volocity software (PerkinElmer). These images were used to create a composite image that reduced the spatial effects of bacteria in different focal planes. The average *gfp* units per voxel (cubic pixel) was quantified, for at least 100 bacteria with a minimum volume of 4 µm<sup>3</sup>, using Volocity Quantification software (Perkin-Elmer). These values were exported and plotted in GraphPad Prism 5 (GraphPad Software, USA).

### Expression on contact with EBL cell lines

Embryonic bovine cell (German Collection of Microorganisms and Cell Cultures, no. ACC192, provided by Dr Arvind Mahajan, University of Edinburgh) were prepared and cultured as described previously [47]. The ZAP193 strain transformed with the appropriate GFP reporter plasmids was cultured in MEM-HEPES to OD<sub>600</sub> 0.8 at 37°C, added to the multichamber slide, and centrifuged onto the EBL cells (1000×g) for 5 min (Time 0). The cells were stained at intervals by removal of the culture and addition of CellMask™ Deep Red plasma membrane stain (Invitrogen) before fixation with 4% paraformaldehyde. Time points analysed were 0, 5, 30, 180, and 420 min after addition. Immunostaining was performed using Mast α-O157 antibody and α-rabbit AlexaFluor-555 conjugate secondary antibody. Fluorescence analysis using Zeiss and Volocity software was then performed as described previously.

### RT-PCR analysis

Triplicate ZAP193, ZAP193ΔgrlA and ZAP193Δler were cultured in MEM-HEPES media to an OD<sub>600</sub> = 1.2. Bacterial pellets were suspended in RNeasy Protect Bacteria Reagent (Qiagen). Total RNA was extracted using Qiagen RNeasy Mini kit and cDNA synthesis was carried out using a Qiagen QuantiTect™ Reverse Transcription kit. Duplicate qPCRs were carried out using a Qiagen Quantifast™ SYBR® green PCR kit and

Stratagene MX3000 and primers listed in Table S2. All the experiments were performed according to manufacturer's instructions.

### Transfection of HEK293T cells

HEK293T cells [29] were cultured in DMEM (Invitrogen 21989) supplemented with 1 mM L-Glutamine, 10% foetal calf serum and penicillin/streptomycin. HEK293T cells were plated at a density of 5 × 10<sup>4</sup> cells per well of a 24 well plate and, once 90% confluent, transfected with 0.4 µg of control (pCMV) or expression plasmid (pCMVNleH1, pCMVNleH1K159A, pCMVNleH1E173A, pCMVNleH1D258A pCMVNleH2 or pCMVospG (DNA 2.0), 0.4 µg NF-κB luciferase reporter plasmid (Stratagene) and 0.1 µg β-galactosidase plasmid (a gift from Dr. Alison Michie). TNF-α (25 ng/ml) was added 40 hours after transfection. 24 hours after stimulation, cells were washed twice with PBS before lysates prepared and analysed with Dual-Light® System (Applied Biosystems). Luciferase activity was determined and normalized to β galactosidase activity as described [48]. Each assay was performed in triplicate, measured in duplicate and repeated three times.

### Supporting Information

**Figure S1 655 bp of upstream untranslated region (UTR) of *E. coli* O157:H7 EDL933 NleH1 (z0989) and NleH2 (z6021) were aligned using ClustalW.** Primers designed to construct translational fusions to GFP are labelled; green for NleH1 and blue for NleH2. (TIFF)

**Figure S2 pAHE8 (NleH1-GFP) and pAHE22 (NleH2-GFP) were transformed into ZAP193 (A), ZAP193Δler (B) and ZAP193ΔgrlA (C) and at OD<sub>600</sub> = 0.8 fixed with 4% paraformaldehyde onto a microscope slide.** Expression of NleH-GFP (green) and immunostained EspA filaments (Alexa-Fluor555; red) were observed using the appropriate filter sets. Micrographs are the composite image from 16 z-slices with 0.15 µm spacing. (TIFF)

**Table S1 Sequences containing promoter regions were obtained from coliBASE and aligned using ClustalW.** (DOC)

**Table S2 Oligonucleotides used in this study.** (DOCX)

### Acknowledgments

The authors thank Miss Jennifer Lonsdale for her valuable help with the microscopy, Mr Sean McAteer for providing the GrlA deletion strain, Dr Vanessa Sperandio for defined *qseC* *E. coli* K12 mutant, Dr Gail Ferguson for defined *rpoS* *E. coli* K12 mutant, and Dr Arvind Mahajan for the EBL cell line.

### Author Contributions

Conceived and designed the experiments: AJR AH TJE TJM. Performed the experiments: AH CLA TJE DW. Analyzed the data: AH AJR TJE. Wrote the paper: AJR AH.

### References

- Chen HD, Frankel G (2005) Enteropathogenic *Escherichia coli*: unravelling pathogenesis. FEMS Microbiol Rev 29: 83–98.
- Giron JA, Torres AG, Freer E, Kaper JB (2002) The flagella of enteropathogenic *Escherichia coli* mediate adherence to epithelial cells. Mol Microbiol 44: 361–379.

3. Mahajan A, Currie CG, Mackie S, Tree J, McAteer S, et al. (2009) An investigation of the expression and adhesion function of H7 flagella in the interaction of *Escherichia coli* O157:H7 with bovine intestinal epithelium. *Cell Microbiol* 11: 121–137.
4. Kenny B, DeVinney R, Stein M, Reinscheid DJ, Frey EA, et al. (1997) Enteropathogenic *E. coli* (EPEC) transfers its receptor for intimate adherence into mammalian cells. *Cell* 91: 511–520.
5. Deng W, de Hoog CL, Yu HB, Li Y, Croxen MA, et al. (2010) A comprehensive proteomic analysis of the type III secretome of *Citrobacter rodentium*. *J Biol Chem* 285: 6790–6800.
6. Deng W, Li Y, Hardwidge PR, Frey EA, Pfuetzner RA, et al. (2005) Regulation of type III secretion hierarchy of translocators and effectors in attaching and effacing bacterial pathogens. *Infect Immun* 73: 2135–2146.
7. Tobe T, Beatson SA, Taniguchi H, Abe H, Bailey CM, et al. (2006) An extensive repertoire of type III secretion effectors in *Escherichia coli* O157 and the role of lambdaoid phages in their dissemination. *Proceedings of the National Academy of Sciences of the United States of America* 103: 14941–14946.
8. Marches O, Ledger TN, Boury M, Ohara M, Tu X, et al. (2003) Enteropathogenic and enterohaemorrhagic *Escherichia coli* deliver a novel effector called Cif, which blocks cell cycle G2/M transition. *Mol Microbiol* 50: 1553–1567.
9. Mundy R, MacDonald TT, Dougan G, Frankel G, Wiles S (2005) *Citrobacter rodentium* of mice and man. *Cell Microbiol* 7: 1697–1706.
10. Mellies JL, Barron AM, Carmona AM (2007) Enteropathogenic and enterohaemorrhagic *Escherichia coli* virulence gene regulation. *Infect Immun* 75: 4199–4210.
11. Tree JJ, Roe AJ, Flockhart A, McAteer SP, Xu X, et al. (2011) Transcriptional regulators of the GAD acid stress island are carried by effector protein-encoding prophages and indirectly control type III secretion in enterohaemorrhagic *Escherichia coli* O157:H7. *Mol Microbiol* 80: 1349–1365.
12. Elliott SJ, Sperandio V, Giron JA, Shin S, Mellies JL, et al. (2000) The locus of enterocyte effacement (LEE)-encoded regulator controls expression of both LEE- and non-LEE-encoded virulence factors in enteropathogenic and enterohaemorrhagic *Escherichia coli*. *Infect Immun* 68: 6115–6126.
13. Roe AJ, Tysall L, Dransfield T, Wang D, Fraser-Pitt D, et al. (2007) Analysis of the expression, regulation and export of NleA-E in *Escherichia coli* O157:H7. *Microbiology* 153: 1350–1360.
14. Bustamante VH, Santana FJ, Calva E, Puente JL (2001) Transcriptional regulation of type III secretion genes in enteropathogenic *Escherichia coli*: Ler antagonizes H-NS-dependent repression. *Mol Microbiol* 39: 664–678.
15. Beltrametti F, Kresse AU, Guzman CA (1999) Transcriptional regulation of the esp genes of enterohaemorrhagic *Escherichia coli*. *J Bacteriol* 181: 3409–3418.
16. Laaberki MH, Janabi N, Oswald E, Repollo F (2006) Concert of regulators to switch on LEE expression in enterohaemorrhagic *Escherichia coli* O157:H7: interplay between Ler, GrlA, HNS and RpoS. *Int J Med Microbiol* 296: 197–210.
17. Deng WY, Puente JL, Gruenheid S, Li Y, Vallance BA, et al. (2004) Dissecting virulence: Systematic and functional analyses of a pathogenicity island. *Proceedings of the National Academy of Sciences of the United States of America* 101: 3597–3602.
18. Huang LH, Syu WJ (2008) GrlA of enterohaemorrhagic *Escherichia coli* O157:H7 activates LEE1 by binding to the promoter region. *J Microbiol Immunol Infect* 41: 9–16.
19. Barba J, Bustamante VH, Flores-Valdez MA, Deng W, Finlay BB, et al. (2005) A positive regulatory loop controls expression of the locus of enterocyte effacement-encoded regulators Ler and GrlA. *J Bacteriol* 187: 7918–7930.
20. Jobichen C, Li M, Yerushalmi G, Tan YW, Mok YK, et al. (2007) Structure of GrlR and the implication of its EDED motif in mediating the regulation of type III secretion system in EHEC. *PLoS Pathog* 3: e69.
21. Abe H, Miyahara A, Oshima T, Tashiro K, Ogura Y, et al. (2008) Global regulation by horizontally transferred regulators establishes the pathogenicity of *Escherichia coli*. *DNA Res* 15: 25–38.
22. Iyoda S, Watanabe H (2004) Positive effects of multiple pch genes on expression of the locus of enterocyte effacement genes and adherence of enterohaemorrhagic *Escherichia coli* O157:H7 to HEp-2 cells. *Microbiology* 150: 2357–2571.
23. Porter ME, Mitchell P, Free A, Smith DG, Gally DL (2005) The LEE1 promoters from both enteropathogenic and enterohaemorrhagic *Escherichia coli* can be activated by PerC-like proteins from either organism. *J Bacteriol* 187: 458–472.
24. Kim DW, Lenzen G, Page AL, Legrain P, Sansonetti PJ, et al. (2005) The *Shigella flexneri* effector OspG interferes with innate immune responses by targeting ubiquitin-conjugating enzymes. *Proceedings of the National Academy of Sciences of the United States of America* 102: 14046–14051.
25. Garcia-Angulo VA, Deng W, Thomas NA, Finlay BB, Puente JL (2008) Regulation of expression and secretion of NleH, a new non-locus of enterocyte effacement-encoded effector in *Citrobacter rodentium*. *J Bacteriol* 190: 2388–2399.
26. Hemrajani C, Marches O, Wiles S, Girard F, Dennis A, et al. (2008) Role of NleH, a type III secreted effector from attaching and effacing pathogens, in colonization of the bovine, ovine and murine gut. *Infect Immun*.
27. Gao X, Wan F, Mateo K, Callegari E, Wang D, et al. (2009) Bacterial effector binding to ribosomal protein s3 subverts NF-kappaB function. *PLoS Pathog* 5: e1000708.
28. Hemrajani C, Berger CN, Robinson KS, Marches O, Mousnier A, et al. (2010) NleH effectors interact with Bax inhibitor-1 to block apoptosis during enteropathogenic *Escherichia coli* infection. *Proc Natl Acad Sci U S A* 107: 3129–3134.
29. Graham FL, Smiley J, Russell WC, Nairn R (1977) Characteristics of a human cell line transformed by DNA from human adenovirus type 5. *The Journal of general virology* 36: 59–74.
30. Roe AJ, Yull H, Naylor SW, Woodward MJ, Smith DG, et al. (2003) Heterogeneous surface expression of EspA translocon filaments by *Escherichia coli* O157:H7 is controlled at the posttranscriptional level. *Infect Immun* 71: 5900–5909.
31. Roe AJ, Naylor SW, Spears KJ, Yull HM, Dransfield TA, et al. (2004) Coordinate single-cell expression of LEE4- and LEE5-encoded proteins of *Escherichia coli* O157:H7. *Mol Microbiol* 54: 337–352.
32. Roe AJ, Hoey DEE, Gally DL (2003) Regulation, secretion and activity of type III-secreted proteins of enterohaemorrhagic *Escherichia coli* O157. *Biochemical Society Transactions* 31: 98–103.
33. Schwidder M, Hensel M, Schmidt H (2011) Regulation of nleA in Shiga toxin-producing *Escherichia coli* O84:H4 strain 4795/97. *J Bacteriol* 193: 832–841.
34. Gruenheid S, Sekirov I, Thomas NA, Deng W, O'Donnell P, et al. (2004) Identification and characterization of NleA, a non-LEE-encoded type III translocated virulence factor of enterohaemorrhagic *Escherichia coli* O157:H7. *Mol Microbiol* 51: 1233–1249.
35. Thanabalasuriar A, Koutsouris A, Welfen A, Mimeo M, Hecht G, et al. (2010) The bacterial virulence factor NleA is required for the disruption of intestinal tight junctions by enteropathogenic *Escherichia coli*. *Cell Microbiol* 12: 31–41.
36. Dahan S, Knutton S, Shaw RK, Crepin VF, Dougan G, et al. (2004) Transcriptome of enterohaemorrhagic *Escherichia coli* O157 adhering to eukaryotic plasma membranes. *Infect Immun* 72: 5452–5459.
37. Tatsuno I, Nagano K, Taguchi K, Rong L, Mori H, et al. (2003) Increased adherence to Caco-2 cells caused by disruption of the yhiE and yhiF genes in enterohaemorrhagic *Escherichia coli* O157:H7. *Infect Immun* 71: 2598–2606.
38. Kelly M, Hart E, Mundy R, Marches O, Wiles S, et al. (2006) Essential role of the type III secretion system effector NleB in colonization of mice by *Citrobacter rodentium*. *Infect Immun* 74: 2328–2337.
39. Echtenkamp F, Deng W, Wickham ME, Vazquez A, Puente JL, et al. (2008) Characterization of the NleF effector protein from attaching and effacing bacterial pathogens. *FEMS Microbiol Lett* 281: 98–107.
40. Wickham ME, Lupp C, Vazquez A, Mascarenhas M, Coburn B, et al. (2007) *Citrobacter rodentium* virulence in mice associates with bacterial load and the type III effector NleE. *Microbes Infect* 9: 400–407.
41. Dziva F, van Diemen PM, Stevens MP, Smith AJ, Wallis TS (2004) Identification of *Escherichia coli* O157:H7 genes influencing colonization of the bovine gastrointestinal tract using signature-tagged mutagenesis. *Microbiology* 150: 3631–3645.
42. Visidou I, Marches O, Dziva F, Mundy R, Frankel G, et al. (2006) Identification and characterization of EspK, a type III secreted effector protein of enterohaemorrhagic *Escherichia coli* O157:H7. *FEMS Microbiol Lett* 263: 32–40.
43. van Diemen PM, Dziva F, Stevens MP, Wallis TS (2005) Identification of enterohaemorrhagic *Escherichia coli* O26:H- genes required for intestinal colonization in calves. *Infect Immun* 73: 1735–1743.
44. Royan SV, Jones RM, Koutsouris A, Roxas JL, Falzari K, et al. (2010) Enteropathogenic *E. coli* non-LEE encoded effectors NleH1 and NleH2 attenuate NF-kappaB activation. *Mol Microbiol* 78: 1232–1245.
45. Wan F, Weaver A, Gao X, Bem M, Hardwidge PR, et al. (2011) IKKbeta phosphorylation regulates RPS3 nuclear translocation and NF-kappaB function during infection with *Escherichia coli* strain O157:H7. *Nat Immunol* 12: 335–343.
46. Wan F, Anderson DE, Barnitz RA, Snow A, Bidere N, et al. (2007) Ribosomal protein S3: a KH domain subunit in NF-kappaB complexes that mediates selective gene regulation. *Cell* 131: 927–939.
47. Roe AJ, Naylor SW, Spears KJ, Yull HM, Dransfield TA, et al. (2004) Coordinate single-cell expression of LEE4- and LEE5-encoded proteins of *Escherichia coli* O157:H7. *Molecular Microbiology* 54: 337–352.
48. Philpott DJ, Yamaoka S, Israel A, Sansonetti PJ (2000) Invasive *Shigella flexneri* activates NF-kappa B through a lipopolysaccharide-dependent innate intracellular response and leads to IL-8 expression in epithelial cells. *J Immunol* 165: 903–914.
49. Perna NT, Plunkett G, 3rd, Burland V, Mau B, Glasner JD, et al. (2001) Genome sequence of enterohaemorrhagic *Escherichia coli* O157:H7. *Nature* 409: 529–533.
50. Low AS, Holden N, Rosser T, Roe AJ, Constantinidou C, et al. (2006) Analysis of fimbrial gene clusters and their expression in enterohaemorrhagic *Escherichia coli* O157:H7. *Environmental microbiology* 8: 1033–1047.
51. Flockhart AF, Tree JJ, Xu X, Karpiyevich M, McAteer SP, et al. (2011) Identification of a novel prophage regulator in *Escherichia coli* controlling the expression of type III secretion. *Molecular Microbiology*.
52. Baba T, Ara T, Hasegawa M, Takai Y, Okumura Y, et al. (2006) Construction of *Escherichia coli* K-12 in-frame, single-gene knockout mutants: the Keio collection. *Molecular systems biology* 2: 2006 0008.
53. Casadaban MJ, Cohen SN (1980) Analysis of gene control signals by DNA fusion and cloning in *Escherichia coli*. *Journal of molecular biology* 138: 179–207.
54. Sperandio V, Torres AG, Kaper JB (2002) Quorum sensing *Escherichia coli* regulators B and C (QseBC): a novel two-component regulatory system involved in the regulation of flagella and motility by quorum sensing in *E. coli*. *Molecular Microbiology* 43: 809–821.